Stability of four-body kite central configurations

Simonas Stasevičius

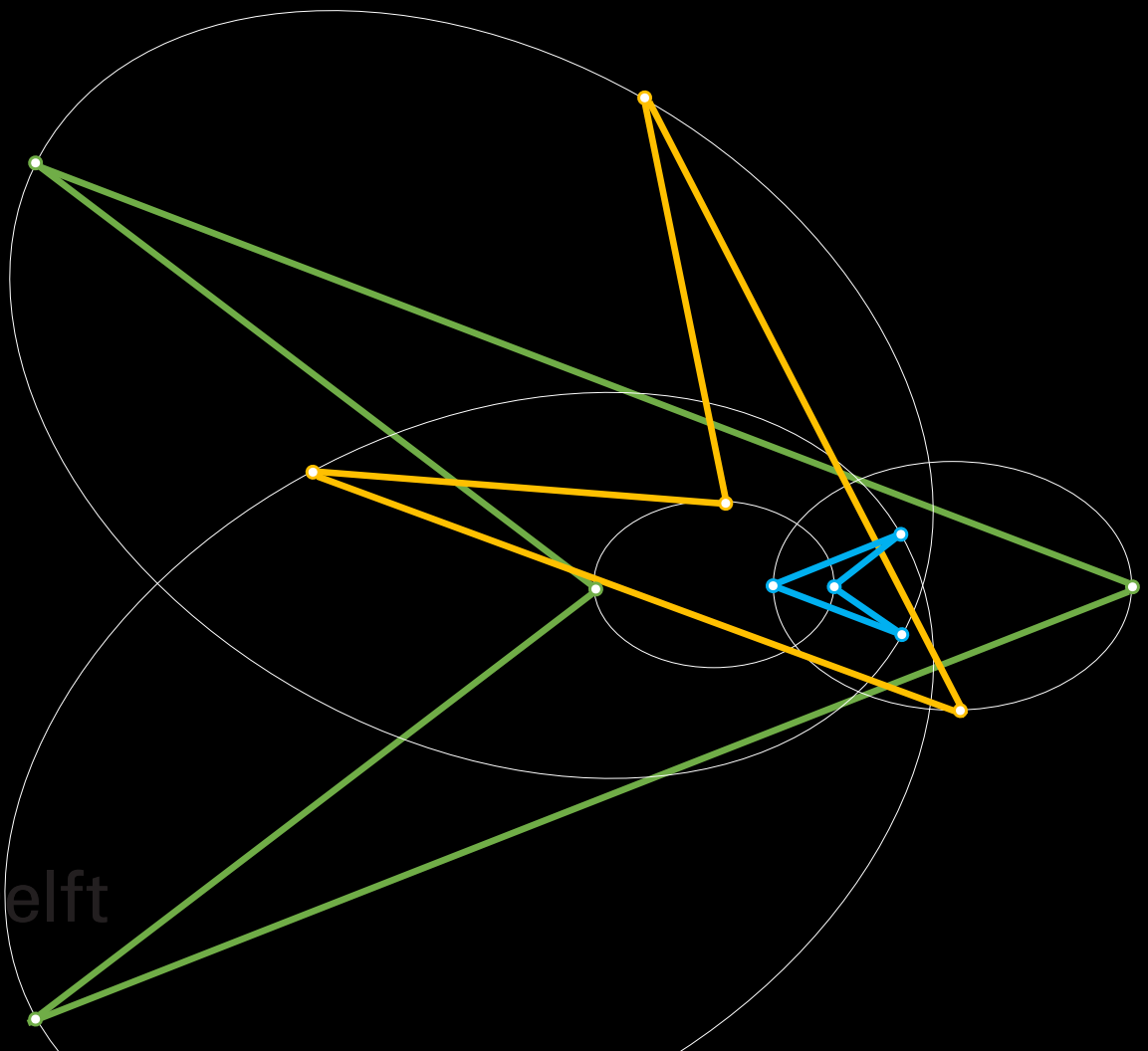

TU Delft

Stability of four-body kite central configurations

by

Simonas Stasevičius

to obtain the degree of Master of Science
at Delft University of Technology,
to be defended publicly on Thursday December 22, 2022 at 13:00.

Student number:	4547233	
Thesis committee:	Ir. R. Noomen,	TU Delft, supervisor
	Dr. ir. W. T. van Horssen,	TU Delft, supervisor
	Dr. D. M. Stam	TU Delft, chair
	Dr. P. M. Visser	TU Delft, examiner

An electronic version of this thesis is available at `http://repository.tudelft.nl/`.

TU Delft

Preface

I would like to express my gratitude to my supervisors Ron Noomen and Wim van Horssen for their well-meaning efforts, their guidance, for their time invested in this project, for offering their wise advice and for staying patient with me.

Simonas Stasevičius
Amsterdam, December 2022

Abstract

Central configurations provide the only closed-form analytical solutions of the n-body problem. All possible central configurations of three bodies have been extensively studied along with the stability of the associated periodic orbits. Stable cases have been found for the Lagrangian triangle configuration, which we see occurring with the Trojan asteroids. However, the knowledge about four-body central configurations remains limited. An explicit parameterization of a family of kite shaped four-body central configurations has recently been published. The present research investigates the stability of periodic solutions provided by these central configurations. An analytical treatment of linear stability is carried out and the eigenvalues for circular periodic orbits are calculated. This is complemented with a numerical estimation of Floquet multipliers to determine the linear stability of eccentric periodic orbits. While most of the kite configurations are found to be unstable, regions of linearly stable cases are discovered for both circular and eccentric orbits. Further, numerical simulations of the non-linear system are performed as an independent approach to validate the linear stability results. Perfect agreement with the linear analysis is found, suggesting that stable kites may be observed in the universe.

Contents

1 Introduction **3**
1.1 Background . . . 3
1.2 Applications . . . 4
1.2.1 One massive object . . . 4
1.2.2 Two massive objects . . . 5
1.2.3 Three or four massive objects . . . 6
1.3 Research aim . . . 6
1.4 Structure . . . 6

2 Kite central configurations **9**
2.1 Convex configurations . . . 9
2.2 Concave configurations . . . 10
2.2.1 First concave case . . . 10
2.2.2 Second concave case . . . 12

3 Reduction of symmetries **15**
3.1 Hamiltonian formulation . . . 15
3.2 Canonical transformations . . . 16
3.3 Jacobi coordinates . . . 17
3.4 Polar coordinates . . . 20
3.5 Eliminating angular momentum . . . 23
3.6 Further elimination . . . 25

I Linear stability **27**

4 Convex cases **29**
4.1 Periodic solution . . . 29
4.2 Convex case . . . 30
4.3 Linearization . . . 34
4.4 Further reduction . . . 48
4.5 Simplification . . . 61
4.6 Circular square case . . . 64
4.7 Circular cases . . . 68
4.7.1 Mathematica procedure . . . 70
4.8 Perturbations in eccentricity . . . 71
4.8.1 Method . . . 71
4.8.2 Application . . . 76
4.9 Eccentric cases . . . 78
4.9.1 Method of integration . . . 79
4.9.2 Results . . . 80
4.10 Closing remarks . . . 87

5 First concave cases **91**
5.1 Linearization . . . 91
5.2 Circular cases . . . 96
5.3 Eccentric cases . . . 96
5.4 Closing remarks . . . 96

6 Second concave cases **101**
6.1 Linearization . . . 101
6.2 Circular cases . . . 106
6.3 Eccentric cases . . . 106
6.4 Closing remarks . . . 109

7 Verification and validation **111**
7.1 Verification of linear stability . . . 111
7.1.1 Coefficients of the Hessian . . . 111
7.1.2 Decoupling . . . 111
7.1.3 Final matrix . . . 111
7.1.4 Perturbation method . . . 111
7.1.5 Numerical integrators . . . 112
7.1.6 Monodromy matrices . . . 112
7.1.7 Characteristic multipliers . . . 112
7.1.8 Linear stability . . . 112

II Non-linear stability **113**

8 Long-term numerical integration **115**
8.1 The system . . . 115
8.2 Numerical integration technique . . . 115
8.3 Convex configurations . . . 117
8.3.1 Square configuration . . . 118
8.3.2 Case $\boldsymbol{\alpha = 59.9°}$, $\boldsymbol{\beta = 15.1°}$, $\boldsymbol{e = 0.3}$ . . . 120
8.3.3 Case $\boldsymbol{\alpha = 39.7°}$, $\boldsymbol{\beta = 25.3°}$, $\boldsymbol{e = 0.2}$ . . . 123
8.4 Concave configurations of the first kind . . . 125
8.4.1 Case $\boldsymbol{\alpha = 50°}$, $\boldsymbol{\beta = 5°}$, $\boldsymbol{e = 0.1}$ . . . 125
8.5 Concave configurations of the second kind . . . 127
8.5.1 Case $\boldsymbol{\alpha = 74°}$, $\boldsymbol{\beta = 59°}$, $\boldsymbol{e = 0.1}$ . . . 127
8.5.2 Case $\boldsymbol{\alpha = 65°}$, $\boldsymbol{\beta = 55°}$, $\boldsymbol{e = 0}$ . . . 129
8.6 Conclusions . . . 131

III Conclusions and recommendations **133**

9 Conclusions **135**
9.1 Research questions . . . 135
9.2 Research objective . . . 136
9.3 Recommendations . . . 136

Bibliography **139**

Appendices **141**

A Non-linear numerical integration plots **143**
A.1 Case $\alpha = 59.9°$, $\beta = 15.1°$, $e = 0.3$ . . . 143
A.1.1 Perturbation in $r_3(0)$ . . . 143
A.1.2 Perturbation in $\gamma(0)$ . . . 144
A.1.3 Perturbation in $r_4(0)$ . . . 145
A.1.4 Perturbation in $\phi(0)$ . . . 146
A.1.5 Perturbation in $R_2(0)$ . . . 147
A.1.6 Perturbation in $R_3(0)$ . . . 148
A.1.7 Perturbation in $\Gamma(0)$ . . . 149
A.1.8 Perturbation in $R_4(0)$ . . . 150
A.1.9 Perturbation in $\Phi(0)$ . . . 151

A.2 Case $\alpha = 39.7°$, $\beta = 25.3°$, $e = 0.2$ 152
A.2.1 Perturbation in $r_3(0)$ 152
A.2.2 Perturbation in $\gamma(0)$. 153
A.2.3 Perturbation in $r_4(0)$ 154
A.2.4 Perturbation in $\phi(0)$ 155
A.2.5 Perturbation in $R_2(0)$ 156
A.2.6 Perturbation in $R_3(0)$ 157
A.2.7 Perturbation in $\Gamma(0)$. 158
A.2.8 Perturbation in $R_4(0)$ 159
A.2.9 Perturbation in $\Phi(0)$ 160

Nomenclature

List of abbreviations

Abbreviation	Meaning
CC	Central Configuration
c.o.m.	center of mass
RE	Relative Equilibrium
RK	Runge-Kutta

List of symbols

Greek symbol	Description	Units
α	Angular variable for description of kite configurations	rad
$\alpha(t)$	Complex scaling function of periodic solution	-
β	Angular variable for description of kite configurations	rad
Γ	Momentum conjugate to γ	$\mathrm{kg\,m^2\,s^{-1}}$
γ	Angle from $\boldsymbol{u}_2$ to $\boldsymbol{u}_3$	rad
$\gamma(t)$	Convex periodic solution	-
Δ	Determinant	-
Θ_i	Momentum conjugate to θ_i	$\mathrm{kg\,m^2\,s^{-1}}$
θ_i	Angle of the ith Jacobi variable $\boldsymbol{u}_i$	rad
$\theta(t)$	True anomaly	rad
κ_1	Distance between bodies 1 and 3	m
κ_2	Distance between bodies 1 and 4	m
κ_3	Distance between bodies 2 and 3	m
κ_4	Distance between bodies 2 and 4	m
κ_5	Distance between bodies 3 and 4	m
Λ	Proportionality constant relating length to mass units	-
λ	Eigenvalue	-
ξ_i	State variable of the decoupled linear system	-
ρ	Characteristic multiplier	-
Φ	Momentum conjugate to ϕ	$\mathrm{kg\,m^2\,s^{-1}}$
Ψ	Momentum conjugate to ψ	$\mathrm{kg\,m^2\,s^{-1}}$
ψ	Angle variable equal to θ_2	rad
ψ	Angle from $\boldsymbol{u}_3$ to $\boldsymbol{u}_4$	rad
ω	Angular momentum of Kepler solution	$\mathrm{kg\,m^2\,s^{-1}}$

Latin symbol	Description	Units
c_i	Initial value of r_i	m
c	Total angular momentum of periodic solution	$\mathrm{kg\,m^2\,s^{-1}}$
e	Eccentricity of Kepler solution	-
$\boldsymbol{G}_k$	Total linear momentum of the first k bodies	kg m/s
G	Universal gravitational constant	$\mathrm{N\,m^2\,kg^{-2}}$
H	Hamiltonian function	J
h	Total energy	J
J	Canonical matrix	-
$K_{x,y}$	Factor of a double derivative dependent on the geometry	-
$k_{l,m}$	Coefficient scaling a double derivative as part of a v coefficient	-
M_i	Reduced mass	kg
M_{ij}	Dimensionless mass parameters	-
m	Mass	kg
p	Canonical momentum variable	-
q	Canonical position variable	-
R_i	Momentum conjugate to r_i	kg m/s
r_i	Length of the Jacobi variable $\boldsymbol{u}_i$	m
$r(t)$	Scaling of Kepler solution	-
T	Period	s
T	Kinetic energy	J
U	Potential energy	J
$\boldsymbol{u}_i$	Jacobi variable to the i-th body	m
$\boldsymbol{v}_i$	Momentum conjugate to $\boldsymbol{u}_i$	kg m/s
$v_{i,j}$	Coefficient of V matrix	-
$W_{x,y}$	Factor of a double derivative dependent on the geometry	-
y	Initial distance between the symmetry line and one of the equal-mass bodies	m

Operator	Description
$\wedge$	Exterior product

1 Introduction

1.1. Background

The n-body problem is a classic problem of mathematics and physics, where the aim is to predict the motion of n point-masses, which attract each other by Newton's law of gravitation; all other forces are ignored. It is the basis for the entire discipline of celestial mechanics. Newton's second law together with Newton's law of gravitation results in a system of second-order ordinary differential equations

$$m_i \ddot{\boldsymbol{q}}_i = \sum_{j \neq i}^{n} \frac{G m_i m_j \left(\boldsymbol{q}_j - \boldsymbol{q}_i\right)}{\left\| \boldsymbol{q}_j - \boldsymbol{q}_i \right\|^3}, \quad i = 1, \ldots, n, \tag{1.1}$$

where m_i are the masses, $\boldsymbol{q}_i \in \mathbb{R}^3$ are the position vectors of objects i and G is the universal gravitational constant. Solving the n-body problem amounts to solving the initial-value problem: for given initial position and velocity vectors $\boldsymbol{q}_i(0)$, $\dot{\boldsymbol{q}}_i(0)$ find the vector function $\boldsymbol{q}(t)$ which provides the positions of the bodies in terms of the time t.

The problem dates back to Newton's *Philosophiæ Naturalis Principia Mathematica* [22] and has been tackled by a great many minds since then. Finding a general solution was of great importance, because that would allow an exact prediction of the evolution of planetary systems like our own or, in fact, any system of celestial objects. Newton started from the laws of Kepler and proceeded to prove that a body moving on an ellipse, parabola or hyperbola according to the second law of Kepler is attracted to the focus by the inverse square law [31]. Proving that two-body motion follows conic sections starting from the force law Eq. (1.1) back then was called the "inverse problem" [31]. The two-body "inverse problem" (complete solution of Eq. (1.1) for $n = 2$) was solved by Johann Bernoulli in 1710 [4, 6]. It took two centuries before an exact series solution was obtained for three bodies in 1912 by Karl Sundman and then another eight decades until Quidong Wang in 1991 provided a convergent power-series solution for the full n-body problem (excluding only collisions) [6, 25]. The series solutions of Sundman and Wang, even though convergent and exact, are impractical for actual calculations, "because the speed of convergence of the resulting solution is terribly slow. One has to sum, for example, an incredible number of terms, even for an approximate solution of first order in q, p, t." [25]. Hence, it seems that for three or more bodies we have to rely mostly on numerical methods or some special cases which allow a tractable analytical treatment.

A class of such special cases is called *central configurations*. These are characterized by the property that the resultant force on each body is directed to the center of mass of the configuration and directly proportional to the body's distance from it. Such configurations allow so-called *homographic* or *self-similar* solutions, where the bodies remain in the same geometry for all time as they move on conic sections about the center of mass [20]. For example, any arrangement of two bodies is a trivial central configuration, as in these cases the two bodies remain on a straight line as they move along conic sections. The first non-trivial central configurations were found by Euler in 1767 and consist of three bodies positioned on a straight line [7, 20]. Euler found that for any ordering of arbitrary three masses there exists a unique equivalence class of central collinear configurations (they may be scaled and rotated, but the ratios of the distances are unique). In fact, Moulton showed in 1910 that the same holds for any number of point-masses positioned on a line [20, 21].

The only other possible central configuration of three bodies was found by Lagrange in 1772 [13, 20]. It is the equilateral triangle configuration and holds for any masses. The bodies remain on the vertices of

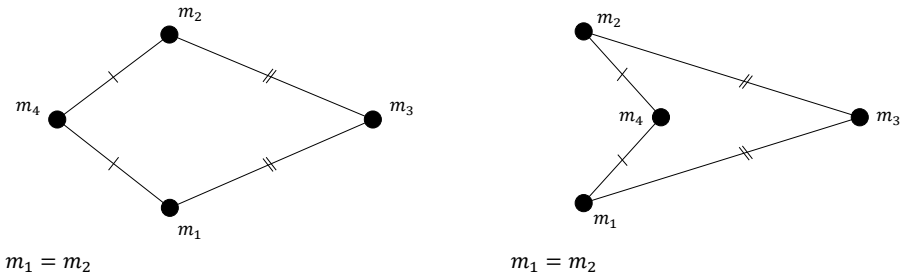

Figure 1.1: Convex and concave kite central configurations.

an equilateral triangle for all time, given correct initial velocities that set their orbits on appropriate conic sections.

Considering four-body central configurations, many more possibilities exist. Some well-known cases are the trapezoidal configurations [38], the square central configuration [16] and the equilateral triangle with a body in the middle [15]. The last two fall into a family of *kite central configurations*, where two bodies with equal mass are positioned symmetrically with respect to the axis on which the other two bodies lie. Such shapes are known as kite geometries and can be of two types: convex and concave. The convex kite contains no body in the interior of the triangle formed by the other three, such as the square, while in the concave case one body lies inside the triangle formed by the other three, such as the equilateral triangle configuration with one body in the center. The two types of kite central configurations are illustrated in Fig. 1.1.

The family of kite central configurations was given an elegant treatment recently in [40], where a description of all possible cases is given and explicit algebraic expressions for the masses which make the configurations central are derived in terms of the angles of the geometry. Further, in [34] the possibility of binary star systems occuring as any of the cases discussed in [40] is assessed and the mass-geometry relations are further simplified.

An essential question about such configurations is the question of their stability. For instance, all collinear configurations are known to be unstable, while the Lagrangian triangle configurations are linearly stable only for a dominant mass [20]. This work concerns the problem of stability of four-body kite central configurations, pictured in Fig. 1.1.

1.2. Applications

The applications of such results may be numerous. First of all, there is significant interest in central configurations and their properties from the pure mathematics perspective. The finiteness of the number of central configurations for a choice of positive masses is one of the unsolved questions in the set of 18 mathematical problems for the 21st century compiled by Stephen Smale [30], which shows significant interest in central configurations topics from the mathematical community. Contributing to the body of knowledge regarding this topic is an end in itself and hopefully the methods and results developed and generated here may be used in future explorations of this interesting niche of mathematics.

Considering the physical relevance, there are several possible scenarios of different scales where astronomical bodies could exist in a kite four-body central configuration. The research presented in this thesis, in turn, will reveal which of these scenarios can actually exist long-term and which would be inherently unstable, giving insight into the possible occurence of such systems in the actual universe.

1.2.1. One massive object

A qualitative distinction may be made for the cases where one of the four masses is much larger than the other three, as very often systems of celestial bodies exist in these kinds of hierarchical configurations. Then, one possibility corresponding to this scenario is a star with three planets orbiting around it with equal periods. Take, for instance, the mass m_3 to be the star. Then, it is possible that planets m_1 and m_2 are situated in one orbit, while planet m_4 is orbiting further away, making a convex configuration. It is even possible that the three planets m_1, m_2 and m_4 are of (approximately) the same mass, which would correspond to a situation where they all orbit the star m_3 along the same orbit, following each other. Even though we know these situations do not occur in the Solar System, if they are found to be stable, we could reasonably expect to find

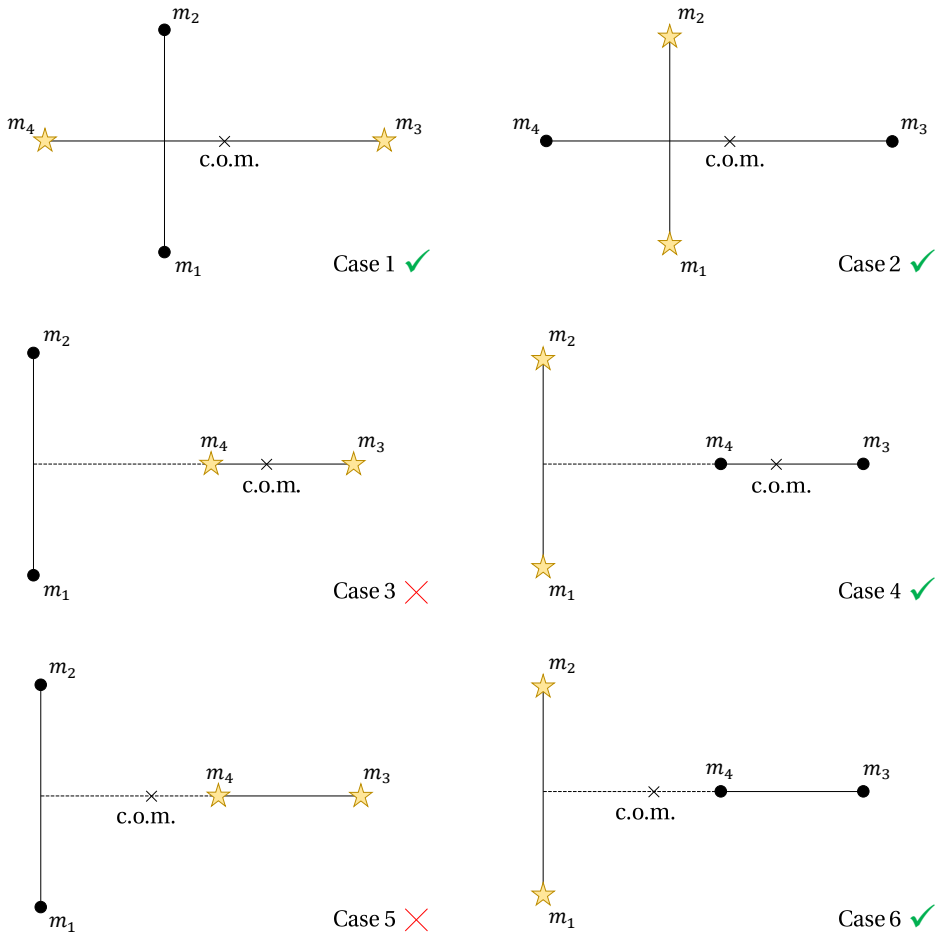

Figure 1.2: The possible kite central configurations for the mass constraints of binary star systems, as found in [34].

such configurations in exoplanetary systems.

Another scenario is the situation where the objects m_1, m_2 and m_4 are much less massive, such as asteroids, pebbles, dust, etc. The massive object m_3 can then either be a star or a planet. An example could be ring particles orbiting a planet in a "lumpy ring" [20], which may even be found in the Solar System, for instance, in the rings of Uranus or Neptune. This scenario corresponds to a limit case, where three masses are negligible compared to the fourth one.

1.2.2. Two massive objects

Another possibility is that of two massive objects and two smaller ones. An important and exciting example is that of a binary star system with two planets. The kite central configurations which such a system might assume were specifically singled out in [34]. It is assumed in that article that each star is at least 10 times more massive than any of the planets and that the stellar masses are within a factor of 10 of each other. According to [34] virtually every known binary star system satisfies these criteria. Using the mass constraints the plausible configuration space is heavily reduced and it is found that for the concave configurations, the stars would necessarily have to take the positions of the equal mass bodies, positioned equidistantly from the axis of symmetry, see Fig. 1.2. The reason cases 3 and 5 in Fig. 1.2 are impossible is because, in order to have a concave kite central configuration, only the center body m_4 can be 10 times more massive than the symmetric bodies m_1 and m_2 . Body m_3 is only allowed to be slightly more massive than the symmetric bodies, as can be seen in Figs. 2.6 and 2.8.

There is no lower limit imposed on the masses in [34], so these results apply just as well to two clusters of asteroids or dust near two planets or stars, such as the Trojan and Greek asteroids, situated at the vertices of Lagrangian equilateral triangles with Jupiter and Sun at the other two vertices.

1.2.3. Three or four massive objects

Multiple (three or more) star systems are a well-known phenomenon, in fact, "nearly half of all stars reside in multiple star systems" [24] and "approximately two thirds of the stars in our Galaxy exist as part of multi-stellar systems. <...> The number of quadruple stellar systems in the Galaxy is estimated to be of the order of thousands of millions." [2]. Given the extremely big number of such systems, it seems plausible that some of them might be arranged in a kite central configuration, either with three stars and one planet or a complete four-star kite configuration. This study will reveal whether such systems can be long-term stable and, if so, can help predict the masses or geometries of observed multiple star systems and/or help anticipate a planet in a kite configuration with the stars.

1.3. Research aim

Having introduced the context and relevance of the problem, we now explicitly define the goals of the present research project. To this end, we state a research objective and a research question with sub-questions.

The objective is the main reason for executing this work and the success of our efforts will depend on the extent that this objective is achieved.

Research objective. *Contribute to the body of knowledge of celestial mechanics through a stability assessment of the four-body kite central configuration family.*

To guide our efforts towards this goal, we have the main research question.

Research question. *What are the stability properties of kite central configurations of four bodies?*

The pursuit of an answer to this research question is motivated, for instance, by the following statement in [10]: "Whether the new four-body central configurations are stable is an interesting, unexplored question and is an inviting direction for future research", where the configurations being referred to are the kite CCs. This specific research gap is also referred to in [34]: "A proper stability analysis of planar four-body central configurations with two equal masses and an axis of symmetry connecting the unequal masses has not yet been carried out, and could represent a significant undertaking."

To give additional structure to our investigation we distinguish three research sub-questions, answering each of which will constitute a part of the solution to the main question and move us closer towards the research objective.

Sub-question 1. *Are the homographic solutions provided by the kite central configurations linearly stable?*

This sub-question is addressed in Part I. An attempt is made to take this treatment as far as possible using exact, analytical methods and only utilize the help of numerical techniques where an exact solution is no longer feasible.

Sub-question 2. *Do the homographic solutions provided by kite central configurations possess non-linear stability?*

An investigation into this sub-question is presented in Part II. We turn to a purely numerical approach for this question.

Sub-question 3. *Can kite central configurations occur in real astronomical systems?*

The answer to this sub-question is inferred from the two previous answers in Part III.

1.4. Structure

We now present an overview of the organization of the rest of this report. In the following chapter (Chapter 2), a description and parameterization of kite central configurations and their types are given. Moving on, in Chapter 3 we start the mathematical treatment of the dynamics: state variables are introduced and a series of coordinate transformations are performed to reduce the dimensions of the system of differential equations.

The question of linear stability is treated in Part I. First for the convex type of kite CCs in Chapter 4, then for the first concave kind in Chapter 5 and, finally, for kite CCs of the second concave kind in Chapter 6. The entire procedure to determine linear stability is developed and explained in Chapter 4, whereas Chapters 5 and 6 contain solely the application of said procedure to the concave cases.

Having dealt with the linear stability, Part II contains a numerical investigation into non-linear stability of the kite periodic solutions. We again divide the treatment into three parts, corresponding to each type of kite CC. Section 8.3 deals with the convex cases, while Sections 8.4 and 8.5 contain the non-linear stability results for the first and second concave cases, respectively.

Finally, in Part III we summarize, draw conclusions, assess the extent to which the objective has been achieved as well as give recommendations for future work.

2

Kite central configurations

In this chapter the kite central configurations are illustrated and the relationship between the geometry and the point masses is demonstrated. The description of the kite central configurations in [40] divides them into three categories: the convex case, first concave case and second concave case.

2.1. Convex configurations

The convex kite configurations are described by two angles α and β, as shown in Fig. 2.1, with [40]

$$\begin{aligned} \alpha &= 30° + 2\kappa \\ \beta &= 30° + \lambda\kappa \end{aligned} \quad \text{where} \quad \begin{aligned} 0 &\leq \kappa \leq 15° \\ -1 &\leq \lambda \leq 2 \end{aligned} \tag{2.1}$$

describing the domain shown in Fig. 2.2. The angle α is allowed to take on values from 30° to 60°, while β ($\leq \alpha$ because mirror images of the configurations are considered equivalent) can take on a range of values that is increasing with α (increasing κ), the widest range being $15° \leq \beta \leq 60°$ at $\alpha = 60°$ ($\kappa = 15°$). At this edge of the domain m_4 is infinitesimal, while the other three bodies sit on the vertices of an equilateral triangle.

Looking now at the leftmost edge of the green area in Fig. 2.2, we see that on this line $m_3 = m_4$, which represents the situation with two pairs of equal masses in a rhombus geometry. Going downwards, we reach the point 'S', which is a singularity where all mass is in bodies 3 and 4 (bodies on the symmetry axis) and infinitesimal masses 1 and 2 are situated at the triangular Lagrange points. Finally, the rightmost edge of the domain represents the limit case where β is minimal, all mass is in m_3, and the three infinitesimal masses are situated on a circle centered on m_3. This is the convex coorbital case, such as the "lumpy ring" situation mentioned in Section 1.2.1.

Using the mass relationships derived by [34] we obtain a range of convex kite central configurations as shown in Fig. 2.3. One can notice that increasing α tends to make the symmetric bodies 1 and 2 more massive,

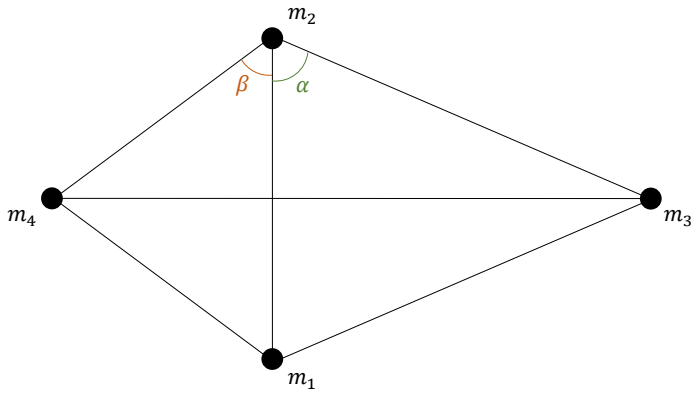

Figure 2.1: The parameterization of the convex kite configurations in [40].

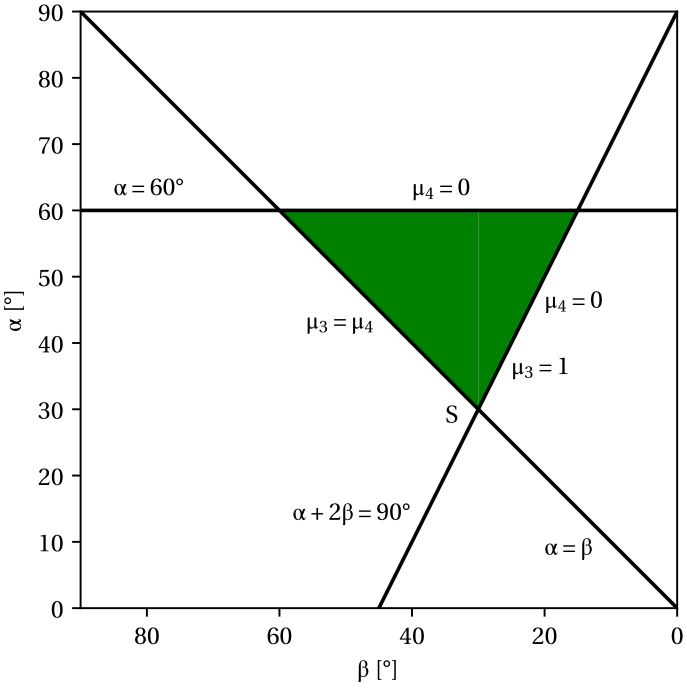

Figure 2.2: The region of possible convex kite central configurations parameterized in terms of α and β. $0 \le \mu_3 \le 1$ and $0 \le \mu_4 \le 1$ denote normalized masses m_3 and m_4, respectively, 1 being the total mass of the four-body configuration. 'S' denotes the singular case where all mass is in bodies 3 and 4 and infinitesimal masses 1 and 2 are situated at vertices of equilateral triangles, i.e. the fourth and fifth Lagrange points of masses 3 and 4. In this case bodies 3 and 4 can take on any masses as long as $\mu_3 + \mu_4 = 1$. Figure reproduced from [40], with body indices adjusted to be consistent with the present work.

while increasing β has the effect of equalizing the masses of bodies 3 and 4.

2.2. Concave configurations

2.2.1. First concave case

In the concave cases, one of the bodies is inside the triangle defined by the other three. In the first concave case this body (m_4) is behind the center of mass of the configuration marked by x in Fig. 2.4. The direction of the angle β is now changed, as seen in Fig. 2.4. The domain of the first concave configurations is given by [34]

$$\begin{aligned} \alpha &= 45° + \kappa \\ \beta &= \lambda\kappa \end{aligned} \quad \text{where} \quad \begin{aligned} 0 &\le \kappa \le 15° \\ 0 &\le \lambda \le 2 \end{aligned} \tag{2.2}$$

which describes the green triangle on the left in Fig. 2.5. The angle α can range between 45° and 60°, which is parameterized by κ, while the range of β increases with increasing α, reaching 0° to 30° at $\alpha = 60°$ ($\kappa = 15°$). At this edge of the domain (top bound on the left triangle in Fig. 2.5) masses 1, 2 and 3 sit on the vertices of an equilateral triangle, making a Lagrange triangle central configuration, while mass 4 is infinitesimal, sitting on the symmetry axis of this triangle. That is until $\beta = 30°$ is reached, where we get the singular case of m_4 in the center of mass of the Lagrange triangle taking on any mass value and the other three bodies on the vertices taking on arbitrary equal mass values.

The bottom edge of the triangle in Fig. 2.5 corresponds to the cases where β is maximum and all mass is in the interior body m_4. Then, the three infinitesimal masses are situated on a circle centered on m_4 and the configuration is concave coorbital (e.g. three satellites orbiting Earth in the same plane with equal periods and, thus, equal semi-major axes). Finally, the leftmost edge of the domain corresponds to collinear configurations, where $\beta = 0°$, $m_3 = 0$ and masses 4, 1 and 2 are positioned in a Euler central configuration on a straight line. Going from bottom to top, first all mass is in body 4 at $\alpha = 45°$, then m_4 decreases until it is zero at $\alpha = 60°$ and all mass is in the equal mass bodies 1 and 2.

A range of possible concave configurations of the first kind is shown in Fig. 2.6. In this case, increasing α seems to shrink the central body, while increasing β grows the central body.

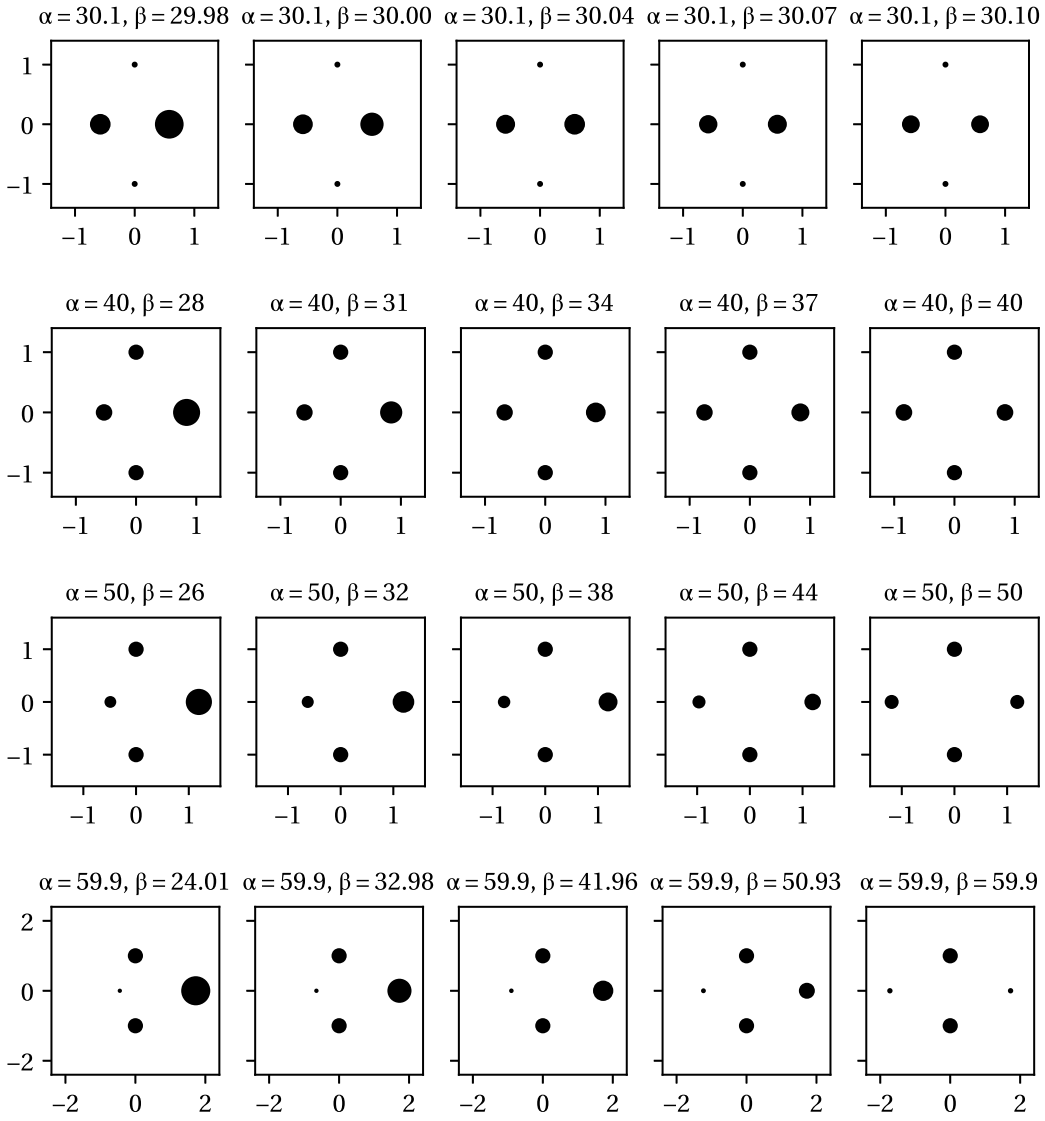

Figure 2.3: A range of possible convex kite central configurations. The radii of the bodies are proportional to cube roots of the masses, such that the volumes would be directly proportional to the masses. Unit radius is chosen for optimal viewing in each case and is not to scale. Unit distance is chosen to be the distance from the axis of symmetry to one of the equal masses. All angles are in degrees.

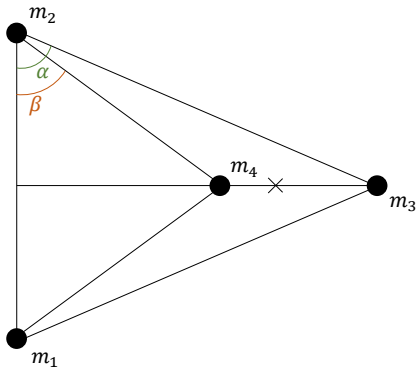

Figure 2.4: The parameterization of the first concave kite configurations in [40]. The center of mass is marked by x.

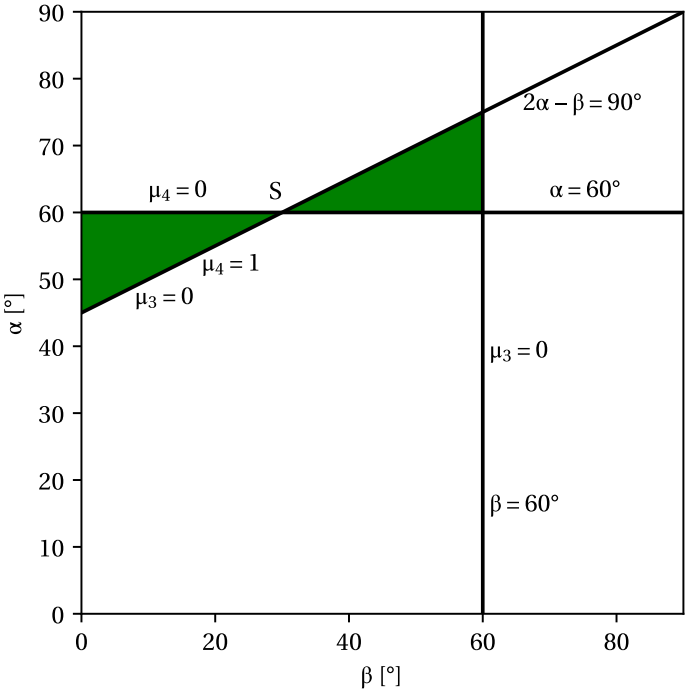

Figure 2.5: The region of possible concave kite central configurations parameterized in terms of α and β. $0 \le \mu_3 \le 1$ and $0 \le \mu_4 \le 1$ denote normalized masses m_3 and m_4, respectively, 1 being the total mass of the four-body configuration. 'S' denotes the singular case where body 4 is in the center of mass of an equilateral triangle made by the three remaining masses. In this case body 4 can take on any mass in the range $0 \le \mu_4 \le 1$ and the remaining masses are equal, with values in the range $0 \le \mu_3 \le 1$ [40]. Figure reproduced from [40], with body indices adjusted to be consistent with the present work.

2.2.2. Second concave case

The second concave case differs from the first as the interior body m_4 is now in front of the center of mass in Fig. 2.7. The second concave cases satisfies [34]

$$\begin{aligned} \alpha &= 60° + \kappa \\ \beta &= 60° + \lambda\,(15° - \kappa) \end{aligned} \quad \text{where} \quad \begin{aligned} 0 &\le \kappa \le 15° \\ -2 &\le \lambda \le 0 \end{aligned} \tag{2.3}$$

which corresponds to the green area on the right in Fig. 2.5. Now α ranges from 60° to 75°, again parameterized by κ. However, this time the range of permissible β angles decreases with increasing α. The range is maximum at $\alpha = 60°$, with $30° \le \beta \le 60°$.

Similarly to the first concave case, the bottom domain boundary at $\alpha = 60°$ in Fig. 2.5 marks the cases where m_4 is infinitesimal, placed on the symmetry axis of an equilateral triangle formed by the remaining three bodies. At the bottom right corner $\alpha = 60°$, $\beta = 60°$, we have that both m_3 and m_4 are infinitesimal and positioned on the same vertex of an equilateral triangle with bodies 1 and 2 of equal mass at the other vertices. Going up from this point, mass 3 is still infinitesimal, while mass 4 increases until all mass is in m_4 at the top most point $\alpha = 75°$, $\beta = 60°$. This point is part of the slope $2\alpha - \beta = 90°$, which, as in the first concave case, marks the coorbital concave configurations, where three bodies of equal infinitesimal mass orbit body 4 in the center.

A range of possible concave configurations of the second kind is shown in Fig. 2.8. Here we see an opposite pattern from the first concave case: increasing α makes the central body massive, while increasing β shrinks it.

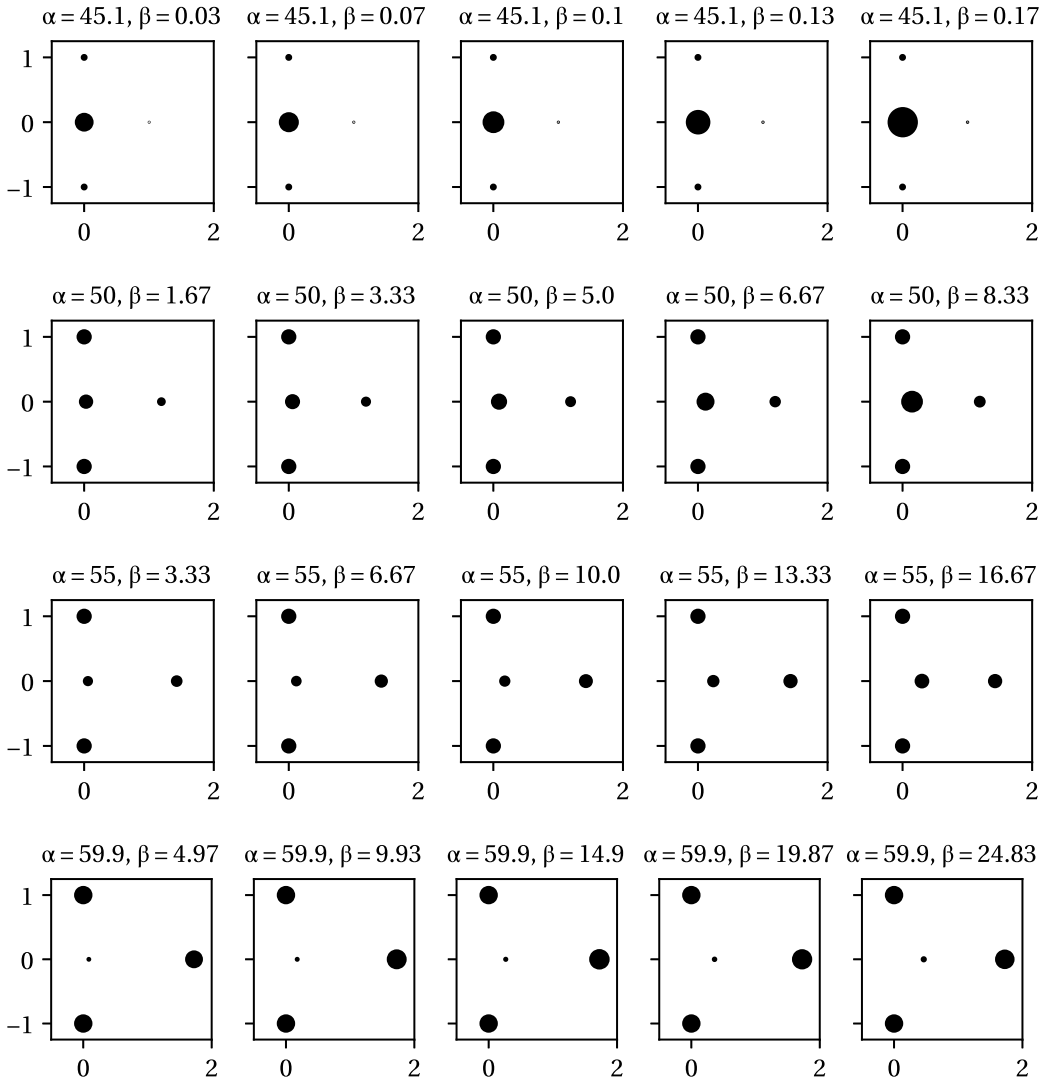

Figure 2.6: A range of possible concave kite central configurations of the first kind. The radii of the bodies are proportional to cube roots of the masses, such that the volumes would be directly proportional to the masses. Unit radius is chosen for optimal viewing in each case and is not to scale. Unit distance is chosen to be the distance from the axis of symmetry to one of the equal masses. All angles are in degrees.

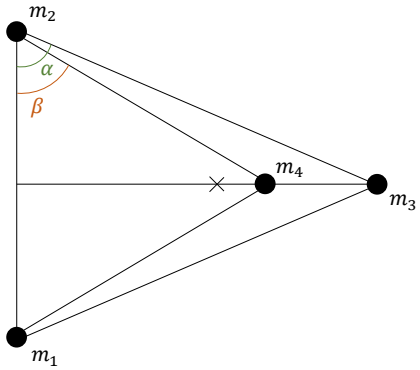

Figure 2.7: The parameterization of the second concave kite configurations in [40]. The center of mass is marked by x.

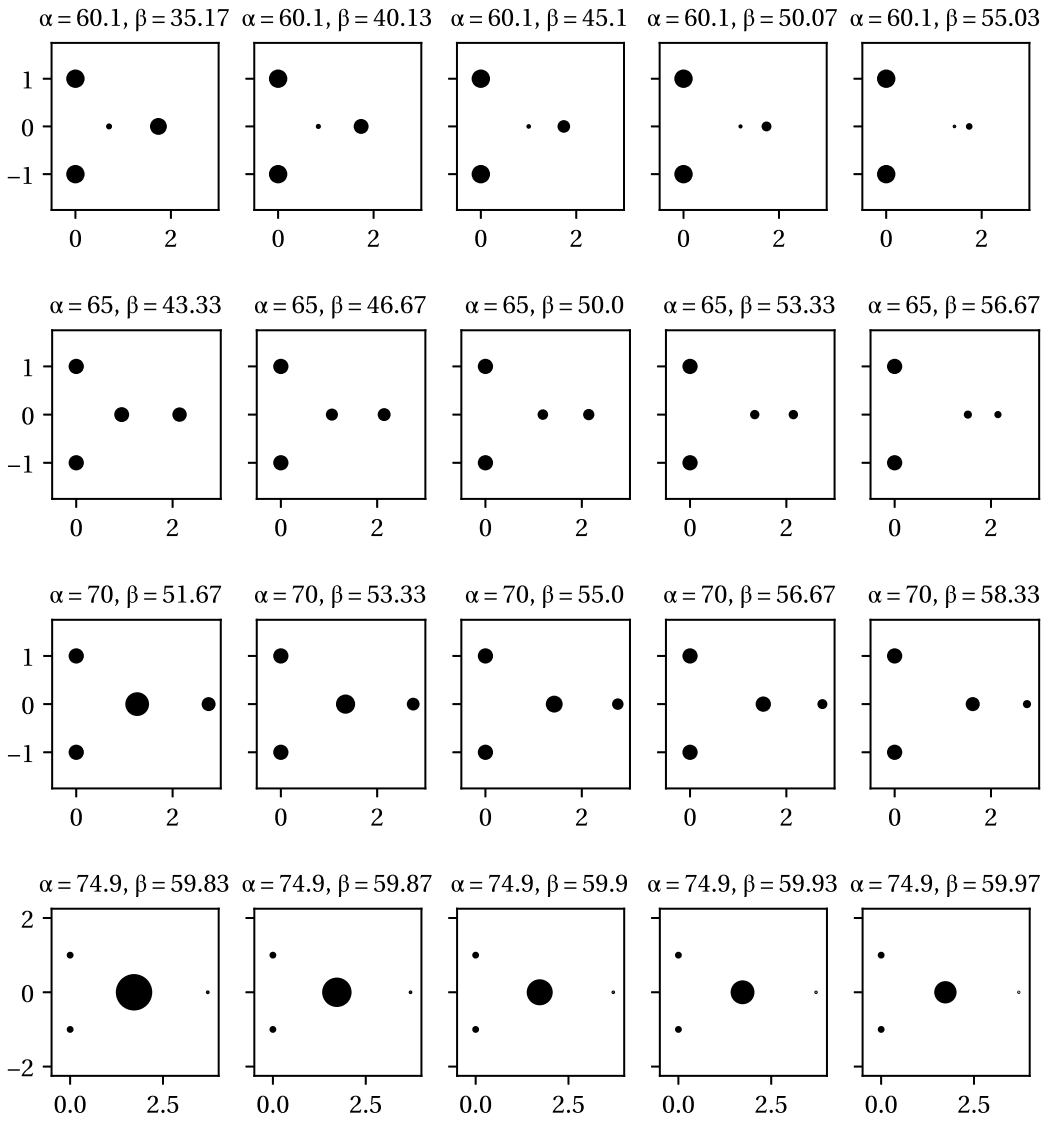

Figure 2.8: A range of possible concave kite central configurations of the second kind. The radii of the bodies are proportional to cube roots of the masses, such that the volumes would be directly proportional to the masses. Unit radius is chosen for optimal viewing in each case and is not to scale. Unit distance is chosen to be the distance from the axis of symmetry to one of the equal masses. All angles are in degrees.

3

Reduction of symmetries

The idea of this chapter is to simplify our dynamical system which is described by eight position variables q_i and eight momentum variables p_i by changing to coordinates where fewer state variables are needed to contain the essential information about the system. This can be achieved with the use of symmetries and first integrals. By *symmetry* we refer to the property of the dynamical system that the differential equations are unchanged under some transformation. For example, rotating the coordinate frame does not influence the dynamics of our four-body system and this is called rotational symmetry. By Noether's theorem, symmetries have conservation laws associated to them, which implies a first integral. In the case of the rotational symmetry we have the total angular momentum as the associated conserved quantity.

If we find coordinates where one position variable is the rotation angle of the system, this variable can be discarded, as its value is irrelevant for the dynamics. Similarly, when a momentum variable is equal to the total angular momentum of the system, we can set this variable to a constant, because the total angular momentum is conserved. Together, this would result in two less state variables, as all information about the evolution of the system is now contained in the rest of the variables. This is possible, because the symmetry allows us to eliminate information irrelevant to the stability and a first integral constrains the possible states the system can take to only the set where the conserved quantity is constant.

The planar n-body problem has two translational symmetries from the fact that we can vary the horizontal or vertical position of the whole system with no impact on the dynamics and one rotational symmetry from invariance of the system to rotation in the plane. Corresponding to these three symmetries are the three first integrals: linear momentum in two directions and angular momentum. In this chapter we use these to reduce our system from 16-dimensional one to a 10-dimensional one. This will set the stage for linearization of the system in Part I, where double partial derivatives with respect to each pair of variables have to be calculated. Linearizing the reduced system will require 55 of these double derivatives, instead of 136, were we to proceed with the 16-dimensional system. Further, the symmetries and integrals would show up as +1 eigenvalues of the monodromy matrix of the linearized system [27], as will be seen in Section 4.4. The reduction procedure gets rid of these trivial multipliers and only the essential multipliers that actually determine linear stability are left. Lastly, with further treatment in Part I we will remove two more dimensions, leading to an eight-dimensional system which allows an analytical computation of the eigenvalues. If we left any more dimensions than that, analytical computations would become unfeasible, which is why the dimensionality reduction of this chapter is instrumental for the analytical treatment of stability of kite central configurations.

3.1. Hamiltonian formulation

A mechanical system in which the forces are derived from a potential function can be described in a Hamiltonian formulation [17]. In this formulation, the equations of motion are derived from a Hamiltonian function $H(\boldsymbol{q},\boldsymbol{p})$ through Hamilton's equations [17]:

$$\dot{q}_i = \frac{\partial H}{\partial p_i} \qquad \dot{p}_i = -\frac{\partial H}{\partial q_i} \tag{3.1}$$

where $q_i(t)$ is the i-th position variable, $p_i(t)$ is the corresponding, or conjugate, momentum variable, $\boldsymbol{q}$ the vector containing all the position variables and $\boldsymbol{p}$ the vector containing all the momentum variables.

As we will see in this chapter, using the theory of Hamiltonian mechanics will allow us to perform multiple coordinate changes easily where all information about the dynamics is always completely contained in the Hamiltonian function.

The Hamiltonian function in this case is equal to the total energy of the mechanical system [17]:

$$H(\boldsymbol{q},\boldsymbol{p}) = T(\boldsymbol{p}) + U(\boldsymbol{q}) \tag{3.2}$$

where T is the kinetic energy and U is the potential energy. The Hamiltonian function H for a conservative dynamical system is independent of time, because energy is conserved.

The kinetic energy for the four-body problem is [17]

$$T = \frac{1}{2}\sum_{i=1}^{4} m_i \left\|\dot{\boldsymbol{q}}_i\right\|^2 = \frac{1}{2}\left(m_1\left\|\dot{\boldsymbol{q}}_1\right\|^2 + m_2\left\|\dot{\boldsymbol{q}}_2\right\|^2 + m_3\left\|\dot{\boldsymbol{q}}_3\right\|^2 + m_4\left\|\dot{\boldsymbol{q}}_4\right\|^2\right) \tag{3.3}$$

where $\boldsymbol{q}_i$ is the position vector to the i-th body from the barycenter in an inertial frame. Introducing the linear momentum of the i-th body $\boldsymbol{p}_i = m_i\dot{\boldsymbol{q}}_i$ we write the kinetic energy as

$$T = \frac{1}{2}\left(\frac{\|\boldsymbol{p}_1\|^2}{m_1} + \frac{\|\boldsymbol{p}_2\|^2}{m_2} + \frac{\|\boldsymbol{p}_3\|^2}{m_3} + \frac{\|\boldsymbol{p}_4\|^2}{m_4}\right) \tag{3.4}$$

The potential energy is given by [17]

$$U = -\sum_{1\le i<j\le 4}\frac{Gm_im_j}{\left\|\boldsymbol{q}_i-\boldsymbol{q}_j\right\|} = -\frac{Gm_1m_2}{\left\|\boldsymbol{q}_1-\boldsymbol{q}_2\right\|} - \frac{Gm_1m_3}{\left\|\boldsymbol{q}_1-\boldsymbol{q}_3\right\|} - \frac{Gm_1m_4}{\left\|\boldsymbol{q}_1-\boldsymbol{q}_4\right\|} - \frac{Gm_2m_3}{\left\|\boldsymbol{q}_2-\boldsymbol{q}_3\right\|} - \frac{Gm_2m_4}{\left\|\boldsymbol{q}_2-\boldsymbol{q}_4\right\|} - \frac{Gm_3m_4}{\left\|\boldsymbol{q}_3-\boldsymbol{q}_4\right\|} \tag{3.5}$$

Applying Eq. (3.1) to Eq. (3.2) with Eqs. (3.4) and (3.5) yields the familiar Eq. (1.1).

3.2. Canonical transformations

The vectors $\boldsymbol{q}$ and $\boldsymbol{p}$ together describe the state of the system completely. Meaning that, given a state of the system $(\boldsymbol{q},\boldsymbol{p})$, all the subsequent and previous states are uniquely determined by the system of differential equations (3.1). The set of all points $\{(\boldsymbol{q},\boldsymbol{p})\}$, that is, every possible combination of the position variables q_i and their conjugate momenta p_i is called *the phase space*. It represents the set of all possible states the system can take and therefore includes all possible solutions of Eq. (3.1). For a system with n degrees of freedom, there will be n position variables $q_1,\ldots,q_n$ and a single state will be described by $2n$ numbers $(q_1,\ldots,q_n,p_1,\ldots,p_n)$. Therefore, the dimension of the phase space of such a system will be $2n$. In our case, each body has two independent directions where it may move in the plane, so the system has 8 degrees of freedom, and the phase space is of dimension 16: $\{(\boldsymbol{q},\boldsymbol{p})\} = \mathbb{R}^{16}$.

Consider a transformation $g : \mathbb{R}^{2n} \to \mathbb{R}^{2n}$ which maps points in phase space to points in phase space. There is a special class of such transformations which preserve the differential 2-form [3]

$$\sum_i dp_i \wedge dq_i \tag{3.6}$$

and they are called *canonical transformations*; dp_i and dq_i are differentials [32]: for our purposes, simply functions that take a vector as an argument and output the p_i-th and q_i-th components respectively. By the "wedge product" operation $\wedge$ the two differentials combine as in Eq. (3.6) to produce a 2-form: a function that takes two vectors as arguments and outputs a single number. The 2-form in Eq. (3.6) operates the following way:

$$\sum_i dp_i \wedge dq_i(\boldsymbol{x},\boldsymbol{y}) = \sum_i X_iy_i - Y_ix_i \tag{3.7}$$

The property that this 2-form is preserved means that two vectors in phase space $\boldsymbol{x} = (x_1,\ldots,x_n,X_1,\ldots,X_n)$ and $\boldsymbol{y} = (y_1,\ldots,y_n,Y_1,\ldots,Y_n)$ transformed with a canonical transformation g to $g(\boldsymbol{x}) = \boldsymbol{a} = (a_1,\ldots,a_n,A_1,\ldots,A_n)$ and $g(\boldsymbol{y}) = \boldsymbol{b} = (b_1,\ldots,b_n,B_1,\ldots,B_n)$ will satisfy the following property

$$\begin{gathered}\sum_i dp_i \wedge dq_i(\boldsymbol{x},\boldsymbol{y}) = \sum_i dp_i \wedge dq_i(\boldsymbol{a},\boldsymbol{b}) = \\ \sum_i X_iy_i - Y_ix_i = \sum_i A_ib_i - B_ia_i\end{gathered} \tag{3.8}$$

As we will see, a very useful property of these transformations is that given a canonical transformation $\boldsymbol{Q} = \boldsymbol{Q}(\boldsymbol{q},\boldsymbol{p})$, $\boldsymbol{P} = \boldsymbol{P}(\boldsymbol{q},\boldsymbol{p})$ of variables $\boldsymbol{q}$ and $\boldsymbol{p}$ which satisfy Hamilton's equations Eq. (3.1) for a Hamiltonian function $H(\boldsymbol{q},\boldsymbol{p})$, we have that the new phase space coordinates $(\boldsymbol{Q},\boldsymbol{P})$ again satisfy Hamilton's equations [3]:

$$\dot{Q}_i = \frac{\partial K}{\partial P_i} \qquad \dot{P}_i = -\frac{\partial K}{\partial Q_i} \tag{3.9}$$

where K is the same Hamiltonian function expressed in new variables $K(\boldsymbol{Q},\boldsymbol{P}) = H(\boldsymbol{q},\boldsymbol{p})$.

Using canonical transformations, coordinates can be changed simply by substituting the transformation relations in the Hamiltonian function and the new equations of motion are then simply obtained through Eq. (3.1). Alternatively, one would have to change the coordinates directly in the equations of motion, which requires expressing the derivative terms in new variables and can quickly get cumbersome. Especially since we perform a series of coordinate changes in this chapter, not having to rewrite the equations of motion in each step really saves a lot of work.

More importantly, because of the nature of canonical coordinates and the Hamiltonian formulation, once we change to a coordinate corresponding to a symmetry, as explained at the start of this chapter, it no longer appears in the Hamiltonian function, because it has no influence on the dynamics. Such a coordinate is said to be *cyclic*. Then, the partial derivative of the Hamiltonian with respect to the cyclic variable is zero and we see immediately from Eq. (3.1) that the conjugate momentum to the cyclic variable is constant, because it is the first integral associated with the symmetry. So, using canonical transformations, we arrive at the reduction from the symmetry and the first integral simultaneously.

3.3. Jacobi coordinates

Jacobi coordinates are a standard tool in the analysis of the n-body problem. In conservative systems these coordinates allow reducing the dimensions of the problem by four by eliminating the information about the position of the center of mass and the total linear momentum from the equations. These coordinates start from a chosen body in the system and the first position vector then points to the next body. The next position vector starts from the center of mass of the previous bodies and points to the next chosen body of the system and so on. In this way only the relative positions of the bodies are described by the coordinates. In our case these coordinates are ideal, because, not only do we reduce the system's many dimensions, but also by choosing the two equal masses as the first bodies we obtain a very natural representation of the configuration with position vectors laying perpendicular and parallel to each other, as seen on the right in Figure 3.1. This will lead to simplifications later, when we plug in the periodic solution to the equations of motion.

The procedure to generate Jacobi coordinates is taken from [17]:

$$\begin{aligned} \boldsymbol{u}_k &= \boldsymbol{q}_k - \boldsymbol{g}_{k-1} \\ \boldsymbol{g}_k &= \frac{1}{\mu_k}\left(m_k\boldsymbol{q}_k + \mu_{k-1}\boldsymbol{g}_{k-1}\right) \\ \mu_k &= \mu_{k-1} + m_k \end{aligned} \tag{3.10}$$

with

$$\boldsymbol{g}_1 = \boldsymbol{q}_1 \qquad \mu_1 = m_1 \tag{3.11}$$

where $\boldsymbol{u}_k$ is the k-th Jacobi position vector, $\boldsymbol{g}_k$ is the center of mass of the first k bodies and μ_k is the total mass of the first k bodies. For the four-body problem this yields:

$$\begin{aligned} \mu_2 &= \mu_1 + m_2 = m_1 + m_2 \\ \boldsymbol{g}_2 &= \frac{m_2\boldsymbol{q}_2 + \mu_1\boldsymbol{g}_1}{\mu_2} = \frac{m_2\boldsymbol{q}_2 + m_1\boldsymbol{q}_1}{m_1+m_2} \\ \boldsymbol{u}_2 &= \boldsymbol{q}_2 - \boldsymbol{g}_1 = \boldsymbol{q}_2 - \boldsymbol{q}_1 \end{aligned} \tag{3.12}$$

$$\begin{aligned} \mu_3 &= \mu_2 + m_3 = m_1 + m_2 + m_3 \\ \boldsymbol{g}_3 &= \frac{m_3\boldsymbol{q}_3 + \mu_2\boldsymbol{g}_2}{\mu_3} = \frac{m_3\boldsymbol{q}_3 + (m_1+m_2)\,\frac{m_1\boldsymbol{q}_1+m_2\boldsymbol{q}_2}{m_1+m_2}}{m_1+m_2+m_3} = \frac{m_1\boldsymbol{q}_1 + m_2\boldsymbol{q}_2 + m_3\boldsymbol{q}_3}{m_1+m_2+m_3} \\ \boldsymbol{u}_3 &= \boldsymbol{q}_3 - \boldsymbol{g}_2 = \boldsymbol{q}_3 - \frac{m_1\boldsymbol{q}_1 + m_2\boldsymbol{q}_2}{m_1+m_2} \end{aligned} \tag{3.13}$$

$$\begin{aligned}\mu_4 &= \mu_3 + m_4 = m_1 + m_2 + m_3 + m_4\\ \boldsymbol{g}_4 &= \frac{m_4\boldsymbol{q}_4 + \mu_3\boldsymbol{g}_3}{\mu_4} = \frac{m_1\boldsymbol{q}_1 + m_2\boldsymbol{q}_2 + m_3\boldsymbol{q}_3 + m_4\boldsymbol{q}_4}{m_1 + m_2 + m_3 + m_4}\\ \boldsymbol{u}_4 &= \boldsymbol{q}_4 - \boldsymbol{g}_3 = \boldsymbol{q}_4 - \frac{m_1\boldsymbol{q}_1 + m_2\boldsymbol{q}_2 + m_3\boldsymbol{q}_3}{m_1 + m_2 + m_3}\end{aligned} \tag{3.14}$$

The conjugate momenta are generated using [17]:

$$\begin{aligned}\boldsymbol{v}_k &= \frac{\mu_{k-1}}{\mu_k}\boldsymbol{p}_k - \frac{m_k}{\mu_k}\boldsymbol{G}_{k-1}\\ \boldsymbol{G}_k &= \boldsymbol{p}_k + \boldsymbol{G}_{k-1}\end{aligned} \tag{3.15}$$

with

$$\boldsymbol{G}_1 = \boldsymbol{p}_1 \tag{3.16}$$

where $\boldsymbol{v}_k$ is the k-th Jacobi momentum variable and $\boldsymbol{G}_k$ is the total linear momentum of the first k bodies. In our case we get:

$$\begin{aligned}\boldsymbol{v}_2 &= \frac{\mu_1}{\mu_2}\boldsymbol{p}_2 - \frac{m_2}{\mu_2}\boldsymbol{G}_1 = \frac{m_1}{m_1 + m_2}\boldsymbol{p}_2 - \frac{m_2}{m_1 + m_2}\boldsymbol{p}_1\\ \boldsymbol{G}_2 &= \boldsymbol{p}_2 + \boldsymbol{G}_1 = \boldsymbol{p}_2 + \boldsymbol{p}_1\end{aligned} \tag{3.17}$$

$$\begin{aligned}\boldsymbol{v}_3 &= \frac{\mu_2}{\mu_3}\boldsymbol{p}_3 - \frac{m_3}{\mu_3}\boldsymbol{G}_2 = \frac{m_1 + m_2}{m_1 + m_2 + m_3}\boldsymbol{p}_3 - \frac{m_3}{m_1 + m_2 + m_3}\left(\boldsymbol{p}_1 + \boldsymbol{p}_2\right)\\ \boldsymbol{G}_3 &= \boldsymbol{p}_3 + \boldsymbol{G}_2 = \boldsymbol{p}_1 + \boldsymbol{p}_2 + \boldsymbol{p}_3\end{aligned} \tag{3.18}$$

$$\boldsymbol{v}_4 = \frac{\mu_3}{\mu_4}\boldsymbol{p}_4 - \frac{m_4}{\mu_4}\boldsymbol{G}_3 = \frac{m_1 + m_2 + m_3}{m_1 + m_2 + m_3 + m_4}\boldsymbol{p}_4 - \frac{m_4}{m_1 + m_2 + m_3 + m_4}\left(\boldsymbol{p}_1 + \boldsymbol{p}_2 + \boldsymbol{p}_3\right) \tag{3.19}$$

Recall that $\boldsymbol{p}_i = m_i\dot{\boldsymbol{q}}_i$ and notice that the mass factors in front of the $\boldsymbol{p}_i$ in Eqs. (3.17) to (3.19) multiply with the masses m_i such that each Jacobi momentum variable $\boldsymbol{v}_i$ represents the relative velocity of particle m_i with respect to the velocity of the center of mass of the previous $i-1$ particles, scaled by a mass ratio $M_i = m_i\frac{\mu_{i-1}}{\mu_i}$:

$$\boldsymbol{v}_2 = m_2\frac{m_1}{m_1 + m_2}\left(\dot{\boldsymbol{q}}_2 - \dot{\boldsymbol{q}}_1\right) = M_2\left(\dot{\boldsymbol{q}}_2 - \dot{\boldsymbol{q}}_1\right) \tag{3.20}$$

$$\boldsymbol{v}_3 = m_3\frac{m_1 + m_2}{m_1 + m_2 + m_3}\left(\dot{\boldsymbol{q}}_3 - \frac{m_1\dot{\boldsymbol{q}}_1 + m_2\dot{\boldsymbol{q}}_2}{m_1 + m_2}\right) = M_2\left(\dot{\boldsymbol{q}}_3 - \frac{m_1\dot{\boldsymbol{q}}_1 + m_2\dot{\boldsymbol{q}}_2}{m_1 + m_2}\right) \tag{3.21}$$

$$\boldsymbol{v}_4 = m_4\frac{m_1 + m_2 + m_3}{m_1 + m_2 + m_3 + m_4}\left(\dot{\boldsymbol{q}}_4 - \frac{m_1\dot{\boldsymbol{q}}_1 + m_2\dot{\boldsymbol{q}}_2 + m_3\dot{\boldsymbol{q}}_3}{m_1 + m_2 + m_3}\right) = M_4\left(\dot{\boldsymbol{q}}_4 - \frac{m_1\dot{\boldsymbol{q}}_1 + m_2\dot{\boldsymbol{q}}_2 + m_3\dot{\boldsymbol{q}}_3}{m_1 + m_2 + m_3}\right) \tag{3.22}$$

The mass factor $M_2 = \frac{m_1 m_2}{m_1 + m_2}$ is known as "reduced mass" in the context of the two-body problem [8], as it is the effective mass that one uses when writing the two-body problem as a "one-body" problem of the relative position vector between the bodies. What we have in our case is essentially three two-body systems, with the center of mass of the bodies in the first system, becoming the first body in the next and likewise the c.o.m. of the bodies in this system becoming the first body of the third system. Then, the M_i are just the "reduced masses" of the three respective systems and $\boldsymbol{v}_i$ are the linear momenta of these two-body systems.

To express the potential terms in Jacobi coordinates, the distances between the bodies need to be expressed in the new variables:

$$\begin{aligned}\frac{m_2}{m_1 + m_2}\boldsymbol{u}_2 + \boldsymbol{u}_3 &= \frac{m_2}{m_1 + m_2}\boldsymbol{q}_2 - \frac{m_2}{m_1 + m_2}\boldsymbol{q}_1 + \boldsymbol{q}_3 - \frac{m_1}{m_1 + m_2}\boldsymbol{q}_1 - \frac{m_2}{m_1 + m_2}\boldsymbol{q}_2 =\\ &= \boldsymbol{q}_3 - \frac{m_1 + m_2}{m_1 + m_2}\boldsymbol{q}_1 = \boldsymbol{q}_3 - \boldsymbol{q}_1\end{aligned} \tag{3.23}$$

$$\begin{aligned}\boldsymbol{u}_4 + \frac{m_2 + m_3}{m_1 + m_2 + m_3}\boldsymbol{u}_2 &= \boldsymbol{q}_4 - \frac{m_1\boldsymbol{q}_1 - m_2\boldsymbol{q}_2 - m_3\boldsymbol{q}_3 + (m_2 + m_3)\boldsymbol{q}_2 - (m_2 + m_3)\boldsymbol{q}_1}{m_1 + m_2 + m_3} =\\ &= \boldsymbol{q}_4 - \boldsymbol{q}_1 + \frac{m_3}{m_1 + m_2 + m_3}\left(\boldsymbol{q}_2 - \boldsymbol{q}_3\right)\end{aligned} \tag{3.24}$$

$$\boldsymbol{u}_3 - \frac{m_1}{m_1 + m_2}\boldsymbol{u}_2 = \boldsymbol{q}_3 + \frac{-m_1\boldsymbol{q}_1 - m_2\boldsymbol{q}_2 - m_1\boldsymbol{q}_2 + m_1\boldsymbol{q}_1}{m_1 + m_2} = \boldsymbol{q}_3 - \boldsymbol{q}_2 \tag{3.25}$$

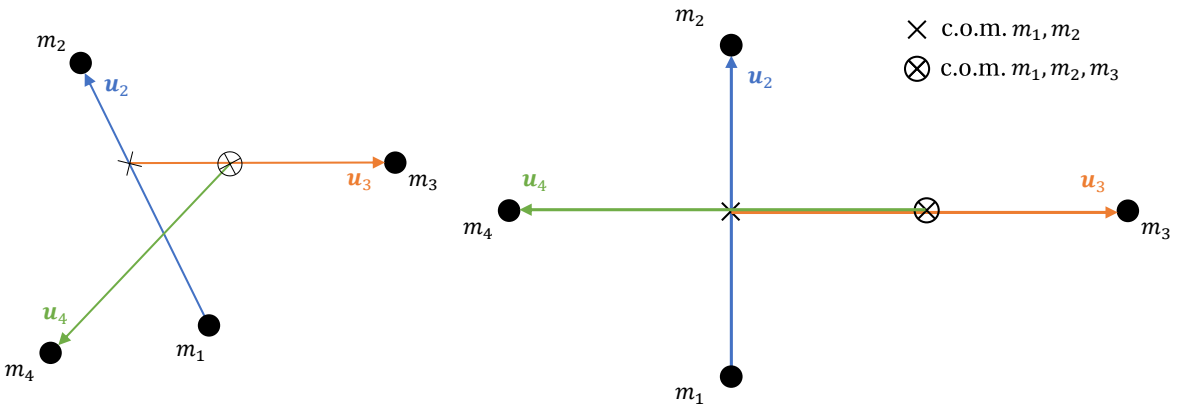

Figure 3.1: Jacobi coordinates for the general four-body problem on the left and for a four-body convex kite configuration on the right.

$$\begin{aligned}\boldsymbol{q}_4-\boldsymbol{q}_1 &= \boldsymbol{u}_4+\frac{m_2+m_3}{m_1+m_2+m_3}\boldsymbol{u}_2-\frac{m_3}{m_1+m_2+m_3}\left(\boldsymbol{q}_2-\boldsymbol{q}_3\right)= \\ &= \boldsymbol{u}_4+\frac{m_2+m_3}{m_1+m_2+m_3}\boldsymbol{u}_2+\frac{m_3}{m_1+m_2+m_3}\boldsymbol{u}_3-\frac{m_3}{m_1+m_2+m_3}\cdot\frac{m_1}{m_1+m_2}\boldsymbol{u}_2\end{aligned} \tag{3.26}$$

$$\begin{aligned}\boldsymbol{u}_4-\frac{m_1+m_3}{m_1+m_2+m_3}\boldsymbol{u}_2 &= \boldsymbol{q}_4+\frac{-m_1\boldsymbol{q}_1-m_2\boldsymbol{q}_2-m_3\boldsymbol{q}_3-(m_1+m_3)\,\boldsymbol{q}_2+(m_1+m_3)\,\boldsymbol{q}_1}{m_1+m_2+m_3}= \\ &= \boldsymbol{q}_4-\boldsymbol{q}_2+\frac{m_3}{m_1+m_2+m_3}\left(\boldsymbol{q}_1-\boldsymbol{q}_3\right)\end{aligned} \tag{3.27}$$

$$\begin{aligned}\boldsymbol{q}_4-\boldsymbol{q}_2 &= \boldsymbol{u}_4-\frac{m_1+m_3}{m_1+m_2+m_3}\boldsymbol{u}_2+\frac{m_3}{m_1+m_2+m_3}\left(\boldsymbol{q}_3-\boldsymbol{q}_1\right)= \\ &= \boldsymbol{u}_4-\frac{m_1+m_3}{m_1+m_2+m_3}\boldsymbol{u}_2+\frac{m_3}{m_1+m_2+m_3}\boldsymbol{u}_3+\frac{m_3}{m_1+m_2+m_3}\cdot\frac{m_2}{m_1+m_2}\boldsymbol{u}_2\end{aligned} \tag{3.28}$$

$$\begin{aligned}\frac{m_1+m_2}{m_1+m_2+m_3}\boldsymbol{u}_3-\boldsymbol{u}_4 &= \frac{(m_1+m_2)\,\boldsymbol{q}_3-m_1\boldsymbol{q}_1-m_2\boldsymbol{q}_2+m_1\boldsymbol{q}_1+m_2\boldsymbol{q}_2+m_3\boldsymbol{q}_3}{m_1+m_2+m_3}-\boldsymbol{q}_4= \\ &= \boldsymbol{q}_3-\boldsymbol{q}_4\end{aligned} \tag{3.29}$$

Introduce the mass parameters

$$\begin{aligned}M_{12}&=\frac{m_1}{m_1+m_2} & M_{22}&=\frac{m_2}{m_1+m_2} \\ M_{13}&=\frac{m_1}{m_1+m_2+m_3} & M_{23}&=\frac{m_2}{m_1+m_2+m_3} & M_{33}&=\frac{m_3}{m_1+m_2+m_3}\end{aligned} \tag{3.30}$$

Then, the distances become

$$\begin{aligned}\boldsymbol{q}_2-\boldsymbol{q}_1&=\boldsymbol{u}_2\\ \boldsymbol{q}_3-\boldsymbol{q}_1&=M_{22}\boldsymbol{u}_2+\boldsymbol{u}_3\\ \boldsymbol{q}_4-\boldsymbol{q}_1&=\boldsymbol{u}_4+\left(M_{23}+M_{33}-M_{33}M_{12}\right)\boldsymbol{u}_2+M_{33}\boldsymbol{u}_3\\ \boldsymbol{q}_3-\boldsymbol{q}_2&=\boldsymbol{u}_3-M_{12}\boldsymbol{u}_2\\ \boldsymbol{q}_4-\boldsymbol{q}_2&=\boldsymbol{u}_4+\left(M_{33}M_{22}-M_{13}-M_{33}\right)\boldsymbol{u}_2+M_{33}\boldsymbol{u}_3\\ \boldsymbol{q}_3-\boldsymbol{q}_4&=\left(M_{13}+M_{23}\right)\boldsymbol{u}_3-\boldsymbol{u}_4\end{aligned} \tag{3.31}$$

It can be checked using the definitions (3.15) that the following identity holds for $k=2,3,4$ [17]

$$\frac{\|\boldsymbol{G}_{k-1}\|^2}{2\mu_{k-1}}+\frac{\|\boldsymbol{p}_k\|^2}{2m_k}=\frac{\|\boldsymbol{G}_k\|^2}{2\mu_k}+\frac{\|\boldsymbol{v}_k\|^2}{2M_k} \tag{3.32}$$

Using Eq. (3.32) the kinetic energy can be expressed by [17]:

$$\begin{aligned} T = \sum_{k=1}^{4} \frac{\|\boldsymbol{p}_k\|^2}{2m_k} &= \frac{\|\boldsymbol{p}_1\|^2}{2m_1} - \frac{\|\boldsymbol{G}_1\|^2}{2\mu_1} + \frac{\|\boldsymbol{G}_2\|^2}{2\mu_2} + \frac{\|\boldsymbol{v}_2\|^2}{2M_2} - \frac{\|\boldsymbol{G}_2\|^2}{2\mu_2} + \frac{\|\boldsymbol{G}_3\|^2}{2\mu_3} + \frac{\|\boldsymbol{v}_3\|^2}{2M_3} - \frac{\|\boldsymbol{G}_3\|^2}{2\mu_3} + \frac{\|\boldsymbol{G}_4\|^2}{2\mu_4} + \frac{\|\boldsymbol{v}_4\|^2}{2M_4} \\ &= \frac{\|\boldsymbol{p}_1\|^2}{2m_1} - \frac{\|\boldsymbol{G}_1\|^2}{2\mu_1} + \frac{\|\boldsymbol{v}_2\|^2}{2M_2} + \frac{\|\boldsymbol{v}_3\|^2}{2M_3} + \frac{\|\boldsymbol{G}_4\|^2}{2\mu_4} + \frac{\|\boldsymbol{v}_4\|^2}{2M_4} \end{aligned} \tag{3.33}$$

Then, using Eqs. (3.11) and (3.16) we get

$$T = \frac{\|\boldsymbol{G}_4\|^2}{2\mu_4} + \sum_{k=2}^{4} \frac{\|\boldsymbol{v}_k\|^2}{2M_k} \tag{3.34}$$

Since the total linear momentum is conserved, $\boldsymbol{G_4}$ is a constant that influences the value of kinetic energy, but has no influence over the dynamics of the system. Therefore, we do not lose generality by setting the total linear momentum to zero $\boldsymbol{G}_4 = 0$ [17] (we set the center of mass to be stationary) to get

$$T = \sum_{k=2}^{4} \frac{\|\boldsymbol{v}_k\|^2}{2M_k} \tag{3.35}$$

Now introducing the following compound mass parameters for brevity of the expressions:

$$\begin{aligned} M_{c1} &= M_{23} + M_{33} - M_{33}M_{12} \\ M_{c2} &= M_{33}M_{22} - M_{13} - M_{33} \\ M_{c3} &= M_{13} + M_{23} \end{aligned} \tag{3.36}$$

we get that the Hamiltonian in terms of the Jacobian variables $\boldsymbol{u}_2$, $\boldsymbol{u}_3$, $\boldsymbol{u}_4$, $\boldsymbol{v}_2$, $\boldsymbol{v}_3$, $\boldsymbol{v}_4$ is

$$\begin{aligned} H = &\frac{\|\boldsymbol{v}_2\|^2}{2M_2} + \frac{\|\boldsymbol{v}_3\|^2}{2M_3} + \frac{\|\boldsymbol{v}_4\|^2}{2M_4} \\ &- \frac{Gm_1m_2}{\|\boldsymbol{u}_2\|} - \frac{Gm_1m_3}{\|M_{22}\boldsymbol{u}_2 + \boldsymbol{u}_3\|} - \frac{Gm_1m_4}{\|\boldsymbol{u}_4 + M_{c1}\boldsymbol{u}_2 + M_{33}\boldsymbol{u}_3\|} \\ &- \frac{Gm_2m_3}{\|\boldsymbol{u}_3 - M_{12}\boldsymbol{u}_2\|} - \frac{Gm_2m_4}{\|\boldsymbol{u}_4 + M_{c2}\boldsymbol{u}_2 + M_{33}\boldsymbol{u}_3\|} - \frac{Gm_3m_4}{\|M_{c3}\boldsymbol{u}_3 - \boldsymbol{u}_4\|} \end{aligned} \tag{3.37}$$

Clearly, we have six Jacobian variables, each of which has two components in $\mathbb{R}^2$, therefore the dimension of our system is 12. This is already significantly simplified from the 16-dimensional system we started with. It will especially become clear when linearizing how much labour we avoid by not carrying around unnecessary information.

3.4. Polar coordinates

Now we wish to reduce the system by two more dimensions using the rotational symmetry and angular momentum integral. Since the rotation of the system is naturally described by angles and their rates of change we first introduce polar coordinates, as shown in Figure 3.2.

$$\begin{aligned} u_{21} &= r_2\cos\theta_2 \qquad u_{22} = r_2\sin\theta_2 \\ u_{31} &= r_3\cos\theta_3 \qquad u_{32} = r_3\sin\theta_3 \\ u_{41} &= r_4\cos\theta_4 \qquad u_{42} = r_4\sin\theta_4 \end{aligned} \tag{3.38}$$

We use the generating function S_2, given in [17], to generate the conjugate momenta:

$$S_2 = v_{21}r_2\cos\theta_2 + v_{22}r_2\sin\theta_2 + v_{31}r_3\cos\theta_3 + v_{32}r_3\sin\theta_3 + v_{41}r_4\cos\theta_4 + v_{42}r_4\sin\theta_4 \tag{3.39}$$

$$\begin{aligned} R_2 &= \frac{\partial S_2}{\partial r_2} = v_{21}\cos\theta_2 + v_{22}\sin\theta_2 & R_3 &= \frac{\partial S_2}{\partial r_3} = v_{31}\cos\theta_3 + v_{32}\sin\theta_3 \\ \Theta_2 &= \frac{\partial S_2}{\partial \theta_2} = -v_{21}r_2\sin\theta_2 + v_{22}r_2\cos\theta_2 & \Theta_3 &= \frac{\partial S_2}{\partial \theta_3} = -v_{31}r_3\sin\theta_3 + v_{32}r_3\cos\theta_3 \\ R_4 &= \frac{\partial S_2}{\partial r_4} = v_{41}\cos\theta_4 + v_{42}\sin\theta_4 \\ \Theta_4 &= \frac{\partial S_2}{\partial \theta_4} = -v_{41}r_4\sin\theta_4 + v_{42}r_4\cos\theta_4 \end{aligned} \tag{3.40}$$

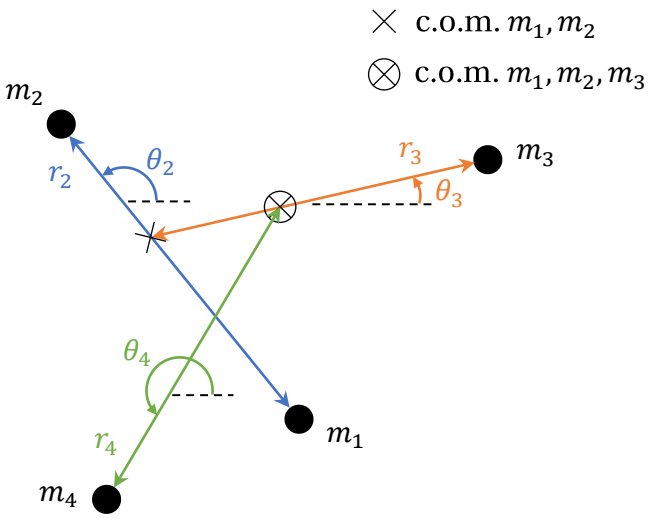

Figure 3.2: Polar coordinates.

We see that the conjugate momenta of the distance variables R_i are the components of $\boldsymbol{v}_i$ that change the magnitude of $\boldsymbol{u}_i$, in other words, they are proportional to the rate of change of the corresponding lengths r_i and have units of linear momentum. Meanwhile, the conjugate momenta of the angle variables Θ_i are the angular momenta of the three respective two-body problems associated to the three Jacobi variables (as explained in Section 3.3) and are proportional to the rate of change of the corresponding angles θ_i.

Rearranging we obtain:

$$\begin{aligned} v_{22} &= \frac{R_2 - v_{21}\cos\theta_2}{\sin\theta_2} \\ v_{21} &= v_{22}\frac{\cos\theta_2}{\sin\theta_2} - \frac{\Theta_2}{r_2\sin\theta_2} \end{aligned} \tag{3.41}$$

Solving the system:

$$\begin{aligned} v_{21} &= R_2\frac{\cos\theta_2}{\sin^2\theta_2} - v_{21}\frac{\cos^2\theta_2}{\sin^2\theta_2} - \frac{\Theta_2}{r_2\sin\theta_2} \\ \implies v_{21} &= R_2\cos\theta_2 - \frac{\Theta_2}{r_2}\sin\theta_2 \\ \implies v_{22} &= \frac{R_2}{\sin\theta_2} - R_2\frac{\cos^2\theta_2}{\sin\theta_2} + \frac{\Theta_2}{r_2}\cos\theta_2 = R_2\sin\theta_2 + \frac{\Theta_2}{r_2}\cos\theta_2 \end{aligned} \tag{3.42}$$

The rest of the momenta are obtained in the same way and only differ by indices:

$$\begin{aligned} v_{31} &= R_3\cos\theta_3 - \frac{\Theta_3}{r_3}\sin\theta_3 \qquad & v_{41} &= R_4\cos\theta_4 - \frac{\Theta_4}{r_4}\sin\theta_4 \\ v_{32} &= R_3\sin\theta_3 + \frac{\Theta_3}{r_3}\cos\theta_3 \qquad & v_{42} &= R_4\sin\theta_4 + \frac{\Theta_4}{r_4}\cos\theta_4 \end{aligned} \tag{3.43}$$

The kinetic terms then become:

$$\begin{aligned}\|\boldsymbol{v}_2\|^2 = v_{21}^2 + v_{22}^2 &= R_2^2\cos^2\theta_2 - 2R_2\cos\theta_2\frac{\Theta_2}{r_2}\sin\theta_2 + \frac{\Theta_2^2}{r_2^2}\sin^2\theta_2 + \\ &+ R_2^2\sin^2\theta_2 + 2R_2\sin\theta_2\frac{\Theta_2}{r_2}\cos\theta_2 + \frac{\Theta_2^2}{r_2^2}\cos^2\theta_2 = \\ &= R_2^2 + \frac{\Theta_2^2}{r_2^2} \\ \|\boldsymbol{v}_3\|^2 = v_{31}^2 + v_{32}^2 &= R_3^2 + \frac{\Theta_3^2}{r_3^2} \\ \|\boldsymbol{v}_4\|^2 = v_{41}^2 + v_{42}^2 &= R_4^2 + \frac{\Theta_4^2}{r_4^2}\end{aligned} \tag{3.44}$$

Similarly, the potential terms can be expressed in polar coordinates:

$$\|\boldsymbol{u}_2\| = \sqrt{u_{21}^2 + u_{22}^2} = \sqrt{r_2^2\cos^2\theta_2 + r_2^2\sin^2\theta_2} = r_2 \tag{3.45}$$

$$\begin{aligned}&\|M_{22}\boldsymbol{u}_2 + \boldsymbol{u}_3\| = \sqrt{(M_{22}u_{21} + u_{31})^2 + (M_{22}u_{22} + u_{32})^2} \\ &= \sqrt{M_{22}^2u_{21}^2 + 2M_{22}u_{21}u_{31} + u_{31}^2 + M_{22}^2u_{22}^2 + 2M_{22}u_{22}u_{32} + u_{32}^2} \\ &= \sqrt{M_{22}^2r_2^2\cos^2\theta_2 + 2M_{22}r_2\cos\theta_2 r_3\cos\theta_3 + r_3^2\cos^2\theta_3 + M_{22}^2r_2^2\sin^2\theta_2 + 2M_{22}r_2\sin\theta_2 r_3\sin\theta_3 + r_3^2\sin^2\theta_3} \\ &= \sqrt{M_{22}^2r_2^2 + 2M_{22}r_2r_3\cos(\theta_2-\theta_3) + r_3^2} \\ &= \kappa_1\end{aligned} \tag{3.46}$$

$$\begin{aligned}&\|\boldsymbol{u}_4 + M_{c1}\boldsymbol{u}_2 + M_{33}\boldsymbol{u}_3\| = \sqrt{(u_{41} + M_{c1}u_{21} + M_{33}u_{31})^2 + (u_{42} + M_{c1}u_{22} + M_{33}u_{32})^2} \\ &= \sqrt{\begin{aligned}&u_{41}^2 + M_{c1}u_{21}u_{41} + M_{33}u_{31}u_{41} + u_{41}M_{c1}u_{21} + M_{c1}^2u_{21}^2 + M_{33}u_{31}M_{c1}u_{21} \\ &+ u_{41}M_{33}u_{31} + M_{c1}u_{21}M_{33}u_{31} + M_{33}^2u_{31}^2 + u_{42}^2 + M_{c1}u_{22}u_{42} + M_{33}u_{32}u_{42} \\ &+ u_{42}M_{c1}u_{22} + M_{c1}^2u_{22}^2 + M_{33}u_{32}M_{c1}u_{22} + u_{42}M_{33}u_{32} + M_{c1}u_{22}M_{33}u_{32} + M_{33}^2u_{32}^2\end{aligned}} \\ &= \sqrt{\begin{aligned}&r_4^2 + M_{c1}^2r_2^2 + M_{33}^2r_3^2 + 2M_{c1}r_2\cos\theta_2 r_4\cos\theta_4 + 2M_{33}r_3\cos\theta_3 r_4\cos\theta_4 + 2M_{33}M_{c1}r_3\cos\theta_3 r_2\cos\theta_2 \\ &+2M_{c1}r_2\sin\theta_2 r_4\sin\theta_4 + 2M_{33}r_3\sin\theta_3 r_4\sin\theta_4 + 2M_{33}M_{c1}r_3\sin\theta_3 r_2\sin\theta_2\end{aligned}} \\ &= \sqrt{M_{c1}^2r_2^2 + M_{33}^2r_3^2 + r_4^2 + 2M_{c1}r_2r_4\cos(\theta_2-\theta_4) + 2M_{33}r_3r_4\cos(\theta_3-\theta_4) + 2M_{33}M_{c1}r_2r_3\cos(\theta_2-\theta_3)} \\ &= \kappa_2\end{aligned} \tag{3.47}$$

$$\|\boldsymbol{u}_3 - M_{12}\boldsymbol{u}_2\| = \sqrt{r_3^2 + M_{12}^2r_2^2 - 2M_{12}r_2r_3\cos(\theta_2-\theta_3)} = \kappa_3 \tag{3.48}$$

$$\|\boldsymbol{u}_4 + M_{c2}\boldsymbol{u}_2 + M_{33}\boldsymbol{u}_3\| =$$

$$= \sqrt{r_4^2 + M_{c2}^2r_2^2 + M_{33}r_3^2 + 2M_{c2}r_2r_4\cos(\theta_2-\theta_4) + 2M_{33}r_3r_4\cos(\theta_3-\theta_4) + 2M_{33}M_{c2}r_3r_2\cos(\theta_3-\theta_2)} \tag{3.49}$$

$$= \kappa_4$$

$$\|M_{c3}\boldsymbol{u}_3 - \boldsymbol{u}_4\| = \sqrt{M_{c3}^2r_3^2 + r_4^2 - 2M_{c3}r_3r_4\cos(\theta_3-\theta_4)} = \kappa_5 \tag{3.50}$$

Substituting all results into the Hamiltonian yields:

$$\begin{aligned}H = &\left(R_2^2 + \frac{\Theta_2^2}{r_2^2}\right)\frac{1}{2M_2} + \left(R_3^2 + \frac{\Theta_3^2}{r_3^2}\right)\frac{1}{2M_3} + \left(R_4^2 + \frac{\Theta_4^2}{r_4^2}\right)\frac{1}{2M_4} \\ &- \frac{Gm_1m_2}{r_2} - \frac{Gm_1m_3}{\kappa_1} - \frac{Gm_1m_4}{\kappa_2} \\ &- \frac{Gm_2m_3}{\kappa_3} - \frac{Gm_2m_4}{\kappa_4} - \frac{Gm_3m_4}{\kappa_5}\end{aligned} \tag{3.51}$$

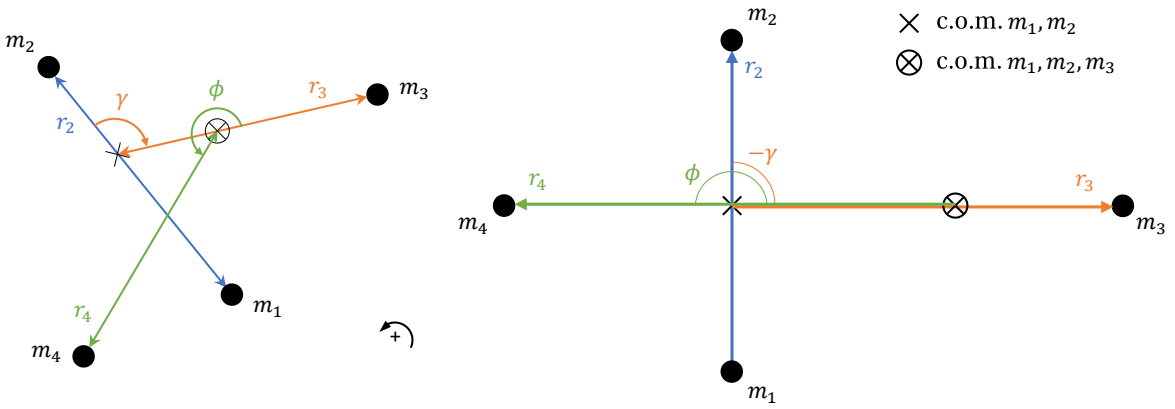

Figure 3.3: Polar coordinates with rotational symmetry eliminated for the general four-body problem on the left and for a four-body convex kite configuration on the right. The positive angle direction is counterclockwise. The angles in the left diagram have arrows to indicate sign, whereas the minus sign indicates that the magnitude of an angle is negative in the right diagram.

3.5. Eliminating angular momentum

The rotational symmetry and angular momentum are not eliminated yet. For that we wish to make the rotation of the whole system disappear from the Hamiltonian and to have a momentum variable correspond to the total angular momentum, which can then be set to a constant. However, the fact that the angles in the Hamiltonian (3.51) appear only in pairs tells us that a single angle coordinate, representing the absolute rotation of the system, does not influence the Hamiltonian. Hence, we make θ_2 a cyclic coordinate (a coordinate which does not appear in the Hamiltonian) and make the other coordinates represent the angular differences with the following canonical coordinate transformation

$$\Theta_2, \Theta_3, \Theta_4, \theta_2, \theta_3, \theta_4 \to \Psi, \Gamma, \Phi, \psi, \gamma, \phi$$

where we set (cf. Fig. 3.2 and Fig. 3.3)

$$\begin{aligned} \psi &= \theta_2 \\ \gamma &= \theta_3 - \theta_2 \\ \phi &= \theta_4 - \theta_3 \end{aligned} \tag{3.52}$$

From Figure 3.3 we see that $\psi = \theta_2$ describes the absolute rotation of the configuration with respect to some arbitrary datum, while γ and ϕ describe the relative rotations of the bodies with respect to one another.

Now, since we have one cyclic coordinate, by Noether's theorem [17] we know that its conjugate momentum must be a conserved quantity, which we anticipate to be the total angular momentum. The conjugate momenta are derived using the fact that a symplectic transformation must preserve the 2-form

$$\sum_i dp_i \wedge dq_i$$

Introduce two arbitrary vectors in the Θ_i, θ_i coordinate basis:

$$\begin{aligned} \boldsymbol{v}_1 &= (\Theta_{12}, \Theta_{13}, \Theta_{14}, \theta_{12}, \theta_{13}, \theta_{14}) \\ \boldsymbol{v}_2 &= (\Theta_{22}, \Theta_{23}, \Theta_{24}, \theta_{22}, \theta_{23}, \theta_{24}) \end{aligned}$$

which give

$$\begin{aligned} &dp_1 \wedge dq_1(\boldsymbol{v}_1, \boldsymbol{v}_2) + dp_2 \wedge dq_2(\boldsymbol{v}_1, \boldsymbol{v}_2) + dp_3 \wedge dq_3(\boldsymbol{v}_1, \boldsymbol{v}_2) = \\ &= (\Theta_{12}\theta_{22} - \Theta_{22}\theta_{12}) + (\Theta_{13}\theta_{23} - \Theta_{23}\theta_{13}) + (\Theta_{14}\theta_{24} - \Theta_{24}\theta_{14}) \end{aligned} \tag{3.53}$$

Now denote the transformed vectors, i.e. the same vectors in the new coordinate basis as

$$\begin{aligned} \boldsymbol{v}_1' &= \big(\Psi_1, \Gamma_1, \Phi_1, \psi_1, \gamma_1, \phi_1\big) = (\Psi_1, \Gamma_1, \Phi_1, \theta_{12}, \theta_{13} - \theta_{12}, \theta_{14} - \theta_{13}) \\ \boldsymbol{v}_2' &= \big(\Psi_2, \Gamma_2, \Phi_2, \psi_2, \gamma_2, \phi_2\big) = (\Psi_2, \Gamma_2, \Phi_2, \theta_{22}, \theta_{23} - \theta_{22}, \theta_{24} - \theta_{23}) \end{aligned}$$

which give

$$\begin{aligned} dp_1 \wedge dq_1(\boldsymbol{v}_1', \boldsymbol{v}_2') + dp_2 \wedge dq_2(\boldsymbol{v}_1', \boldsymbol{v}_2') + dp_3 \wedge dq_3(\boldsymbol{v}_1', \boldsymbol{v}_2') = \\ = (\Psi_1\theta_{22} - \Psi_2\theta_{12}) + (\Gamma_1(\theta_{23} - \theta_{22}) - \Gamma_2(\theta_{13} - \theta_{12})) + (\Phi_1(\theta_{24} - \theta_{23}) - \Phi_2(\theta_{14} - \theta_{13})) = \\ = \theta_{12}(-\Psi_2 + \Gamma_2) + \theta_{22}(\Psi_1 - \Gamma_1) + \theta_{13}(\Phi_2 - \Gamma_2) + \theta_{23}(\Gamma_1 - \Phi_1) + \theta_{14}(-\Phi_2) + \theta_{24}\Phi_1 = \\ = \theta_{12}(-\Theta_{22}) + \theta_{22}\Theta_{12} + \theta_{13}(-\Theta_{23}) + \theta_{23}\Theta_{13} + \theta_{14}(-\Theta_{24}) + \theta_{24}\Theta_{14} \end{aligned} \tag{3.54}$$

Therefore:

$$\begin{aligned} &\Psi_2 - \Gamma_2 = \Theta_{22} \\ &\Psi_1 - \Gamma_1 = \Theta_{12} \\ &\Gamma_2 - \Phi_2 = \Theta_{23} \\ &\Gamma_1 - \Phi_1 = \Theta_{13} \\ &\Phi_2 = \Theta_{24} \\ &\Phi_1 = \Theta_{14} \end{aligned} \implies \begin{aligned} &\Psi = \Theta_2 + \Gamma = \Theta_2 + \Theta_3 + \Theta_4 = c \\ &\Gamma = \Theta_3 + \Phi = \Theta_3 + \Theta_4 \\ &\Phi = \Theta_4 \end{aligned} \implies \begin{aligned} &\Theta_2 = c - \Gamma \\ &\Theta_3 = \Gamma - \Phi \\ &\Theta_4 = \Phi \end{aligned} \tag{3.55}$$

Clearly, Ψ is the total angular momentum, as expected, and is set to a constant value c.

Making the substitutions gives

$$\kappa_1 = \sqrt{M_{22}^2 r_2^2 + r_3^2 + 2M_{22} r_2 r_3 \cos(\gamma)} \tag{3.56}$$

$$\kappa_2 = \sqrt{M_{c1}^2 r_2^2 + M_{33}^2 r_3^2 + r_4^2 + 2M_{c1} r_2 r_4 \cos(\gamma + \phi) + 2M_{33} r_3 r_4 \cos(\phi) + 2M_{33} M_{c1} r_2 r_3 \cos(\gamma)} \tag{3.57}$$

$$\kappa_3 = \sqrt{M_{12}^2 r_2^2 + r_3^2 - 2M_{12} r_2 r_3 \cos(\gamma)} \tag{3.58}$$

$$\kappa_4 = \sqrt{M_{c2}^2 r_2^2 + M_{33}^2 r_3^2 + r_4^2 + 2M_{c2} r_2 r_4 \cos(\gamma + \phi) + 2M_{33} r_3 r_4 \cos(\phi) + 2M_{33} M_{c2} r_2 r_3 \cos(\gamma)} \tag{3.59}$$

$$\kappa_5 = \sqrt{M_{c3}^2 r_3^2 + r_4^2 - 2M_{c3} r_3 r_4 \cos(\phi)} \tag{3.60}$$

and the Hamiltonian becomes

$$\begin{aligned} H = &\left(R_2^2 + \frac{(c-\Gamma)^2}{r_2^2}\right)\frac{1}{2M_2} + \left(R_3^2 + \frac{(\Gamma-\Phi)^2}{r_3^2}\right)\frac{1}{2M_3} + \left(R_4^2 + \frac{\Phi^2}{r_4^2}\right)\frac{1}{2M_4} \\ &- \frac{Gm_1m_2}{r_2} - \frac{Gm_1m_3}{\kappa_1} - \frac{Gm_1m_4}{\kappa_2} \\ &- \frac{Gm_2m_3}{\kappa_3} - \frac{Gm_2m_4}{\kappa_4} - \frac{Gm_3m_4}{\kappa_5} \end{aligned} \tag{3.61}$$

Thus, the problem has been reduced from 16-dimensional to a 10-dimensional one with the variables r_2, r_3, γ, r_4, ϕ, R_2, R_3, Γ, R_4, Φ.

Applying Hamilton's equations yields:

$$\dot{r}_2 = \frac{\partial H}{\partial R_2} = \frac{R_2}{M_2} \quad \dot{r}_3 = \frac{\partial H}{\partial R_3} = \frac{R_3}{M_3} \quad \dot{r}_4 = \frac{\partial H}{\partial R_4} = \frac{R_4}{M_4} \tag{3.62}$$

$$\begin{aligned} \dot{R}_2 = -\frac{\partial H}{\partial r_2} = &\frac{(c-\Gamma)^2}{M_2}\frac{1}{r_2^3} - \frac{Gm_1m_2}{r_2^2} - \frac{Gm_1m_3}{\kappa_1^3}\left(M_{22}^2 r_2 + M_{22} r_3 \cos\gamma\right) \\ &- \frac{Gm_1m_4}{\kappa_2^3}\left(M_{c1}^2 r_2 + M_{c1} r_4 \cos(\gamma+\phi) + M_{33} M_{c1} r_3 \cos\gamma\right) - \frac{Gm_2m_3}{\kappa_3^3}\left(M_{12}^2 r_2 - M_{12} r_3 \cos\gamma\right) \\ &- \frac{Gm_2m_4}{\kappa_4^3}\left(M_{c2}^2 r_2 + M_{c2} r_4 \cos(\gamma+\phi) + M_{33} M_{c2} r_3 \cos\gamma\right) \end{aligned} \tag{3.63}$$

$$\begin{aligned} \dot{R}_3 = -\frac{\partial H}{\partial r_3} = &\frac{(\Gamma-\Phi)^2}{M_3}\frac{1}{r_3^3} - \frac{Gm_1m_3}{\kappa_1^3}\left(r_3 + M_{22} r_2 \cos\gamma\right) - \frac{Gm_1m_4}{\kappa_2^3}\left(M_{33}^2 r_3 + M_{33} r_4 \cos\phi + M_{33} M_{c1} r_2 \cos\gamma\right) \\ &- \frac{Gm_2m_3}{\kappa_3^3}\left(r_3 - M_{12} r_2 \cos\gamma\right) - \frac{Gm_2m_4}{\kappa_4^3}\left(M_{33}^2 r_3 + M_{33} r_4 \cos\phi + M_{33} M_{c2} r_2 \cos\gamma\right) \\ &- \frac{Gm_3m_4}{\kappa_5^3}\left(M_{c3}^2 r_3 - M_{c3} r_4 \cos\phi\right) \end{aligned} \tag{3.64}$$

$$\begin{aligned}\dot{R}_4 = -\frac{\partial H}{\partial r_4} = \frac{\Phi^2}{M_4}\frac{1}{r_4^3} - \frac{Gm_1m_4}{\kappa_2^3}\left(r_4 + M_{c1}r_2\cos(\gamma+\phi) + M_{33}r_3\cos\phi\right) \\ - \frac{Gm_2m_4}{\kappa_4^3}\left(r_4 + M_{c2}r_2\cos(\gamma+\phi) + M_{33}r_3\cos\phi\right) - \frac{Gm_3m_4}{\kappa_5^3}\left(r_4 - M_{c3}r_3\cos\phi\right)\end{aligned} \tag{3.65}$$

And for the angular variables:

$$\dot{\gamma} = \frac{\partial H}{\partial \Gamma} = \frac{\Gamma - c}{M_2 r_2^2} + \frac{\Gamma - \Phi}{M_3 r_3^2} \quad \dot{\phi} = \frac{\partial H}{\partial \Phi} = \frac{\Phi - \Gamma}{M_3 r_3^2} + \frac{\Phi}{M_4 r_4^2} \tag{3.66}$$

$$\begin{aligned}\dot{\Gamma} = -\frac{\partial H}{\partial \gamma} =& \frac{Gm_1m_3}{\kappa_1^3}M_{22}r_2r_3\sin\gamma + \frac{Gm_1m_4}{\kappa_2^3}\left(M_{c1}r_2r_4\sin(\gamma+\phi) + M_{33}M_{c1}r_2r_3\sin\gamma\right) \\ & - \frac{Gm_2m_3}{\kappa_3^3}M_{12}r_2r_3\sin\gamma + \frac{Gm_2m_4}{\kappa_4^3}\left(M_{c2}r_2r_4\sin(\gamma+\phi) + M_{33}M_{c2}r_2r_3\sin\gamma\right)\end{aligned} \tag{3.67}$$

$$\begin{aligned}\dot{\Phi} = -\frac{\partial H}{\partial \phi} =& \frac{Gm_1m_4}{\kappa_2^3}\left(M_{c1}r_2r_4\sin(\gamma+\phi) + M_{33}r_3r_4\sin\phi\right) \\ & + \frac{Gm_2m_4}{\kappa_4^3}\left(M_{c2}r_2r_4\sin(\gamma+\phi) + M_{33}r_3r_4\sin\phi\right) - \frac{Gm_3m_4}{\kappa_5^3}M_{c3}r_3r_4\sin\phi\end{aligned} \tag{3.68}$$

Note that $\frac{(c-\Gamma)^2}{M_2}\frac{1}{r_2^3}$, $\frac{(\Gamma-\Phi)^2}{M_3}\frac{1}{r_3^3}$ and $\frac{\Phi^2}{M_4}\frac{1}{r_4^3}$ in Eqs. (3.63) to (3.65) are centrifugal force terms, arising because of the rotating reference frame:

$$\frac{(c-\Gamma)^2}{M_2}\frac{1}{r_2^3} = \frac{\Theta_2^2}{M_2}\frac{1}{r_2^3} = \frac{\left(M_2r_2^2\dot{\theta}_2\right)^2}{M_2r_2^3} = M_2r_2\dot{\theta}_2^2 \tag{3.69}$$

$$\frac{(\Gamma-\Phi)^2}{M_3}\frac{1}{r_3^3} = \frac{\Theta_3^2}{M_3}\frac{1}{r_3^3} = \frac{\left(M_3r_3^2\dot{\theta}_3\right)^2}{M_3r_3^3} = M_3r_3\dot{\theta}_3^2 \tag{3.70}$$

$$\frac{\Phi^2}{M_4}\frac{1}{r_4^3} = \frac{\Theta_4^2}{M_4}\frac{1}{r_4^3} = \frac{\left(M_4r_4^2\dot{\theta}_4\right)^2}{M_4r_4^3} = M_4r_4\dot{\theta}_4^2 \tag{3.71}$$

where we used the definitions Eq. (3.55) and the fact that we can express the angular momenta of each two-body problem Θ_i, (as discussed in Section 3.4) in terms of the angular velocities and moments of inertia, which, in turn, can be expressed using the reduced masses of each two-body problem (as introduced in Section 3.3): $\Theta_i = M_i r_i^2 \dot{\theta}_i$.

3.6. Further elimination

It is possible to reduce the equations of motion further. Since the total energy is constant, H = constant = h, the independent variable can be changed from time t to one of the state variables $r_2, r_3, \gamma, r_4, \phi, R_2, R_3, \Gamma, R_4, \Phi$. Suppose we would like to make r_2 the new independent variable. Then, its conjugate momentum, R_2, becomes the new Hamiltonian function [23]:

$$R_2 = K(h, r_2, r_3, \gamma, r_4, \phi, R_3, \Gamma, R_4, \Phi) \tag{3.72}$$

where $K = R_2$ is the new Hamiltonian function and r_2 is the new independent variable. In this way, one more state variable can be eliminated. Note that this Hamiltonian is no longer autonomous, nor is it equal to the total energy [23], as its value now depends on the independent variable r_2 and is no longer constant. Any other state variable could have been chosen as the new Hamiltonian, however, explicit expressions are easy to get only for the momentum variables, since they appear only once as squared terms in H. Each position variable appears multiple times under square roots in the denominator, which would be very difficult to get an explicit expression in the form of Equation 3.72. Thus, our best bet is to make one of the momentum

variables the new Hamiltonian. For $R_2 = K$ we get:

$$K = R_2 = \pm \sqrt{\begin{array}{l} 2M_2 h - \dfrac{(c-\Gamma)^2}{r_2^2} - \dfrac{M_2}{M_3}\left(R_3^2 + \dfrac{(\Gamma-\Phi)^2}{r_3^2}\right) - \dfrac{M_2}{M_4}\left(R_4^2 + \dfrac{\Phi^2}{r_4^2}\right) \\ +2\dfrac{Gm_1m_2M_2}{r_2} + 2\dfrac{Gm_1m_3M_2}{\kappa_1} + 2\dfrac{Gm_1m_4M_2}{\kappa_2} + 2\dfrac{Gm_2m_3M_2}{\kappa_3} + 2\dfrac{Gm_2m_4M_2}{\kappa_4} + 2\dfrac{Gm_3m_4M_2}{\kappa_5} \end{array}} \tag{3.73}$$

We notice immediately that K can take on two values, a positive and a negative one, which correspond to the two directions of time, since time has been eliminated and the dynamics do not change with the direction of time for a conservative system. The equations of motion are then obtained from Hamilton's equations:

$$\begin{array}{ll} \dfrac{dr_3}{dr_2} = \dfrac{\partial K}{\partial R_3} & \dfrac{dR_3}{dr_2} = -\dfrac{\partial K}{\partial r_3} \\ \dfrac{dr_4}{dr_2} = \dfrac{\partial K}{\partial R_4} & \dfrac{dR_4}{dr_2} = -\dfrac{\partial K}{\partial r_4} \\ \dfrac{d\phi}{dr_2} = \dfrac{\partial K}{\partial \Phi} & \dfrac{d\Phi}{dr_2} = -\dfrac{\partial K}{\partial \phi} \\ \dfrac{d\gamma}{dr_2} = \dfrac{\partial K}{\partial \Gamma} & \dfrac{d\Gamma}{dr_2} = -\dfrac{\partial K}{\partial \gamma} \end{array} \tag{3.74}$$

The fact that the expression for K is entirely under a square root means that each first derivative of the equations of motion is going to have a $\frac{1}{2K}$ factor in front. This becomes a major inconvenience when we attempt to linearize the system, because every state variable now appears in every first derivative under K. This causes all second derivatives to be non-zero. Thus, even though there are two variables less in this reduced formulation, linearizing this system would be much more computationally heavy than the previous formulation and we will continue with time as the independent variable and a four-body system still described by 10 parameters.

I

Linear stability

4

Convex cases

In this chapter we investigate the stability of one subset of kite configurations: the convex cases. An attempt is made to take this assessment as far as possible with analytical techniques. To that aim, we linearize the equations of motion, so that the theory of Floquet can be applied and linear stability can be determined. The linearized system is evaluated at the periodic solution, so that the linear equations describe the perturbations from the central configuration. The procedure we follow closely resembles the one followed in [27] for linear stability determination of circular and eccentric three body Lagrange triangle periodic solutions. Before proceeding, it might be worth mentioning that this chapter includes a fair share of lenghty and at times somewhat tedious computations, however we feel they are quite fundamental for the understanding of our mathematical model and, therefore, they are left in the text instead of an appendix.

4.1. Periodic solution

For describing the periodic solution corresponding to a central configuration we identify the plane $\mathbb{R}^2$ with the complex plane $\mathbb{C}$. Then, for a central configuration we require:

$$q_i(t) = \alpha(t) z_i \tag{4.1}$$

where $q_i \in \mathbb{C}$ is the inertial position of the i-th body, $\alpha(t) \in \mathbb{C}$ is a scaling factor and $z_i \in \mathbb{C}$ is the initial position of the i-th body. Since multiplying a complex number by another complex number is equivalent to a scaling and a rotation in the complex plane, this equation says that at any time, the positions of all bodies can be obtained by applying the same scaling and rotation to the initial positions, since the geometry is required to stay the same in a central configuration. Substituting this constraint into the Newtonian equations of motion

$$\ddot{q}_i = \sum_{i \neq j} \frac{G m_j \left(q_j - q_i\right)}{\left\| q_j - q_i \right\|^3} \tag{4.2}$$

gives

$$\ddot{\alpha} |\alpha|^3 \alpha^{-1} z_i = \sum_{i \neq j} \frac{G m_j \left(z_j - z_i\right)}{\left\| z_j - z_i \right\|^3} \tag{4.3}$$

Because all z_i are constants, so must be the term on the left hand side:

$$\ddot{\alpha} |\alpha|^3 \alpha^{-1} = \text{constant} = G\Lambda \tag{4.4}$$

where Λ is a proportionality constant, depending on the masses and geometry of the configuration. Then we have the conditions on initial positions to have a central configuration:

$$\Lambda z_i = \sum_{i \neq j} \frac{m_j \left(z_j - z_i\right)}{\left\| z_j - z_i \right\|^3} \tag{4.5}$$

This means that in a central configuration the net acceleration on each body has to be directly proportional to the body's distance from the barycenter and directed towards the barycenter. Hence the name "central

configuration". Rearranging Equation 4.4 we obtain

$$\ddot{\alpha} = \frac{G\Lambda\alpha}{|\alpha|^3} \tag{4.6}$$

Note that the solutions of Equation 4.6 are simply the Kepler orbits described by [36]

$$\begin{aligned} r(t) &= -\frac{\omega^2/G\Lambda}{1+e\cos\theta(t)} \\ \dot{\theta}(t) &= \frac{\omega}{r^2(t)}, \qquad \theta(0)=0 \end{aligned} \tag{4.7}$$

where r is the magnitude of α and θ is the angle from the real axis. We choose the argument of perihelion and initial true anomaly as zero. The period is obtained from Kepler's third law [36]:

$$T = 2\pi\sqrt{\frac{a^3}{-G\Lambda}} = 2\pi\sqrt{a^3} \tag{4.8}$$

where $-G\Lambda$ is the gravitational parameter and a is the semi-major axis of the orbit, given by [36]:

$$a = \frac{\omega^2/-G\Lambda}{1-e^2} \tag{4.9}$$

For simplicity of expressions we set the proportionality constant $\Lambda = -1/G$ such that $-G\Lambda = 1$. This simply fixes the scale of the configuration in such a way that Eq. (4.5) holds. The semi-major axis then becomes

$$a = \frac{\omega^2}{1-e^2}, \tag{4.10}$$

which in turn gives for the period

$$T = 2\pi\frac{\omega^3}{\left(1-e^2\right)^{\frac{3}{2}}}. \tag{4.11}$$

The complex variables are then

$$\begin{aligned} \alpha(t) &= r(t)e^{i\theta(t)} \\ z_i &= |z_i|\,e^{i\eta_i} \end{aligned} \tag{4.12}$$

where η_i is the angle of the i-th body from the real axis. Then, the position of the i-th body in time is described by:

$$q_i(t) = \alpha(t)z_i = r(t)\,|z_i|\,e^{i(\theta(t)+\eta_i)} \tag{4.13}$$

or, turning back to the plane $\mathbb{R}^2$ again:

$$\boldsymbol{q}_i = r(t)\,\|\boldsymbol{z}_i\| \begin{bmatrix} \cos(\theta(t)+\eta_i) \\ \sin(\theta(t)+\eta_i) \end{bmatrix} \tag{4.14}$$

4.2. Convex case

Here, we introduce the common mass of the kite central configurations:

$$m_1 = m_2 = m \tag{4.15}$$

The proportionality constant is given by [40]:

$$\Lambda = -\frac{m_3}{d_1^3} - \frac{m_4}{d_2^3} - \frac{1}{4}\frac{m}{y^3} \tag{4.16}$$

Since we set $\Lambda G = -1$, then

$$\frac{-1}{G} = -\frac{m_3}{d_1^3} - \frac{m_4}{d_2^3} - \frac{1}{4}\frac{m}{y^3} \tag{4.17}$$

$$r(t) = \frac{\omega^2}{1+e\cos\theta(t)} \tag{4.18}$$

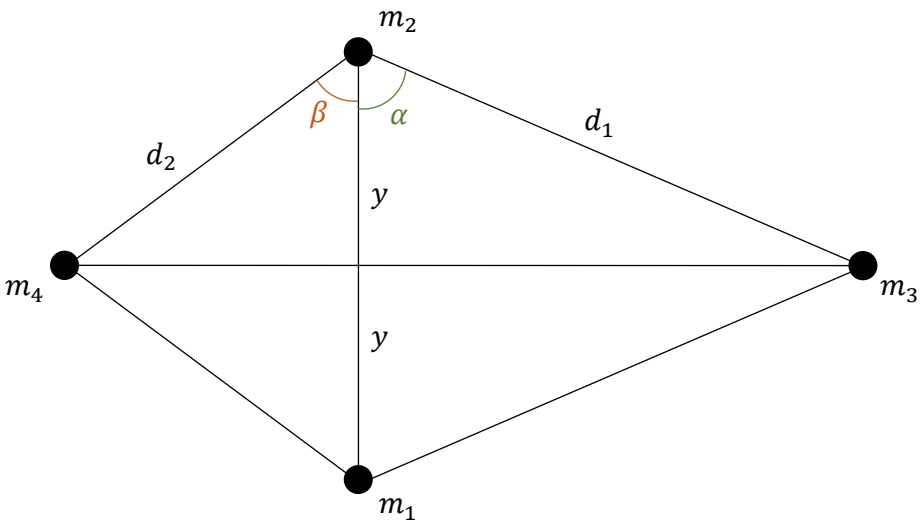

Figure 4.1: Convex kite geometry.

Looking at Equation 3.62, Equation 4.14 and Figure 4.1 we express the state variables for the periodic solution in terms of the Kepler orbit and geometric parameters of the convex central configuration:

$$\begin{aligned} r_2 &= c_2 r(t) & R_2 &= M_2 c_2 R(t) \\ r_3 &= c_3 r(t) & R_3 &= M_3 c_3 R(t) \\ r_4 &= c_4 r(t) & R_4 &= M_4 c_4 R(t) \\ \gamma &= -\frac{\pi}{2} & \Gamma &= M_3 c_3^2 \omega + M_4 c_4^2 \omega \\ \phi &= \pi & \Phi &= M_4 c_4^2 \omega \end{aligned} \tag{4.19}$$

where

$$\begin{aligned} c_2 &= 2y \\ c_3 &= y \tan \alpha \\ c_4 &= \|z_4\| \frac{M}{m_1 + m_2 + m_3} \end{aligned} \tag{4.20}$$

and $R(t) = \dot{r}(t)$. The expressions for Γ and Φ are obtained from

$$\begin{aligned} \Theta_3 &= M_3 r_3^2 \dot{\theta}_3 = M_3 c_3^2 r^2 \frac{\omega}{r^2} = M_3 c_3^2 \omega \\ \Theta_4 &= M_4 r_4^2 \dot{\theta}_4 = M_4 c_4^2 r^2 \frac{\omega}{r^2} = M_4 c_4^2 \omega \end{aligned} \tag{4.21}$$

and therefore

$$\begin{aligned} \Gamma &= \Theta_3 + \Theta_4 = M_3 c_3^2 \omega + M_4 c_4^2 \omega \\ \Phi &= \Theta_4 = M_4 c_4^2 \omega \end{aligned} \tag{4.22}$$

Also note that

$$\begin{aligned} c &= \Theta_2 + \Theta_3 + \Theta_4 = M_2 r_2^2 \dot{\theta}_2 + M_3 r_3^2 \dot{\theta}_3 + M_4 r_4^2 \dot{\theta}_4 \\ &= M_2 c_2^2 r^2 \frac{\omega}{r^2} + M_3 c_3^2 r^2 \frac{\omega}{r^2} + M_4 c_4^2 r^2 \frac{\omega}{r^2} \\ &= M_2 c_2^2 \omega + M_3 c_3^2 \omega + M_4 c_4^2 \omega \end{aligned} \tag{4.23}$$

The mass ratios in terms of the angles are [34]

$$\begin{aligned}\frac{m_3}{m_1}=\frac{m_3}{m_2}&=\frac{\tan\beta\left(\tan\alpha+\tan\beta\right)^2\left(8\cos^3\beta-1\right)}{4\left[\left(\sin\alpha+\cos\alpha\tan\beta\right)^3-1\right]}=\frac{tn_\beta}{4sc_\alpha}\\ \frac{m_4}{m_1}=\frac{m_4}{m_2}&=\frac{\tan\alpha\left(\tan\alpha+\tan\beta\right)^2\left(8\cos^3\alpha-1\right)}{4\left[\left(\sin\beta+\cos\beta\tan\alpha\right)^3-1\right]}=\frac{tn_\alpha}{4sc_\beta}\end{aligned} \tag{4.24}$$

with

$$\begin{aligned}\alpha&=30^\circ+2\kappa\\ \beta&=30^\circ+\lambda\kappa\end{aligned}\quad\text{where}\quad\begin{aligned}0\le\kappa&\le15^\circ\\ -1\le\lambda&\le2\end{aligned}$$

The distances between the bodies are:

$$\begin{aligned}\frac{\kappa_1}{r}=\frac{\kappa_3}{r}=\frac{r_{23}}{r}=\frac{r_{13}}{r}&=d_1=y\sec\alpha=\frac{y}{\cos\alpha}\\ \frac{\kappa_2}{r}=\frac{\kappa_4}{r}=\frac{r_{24}}{r}=\frac{r_{14}}{r}&=d_2=y\sec\beta=\frac{y}{\cos\beta}\\ \frac{\kappa_5}{r}=\frac{r_{34}}{r}&=d_{34}=y\left(\tan\alpha+\tan\beta\right)\end{aligned} \tag{4.25}$$

Applying these to Equation 4.17 we get a useful equation relating the distance parameter y to the masses and geometry of the configuration:

$$y^3=G\left(\frac{m}{4}+m_3\cos^3\alpha+m_4\cos^3\beta\right) \tag{4.26}$$

The mass parameters become

$$\begin{aligned}M_{12}=M_{22}&=\frac{m_1}{m_1+m_2}=\frac{m_2}{m_1+m_2}=\frac{1}{2}\\ M_{13}=M_{23}&=\frac{m_1}{m_1+m_2+m_3}=\left(\frac{m_1}{m_1}+\frac{m_2}{m_1}+\frac{m_3}{m_1}\right)^{-1}=\left(2+\frac{tn_\beta}{4sc_\alpha}\right)^{-1}=\frac{4sc_\alpha}{8sc_\alpha+tn_\beta}\\ M_{33}&=\frac{m_3}{m_1+m_2+m_3}=\left(\frac{m_1}{m_3}+\frac{m_2}{m_3}+\frac{m_3}{m_3}\right)^{-1}=\left(2\frac{4sc_\alpha}{tn_\beta}+1\right)^{-1}=\frac{tn_\beta}{8sc_\alpha+tn_\beta}\end{aligned} \tag{4.27}$$

$$\begin{aligned}M_{c1}&=M_{23}+M_{33}-M_{33}M_{12}=M_{23}+\frac{1}{2}M_{33}=\frac{m_2+\frac{1}{2}m_3}{m_1+m_2+m_3}=\frac{m+\frac{1}{2}m_3}{2m+m_3}=\frac{1}{2}\\ M_{c2}&=M_{33}M_{22}-M_{13}-M_{33}=-\frac{1}{2}M_{33}-M_{13}=-M_{c1}=-\frac{1}{2}\\ M_{c3}&=M_{13}+M_{23}=2M_{13}=2M_{23}=\frac{8sc_\alpha}{8sc_\alpha+tn_\beta}\end{aligned} \tag{4.28}$$

and

$$\begin{aligned}M_2&=m_2\frac{m_1}{m_1+m_2}=m_2M_{12}=\frac{m}{2}\\ M_3&=m_3\frac{m_1+m_2}{m_1+m_2+m_3}=m_3\left(M_{13}+M_{23}\right)=2m_3M_{13}=2m_3M_{23}\\ M_4&=m_4\frac{m_1+m_2+m_3}{m_1+m_2+m_3+m_4}=m_4M_{34}\end{aligned} \tag{4.29}$$

Furthermore, applying the condition on κ_2 from Equation 4.25, we get

$$\begin{aligned}
\kappa_2^2 =& \frac{1}{4}c_2^2 r^2 + M_{33}^2 c_3^2 r^2 + c_4^2 r^2 - 2M_{33}c_3c_4 r^2 = r^2 \frac{y^2}{\cos^2\beta} \\
& y^2 + y^2 \frac{m_3^2}{(m_1+m_2+m_3)^2}\tan^2\alpha + \|\boldsymbol{z}_4\|^2 \frac{M^2}{(m_1+m_2+m_3)^2} - 2\frac{m_3 M}{(m_1+m_2+m_3)^2} y\tan\alpha\|\boldsymbol{z}_4\| = \frac{y^2}{\cos^2\beta} \\
& y^2 + \frac{y^2\tan^2\alpha m_3^2 + \|\boldsymbol{z}_4\|^2 M^2 - 2m_3 M y\tan\alpha\|\boldsymbol{z}_4\|}{(m_1+m_2+m_3)^2} = \frac{y^2}{\cos^2\beta} \\
& y^2 + \frac{\left(m_3 y\tan\alpha - \|\boldsymbol{z}_4\| M\right)^2}{(m_1+m_2+m_3)^2} = \frac{y^2}{\cos^2\beta} \\
& \frac{\left(m_3 y\tan\alpha - \|\boldsymbol{z}_4\| M\right)^2}{(m_1+m_2+m_3)^2} = y^2\left(\frac{1}{\cos^2\beta} - 1\right) = y^2\frac{\sin^2\beta}{\cos^2\beta} \\
\implies & m_3 y\tan\alpha - \|\boldsymbol{z}_4\| M = \pm y\tan\beta\,(m_1+m_2+m_3) \\
\implies & \|\boldsymbol{z}_4\| = \frac{m_3 y\tan\alpha \pm (m_1+m_2+m_3)\, y\tan\beta}{M}
\end{aligned} \tag{4.30}$$

Thus

$$c_4 = \|\boldsymbol{z}_4\|\frac{M}{m_1+m_2+m_3} = \frac{m_3 y\tan\alpha \pm (m_1+m_2+m_3)\, y\tan\beta}{M}\frac{M}{m_1+m_2+m_3} = M_{33}y\tan\alpha \pm y\tan\beta \tag{4.31}$$

To find the right sign in this equality we calculate the other κ at the periodic solution, which also serves to verify that the state variables and mass parameters have been set up correctly.

$$\begin{aligned}
\kappa_1 &= \sqrt{M_{22}^2 r_2^2 + r_3^2 + 2M_{22}r_2r_3\cos\gamma} = \sqrt{M_{22}^2c_2^2r^2 + c_3^2r^2} = r\sqrt{M_{22}^2c_2^2 + c_3^2} \\
&= r\sqrt{\frac{1}{4}4y^2 + y^2\tan^2\alpha} = ry\sqrt{1+\tan^2\alpha} = ry\sqrt{\frac{1}{\cos^2\alpha}} = \frac{ry}{\cos\alpha} \\
\kappa_3 &= \sqrt{M_{12}^2 r_2^2 + r_3^2 - 2M_{12}r_2r_3\cos\gamma} = \sqrt{M_{12}^2c_2^2r^2 + c_3^2r^2} = r\sqrt{\frac{1}{4}4y^2 + y^2\tan^2\alpha} = ry\sqrt{1+\tan\alpha} = \frac{ry}{\cos\alpha} = \kappa_1 \\
\kappa_4 &= \sqrt{M_{c2}^2c_2^2r^2 + M_{33}^2c_3^2r^2 + c_4^2r^2 - 2M_{33}c_3c_4r^2} \\
&= ry\sqrt{1 + M_{33}^2\tan^2\alpha + M_{33}^2\tan^2\alpha - 2M_{33}\tan\alpha\tan\beta + \tan^2\beta - 2M_{33}^2\tan^2\alpha + 2M_{33}\tan\alpha\tan\beta} \\
&= ry\sqrt{1+\tan^2\beta} = ry\sqrt{1+\tan^2\beta} = \frac{ry}{\cos\beta} = \kappa_2 \\
\kappa_5 &= \sqrt{M_{c3}^2r_3^2 + r_4^2 - 2M_{c3}r_3r_4\cos\phi} = \sqrt{4M_{13}^2c_3^2r^2 + c_4^2r^2 + 4M_{13}c_3c_4r^2} \\
&= ry\sqrt{4M_{13}^2\tan^2\alpha + M_{33}^2\tan^2\alpha \pm 2M_{33}\tan\alpha\tan\beta + \tan^2\beta + 4M_{13}M_{33}\tan^2\alpha \pm 4M_{13}\tan\alpha\tan\beta} \\
&= ry\sqrt{\pm 2\tan\alpha\tan\beta\,(M_{33}+2M_{13}) + \tan^2\alpha\left(4M_{13}^2 + M_{33}^2 + 4M_{13}M_{33}\right) + \tan^2\beta} \\
&= ry\sqrt{\pm 2\tan\alpha\tan\beta + \tan^2\alpha + \tan^2\beta} = ry\sqrt{\left(\tan\alpha \pm \tan\beta\right)^2} = ry\left(\tan\alpha \pm \tan\beta\right)
\end{aligned} \tag{4.32}$$

Since $\kappa_5 = yr\left(\tan\alpha + \tan\beta\right)$ we must have that

$$\|\boldsymbol{z}_4\| = \frac{m_3 y\tan\alpha + (m_1+m_2+m_3)\, y\tan\beta}{M} \tag{4.33}$$

Comparing this with Eq. (4.31) we find

$$c_4 = M_{33}y\tan\alpha + y\tan\beta \tag{4.34}$$

c_4 can be expressed purely in terms of geometric parameters, as c_2 and c_3 are by expressing the mass ratio M_{33} in terms of α and β, as in Eq. (4.27).

4.3. Linearization

As Moeckel shows in [19], attempting to prove the stability of a full non-linear relative equilibrium (RE) solution (name for a circular periodic solution of a central configuration, since it becomes stationary in a rotating frame) of an n-body problem is hopeless. A classic approach to prove or disprove non-linear stability is by finding a Lyapunov function [19, 35] which can be the Hamiltonian or some other integral. One then proceeds to prove that the equilibrium point (relative equilibrium in a rotating frame) in phase space rests at an isolated minimum or maximum of the Lyapunov function. The idea is that the solution must stay on a manifold defined by a constant conserved quantity. If our solution in phase space rests at a local minimum of the total energy, for instance, we would know that it is a stable solution. This is because all regions surrounding an isolated minimum would be of a higher energy level and, since energy is conserved, the solution could never climb out of the energy "hole".

Apparently, "this approach never works for RE's" [19], because one can always find a direction at an RE point in phase space where the Hamiltonian function will increase and one where it will decrease, preventing the point from ever being at an isolated minimum/maximum, as proved in [19]. Thus we proceed to investigate linear stability, just as is done for three bodies in [19, 27, 28].

The equations of motion of a Hamiltonian system are given by Hamilton's equations (Eq. (3.1)):

$$\begin{bmatrix} \dot{q}_1 \\ \vdots \\ \dot{q}_n \\ \dot{p}_1 \\ \vdots \\ \dot{p}_n \end{bmatrix} = \begin{bmatrix} \frac{\partial H}{\partial p_1} \\ \vdots \\ \frac{\partial H}{\partial p_n} \\ -\frac{\partial H}{\partial q_1} \\ \vdots \\ -\frac{\partial H}{\partial q_n} \end{bmatrix} \tag{4.35}$$

Or

$$\dot{\boldsymbol{x}} = f(\boldsymbol{x}) = JDH(\boldsymbol{x}) \tag{4.36}$$

in shorthand, where $\boldsymbol{x} \in \mathbb{R}^{2n}$ is the state vector, $f(\boldsymbol{x}) : \mathbb{R}^{2n} \to \mathbb{R}^{2n}$ is the vector valued function that maps the vector of state variables to the vector of their derivatives, $DH(\boldsymbol{x})$ is the gradient vector of the Hamiltonian and J is the canonical matrix

$$\begin{bmatrix} 0 & I \\ -I & 0 \end{bmatrix} \tag{4.37}$$

We denote the periodic orbit, given by expressions (4.19), by

$$\boldsymbol{\gamma}(t) = \begin{bmatrix} c_2 r(t) \\ c_3 r(t) \\ -\pi/2 \\ c_4 r(t) \\ \pi \\ M_2 c_2 R(t) \\ M_3 c_3 R(t) \\ M_3 c_3^2 \omega + M_4 c_4^2 \omega \\ M_4 c_4 R(t) \\ M_4 c_4^2 \omega \end{bmatrix} \tag{4.38}$$

To linearize the system around the periodic solution we set $\boldsymbol{x} = \boldsymbol{\gamma}(t) + \boldsymbol{y}$ [35], where y is a perturbation vector, representing deviations from the periodic solution. Substitute into Eq. (4.36) and write the Taylor expansion to get

$$\dot{\boldsymbol{\gamma}}(t) + \dot{\boldsymbol{y}} = f(\boldsymbol{\gamma}(t) + \boldsymbol{y}) = f(\boldsymbol{\gamma}(t)) + \boldsymbol{y}^T Df(\boldsymbol{\gamma}(t)) + \cdots \tag{4.39}$$

where $Df(\boldsymbol{\gamma}(t))$ is the gradient vector vector evaluated at the periodic solution, $\cdots$ denotes the higher order terms and we have assumed that $f(\boldsymbol{x})$ has a Taylor expansion to at least degree two. Notice that since $\boldsymbol{\gamma}(t)$ is a solution of Eq. (4.36), we have $\dot{\boldsymbol{\gamma}}(t) = f(\boldsymbol{\gamma}(t))$, so canceling this solution out we get:

$$\dot{\boldsymbol{y}} = \boldsymbol{y}^T Df(\boldsymbol{\gamma}(t)) + \cdots \tag{4.40}$$

By linearizing we get rid of the higher order terms and obtain the equations of motion linearized around $\boldsymbol{\gamma}(t)$:

$$\dot{\boldsymbol{y}} = \boldsymbol{y}^T Df(\boldsymbol{\gamma}(t)) = JD^2H(\boldsymbol{\gamma}(t))\boldsymbol{y} \tag{4.41}$$

where $D^2H(\boldsymbol{\gamma}(t))$ is the Hessian of H evaluated at the periodic solution.

$$D^2H(\boldsymbol{\gamma}(t)) = \begin{bmatrix} \frac{\partial^2 H}{\partial q_1 \partial q_1}\Big|_{\boldsymbol{\gamma}(t)} & \cdots & \frac{\partial^2 H}{\partial q_1 \partial q_n}\Big|_{\boldsymbol{\gamma}(t)} & \frac{\partial^2 H}{\partial q_1 \partial p_1}\Big|_{\boldsymbol{\gamma}(t)} & \cdots & \frac{\partial^2 H}{\partial q_1 \partial p_n}\Big|_{\boldsymbol{\gamma}(t)} \\ \vdots & & \vdots & \vdots & & \vdots \\ \frac{\partial^2 H}{\partial q_n \partial q_1}\Big|_{\boldsymbol{\gamma}(t)} & \cdots & \frac{\partial^2 H}{\partial q_n \partial q_n}\Big|_{\boldsymbol{\gamma}(t)} & \frac{\partial^2 H}{\partial q_n \partial p_1}\Big|_{\boldsymbol{\gamma}(t)} & \cdots & \frac{\partial^2 H}{\partial q_n \partial p_n}\Big|_{\boldsymbol{\gamma}(t)} \\ \frac{\partial^2 H}{\partial p_1 \partial q_1}\Big|_{\boldsymbol{\gamma}(t)} & \cdots & \frac{\partial^2 H}{\partial p_1 \partial q_n}\Big|_{\boldsymbol{\gamma}(t)} & \frac{\partial^2 H}{\partial p_1 \partial p_1}\Big|_{\boldsymbol{\gamma}(t)} & \cdots & \frac{\partial^2 H}{\partial p_1 \partial p_n}\Big|_{\boldsymbol{\gamma}(t)} \\ \vdots & & \vdots & \vdots & & \vdots \\ \frac{\partial^2 H}{\partial p_n \partial q_1}\Big|_{\boldsymbol{\gamma}(t)} & \cdots & \frac{\partial^2 H}{\partial p_n \partial q_n}\Big|_{\boldsymbol{\gamma}(t)} & \frac{\partial^2 H}{\partial p_n \partial p_1}\Big|_{\boldsymbol{\gamma}(t)} & \cdots & \frac{\partial^2 H}{\partial p_n \partial p_n}\Big|_{\boldsymbol{\gamma}(t)} \end{bmatrix} \tag{4.42}$$

The double derivative terms in Eq. (4.42) with respect to our position variables r_2, r_3, γ, r_4, ϕ and conjugate momenta R_2, R_3, Γ, R_4 and Φ are computed as follows

$$\begin{aligned} \frac{\partial^2 H}{\partial r_2^2} =& \frac{\partial}{\partial r_2}\begin{bmatrix} -\frac{(c-\Gamma)^2}{M_2}\frac{1}{r_2^3} + \frac{Gm_1m_2}{r_2^2} + \frac{Gm_1m_3}{\kappa_1^3}\left(M_{22}^2 r_2 + M_{22} r_3\cos\gamma\right) \\ + \frac{Gm_1m_4}{\kappa_2^3}\left(M_{c1}^2 r_2 + M_{c1} r_4\cos(\gamma+\phi) + M_{33}M_{c1} r_3\cos\gamma\right) + \frac{Gm_2m_3}{\kappa_3^3}\left(M_{12}^2 r_2 - M_{12} r_3\cos\gamma\right) \\ + \frac{Gm_2m_4}{\kappa_4^3}\left(M_{c2}^2 r_2 + M_{c2} r_4\cos(\gamma+\phi) + M_{33}M_{c2} r_3\cos\gamma\right) \end{bmatrix} \\ =& 3\frac{(c-\Gamma)^2}{M_2}\frac{1}{r_2^4} - 2\frac{Gm_1m_2}{r_2^3} - 3\frac{Gm_1m_3}{\kappa_1^5}\left(M_{22}^2 r_2 + M_{22} r_3\cos\gamma\right)^2 + \frac{Gm_1m_3}{\kappa_1^3}M_{22}^2 \\ & - 3\frac{Gm_1m_4}{\kappa_2^5}\left(M_{c1}^2 r_2 + M_{c1} r_4\cos(\gamma+\phi) + M_{33}M_{c1} r_3\cos\gamma\right)^2 + \frac{Gm_1m_4}{\kappa_2^3}M_{c1}^2 \\ & - 3\frac{Gm_2m_3}{\kappa_3^5}\left(M_{12}^2 r_2 - M_{12} r_3\cos\gamma\right)^2 + \frac{Gm_2m_3}{\kappa_3^3}M_{12}^2 \\ & - 3\frac{Gm_2m_4}{\kappa_4^5}\left(M_{c2}^2 r_2 + M_{c2} r_4\cos(\gamma+\phi) + M_{33}M_{c2} r_3\cos\gamma\right)^2 + \frac{Gm_2m_4}{\kappa_4^3}M_{c2}^2 \end{aligned} \tag{4.43}$$

Evaluated at the periodic solution $\boldsymbol{\gamma}(t)$ (from Eqs. (4.15), (4.19), (4.25), (4.27) and (4.28)) :

$$\begin{aligned} r_2 &= c_2 r(t) & R_2 &= M_2 c_2 R(t) & \kappa_1 &= \kappa_3 = \frac{ry}{\cos\alpha} \\ r_3 &= c_3 r(t) & R_3 &= M_3 c_3 R(t) & \kappa_2 &= \kappa_4 = \frac{ry}{\cos\beta} \\ r_4 &= c_4 r(t) & R_4 &= M_4 c_4 R(t) & \kappa_5 &= ry\left(\tan\alpha + \tan\beta\right) \\ \gamma &= -\frac{\pi}{2} & \Gamma &= M_3 c_3^2\omega + M_4 c_4^2\omega & M_{12} &= M_{22} = \frac{1}{2} \\ \phi &= \pi & \Phi &= M_4 c_4^2\omega & M_{c1} &= -M_{c2} = \frac{1}{2} \end{aligned}$$

the term becomes

$$\begin{aligned}
\left.\frac{\partial^2 H}{\partial r_2^2}\right|_{\boldsymbol{\gamma}(t)} =& 3\frac{\left(c-M_3c_3^2\omega-M_4c_4^2\omega\right)^2}{M_2}\frac{1}{c_2^4r^4}-2\frac{Gmm}{c_2^3r^3}-3\frac{Gmm_3}{r^5y^5}\cos^5\alpha\left(\frac{1}{4}c_2r\right)^2+\frac{Gmm_3}{r^3y^3}\cos^3\alpha\frac{1}{4}\\
&-3\frac{Gmm_4}{r^5y^5}\cos^5\beta\left(\frac{1}{4}c_2r\right)^2+\frac{Gmm_4}{r^3y^3}\cos^3\beta\frac{1}{4}-3\frac{Gmm_3}{r^5y^5}\cos^5\alpha\left(\frac{1}{4}c_2r\right)^2\\
&+\frac{Gmm_3}{r^3y^3}\cos^3\alpha\frac{1}{4}-3\frac{Gmm_4}{r^5y^5}\cos^5\beta\left(\frac{1}{4}c_2r\right)^2+\frac{Gmm_4}{r^3y^3}\cos^3\beta\frac{1}{4}\\
=&3\frac{\left(M_2c_2^2\omega\right)^2}{M_2}\frac{1}{c_2^4r^4}-2\frac{Gmm}{c_2^3r^3}-6\frac{Gmm_3}{r^3y^5}\cos^5\alpha\left(\frac{1}{4}c_2\right)^2+2\frac{Gmm_3}{r^3y^3}\cos^3\alpha\frac{1}{4}\\
&-6\frac{Gmm_4}{r^3y^5}\cos^5\beta\left(\frac{1}{4}c_2\right)^2+2\frac{Gmm_4}{r^3y^3}\cos^3\beta\frac{1}{4}\\
=&3M_2\frac{\omega^2}{r^4}-\frac{Gmm}{4y^3r^3}-\frac{3}{2}\frac{Gmm_3}{r^3y^3}\cos^5\alpha+\frac{1}{2}\frac{Gmm_3}{r^3y^3}\cos^3\alpha-\frac{3}{2}\frac{Gmm_4}{r^3y^3}\cos^5\beta+\frac{1}{2}\frac{Gmm_4}{r^3y^3}\cos^3\beta\\
=&\boxed{3M_2\frac{\omega^2}{r^4}-\frac{1}{4}\frac{Gmm}{r^3y^3}-\frac{1}{2}\frac{Gmm_3}{r^3y^3}\left(3\cos^5\alpha-\cos^3\alpha\right)-\frac{1}{2}\frac{Gmm_4}{r^3y^3}\left(3\cos^5\beta-\cos^3\beta\right)}
\end{aligned}\tag{4.44}$$

Similarly,

$$\begin{aligned}
\frac{\partial^2 H}{\partial r_2\partial r_3} =& -\frac{3}{2}\frac{Gm_1m_3}{\kappa_1^5}\left(2r_3+2M_{22}r_2\cos\gamma\right)\left(M_{22}^2r_2+M_{22}r_3\cos\gamma\right)+\frac{Gm_1m_3}{\kappa_1^3}M_{22}\cos\gamma\\
&-\frac{3}{2}\frac{Gm_1m_4}{\kappa_2^5}\left(2M_{33}^2r_3+2M_{33}r_4\cos\phi+2M_{33}M_{c1}r_2\cos\gamma\right)\left(M_{c1}^2r_2+M_{c1}r_4\cos(\gamma+\phi)+M_{33}M_{c1}r_3\cos\gamma\right)\\
&+\frac{Gm_1m_4}{\kappa_2^3}M_{33}M_{c1}\cos\gamma\\
&-\frac{3}{2}\frac{Gm_2m_3}{\kappa_3^5}\left(2r_3-2M_{12}r_2\cos\gamma\right)\left(M_{12}^2r_2-M_{12}r_3\cos\gamma\right)-\frac{Gm_2m_3}{\kappa_3^3}M_{12}\cos\gamma\\
&-\frac{3}{2}\frac{Gm_2m_4}{\kappa_4^5}\left(2M_{33}^2r_3+2M_{33}r_4\cos\phi+2M_{33}M_{c2}r_2\cos\gamma\right)\left(M_{c2}^2r_2+M_{c2}r_4\cos(\gamma+\phi)+M_{33}M_{c2}r_3\cos\gamma\right)\\
&+\frac{Gm_2m_4}{\kappa_4^3}M_{33}M_{c2}\cos\gamma
\end{aligned}\tag{4.45}$$

then at the periodic solution $\boldsymbol{\gamma}(t)$

$$\begin{aligned}
\left.\frac{\partial^2 H}{\partial r_2\partial r_3}\right|_{\boldsymbol{\gamma}(t)} =& -3\frac{Gmm_3}{r^5y^5}\cos^5\alpha\cdot c_3r\cdot\frac{1}{4}c_2r-3\frac{Gmm_4}{r^5y^5}\cos^5\beta\cdot\left(M_{33}^2c_3r-M_{33}c_4r\right)\cdot\left(\frac{1}{4}c_2r\right)\\
&-3\frac{Gmm_3}{r^5y^5}\cos^5\alpha\cdot c_3r\cdot\frac{1}{4}c_2r-3\frac{Gmm_4}{r^5y^5}\cos^5\beta\cdot\left(M_{33}^2c_3r-M_{33}c_4r\right)\cdot\left(\frac{1}{4}c_2r\right)\\
=&-\frac{3}{2}\frac{Gmm_3}{r^3y^5}\cos^5\alpha\cdot c_3\cdot c_2-\frac{3}{2}\frac{Gmm_4}{r^3y^5}\cos^5\beta\cdot\left(M_{33}^2c_3-M_{33}c_4\right)\cdot c_2\\
=&-\frac{3}{2}\frac{Gmm_3}{r^3y^5}\cos^5\alpha\cdot y\tan\alpha\cdot 2y-\frac{3}{2}\frac{Gmm_4}{r^3y^5}\cos^5\beta\cdot\left(M_{33}^2y\tan\alpha-M_{33}y\left(M_{33}\tan\alpha+\tan\beta\right)\right)\cdot 2y\\
=&\boxed{-3\frac{Gmm_3}{r^3y^3}\cos^4\alpha\sin\alpha+3\frac{Gmm_4}{r^3y^3}M_{33}\cos^4\beta\sin\beta}
\end{aligned}\tag{4.46}$$

also

$$\begin{aligned}\frac{\partial^2 H}{\partial r_2 \partial r_4} =& -\frac{3}{2}\frac{Gm_1m_4}{\kappa_2^5}\cdot\left(2r_4+2M_{c1}r_2\cos(\gamma+\phi)+2M_{33}r_3\cos\phi\right)\cdot\left(M_{c1}^2r_2+M_{c1}r_4\cos(\gamma+\phi)+M_{33}M_{c1}r_3\cos\gamma\right)\\ &+\frac{Gm_1m_4}{\kappa_2^3}\cdot M_{c1}\cos(\gamma+\phi)\\ &-\frac{3}{2}\frac{Gm_2m_4}{\kappa_4^5}\cdot\left(2r_4+2M_{c2}r_2\cos(\gamma+\phi)+2M_{33}r_3\cos\phi\right)\cdot\left(M_{c2}^2r_2+M_{c2}r_4\cos(\gamma+\phi)+M_{33}M_{c2}r_3\cos\gamma\right)\\ &+\frac{Gm_2m_4}{\kappa_4^3}\cdot M_{c2}\cos(\gamma+\phi)\end{aligned} \tag{4.47}$$

at the periodic solution:

$$\begin{aligned}\left.\frac{\partial H}{\partial r_2\partial r_4}\right|_{\boldsymbol{\gamma}(t)} =& -3\frac{Gmm_4}{r^5y^5}\cos^5\beta\cdot(c_4r-M_{33}c_3r)\cdot\left(\frac{1}{4}c_2r\right)+0\\ &-3\frac{Gmm_4}{r^5y^5}\cos^5\beta\cdot(c_4r-M_{33}c_3r)\cdot\left(\frac{1}{4}c_2r\right)+0\\ =&-\frac{3}{2}\frac{Gmm_4}{r^3y^5}\cos^5\beta\cdot(c_4-M_{33}c_3)\cdot c_2=-\frac{3}{2}\frac{Gmm_4}{r^3y^5}\cos^5\beta\cdot\left(M_{33}y\tan\alpha+y\tan\beta-M_{33}y\tan\alpha\right)\cdot 2y\\ =&\boxed{-3\frac{Gmm_4}{r^3y^3}\cos^4\beta\sin\beta}\end{aligned} \tag{4.48}$$

Derivative with respect to γ:

$$\begin{aligned}\frac{\partial^2 H}{\partial r_2\partial\gamma} =& -\frac{3}{2}\frac{Gm_1m_3}{\kappa_1^5}\cdot -2M_{22}r_2r_3\sin\gamma\cdot\left(M_{22}^2r_2+M_{22}r_3\cos\gamma\right)+\frac{Gm_1m_3}{\kappa_1^3}\cdot -M_{22}r_3\sin\gamma\\ &-\frac{3}{2}\frac{Gm_1m_4}{\kappa_2^5}\cdot\left(-2M_{c1}r_2r_4\sin(\gamma+\phi)-2M_{33}M_{c1}r_2r_3\sin\gamma\right)\cdot\left(M_{c1}^2r_2+M_{c1}r_4\cos(\gamma+\phi)+M_{33}M_{c1}r_3\cos\gamma\right)\\ &+\frac{Gm_1m_4}{\kappa_2^3}\cdot\left(-M_{c1}r_4\sin(\gamma+\phi)-M_{33}M_{c1}r_3\sin\gamma\right)\\ &-\frac{3}{2}\frac{Gm_2m_3}{\kappa_3^5}\cdot 2M_{12}r_2r_3\sin\gamma\cdot\left(M_{12}^2r_2-M_{12}r_3\cos\gamma\right)+\frac{Gm_2m_3}{\kappa_3^3}\cdot M_{12}r_3\sin\gamma\\ &-\frac{3}{2}\frac{Gm_2m_4}{\kappa_4^5}\cdot\left(-2M_{c2}r_2r_4\sin(\gamma+\phi)-2M_{33}M_{c2}r_2r_3\sin\gamma\right)\cdot\left(M_{c2}^2r_2+M_{c2}r_4\cos(\gamma+\phi)+M_{33}M_{c2}r_3\cos\gamma\right)\\ &+\frac{Gm_2m_4}{\kappa_4^3}\cdot\left(-M_{c2}r_4\sin(\gamma+\phi)-M_{33}M_{c2}r_3\sin\gamma\right)\end{aligned} \tag{4.49}$$

at the periodic solution:

$$\begin{aligned}\left.\frac{\partial^2 H}{\partial r_2\partial\gamma}\right|_{\boldsymbol{\gamma}(t)} =& -\frac{3}{2}\frac{Gmm_3}{r^5y^5}\cos^5\alpha\cdot c_2c_3r^2\cdot\frac{1}{4}c_2r+\frac{Gmm_3}{r^3y^3}\cos^3\alpha\cdot\frac{1}{2}c_3r\\ &-\frac{3}{2}\frac{Gmm_4}{r^5y^5}\cos^5\beta\cdot\left(-c_2c_4r^2+M_{33}c_2c_3r^2\right)\cdot\left(\frac{1}{4}c_2r\right)+\frac{Gmm_4}{r^3y^3}\cos^3\beta\cdot\left(-\frac{1}{2}c_4r+M_{33}\frac{1}{2}c_3r\right)\\ &-\frac{3}{2}\frac{Gmm_3}{r^5y^5}\cos^5\alpha\cdot -c_2c_3r^2\cdot\frac{1}{4}c_2r+\frac{Gmm_3}{r^3y^3}\cos^3\alpha\cdot -\frac{1}{2}c_3r\\ &-\frac{3}{2}\frac{Gmm_4}{r^5y^5}\cos^5\beta\cdot\left(c_2c_4r^2-M_{33}c_2c_3r^2\right)\cdot\left(\frac{1}{4}c_2r\right)+\frac{Gmm_4}{r^3y^3}\cos^3\beta\cdot\left(\frac{1}{2}c_4r-M_{33}\frac{1}{2}c_3r\right)\\ =&\boxed{0}\end{aligned} \tag{4.50}$$

Finally, the derivative with respect to ϕ:

$$\begin{aligned}\frac{\partial^2 H}{\partial r_2 \partial \phi} =& -\frac{3}{2}\frac{Gm_1m_4}{\kappa_2^5}\cdot\left(-2M_{c1}r_2r_4\sin(\gamma+\phi)-2M_{33}r_3r_4\sin\phi\right)\cdot\left(M_{c1}^2r_2+M_{c1}r_4\cos(\gamma+\phi)+M_{33}M_{c1}r_3\cos\gamma\right)\\ &-\frac{Gm_1m_4}{\kappa_2^3}M_{c1}r_4\sin(\gamma+\phi)\\ &-\frac{3}{2}\frac{Gm_2m_4}{\kappa_4^5}\cdot\left(-2M_{c2}r_2r_4\sin(\gamma+\phi)-2M_{33}r_3r_4\sin\phi\right)\cdot\left(M_{c2}^2r_2+M_{c2}r_4\cos(\gamma+\phi)+M_{33}M_{c2}r_3\cos\gamma\right)\\ &-\frac{Gm_2m_4}{\kappa_4^3}M_{c2}r_4\sin(\gamma+\phi)\end{aligned} \tag{4.51}$$

at the periodic solution:

$$\begin{aligned}\left.\frac{\partial H}{\partial r_2\partial\phi}\right|_{\boldsymbol{\gamma}(t)} =& -3\frac{Gmm_4}{r^5y^5}\cos^5\beta\cdot-\frac{1}{2}c_2c_4r^2\cdot\frac{1}{4}c_2r-\frac{Gmm_4}{r^3y^3}\cos^3\beta\cdot\frac{1}{2}c_4r\\ &-3\frac{Gmm_4}{r^5y^5}\cos^5\beta\cdot\frac{1}{2}c_2c_4r^2\cdot\frac{1}{4}c_2r-\frac{Gmm_4}{r^3y^3}\cos^3\beta\cdot-\frac{1}{2}c_4r\\ =&\boxed{0}\end{aligned} \tag{4.52}$$

We see that the partial derivatives of $\frac{\partial H}{\partial r_2}=-\dot{R}_2$ with respect to the two angle variables γ and ϕ are zero at the periodic solution. This can be explained by the fact that, looking at Fig. 3.3, an incremental positive change in γ would move the particle m_3 slightly upwards. As a result, slightly weaker upwards acceleration would be exerted on particle m_1, however a slightly stronger downwards acceleration would be exerted on particle m_2. The net result is that the rate of change of the relative distance r_2 remains constant, hence $\left.\frac{\partial \dot{R}_2}{\partial\gamma}\right|_{\boldsymbol{\gamma}(t)}=0$. This is reflected in the equations by the fact that m_1m_3 acceleration terms get an opposite sign from the m_2m_3 acceleration terms in Eq. (4.50) and cancel each other out, where the same thing also happens with m_1m_4 and m_2m_4.

The same reasoning can be applied to the ϕ derivative, only now incremental increase in ϕ will move the particle m_4 slightly downwards. Because of the symmetry of the configuration, again m_1m_4 acceleration terms cancel the m_2m_4 acceleration terms in Eq. (4.52).

We also need the derivatives with respect to the momentum variables:

$$\frac{\partial^2 H}{\partial r_2\partial R_2}=\frac{\partial^2 H}{\partial r_2\partial R_3}=\frac{\partial^2 H}{\partial r_2\partial R_4}=\boxed{0} \tag{4.53}$$

$$\frac{\partial^2 H}{\partial r_2\partial\Phi}=\boxed{0} \tag{4.54}$$

$$\frac{\partial^2 H}{\partial r_2\partial\Gamma}=2\frac{c-\Gamma}{M_2}\frac{1}{r_2^3} \tag{4.55}$$

at the periodic solution:

$$\left.\frac{\partial H}{\partial r_2\partial\Gamma}\right|_{\boldsymbol{\gamma}(t)}=2\frac{M_2c_2^2\omega}{M_2}\frac{1}{c_2^3r^3}=\frac{2\omega}{c_2r^3}=\frac{2\omega}{2yr^3}=\boxed{\frac{\omega}{r^3y}} \tag{4.56}$$

Clearly, the derivatives with respect to R_i and Φ are zero, since, from Eq. (3.63), $\frac{\partial H}{\partial r_2}=-\dot{R}_2$ depends only on gravitational force terms, which, in turn, depend only of the relative positions of the bodies, and the centrifugal force term, which depends on the rotation rate of $\boldsymbol{u}_2$, implicit in $c-\Gamma=\Theta_2$. Thus, out of the momentum variables, only Γ has an influence on $\dot{R}_2$.

Moving on to the r_3 equation:

$$\begin{aligned}\frac{\partial^2 H}{\partial r_3^2}=\frac{\partial}{\partial r_3}\Bigg[&-\frac{(\Gamma-\Phi)^2}{M_3}\frac{1}{r_3^3}+\frac{Gm_1m_3}{\kappa_1^3}\left(r_3+M_{22}r_2\cos\gamma\right)+\frac{Gm_1m_4}{\kappa_2^3}\left(M_{33}^2r_3+M_{33}r_4\cos\phi+M_{33}M_{c1}r_2\cos\gamma\right)\\ &+\frac{Gm_2m_3}{\kappa_3^3}\left(r_3-M_{12}r_2\cos\gamma\right)+\frac{Gm_2m_4}{\kappa_4^3}\left(M_{33}^2r_3+M_{33}r_4\cos\phi+M_{33}M_{c2}r_2\cos\gamma\right)\\ &+\frac{Gm_3m_4}{\kappa_5^3}\left(M_{c3}^2r_3-M_{c3}r_4\cos\phi\right)\Bigg]\end{aligned}$$

$$
\begin{aligned}
=&3\frac{(\Gamma-\Phi)^2}{M_3}\frac{1}{r_3^4}-3\frac{Gm_1m_3}{\kappa_1^5}\cdot\left(r_3+M_{22}r_2\cos\gamma\right)^2+\frac{Gm_1m_3}{\kappa_1^3}\\
&-3\frac{Gm_1m_4}{\kappa_2^5}\cdot\left(M_{33}^2r_3+M_{33}r_4\cos\phi+M_{33}M_{c1}r_2\cos\gamma\right)^2+\frac{Gm_1m_4}{\kappa_2^3}\cdot M_{33}^2\\
&-3\frac{Gm_2m_3}{\kappa_3^5}\cdot\left(r_3-M_{12}r_2\cos\gamma\right)^2+\frac{Gm_2m_3}{\kappa_3^3}\\
&-3\frac{Gm_2m_4}{\kappa_4^5}\cdot\left(M_{33}^2r_3+M_{33}r_4\cos\phi+M_{33}M_{c2}r_2\cos\gamma\right)^2+\frac{Gm_2m_4}{\kappa_4^3}\cdot M_{33}^2\\
&-3\frac{Gm_3m_4}{\kappa_5^5}\cdot\left(M_{c3}^2r_3-M_{c3}r_4\cos\phi\right)^2+\frac{Gm_3m_4}{\kappa_5^3}\cdot M_{c3}^2
\end{aligned}
\tag{4.57}
$$

Evaluated at the periodic solution:

$$
\begin{aligned}
\left.\frac{\partial^2H}{\partial r_3^2}\right|_{\boldsymbol{\gamma}(t)}=&3\frac{\left(M_3c_3^2\omega\right)^2}{M_3}\frac{1}{c_3^4r^4}\\
&-3\frac{Gmm_3}{r^5y^5}\cos^5\alpha\cdot c_3^2r^2+\frac{Gmm_3}{r^3y^3}\cos^3\alpha\\
&-3\frac{Gmm_4}{r^5y^5}\cos^5\beta\cdot\left(M_{33}^2c_3r-M_{33}c_4r\right)^2+\frac{Gmm_4}{r^3y^3}\cos^3\beta\cdot M_{33}^2\\
&-3\frac{Gmm_3}{r^5y^5}\cos^5\alpha\cdot c_3^2r^2+\frac{Gmm_3}{r^3y^3}\cos^3\alpha\\
&-3\frac{Gmm_4}{r^5y^5}\cos^5\beta\cdot\left(M_{33}^2c_3r-M_{33}c_4r\right)^2+\frac{Gmm_4}{r^3y^3}\cos^3\beta\cdot M_{33}^2\\
&-3\frac{Gm_3m_4}{r^5y^5\left(\tan\alpha+\tan\beta\right)^5}\cdot\left(M_{c3}^2c_3r+M_{c3}c_4r\right)^2+\frac{Gm_3m_4}{r^3y^3\left(\tan\alpha+\tan\beta\right)^3}\cdot M_{c3}^2\\
=&3M_3\frac{\omega^2}{r^4}-6\frac{Gmm_3}{r^3y^5}\cos^5\alpha\cdot y^2\tan^2\alpha+2\frac{Gmm_3}{r^3y^3}\cos^3\alpha\\
&-6\frac{Gmm_4}{r^3y^5}\cos^5\beta\cdot\left(M_{33}^2y\tan\alpha-M_{33}\left(M_{33}y\tan\alpha+y\tan\beta\right)\right)^2+2\frac{Gmm_4}{r^3y^3}\cos^3\beta\cdot M_{33}^2\\
&-3\frac{Gm_3m_4}{r^3y^5\left(\tan\alpha+\tan\beta\right)^5}\cdot\left(M_{c3}^2y\tan\alpha+M_{c3}\left(M_{33}y\tan\alpha+y\tan\beta\right)\right)^2\\
&+\frac{Gm_3m_4}{r^3y^3\left(\tan\alpha+\tan\beta\right)^3}\cdot M_{c3}^2\\
=&3M_3\frac{\omega^2}{r^4}-2\frac{Gmm_3}{r^3y^3}\left(3\cos^5\alpha\tan^2\alpha-\cos^3\alpha\right)-2\frac{Gmm_4}{r^3y^3}\left(3M_{33}^2\cos^5\beta\tan^2\beta-M_{33}^2\cos^3\beta\right)\\
&-\frac{Gm_3m_4}{r^3y^3\left(\tan\alpha+\tan\beta\right)^5}\left(3\left(M_{c3}^2\tan\alpha+M_{c3}\left(M_{33}\tan\alpha+\tan\beta\right)\right)^2-M_{c3}^2\left(\tan\alpha+\tan\beta\right)^2\right)\\
=&3M_3\frac{\omega^2}{r^4}-2\frac{Gmm_3}{r^3y^3}\left(3\cos^3\alpha\left(1-\cos^2\alpha\right)-\cos^3\alpha\right)-2\frac{Gmm_4}{r^3y^3}M_{33}^2\left(3\cos^3\beta\left(1-\cos^2\beta\right)-\cos^3\beta\right)\\
&-\frac{Gm_3m_4}{r^3y^3}M_{c3}^2\frac{\tan^2\alpha\left(3M_{c3}^2+6M_{c3}M_{33}+3M_{33}^2-1\right)+2\tan\alpha\tan\beta\left(3M_{c3}+3M_{33}-1\right)+2\tan^2\beta}{\left(\tan\alpha+\tan\beta\right)^5}\\
=&3M_3\frac{\omega^2}{r^4}-2\frac{Gmm_3}{r^3y^3}\left(2\cos^3\alpha-3\cos^5\alpha\right)-2\frac{Gmm_4}{r^3y^3}M_{33}^2\left(2\cos^3\beta-3\cos^5\beta\right)\\
&-\frac{Gm_3m_4}{r^3y^3}M_{c3}^2\frac{\tan^2\alpha\left(3\left(M_{c3}+M_{33}\right)^2-1\right)+2\tan\alpha\tan\beta\left(3\left(M_{c3}+M_{33}\right)-1\right)+2\tan^2\beta}{\left(\tan\alpha+\tan\beta\right)^5}
\end{aligned}
\tag{4.58}
$$

using the fact that $M_{c3}+M_{33}=M_{13}+M_{23}+M_{33}=1$ we get

$$\begin{aligned}\left.\frac{\partial^2 H}{\partial r_3^2}\right|_{\boldsymbol{\gamma}(t)} =& 3M_3\frac{\omega^2}{r^4}-2\frac{Gmm_3}{r^3y^3}\left(2\cos^3\alpha-3\cos^5\alpha\right)-2\frac{Gmm_4}{r^3y^3}M_{33}^2\left(2\cos^3\beta-3\cos^5\beta\right)\\ &-\frac{Gm_3m_4}{r^3y^3}M_{c3}^2\frac{2\tan^2\alpha+4\tan\alpha\tan\beta+2\tan^2\beta}{\left(\tan\alpha+\tan\beta\right)^5}\\ =&\boxed{\begin{aligned}&3M_3\frac{\omega^2}{r^4}-2\frac{Gmm_3}{r^3y^3}\left(2\cos^3\alpha-3\cos^5\alpha\right)-2\frac{Gmm_4}{r^3y^3}M_{33}^2\left(2\cos^3\beta-3\cos^5\beta\right)\\ &-2\frac{Gm_3m_4}{r^3y^3}M_{c3}^2\left(\tan\alpha+\tan\beta\right)^{-3}\end{aligned}}\end{aligned} \tag{4.59}$$

Then, the derivative with respect to γ:

$$\begin{aligned}\frac{\partial^2 H}{\partial r_3\partial\gamma} =& -\frac{3}{2}\frac{Gm_1m_3}{\kappa_1^5}\cdot\left(-2M_{22}r_2r_3\sin\gamma\right)\cdot\left(r_3+M_{22}r_2\cos\gamma\right)+\frac{Gm_1m_3}{\kappa_1^3}\cdot\left(-M_{22}r_2\sin\gamma\right)\\ &-\frac{3}{2}\frac{Gm_1m_4}{\kappa_2^5}\cdot\left(-2M_{c1}r_2r_4\sin(\gamma+\phi)-2M_{33}M_{c1}r_2r_3\sin\gamma\right)\cdot\left(M_{33}^2r_3+M_{33}r_4\cos\phi+M_{33}M_{c1}r_2\cos\gamma\right)\\ &+\frac{Gm_1m_4}{\kappa_2^3}\cdot\left(-M_{33}M_{c1}r_2\sin\gamma\right)\\ &-\frac{3}{2}\frac{Gm_2m_3}{\kappa_3^5}\cdot\left(2M_{12}r_2r_3\sin\gamma\right)\cdot\left(r_3-M_{12}r_2\cos\gamma\right)+\frac{Gm_2m_3}{\kappa_3^3}\cdot\left(M_{12}r_2\sin\gamma\right)\\ &-\frac{3}{2}\frac{Gm_2m_4}{\kappa_4^5}\cdot\left(-2M_{c2}r_2r_4\sin(\gamma+\phi)-2M_{33}M_{c2}r_2r_3\sin\gamma\right)\cdot\left(M_{33}^2r_3+M_{33}r_4\cos\phi+M_{33}M_{c2}r_2\cos\gamma\right)\\ &+\frac{Gm_2m_4}{\kappa_4^3}\cdot\left(-M_{33}M_{c2}r_2\sin\gamma\right)\end{aligned} \tag{4.60}$$

at the periodic solution:

$$\begin{aligned}\left.\frac{\partial^2 H}{\partial r_3\partial\gamma}\right|_{\boldsymbol{\gamma}(t)} =& \frac{3}{2}\frac{Gmm_3}{r^5y^5}\cos^5\alpha\cdot\left(-c_2c_3r^2\right)\cdot\left(c_3r\right)+\frac{Gmm_3}{r^3y^3}\cos^3\alpha\cdot\left(\frac{1}{2}c_2r\right)\\ &\frac{3}{2}\frac{Gmm_4}{r^5y^5}\cos^5\beta\cdot\left(c_2c_4r^2-M_{33}c_2c_3r^2\right)\cdot\left(M_{33}^2c_3r-M_{33}c_4r\right)+\frac{Gmm_4}{r^3y^3}\cos^3\beta\cdot\left(\frac{1}{2}M_{33}c_2r\right)\\ &-\frac{3}{2}\frac{Gmm_3}{r^5y^5}\cos^5\alpha\cdot\left(-c_2c_3r^2\right)\cdot\left(c_3r\right)+\frac{Gmm_3}{r^3y^3}\cos^3\alpha\cdot\left(-\frac{1}{2}c_2r\right)\\ &-\frac{3}{2}\frac{Gmm_4}{r^5y^5}\cos^5\beta\cdot\left(c_2c_4r^2-M_{33}c_2c_3r^2\right)\cdot\left(M_{33}^2c_3r-M_{33}c_4r\right)-\frac{Gmm_4}{r^3y^3}\cos^3\beta\cdot\left(\frac{1}{2}M_{33}c_2r\right)\\ =&\boxed{0}\end{aligned} \tag{4.61}$$

The derivative with respect to r_4:

$$\begin{aligned}\frac{\partial^2 H}{\partial r_3\partial r_4} =& -\frac{3}{2}\frac{Gm_1m_4}{\kappa_2^5}\cdot\left(2r_4+2M_{c1}r_2\cos(\gamma+\phi)+2M_{33}r_3\cos\phi\right)\cdot\left(M_{33}^2r_3+M_{33}r_4\cos\phi+M_{33}M_{c1}r_2\cos\gamma\right)\\ &+\frac{Gm_1m_4}{\kappa_2^3}\cdot\left(M_{33}\cos\phi\right)\\ &-\frac{3}{2}\frac{Gm_2m_4}{\kappa_4^5}\cdot\left(2r_4+2M_{c2}r_2\cos(\gamma+\phi)+2M_{33}r_3\cos\phi\right)\cdot\left(M_{33}^2r_3+M_{33}r_4\cos\phi+M_{33}M_{c2}r_2\cos\gamma\right)\\ &+\frac{Gm_2m_4}{\kappa_4^3}\cdot\left(M_{33}\cos\phi\right)\\ &-\frac{3}{2}\frac{Gm_3m_4}{\kappa_5^5}\cdot\left(2r_4-2M_{c3}r_3\cos\phi\right)\cdot\left(M_{c3}^2r_3-M_{c3}r_4\cos\phi\right)+\frac{Gm_3m_4}{\kappa_5^3}\cdot\left(-M_{c3}\cos\phi\right)\end{aligned} \tag{4.62}$$

at the periodic solution:

$$\begin{aligned}
\left.\frac{\partial^2 H}{\partial r_3 \partial r_4}\right|_{\boldsymbol{\gamma}(t)} =& -3\frac{Gmm_4}{r^5y^5}\cos^5\beta\cdot(c_4r-M_{33}c_3r)\cdot\left(M_{33}^2c_3r-M_{33}c_4r\right)+\frac{Gmm_4}{r^3y^3}\cos^3\beta\cdot-M_{33}\\
&-3\frac{Gmm_4}{r^5y^5}\cos^5\beta\cdot(c_4r-M_{33}c_3r)\cdot\left(M_{33}^2c_3r-M_{33}c_4r\right)+\frac{Gmm_4}{r^3y^3}\cos^3\beta\cdot-M_{33}\\
&-3\frac{Gm_3m_4}{r^5y^5\left(\tan\alpha+\tan\beta\right)^5}\cdot(c_4r+M_{c3}c_3r)\cdot\left(M_{c3}^2c_3r+M_{c3}c_4r\right)+\frac{Gm_3m_4}{r^3y^3\left(\tan\alpha+\tan\beta\right)^3}\cdot M_{c3}\\
=&6\frac{Gmm_4}{r^3y^5}\cos^5\beta\cdot M_{33}\left(c_4-M_{33}c_3\right)^2-2\frac{Gmm_4}{r^3y^3}\cos^3\beta\cdot M_{33}\\
&-3\frac{Gm_3m_4}{r^3y^5\left(\tan\alpha+\tan\beta\right)^5}\cdot M_{c3}\left(c_4+M_{c3}c_3\right)^2+\frac{Gm_3m_4}{r^3y^3\left(\tan\alpha+\tan\beta\right)^3}\cdot M_{c3}\\
=&6\frac{Gmm_4}{r^3y^5}\cos^5\beta\cdot M_{33}\left(M_{33}y\tan\alpha+y\tan\beta-M_{33}y\tan\alpha\right)^2-2\frac{Gmm_4}{r^3y^3}\cos^3\beta\cdot M_{33}\\
&-3\frac{Gm_3m_4}{r^3y^5\left(\tan\alpha+\tan\beta\right)^5}\cdot M_{c3}\left(M_{33}y\tan\alpha+y\tan\beta+M_{c3}y\tan\alpha\right)^2+\frac{Gm_3m_4}{r^3y^3\left(\tan\alpha+\tan\beta\right)^3}\cdot M_{c3}\\
=&6\frac{Gmm_4}{r^3y^3}\cos^5\beta\cdot M_{33}\tan^2\beta-2\frac{Gmm_4}{r^3y^3}\cos^3\beta\cdot M_{33}\\
&-3\frac{Gm_3m_4}{r^3y^3\left(\tan\alpha+\tan\beta\right)^3}\cdot M_{c3}+\frac{Gm_3m_4}{r^3y^3\left(\tan\alpha+\tan\beta\right)^3}\cdot M_{c3}\\
=&2\frac{Gmm_4}{r^3y^3}M_{33}\left(3\cos^5\beta\tan^2\beta-\cos^3\beta\right)-2\frac{Gm_3m_4}{r^3y^3}\frac{M_{c3}}{\left(\tan\alpha+\tan\beta\right)^3}\\
=&\boxed{2\frac{Gmm_4}{r^3y^3}M_{33}\left(2\cos^3\beta-3\cos^5\beta\right)-2\frac{Gm_3m_4}{r^3y^3}M_{c3}\left(\tan\alpha+\tan\beta\right)^{-3}}
\end{aligned}\tag{4.63}$$

Next, the derivative w.r.t. ϕ:

$$\begin{aligned}
\frac{\partial^2 H}{\partial r_3\partial\phi} =& -\frac{3}{2}\frac{Gm_1m_4}{\kappa_2^5}\cdot\left(-2M_{c1}r_2r_4\sin(\gamma+\phi)-2M_{33}r_3r_4\sin\phi\right)\cdot\left(M_{33}^2r_3+M_{33}r_4\cos\phi+M_{33}M_{c1}r_2\cos\gamma\right)\\
&+\frac{Gm_1m_4}{\kappa_2^3}\cdot\left(-M_{33}r_4\sin\phi\right)\\
&-\frac{3}{2}\frac{Gm_2m_4}{\kappa_4^5}\cdot\left(-2M_{c2}r_2r_4\sin(\gamma+\phi)-2M_{33}r_3r_4\sin\phi\right)\cdot\left(M_{33}^2r_3+M_{33}r_4\cos\phi+M_{33}M_{c2}r_2\cos\gamma\right)\\
&+\frac{Gm_2m_4}{\kappa_4^3}\cdot\left(-M_{33}r_4\sin\phi\right)\\
&-\frac{3}{2}\frac{Gm_3m_4}{\kappa_5^5}\cdot\left(2M_{c3}r_3r_4\sin\phi\right)\cdot\left(M_{c3}^2r_3-M_{c3}r_4\cos\phi\right)+\frac{Gm_3m_4}{\kappa_5^3}\cdot\left(M_{c3}r_4\sin\phi\right)
\end{aligned}\tag{4.64}$$

at the periodic solution

$$\begin{aligned}
\left.\frac{\partial^2 H}{\partial r_3\partial\phi}\right|_{\boldsymbol{\gamma}(t)} =& 3\frac{Gmm_4}{r^5y^5}\cos^5\beta\cdot\left(\frac{1}{2}c_2c_4r^2\right)\cdot\left(M_{33}^2c_3r-M_{33}c_4r\right)+0\\
&+3\frac{Gmm_4}{r^5y^5}\cos^5\beta\cdot\left(-\frac{1}{2}c_2c_4r^2\right)\cdot\left(M_{33}^2c_3r-M_{33}c_4r\right)+0\\
&+0+0=\boxed{0}
\end{aligned}\tag{4.65}$$

Then, for the momentum variables we have:

$$\frac{\partial^2 H}{\partial r_3\partial R_2}=\frac{\partial^2 H}{\partial r_3\partial R_3}=\frac{\partial^2 H}{\partial r_3\partial R_4}=\boxed{0}\tag{4.66}$$

$$\frac{\partial^2 H}{\partial r_3\partial\Gamma}=-2\frac{\Gamma-\Phi}{M_3}\frac{1}{r_3^3}\tag{4.67}$$

$$\left.\frac{\partial^2 H}{\partial r_3 \partial \Gamma}\right|_{\boldsymbol{\gamma}(t)} = -2\frac{M_3 c_3^2 \omega}{M_3}\frac{1}{c_3^3 r^3} = -2\frac{\omega}{c_3 r^3} = \boxed{-2\frac{\omega}{r^3 y}\tan^{-1}\alpha} \tag{4.68}$$

$$\frac{\partial^2 H}{\partial r_3 \partial \Phi} = 2\frac{\Gamma-\Phi}{M_3}\frac{1}{r_3^3} \tag{4.69}$$

$$\left.\frac{\partial^2 H}{\partial r_3 \partial \Phi}\right|_{\boldsymbol{\gamma}(t)} = \boxed{2\frac{\omega}{r^3 y}\tan^{-1}\alpha} \tag{4.70}$$

Once again we find all derivatives with respect to R_i are zero, since Eq. (3.64) depends only on the gravitational forces, which are conservative and, thus, depend only on the positions, and on the centrifugal force, which, in this case, depends on the rotation rate of $\boldsymbol{u}_3$, implicit in $\Gamma - \Phi = \Theta_3$.

Now the $\frac{\partial H}{\partial \gamma}$ terms:

$$\begin{aligned}
\frac{\partial^2 H}{\partial \gamma^2} =& \frac{\partial}{\partial \gamma}\left[\begin{array}{l} -\frac{Gm_1m_3}{\kappa_1^3}M_{22}r_2r_3\sin\gamma - \frac{Gm_1m_4}{\kappa_2^3}\left(M_{c1}r_2r_4\sin(\gamma+\phi) + M_{33}M_{c1}r_2r_3\sin\gamma\right) \\ \quad + \frac{Gm_2m_3}{\kappa_3^3}M_{12}r_2r_3\sin\gamma - \frac{Gm_2m_4}{\kappa_4^3}\left(M_{c2}r_2r_4\sin(\gamma+\phi) + M_{33}M_{c2}r_2r_3\sin\gamma\right)\end{array}\right] \\
=& \frac{3}{2}\frac{Gm_1m_3}{\kappa_1^5}\cdot\left(-2M_{22}r_2r_3\sin\gamma\right)\cdot\left(M_{22}r_2r_3\sin\gamma\right) - \frac{Gm_1m_3}{\kappa_1^3}M_{22}r_2r_3\cos\gamma \\
&+ \frac{3}{2}\frac{Gm_1m_4}{\kappa_2^5}\cdot\left(-2M_{c1}r_2r_4\sin(\gamma+\phi) - 2M_{33}M_{c1}r_2r_3\sin\gamma\right)\cdot\left(M_{c1}r_2r_4\sin(\gamma+\phi) + M_{33}M_{c1}r_2r_3\sin\gamma\right) \\
&- \frac{Gm_1m_4}{\kappa_2^3}\left(M_{c1}r_2r_4\cos(\gamma+\phi) + M_{33}M_{c1}r_2r_3\cos\gamma\right) \\
&- \frac{3}{2}\frac{Gm_2m_3}{\kappa_3^5}\cdot\left(2M_{12}r_2r_3\sin\gamma\right)\cdot\left(M_{12}r_2r_3\sin\gamma\right) + \frac{Gm_2m_3}{\kappa_3^3}M_{12}r_2r_3\cos\gamma \\
&+ \frac{3}{2}\frac{Gm_2m_4}{\kappa_4^5}\cdot\left(-2M_{c2}r_2r_4\sin(\gamma+\phi) - 2M_{33}M_{c2}r_2r_3\sin\gamma\right)\cdot\left(M_{c2}r_2r_4\sin(\gamma+\phi) + M_{33}M_{c2}r_2r_3\sin\gamma\right) \\
&- \frac{Gm_2m_4}{\kappa_4^3}\cdot\left(M_{c2}r_2r_4\cos(\gamma+\phi) + M_{33}M_{c2}r_2r_3\cos\gamma\right)
\end{aligned} \tag{4.71}$$

at the periodic solution:

$$\begin{aligned}
\left.\frac{\partial^2 H}{\partial \gamma^2}\right|_{\boldsymbol{\gamma}(t)} =& -3\frac{Gmm_3}{r^5y^5}\cos^5\alpha\cdot\left(-\frac{1}{2}c_2c_3r^2\right)^2 - 3\frac{Gmm_4}{r^5y^5}\cos^5\beta\cdot\left(\frac{1}{2}c_2c_4r^2 - \frac{1}{2}M_{33}c_2c_3r^2\right)^2 \\
&- 3\frac{Gmm_3}{r^5y^5}\cos^5\alpha\cdot\left(-\frac{1}{2}c_2c_3r^2\right)^2 - 3\frac{Gmm_4}{r^5y^5}\cos^5\beta\cdot\left(-\frac{1}{2}c_2c_4r^2 + \frac{1}{2}M_{33}c_2c_3r^2\right)^2 \\
=& -\frac{3}{2}\frac{Gmm_3}{ry^5}\cos^5\alpha\cdot\left(2yy\tan\alpha\right)^2 - \frac{3}{2}\frac{Gmm_4}{ry^5}\cos^5\beta\cdot\left(2yy\left(M_{33}\tan\alpha+\tan\beta\right) - M_{33}2yy\tan\alpha\right)^2 \\
=& \boxed{-6\frac{Gmm_3}{ry}\cos^3\alpha\sin^2\alpha - 6\frac{Gmm_4}{ry}\cos^3\beta\sin^2\beta}
\end{aligned} \tag{4.72}$$

Now the derivative w.r.t. r_4:

$$\begin{aligned}
\frac{\partial^2 H}{\partial \gamma \partial r_4} =& \frac{3}{2}\frac{Gm_1m_4}{\kappa_2^5}\cdot\left(2r_4 + 2M_{c1}r_2\cos(\gamma+\phi) + 2M_{33}r_3\cos\phi\right)\cdot\left(M_{c1}r_2r_4\sin(\gamma+\phi) + M_{33}M_{c1}r_2r_3\sin\gamma\right) \\
&- \frac{Gm_1m_4}{\kappa_2^3}\cdot M_{c1}r_2\sin(\gamma+\phi) \\
&+ \frac{3}{2}\frac{Gm_2m_4}{\kappa_4^5}\cdot\left(2r_4 + 2M_{c2}r_2\cos(\gamma+\phi) + 2M_{33}r_3\cos\phi\right)\cdot\left(M_{c2}r_2r_4\sin(\gamma+\phi) + M_{33}M_{c2}r_2r_3\sin\gamma\right) \\
&- \frac{Gm_2m_4}{\kappa_4^3}\cdot M_{c2}r_2\sin(\gamma+\phi)
\end{aligned} \tag{4.73}$$

at the periodic solution:

$$\begin{aligned}\left.\frac{\partial^2 H}{\partial\gamma\partial r_4}\right|_{\boldsymbol{\gamma}(t)} =& 3\frac{Gmm_4}{r^5y^5}\cos^5\beta\cdot(c_4r-M_{33}c_3r)\cdot\left(\frac{1}{2}c_2c_4r^2-M_{33}\frac{1}{2}c_2c_3r^2\right)-\frac{Gmm_4}{r^3y^3}\cos^3\beta\cdot\frac{1}{2}c_2r\\ &+3\frac{Gmm_4}{r^5y^5}\cos^5\beta\cdot(c_4r-M_{33}c_3r)\cdot\left(-\frac{1}{2}c_2c_4r^2+M_{33}\frac{1}{2}c_2c_3r^2\right)-\frac{Gmm_4}{r^3y^3}\cos^3\beta\cdot-\frac{1}{2}c_2r\\ =&\boxed{0}\end{aligned} \tag{4.74}$$

Next, the ϕ term:

$$\begin{aligned}\frac{\partial^2 H}{\partial\gamma\partial\phi} =& \frac{3}{2}\frac{Gm_1m_4}{\kappa_2^5}\cdot\left(-2M_{c1}r_2r_4\sin(\gamma+\phi)-2M_{33}r_3r_4\sin\phi\right)\cdot\left(M_{c1}r_2r_4\sin(\gamma+\phi)+M_{33}M_{c1}r_2r_3\sin\gamma\right)\\ &-\frac{Gm_1m_4}{\kappa_2^3}\cdot M_{c1}r_2r_4\cos(\gamma+\phi)\\ &+\frac{3}{2}\frac{Gm_2m_4}{\kappa_4^5}\cdot\left(-2M_{c2}r_2r_4\sin(\gamma+\phi)-2M_{33}r_3r_4\sin\phi\right)\cdot\left(M_{c2}r_2r_4\sin(\gamma+\phi)+M_{33}M_{c2}r_2r_3\sin\gamma\right)\\ &-\frac{Gm_2m_4}{\kappa_4^3}\cdot M_{c2}r_2r_4\cos(\gamma+\phi)\end{aligned} \tag{4.75}$$

at the periodic solution:

$$\begin{aligned}\left.\frac{\partial^2 H}{\partial\gamma\partial\phi}\right|_{\boldsymbol{\gamma}(t)} =& -3\frac{Gmm_4}{r^5y^5}\cos^5\beta\cdot\left(\frac{1}{2}c_2c_4r^2\right)\cdot\left(\frac{1}{2}c_2c_4r^2-M_{33}\frac{1}{2}c_2c_3r^2\right)-0\\ &-3\frac{Gmm_4}{r^5y^5}\cos^5\beta\cdot\left(-\frac{1}{2}c_2c_4r^2\right)\cdot\left(-\frac{1}{2}c_2c_4r^2+M_{33}\frac{1}{2}c_2c_3r^2\right)-0\\ =&-\frac{3}{2}\frac{Gmm_4}{ry^5}\cos^5\beta\cdot c_2^2c_4\cdot(c_4-M_{33}c_3)\\ =&-\frac{3}{2}\frac{Gmm_4}{ry^5}\cos^5\beta\cdot4y^2\left(M_{33}\tan\alpha+\tan\beta\right)y\cdot\left(\left(M_{33}\tan\alpha+\tan\beta\right)y-M_{33}y\tan\alpha\right)\\ =&\boxed{-6\frac{Gmm_4}{ry}\cos^4\beta\sin\beta\left(M_{33}\tan\alpha+\tan\beta\right)}\end{aligned} \tag{4.76}$$

Since $\frac{\partial H}{\partial\gamma}=-\dot{\Gamma}$ does not depend on no momentum variables (Eq. (3.67)) we have

$$\frac{\partial^2 H}{\partial\gamma\partial R_2}=\frac{\partial^2 H}{\partial\gamma\partial R_3}=\partial\gamma\partial\Gamma=\frac{\partial^2 H}{\partial\gamma\partial R_4}=\frac{\partial^2 H}{\partial\gamma\partial\Phi}=\boxed{0} \tag{4.77}$$

Moving on, we have for the $\frac{\partial H}{\partial r_4}$ terms:

$$\begin{aligned}\frac{\partial^2 H}{\partial r_4^2} =& \frac{\partial}{\partial r_4}\left[\begin{array}{l}-\frac{\Phi^2}{M_4}\frac{1}{r_4^3}+\frac{Gm_1m_4}{\kappa_2^3}\left(r_4+M_{c1}r_2\cos(\gamma+\phi)+M_{33}r_3\cos\phi\right)\\ \qquad+\frac{Gm_2m_4}{\kappa_4^3}\left(r_4+M_{c2}r_2\cos(\gamma+\phi)+M_{33}r_3\cos\phi\right)+\frac{Gm_3m_4}{\kappa_5^3}\left(r_4-M_{c3}r_3\cos\phi\right)\end{array}\right]\\ =&\ 3\frac{\Phi^2}{M_4}\frac{1}{r_4^4}-3\frac{Gm_1m_4}{\kappa_2^5}\left(r_4+M_{c1}r_2\cos(\gamma+\phi)+M_{33}r_3\cos\phi\right)^2+\frac{Gm_1m_4}{\kappa_2^3}\\ &-3\frac{Gm_2m_4}{\kappa_4^5}\left(r_4+M_{c2}r_2\cos(\gamma+\phi)+M_{33}r_3\cos\phi\right)^2+\frac{Gm_2m_4}{\kappa_4^3}-3\frac{Gm_3m_4}{\kappa_5^5}\left(r_4-M_{c3}r_3\cos\phi\right)^2+\frac{Gm_3m_4}{\kappa_5^3}\end{aligned} \tag{4.78}$$

evaluated at the periodic solution:

$$\begin{aligned}
\left.\frac{\partial^2 H}{\partial r_4^2}\right|_{\boldsymbol{\gamma}(t)} =& 3\frac{M_4^2 c_4^4 \omega^2}{M_4}\frac{1}{c_4^4 r^4} - 3\frac{Gmm_4}{r^5 y^5}\cos^5\beta\,(c_4 r - M_{33}c_3 r)^2 + \frac{Gmm_4}{r^3 y^3}\cos^3\beta \\
& - 3\frac{Gmm_4}{r^5 y^5}\cos^5\beta\,(c_4 r - M_{33}c_3 r)^2 + \frac{Gmm_4}{r^3 y^3}\cos^3\beta \\
& - 3\frac{Gm_3 m_4}{r^5 y^5\left(\tan\alpha+\tan\beta\right)^5}(c_4 r + M_{c3}c_3 r)^2 + \frac{Gm_3 m_4}{r^3 y^3\left(\tan\alpha+\tan\beta\right)^3} \\
=& 3\frac{M_4\omega^2}{r^4} - 6\frac{Gmm_4}{r^3 y^5}\cos^5\beta\left(yM_{33}\tan\alpha + y\tan\beta - M_{33}y\tan\alpha\right)^2 + 2\frac{Gmm_4}{r^3 y^3}\cos^3\beta \\
& - 3\frac{Gm_3 m_4}{r^3 y^5\left(\tan\alpha+\tan\beta\right)^5}\left(yM_{33}\tan\alpha + y\tan\beta + M_{c3}y\tan\alpha\right)^2 + \frac{Gm_3 m_4}{r^3 y^3\left(\tan\alpha+\tan\beta\right)^3} \\
=& 3\frac{M_4\omega^2}{r^4} - 6\frac{Gmm_4}{r^3 y^3}\cos^5\beta\tan^2\beta + 2\frac{Gmm_4}{r^3 y^3}\cos^3\beta - 3\frac{Gm_3 m_4}{r^3 y^3\left(\tan\alpha+\tan\beta\right)^3} + \frac{Gm_3 m_4}{r^3 y^3\left(\tan\alpha+\tan\beta\right)^3} \\
=& 3M_4\frac{\omega^2}{r^4} - 2\frac{Gmm_4}{r^3 y^3}\left(3\cos^5\beta\tan^2\beta - \cos^3\beta\right) - 2\frac{Gm_3 m_4}{r^3 y^3\left(\tan\alpha+\tan\beta\right)^3} \\
=& \boxed{3M_4\frac{\omega^2}{r^4} - 2\frac{Gmm_4}{r^3 y^3}\left(2\cos^3\beta - 3\cos^5\beta\right) - 2\frac{Gm_3 m_4}{r^3 y^3}\left(\tan\alpha+\tan\beta\right)^{-3}}
\end{aligned} \tag{4.79}$$

Next, we have the derivative w.r.t. ϕ:

$$\begin{aligned}
\frac{\partial^2 H}{\partial r_4\partial\phi} =& -\frac{3}{2}\frac{Gm_1 m_4}{\kappa_2^5}\cdot\left(-2M_{c1}r_2 r_4\sin(\gamma+\phi) - 2M_{33}r_3 r_4\sin\phi\right)\cdot\left(r_4 + M_{c1}r_2\cos(\gamma+\phi) + M_{33}r_3\cos\phi\right) \\
& + \frac{Gm_1 m_4}{\kappa_2^3}\cdot\left(-M_{c1}r_2\sin(\gamma+\phi) - M_{33}r_3\sin\phi\right) \\
& - \frac{3}{2}\frac{Gm_2 m_4}{\kappa_4^5}\cdot\left(-2M_{c2}r_2 r_4\sin(\gamma+\phi) - 2M_{33}r_3 r_4\sin\phi\right)\cdot\left(r_4 + M_{c2}r_2\cos(\gamma+\phi) + M_{33}r_3\cos\phi\right) \\
& + \frac{Gm_2 m_4}{\kappa_4^2}\cdot\left(-M_{c2}r_2\sin(\gamma+\phi) - M_{33}r_3\sin\phi\right) \\
& - \frac{3}{2}\frac{Gm_3 m_4}{\kappa_5^5}\cdot\left(2M_{c3}r_3 r_4\sin\phi\right)\cdot\left(r_4 - M_{c3}r_3\cos\phi\right) + \frac{Gm_3 m_4}{\kappa_5^3}\cdot M_{c3}r_3\sin\phi
\end{aligned} \tag{4.80}$$

at the periodic solution:

$$\begin{aligned}
\left.\frac{\partial^2 H}{\partial r_4\partial\phi}\right|_{\boldsymbol{\gamma}(t)} =& -3\frac{Gmm_4}{r^5 y^5}\cos^5\beta\cdot\left(-\frac{1}{2}c_2 c_4 r^2\right)\cdot(c_4 r - M_{33}c_3 r) + \frac{Gmm_4}{r^3 y^3}\cos^3\beta\cdot\left(-\frac{1}{2}c_2 r\right) \\
& - 3\frac{Gmm_4}{r^5 y^5}\cos^5\beta\cdot\left(\frac{1}{2}c_2 c_4 r^2\right)\cdot(c_4 r - M_{33}c_3 r) + \frac{Gmm_4}{r^3 y^3}\cos^3\beta\cdot\left(\frac{1}{2}c_2 r\right) \\
& - 0 + 0 \\
=& \boxed{0}
\end{aligned} \tag{4.81}$$

Similarly to the situation for $\frac{\partial H}{\partial r_2}$ and $\frac{\partial H}{\partial r_3}$, $\frac{\partial H}{\partial r_4} = -\dot{R}_4$ (Eq. (3.65)) does not depend on no momentum variables except $\Phi = \Theta_4$ through the centrifugal force term, which depends on the rotation rate of $\boldsymbol{u}_4$.

$$\frac{\partial^2 H}{\partial r_4\partial R_2} = \frac{\partial^2 H}{\partial r_4\partial R_3} = \frac{\partial^2 H}{\partial r_4\partial R_4} = \frac{\partial^2 H}{\partial r_4\partial\Gamma} = \boxed{0} \tag{4.82}$$

$$\frac{\partial^2 H}{\partial r_4\partial\Phi} = -2\frac{\Phi}{M_4}\frac{1}{r_4^3} \tag{4.83}$$

$$\left.\frac{\partial^2 H}{\partial r_4\partial\Phi}\right|_{\boldsymbol{\gamma}(t)} = -2\frac{M_4 c_4^2\omega}{M_4}\cdot\frac{1}{c_4^3 r^3} = -2\frac{\omega}{c_4 r^3} = \boxed{-2\frac{\omega}{r^3 y}\left(M_{33}\tan\alpha + \tan\beta\right)^{-1}} \tag{4.84}$$

Finally, we compute the linear coefficients for the $\frac{\partial H}{\partial \phi}$ equation. Starting with the derivative w.r.t. ϕ:

$$
\begin{aligned}
\frac{\partial^2 H}{\partial \phi^2} = & \frac{\partial}{\partial \phi}\begin{bmatrix} -\frac{Gm_1m_4}{\kappa_2^3}\left(M_{c1}r_2r_4\sin(\gamma+\phi)+M_{33}r_3r_4\sin\phi\right) \\ -\frac{Gm_2m_4}{\kappa_4^3}\left(M_{c2}r_2r_4\sin(\gamma+\phi)+M_{33}r_3r_4\sin\phi\right)+\frac{Gm_3m_4}{\kappa_5^3}M_{c3}r_3r_4\sin\phi \end{bmatrix} \\
= & \frac{3}{2}\frac{Gm_1m_4}{\kappa_2^5}\cdot\left(-2M_{c1}r_2r_4\sin(\gamma+\phi)-2M_{33}r_3r_4\sin\phi\right)\cdot\left(M_{c1}r_2r_4\sin(\gamma+\phi)+M_{33}r_3r_4\sin\phi\right) \\
& -\frac{Gm_1m_4}{\kappa_2^3}\cdot\left(M_{c1}r_2r_4\cos(\gamma+\phi)+M_{33}r_3r_4\cos\phi\right) \\
& +\frac{3}{2}\frac{Gm_2m_4}{\kappa_4^5}\cdot\left(-2M_{c2}r_2r_4\sin(\gamma+\phi)-2M_{33}r_3r_4\sin\phi\right)\cdot\left(M_{c2}r_2r_4\sin(\gamma+\phi)+M_{33}r_3r_4\sin\phi\right) \\
& -\frac{Gm_2m_4}{\kappa_4^3}\cdot\left(M_{c2}r_2r_4\cos(\gamma+\phi)+M_{33}r_3r_4\cos\phi\right) \\
& -\frac{3}{2}\frac{Gm_3m_4}{\kappa_5^5}\cdot 2M_{c3}r_3r_4\sin\phi\cdot M_{c3}r_3r_4\sin\phi+\frac{Gm_3m_4}{\kappa_5^3}\cdot M_{c3}r_3r_4\cos\phi \\
= & -3\frac{Gm_1m_4}{\kappa_2^5}\cdot\left(M_{c1}r_2r_4\sin(\gamma+\phi)+M_{33}r_3r_4\sin\phi\right)^2-\frac{Gm_1m_4}{\kappa_2^3}\cdot\left(M_{c1}r_2r_4\cos(\gamma+\phi)+M_{33}r_3r_4\cos\phi\right) \\
& -3\frac{Gm_2m_4}{\kappa_4^5}\cdot\left(M_{c2}r_2r_4\sin(\gamma+\phi)+M_{33}r_3r_4\sin\phi\right)^2-\frac{Gm_2m_4}{\kappa_4^3}\cdot\left(M_{c2}r_2r_4\cos(\gamma+\phi)+M_{33}r_3r_4\cos\phi\right) \\
& -3\frac{Gm_3m_4}{\kappa_5^5}\cdot\left(M_{c3}r_3r_4\sin\phi\right)^2+\frac{Gm_3m_4}{\kappa_5^3}\cdot M_{c3}r_3r_4\cos\phi
\end{aligned}
\tag{4.85}
$$

at the periodic solution:

$$
\begin{aligned}
\left.\frac{\partial^2 H}{\partial \phi^2}\right|_{\boldsymbol{\gamma}(t)} = & -3\frac{Gmm_4}{r^5y^5}\cos^5\beta\cdot\left(\frac{1}{2}c_2c_4r^2\right)^2-\frac{Gmm_4}{r^3y^3}\cos^3\beta\cdot\left(-M_{33}c_3c_4r^2\right) \\
& -3\frac{Gmm_4}{r^5y^5}\cos^5\beta\cdot\left(-\frac{1}{2}c_2c_4r^2\right)^2-\frac{Gmm_4}{r^3y^3}\cos^3\beta\cdot\left(-M_{33}c_3c_4r^2\right) \\
& -0-\frac{Gm_3m_4}{r^3y^3\left(\tan\alpha+\tan\beta\right)^3}\cdot M_{c3}c_3c_4r^2 \\
= & -\frac{3}{2}\frac{Gmm_4}{ry^5}\cos^5\beta\cdot\left(2y\left(M_{33}\tan\alpha+\tan\beta\right)\right)^2+2\frac{Gmm_4}{ry^3}\cos^3\beta\cdot M_{33}y\tan\alpha\left(M_{33}\tan\alpha+\tan\beta\right) \\
& -\frac{Gm_3m_4}{ry^3\left(\tan\alpha+\tan\beta\right)^3}\cdot M_{c3}y\tan\alpha\left(M_{33}\tan\alpha+\tan\beta\right) \\
= & -6\frac{Gmm_4}{ry}\cos^5\beta\cdot\left(M_{33}\tan\alpha+\tan\beta\right)^2+2\frac{Gmm_4}{ry}\cos^3\beta\cdot M_{33}\tan\alpha\left(M_{33}\tan\alpha+\tan\beta\right) \\
& -\frac{Gm_3m_4}{ry\left(\tan\alpha+\tan\beta\right)^3}\cdot M_{c3}\tan\alpha\left(M_{33}\tan\alpha+\tan\beta\right) \\
= & 2\frac{Gmm_4}{ry}\left(M_{33}\tan\alpha+\tan\beta\right)\cos^3\beta\left(-3\cos^2\beta\left(M_{33}\tan\alpha+\tan\beta\right)+M_{33}\tan\alpha\right) \\
& -\frac{Gm_3m_4}{ry\left(\tan\alpha+\tan\beta\right)^3}\cdot M_{c3}\tan\alpha\left(M_{33}\tan\alpha+\tan\beta\right) \\
= & \boxed{\begin{aligned} & 2\frac{Gmm_4}{ry}\left(M_{33}\tan\alpha+\tan\beta\right)\cos^3\beta\left(M_{33}\tan\alpha\left(1-3\cos^2\beta\right)-3\cos\beta\sin\beta\right) \\ & -\frac{Gm_3m_4}{ry\left(\tan\alpha+\tan\beta\right)^3}\cdot M_{c3}\tan\alpha\left(M_{33}\tan\alpha+\tan\beta\right)\end{aligned}}
\end{aligned}
\tag{4.86}
$$

Same as in the $\frac{\partial H}{\partial \gamma}$ case, $\frac{\partial H}{\partial \phi} = -\dot{\Phi}$ (Eq. (3.68)) contains no momentum terms and, therefore:

$$\frac{\partial^2 H}{\partial \gamma \partial R_2} = \frac{\partial^2 H}{\partial \gamma \partial R_3} = \frac{\partial^2 H}{\partial \gamma \partial \Gamma} = \frac{\partial^2 H}{\partial \gamma \partial R_4} = \frac{\partial^2 H}{\partial \gamma \partial \Phi} = \boxed{0} \tag{4.87}$$

Now we move on to the momentum equations:

$$\frac{\partial^2 H}{\partial R_2^2} = \frac{\partial}{\partial R_2}\left[\frac{R_2}{M_2}\right] = \boxed{\frac{1}{M_2}} \tag{4.88}$$

$$\frac{\partial^2 H}{\partial R_2 \partial R_3} = \frac{\partial^2 H}{\partial R_2 \partial \Gamma} = \frac{\partial^2 H}{\partial R_2 \partial R_4} = \frac{\partial^2 H}{\partial R_2 \partial \Phi} = \boxed{0} \tag{4.89}$$

$$\frac{\partial^2 H}{\partial R_3^2} = \frac{\partial}{\partial R_3}\left[\frac{R_3}{M_3}\right] = \boxed{\frac{1}{M_3}} \tag{4.90}$$

$$\frac{\partial^2 H}{\partial R_3 \partial \Gamma} = \frac{\partial^2 H}{\partial R_3 \partial R_4} = \frac{\partial^2 H}{\partial R_3 \partial \Phi} = \boxed{0} \tag{4.91}$$

$$\frac{\partial^2 H}{\partial \Gamma^2} = \frac{\partial}{\partial \Gamma}\left[\frac{\Gamma - c}{M_2 r_2^2} + \frac{\Gamma - \Phi}{M_3 r_3^2}\right] = \frac{1}{M_2 r_2^2} + \frac{1}{M_3 r_3^2} = \frac{1}{M_2 c_2^2 r^2} + \frac{1}{M_3 c_3^2 r^2} = \boxed{\frac{1}{4M_2 r^2 y^2} + \frac{1}{M_3 r^2 y^2}\tan^{-2}\alpha} \tag{4.92}$$

$$\frac{\partial^2 H}{\partial \Gamma \partial R_4} = \boxed{0} \tag{4.93}$$

$$\frac{\partial^2 H}{\partial \Gamma \partial \Phi} = \frac{\partial}{\partial \Phi}\left[\frac{\Gamma - c}{M_2 r_2^2} + \frac{\Gamma - \Phi}{M_3 r_3^2}\right] = -\frac{1}{M_3 r_3^2} = -\frac{1}{M_3 c_3^2 r^2} = \boxed{-\frac{1}{M_3 r^2 y^2}\tan^{-2}\alpha} \tag{4.94}$$

$$\frac{\partial^2 H}{\partial R_4^2} = \frac{\partial}{\partial R_4}\left[\frac{R_4}{M_4}\right] = \boxed{\frac{1}{M_4}} \tag{4.95}$$

$$\frac{\partial^2 H}{\partial R_4 \partial \Phi} = \boxed{0} \tag{4.96}$$

$$\begin{aligned}\frac{\partial^2 H}{\partial \Phi^2} &= \frac{\partial}{\partial \Phi}\left[\frac{\Phi - \Gamma}{M_3 r_3^2} + \frac{\Phi}{M_4 r_4^2}\right] = \frac{1}{M_3 r_3^2} + \frac{1}{M_4 r_4^2} = \frac{1}{M_3 c_3^2 r^2} + \frac{1}{M_4 c_4^2 r^2} \\ &= \frac{1}{r^2}\left(\frac{1}{M_3 c_3^2} + \frac{1}{M_4 c_4^2}\right) = \frac{1}{r^2}\left(\frac{1}{M_3 y^2 \tan^2\alpha} + \frac{1}{M_4 y^2 \left(M_{33}\tan\alpha + \tan\beta\right)^2}\right) \\ &= \boxed{\frac{1}{r^2 y^2}\left(\frac{1}{M_3}\tan^{-2}\alpha + \frac{1}{M_4}\left(M_{33}\tan\alpha + \tan\beta\right)^{-2}\right)}\end{aligned} \tag{4.97}$$

Notice that the rates of change of the relative distances $\dot{r}_2 = H_{R_2}$, $\dot{r}_3 = H_{R_3}$, $\dot{r}_4 = H_{R_4}$ only depend on the respective momenta R_2, R_3 and R_4, while both angular rates $\dot{\gamma} = H_\Gamma$ and $\dot{\phi} = H_\Phi$ depend on both Γ and Φ.

Now that all individual terms have been developed and evaluated at the periodic solution $\boldsymbol{\gamma}(t)$, we refer to Eq. (4.41) to produce the matrix of coefficients of the linearized system of equations of motion:

$$JD^2H = \begin{bmatrix}
\frac{\partial^2 H}{\partial R_2 \partial r_2} & \frac{\partial^2 H}{\partial R_2 \partial r_3} & \frac{\partial^2 H}{\partial R_2 \partial \gamma} & \frac{\partial^2 H}{\partial R_2 \partial r_4} & \frac{\partial^2 H}{\partial R_2 \partial \phi} & \frac{\partial^2 H}{\partial R_2^2} & \frac{\partial^2 H}{\partial R_2 \partial R_3} & \frac{\partial^2 H}{\partial R_2 \partial \Gamma} & \frac{\partial^2 H}{\partial R_2 \partial R_4} & \frac{\partial^2 H}{\partial R_2 \partial \Phi} \\
\frac{\partial^2 H}{\partial R_3 \partial r_2} & \frac{\partial^2 H}{\partial R_3 \partial r_3} & \frac{\partial^2 H}{\partial R_3 \partial \gamma} & \frac{\partial^2 H}{\partial R_3 \partial r_4} & \frac{\partial^2 H}{\partial R_3 \partial \phi} & \frac{\partial^2 H}{\partial R_3 \partial R_2} & \frac{\partial^2 H}{\partial R_3^2} & \frac{\partial^2 H}{\partial R_3 \partial \Gamma} & \frac{\partial^2 H}{\partial R_3 \partial R_4} & \frac{\partial^2 H}{\partial R_3 \partial \Phi} \\
\frac{\partial^2 H}{\partial \Gamma \partial r_2} & \frac{\partial^2 H}{\partial \Gamma \partial r_3} & \frac{\partial^2 H}{\partial \Gamma \partial \gamma} & \frac{\partial^2 H}{\partial \Gamma \partial r_4} & \frac{\partial^2 H}{\partial \Gamma \partial \phi} & \frac{\partial^2 H}{\partial \Gamma \partial R_2} & \frac{\partial^2 H}{\partial \Gamma \partial R_3} & \frac{\partial^2 H}{\partial \Gamma^2} & \frac{\partial^2 H}{\partial \Gamma \partial R_4} & \frac{\partial^2 H}{\partial \Gamma \partial \Phi} \\
\frac{\partial^2 H}{\partial R_4 \partial r_2} & \frac{\partial^2 H}{\partial R_4 \partial r_3} & \frac{\partial^2 H}{\partial R_4 \partial \gamma} & \frac{\partial^2 H}{\partial R_4 \partial r_4} & \frac{\partial^2 H}{\partial R_4 \partial \phi} & \frac{\partial^2 H}{\partial R_4 \partial R_2} & \frac{\partial^2 H}{\partial R_4 \partial R_3} & \frac{\partial^2 H}{\partial R_4 \partial \Gamma} & \frac{\partial^2 H}{\partial R_4^2} & \frac{\partial^2 H}{\partial R_4 \partial \Phi} \\
\frac{\partial^2 H}{\partial \Phi \partial r_2} & \frac{\partial^2 H}{\partial \Phi \partial r_3} & \frac{\partial^2 H}{\partial \Phi \partial \gamma} & \frac{\partial^2 H}{\partial \Phi \partial r_4} & \frac{\partial^2 H}{\partial \Phi \partial \phi} & \frac{\partial^2 H}{\partial \Phi \partial R_2} & \frac{\partial^2 H}{\partial \Phi \partial R_3} & \frac{\partial^2 H}{\partial \Phi \partial \Gamma} & \frac{\partial^2 H}{\partial \Phi \partial R_4} & \frac{\partial^2 H}{\partial \Phi^2} \\
-\frac{\partial^2 H}{\partial r_2^2} & -\frac{\partial^2 H}{\partial r_2 \partial r_3} & -\frac{\partial^2 H}{\partial r_2 \partial \gamma} & -\frac{\partial^2 H}{\partial r_2 \partial r_4} & -\frac{\partial^2 H}{\partial r_2 \partial \phi} & -\frac{\partial^2 H}{\partial r_2 \partial R_2} & -\frac{\partial^2 H}{\partial r_2 \partial R_3} & -\frac{\partial^2 H}{\partial r_2 \partial \Gamma} & -\frac{\partial^2 H}{\partial r_2 \partial R_4} & -\frac{\partial^2 H}{\partial r_2 \partial \Phi} \\
-\frac{\partial^2 H}{\partial r_3 \partial r_2} & -\frac{\partial^2 H}{\partial r_3^2} & -\frac{\partial^2 H}{\partial r_3 \partial \gamma} & -\frac{\partial^2 H}{\partial r_3 \partial r_4} & -\frac{\partial^2 H}{\partial r_3 \partial \phi} & -\frac{\partial^2 H}{\partial r_3 \partial R_2} & -\frac{\partial^2 H}{\partial r_3 \partial R_3} & -\frac{\partial^2 H}{\partial r_3 \partial \Gamma} & -\frac{\partial^2 H}{\partial r_3 \partial R_4} & -\frac{\partial^2 H}{\partial r_3 \partial \Phi} \\
-\frac{\partial^2 H}{\partial \gamma \partial r_2} & -\frac{\partial^2 H}{\partial \gamma \partial r_3} & -\frac{\partial^2 H}{\partial \gamma^2} & -\frac{\partial^2 H}{\partial \gamma \partial r_4} & -\frac{\partial^2 H}{\partial \gamma \partial \phi} & -\frac{\partial^2 H}{\partial \gamma \partial R_2} & -\frac{\partial^2 H}{\partial \gamma \partial R_3} & -\frac{\partial^2 H}{\partial \gamma \partial \Gamma} & -\frac{\partial^2 H}{\partial \gamma \partial R_4} & -\frac{\partial^2 H}{\partial \gamma \partial \Phi} \\
-\frac{\partial^2 H}{\partial r_4 \partial r_2} & -\frac{\partial^2 H}{\partial r_4 \partial r_3} & -\frac{\partial^2 H}{\partial r_4 \partial \gamma} & -\frac{\partial^2 H}{\partial r_4^2} & -\frac{\partial^2 H}{\partial r_4 \partial \phi} & -\frac{\partial^2 H}{\partial r_4 \partial R_2} & -\frac{\partial^2 H}{\partial r_4 \partial R_3} & -\frac{\partial^2 H}{\partial r_4 \partial \Gamma} & -\frac{\partial^2 H}{\partial r_4 \partial R_4} & -\frac{\partial^2 H}{\partial r_4 \partial \Phi} \\
-\frac{\partial^2 H}{\partial \phi \partial r_2} & -\frac{\partial^2 H}{\partial \phi \partial r_3} & -\frac{\partial^2 H}{\partial \phi \partial \gamma} & -\frac{\partial^2 H}{\partial \phi \partial r_4} & -\frac{\partial^2 H}{\partial \phi^2} & -\frac{\partial^2 H}{\partial \phi \partial R_2} & -\frac{\partial^2 H}{\partial \phi \partial R_3} & -\frac{\partial^2 H}{\partial \phi \partial \Gamma} & -\frac{\partial^2 H}{\partial \phi \partial R_4} & -\frac{\partial^2 H}{\partial \phi \partial \Phi}
\end{bmatrix} \tag{4.98}$$

Substituting the terms derived in this section we get the coefficient matrix evaluated at $\boldsymbol{\gamma}(t)$:

$$JD^2H(\boldsymbol{\gamma}(t)) = \begin{bmatrix} 0 & 0 & 0 & 0 & 0 & \frac{1}{M_2} & 0 & 0 & 0 & 0 \\ 0 & 0 & 0 & 0 & 0 & 0 & \frac{1}{M_3} & 0 & 0 & 0 \\ a_0 & -a_1 & 0 & 0 & 0 & 0 & 0 & H_{\Gamma^2} & 0 & -a_3 \\ 0 & 0 & 0 & 0 & 0 & 0 & 0 & 0 & \frac{1}{M_4} & 0 \\ 0 & a_1 & 0 & -a_2 & 0 & 0 & 0 & -a_3 & 0 & H_{\Phi^2} \\ -H_{r_2^2} & -H_{r_2,r_3} & 0 & -H_{r_2,r_4} & 0 & 0 & 0 & -a_0 & 0 & 0 \\ -H_{r_3,r_2} & -H_{r_3^2} & 0 & -H_{r_3,r_4} & 0 & 0 & 0 & a_1 & 0 & -a_1 \\ 0 & 0 & -H_{\gamma^2} & 0 & -H_{\gamma,\phi} & 0 & 0 & 0 & 0 & 0 \\ -H_{r_4,r_2} & -H_{r_4,r_3} & 0 & -H_{r_4^2} & 0 & 0 & 0 & 0 & 0 & a_2 \\ 0 & 0 & -H_{\phi,\gamma} & 0 & -H_{\phi^2} & 0 & 0 & 0 & 0 & 0 \end{bmatrix} \tag{4.99}$$

where

$$a_0 = 2\frac{\omega}{r^3}\frac{1}{c_2} = \frac{\omega}{r^3 y} \tag{4.100}$$

$$a_1 = 2\frac{\omega}{r^3}\frac{1}{c_3} = 2\frac{\omega}{r^3 y}\tan^{-1}\alpha \tag{4.101}$$

$$a_2 = 2\frac{\omega}{r^3}\frac{1}{c_4} = \frac{2\omega}{r^3 y\left(M_{33}\tan\alpha + \tan\beta\right)} \tag{4.102}$$

$$a_3 = \frac{1}{M_3 r^2 c_3^2} = \frac{1}{M_3 r^2 y^2 \tan^2\alpha} \tag{4.103}$$

$$H_{\Gamma^2} = \frac{1}{r^2 y^2}\left(\frac{1}{4M_2} + \frac{1}{M_3\tan^2\alpha}\right) \tag{4.104}$$

$$H_{\Phi^2} = \frac{1}{r^2 y^2}\left(\frac{1}{M_3\tan^2\alpha} + \frac{1}{M_4\left(M_{33}\tan\alpha + \tan\beta\right)^2}\right) \tag{4.105}$$

$$\begin{aligned} -H_{r_2^2} = &-3M_2\frac{\omega^2}{r^4} + \frac{1}{4}\frac{Gmm}{r^3 y^3} \\ &+ \frac{1}{2}\frac{Gmm_3}{r^3 y^3}\left(3\cos^5\alpha - \cos^3\alpha\right) + \frac{1}{2}\frac{Gmm_4}{r^3 y^3}\left(3\cos^5\beta - \cos^3\beta\right) \end{aligned} \tag{4.106}$$

$$-H_{r_2,r_3} = -H_{r_3,r_2} = 3\frac{Gmm_3}{r^3 y^3}\cos^4\alpha\sin\alpha - 3\frac{Gmm_4}{r^3 y^3}M_{33}\cos^4\beta\sin\beta \tag{4.107}$$

$$-H_{r_2,r_4} = -H_{r_4,r_2} = 3\frac{Gmm_4}{r^3 y^3}\cos^4\beta\sin\beta \tag{4.108}$$

$$\begin{aligned} -H_{r_3^2} = &-3M_3\frac{\omega^2}{r^4} + 2\frac{Gmm_3}{r^3 y^3}\left(2\cos^3\alpha - 3\cos^5\alpha\right) \\ &+ 2\frac{Gmm_4}{r^3 y^3}M_{33}^2\left(2\cos^3\beta - 3\cos^5\beta\right) + 2\frac{Gm_3 m_4}{r^3 y^3}M_{c3}^2\left(\tan\alpha + \tan\beta\right)^{-3} \end{aligned} \tag{4.109}$$

$$-H_{r_3,r_4} = -H_{r_4,r_3} = -2\frac{Gmm_4}{r^3 y^3}M_{33}\left(2\cos^3\beta - 3\cos^5\beta\right) + 2\frac{Gm_3 m_4}{r^3 y^3}M_{c3}\left(\tan\alpha + \tan\beta\right)^{-3} \tag{4.110}$$

$$-H_{\gamma^2} = 6\frac{Gmm_3}{ry}\cos^3\alpha\sin^2\alpha + 6\frac{Gmm_4}{ry}\cos^3\beta\sin^2\beta \tag{4.111}$$

$$-H_{\gamma,\phi} = -H_{\phi,\gamma} = 6\frac{Gmm_4}{ry}\cos^4\beta\sin\beta\left(M_{33}\tan\alpha + \tan\beta\right) \tag{4.112}$$

$$-H_{r_4^2} = -3M_4\frac{\omega^2}{r^4} + 2\frac{Gmm_4}{r^3 y^3}\left(2\cos^3\beta - 3\cos^5\beta\right) + 2\frac{Gm_3 m_4}{r^3 y^3}\left(\tan\alpha + \tan\beta\right)^{-3} \tag{4.113}$$

$$\begin{aligned} -H_{\phi^2} = &-2\frac{Gmm_4}{ry}\left(M_{33}\tan\alpha + \tan\beta\right)\cos^3\beta\left(M_{33}\tan\alpha\left(1 - 3\cos^2\beta\right) - 3\cos\beta\sin\beta\right) \\ &+ \frac{Gm_3 m_4}{ry\left(\tan\alpha + \tan\beta\right)^3}\cdot M_{c3}\tan\alpha\left(M_{33}\tan\alpha + \tan\beta\right) \end{aligned} \tag{4.114}$$

Keeping in mind that $y^3 \propto Gm$, the coefficients have the form:

$$\begin{aligned}
H_{\Gamma^2} &= \frac{1}{mr^2y^2} K_{\Gamma^2}(\alpha,\beta) &&= \frac{1}{m\omega^4y^2}(1+e\cos\theta)^2 K_{\Gamma^2}(\alpha,\beta)\\
H_{\Phi^2} &= \frac{1}{mr^2y^2} K_{\Phi^2}(\alpha,\beta) &&= \frac{1}{m\omega^4y^2}(1+e\cos\theta)^2 K_{\Phi^2}(\alpha,\beta)\\
-H_{r_2^2} &= \frac{m}{r^3}\left[K_{r_2^2}(\alpha,\beta)+\frac{\omega^2}{r}W_{r_2^2}(\alpha,\beta)\right] &&= \frac{m}{\omega^6}(1+e\cos\theta)^3\left[K_{r_2^2}(\alpha,\beta)+W_{r_2^2}(\alpha,\beta)(1+e\cos\theta)\right]\\
-H_{r_2,r_3} &= \frac{m}{r^3}K_{r_2,r_3}(\alpha,\beta) &&= \frac{m}{\omega^6}(1+e\cos\theta)^3 K_{r_2,r_3}(\alpha,\beta)\\
-H_{r_2,r_4} &= \frac{m}{r^3}K_{r_2,r_4}(\alpha,\beta) &&= \frac{m}{\omega^6}(1+e\cos\theta)^3 K_{r_2,r_4}(\alpha,\beta)\\
-H_{r_3^2} &= \frac{m}{r^3}\left[K_{r_3^2}(\alpha,\beta)+\frac{\omega^2}{r}W_{r_3^2}(\alpha,\beta)\right] &&= \frac{m}{\omega^6}(1+e\cos\theta)^3\left[K_{r_3^2}(\alpha,\beta)+W_{r_3^2}(\alpha,\beta)(1+e\cos\theta)\right]\\
-H_{r_3,r_4} &= \frac{m}{r^3}K_{r_3,r_4}(\alpha,\beta) &&= \frac{m}{\omega^6}(1+e\cos\theta)^3 K_{r_3,r_4}(\alpha,\beta)\\
-H_{\gamma^2} &= \frac{Gm^2}{ry}K_{\gamma^2}(\alpha,\beta) &&= \frac{Gm^2}{\omega^2y}(1+e\cos\theta)K_{\gamma^2}(\alpha,\beta)\\
-H_{\gamma,\phi} &= \frac{Gm^2}{ry}K_{\gamma,\phi}(\alpha,\beta) &&= \frac{Gm^2}{\omega^2y}(1+e\cos\theta)K_{\gamma,\phi}(\alpha,\beta)\\
-H_{r_4^2} &= \frac{m}{r^3}\left[K_{r_4^2}(\alpha,\beta)+\frac{\omega^2}{r}W_{r_4^2}(\alpha,\beta)\right] &&= \frac{m}{\omega^6}(1+e\cos\theta)^3\left[K_{r_4^2}(\alpha,\beta)+W_{r_4^2}(\alpha,\beta)(1+e\cos\theta)\right]\\
-H_{\phi^2} &= \frac{Gm^2}{ry}K_{\phi^2}(\alpha,\beta) &&= \frac{Gm^2}{\omega^2y}(1+e\cos\theta)K_{\phi^2}(\alpha,\beta)
\end{aligned} \tag{4.115}$$

4.4. Further reduction

Having linearized the system, there is more room for reduction and simplification, but we need a few concepts from the theory of linear Hamiltonian systems first.

To start, a matrix A is called *Hamiltonian* if $A^TJ + JA = 0$ holds [17], where J is the canonical matrix, as defined in Eq. (4.37). If and only if A satisfies $A = JR$, where R is a symmetric matrix, is A Hamiltonian, according to Theorem 2.1.1. in [17]. Notice that the Hessian matrix $D^2H(\boldsymbol{\gamma}(t))$ in Eq. (4.42) is symmetric, therefore the matrix of coefficients of the linearized system $JD^2H(\boldsymbol{\gamma}(t))$ is Hamiltonian. A linear system of differential equations, whose matrix of coefficients is Hamiltonian (such as our system Eq. (4.41)) is known as a *linear Hamiltonian system.*

Next, consider a linear periodic system of differential equations

$$\dot{\boldsymbol{z}} = A(t)\boldsymbol{z} \tag{4.116}$$

with $A(t+T) = A(t)$ for all $t \in \mathbb{R}$ and let $Z(t)$ be the fundamental matrix solution of Eq. (4.116) that satisfies $Z(0) = I$. Then, $Z(t+T) = Z(t)Z(T)$ holds for all $t \in \mathbb{R}$ and $Z(T)$ is called the *monodromy matrix* of Eq. (4.116) [17], while the eigenvalues of $Z(T)$ are called the *characteristic multipliers* of Eq. (4.116) [17].

The values of the characteristic multipliers are indicators of the behaviour of the solutions [17]. To see this, consider a characteristic multiplier ρ and its associated eigenvector $\boldsymbol{s}$. $\tilde{\boldsymbol{x}}(t) = Z(t)\boldsymbol{s}$ is a solution of Eq. (4.116). Then [33]:

$$\tilde{\boldsymbol{x}}(t+T) = Z(t+T)\boldsymbol{s} = Z(t)Z(T)\boldsymbol{s} = Z(t)\rho\boldsymbol{s} = \tilde{\boldsymbol{x}}(t)\rho \tag{4.117}$$

Therefore, $|\rho| < 1$ indicates a contraction of the solution after one period, $|\rho| > 1$ indicates expansion and $|\rho| = 1$ indicates an unchanged magnitude. Because of this, the characteristic multipliers can tell us something about the stability of the system.

A *symplectic matrix* T is one, for which $T^TJT = J$ holds, where J is, again, the canonical matrix [17]. An essential fact about linear Hamiltonian systems is that their fundamental matrix solutions are symplectic for all t (Theorem 2.1.3. in [17]) and, as a consequence, so are their monodromy matrices. The monodromy matrix of the linearized Hamiltonian system Eq. (4.41) is, then, also symplectic. There are many well known, useful properties of Hamiltonian and symplectic matrices that will be instrumental in further analysis of the linearized problem.

The linearized system still has two +1 characteristic multipliers left. One of them is because of the fact that, as mentioned in Chapter 3, first integrals show up as +1 eigenvalues of the monodromy matrix [27] and we have not eliminated the energy intergral, as explained in Section 3.6. The second one stems from the fact that the derivative of the periodic solution $\dot{\boldsymbol{\gamma}}(t)$ satisfies the linearized equations Eq. (4.41). To show this fact, we write the equations of motion at the periodic solution as

$$\dot{\boldsymbol{\gamma}}(t) = JDH(\boldsymbol{\gamma}(t)) \tag{4.118}$$

where $DH(\boldsymbol{\gamma}(t))$ is the gradient of the Hamiltonian evaluated at $\boldsymbol{\gamma}(t)$ and J is the canonical matrix (it can be checked that this produces Hamilton's equations in vector form). Now taking the derivative on both sides we get (Jacobian matrix of the gradient of a function is the Hessian of that function)

$$\ddot{\boldsymbol{\gamma}}(t) = JD^2H(\boldsymbol{\gamma}(t))\dot{\boldsymbol{\gamma}}(t) \tag{4.119}$$

which shows that the time derivative of the periodic solution $\dot{\gamma}(t)$ satisfies the linearized equations Eq. (4.41). Note that, while it might be tempting to think that the periodic solution $\boldsymbol{\gamma}(t)$ satisfies the linearized variational equations Eq. (4.41), make no mistake - it does not. $\boldsymbol{\gamma}(t)$ is a periodic solution of the full equations of motion of our four-body system, around which we have linearized to arrive at Eq. (4.41). In the variational equations $\boldsymbol{\gamma}(t)$ is represented by the zero vector solution (no variation from the solution), while $\dot{\gamma}(t)$ is now a non-trivial periodic solution instead of $\boldsymbol{\gamma}(t)$.

Having established this, let $\Psi(t)$ be the fundamental solution of the linearized system Eq. (4.41) with $\Psi(0) = I$ and let $\Psi(T)$ then be the monodromy matrix, where T is the period of our periodic solution $\dot{\boldsymbol{\gamma}}(t)$, which, in turn, can be expressed as $\dot{\boldsymbol{\gamma}}(t) = \Psi(t)\dot{\boldsymbol{\gamma}}(0)$. Then,

$$\dot{\boldsymbol{\gamma}}(t+T) = \Psi(t+T)\dot{\boldsymbol{\gamma}}(0) = \Psi(t)\Psi(T)\dot{\boldsymbol{\gamma}}(0) = \Psi(t)\dot{\boldsymbol{\gamma}}(0) = \dot{\boldsymbol{\gamma}}(t) \tag{4.120}$$

since $\dot{\boldsymbol{\gamma}}(t)$ is T-periodic. So, we find that $\Psi(T)\dot{\boldsymbol{\gamma}}(0) = 1\dot{\boldsymbol{\gamma}}(0)$ must hold, which requires the multiplier associated to the eigenvector $\dot{\boldsymbol{\gamma}}(0)$ to have value +1.

In this section we use a property of Hamiltonian matrices to decouple the linearized system such that the 2×2 system with the remaining +1 multipliers is separated from the 8×8 system which determines the stability. The procedure to achieve this is from [27] and we anticipate the separation of multipliers to be produced by the decoupling since an analogous procedure for three bodies produces the desired result in [27]. By isolating only the stability-determining part of the system we simplify the problem, but we also get a clearer view of the variables that actually matter for stability.

Using the fact that for the Kepler orbit we have

$$\ddot{r} = \frac{\omega^2}{r^3} - \frac{1}{r^2} \qquad \dddot{r} = \left(-\frac{3\omega^2}{r^4} + \frac{2}{r^3}\right)\dot{r} \tag{4.121}$$

we take the time derivative of $\boldsymbol{\gamma}(t)$ (as defined in Eq. (4.38)) to get

$$\dot{\boldsymbol{\gamma}} = \begin{bmatrix} c_2\dot{r} \\ c_3\dot{r} \\ 0 \\ c_4\dot{r} \\ 0 \\ M_2c_2\ddot{r} \\ M_3c_3\ddot{r} \\ 0 \\ M_4c_4\ddot{r} \\ 0 \end{bmatrix} \qquad \ddot{\boldsymbol{\gamma}} = \begin{bmatrix} c_2\ddot{r} \\ c_3\ddot{r} \\ 0 \\ c_4\ddot{r} \\ 0 \\ M_2c_2\left(-\frac{3\omega^2}{r^4} + \frac{2}{r^3}\right)\dot{r} \\ M_3c_3\left(-\frac{3\omega^2}{r^4} + \frac{2}{r^3}\right)\dot{r} \\ 0 \\ M_4c_4\left(-\frac{3\omega^2}{r^4} + \frac{2}{r^3}\right)\dot{r} \\ 0 \end{bmatrix} \tag{4.122}$$

Combining Eqs. (4.99) to (4.102) and (4.122) we find that

$$JD^2H(\boldsymbol{\gamma}(t))\ddot{\boldsymbol{\gamma}} = \begin{bmatrix} \frac{1}{M_2}M_2c_2\ddot{r} \\ \frac{1}{M_3}M_3c_3\ddot{r} \\ \frac{2\omega}{c_2r^3}c_2\dot{r} - \frac{2\omega}{c_3r^3}c_3\dot{r} \\ \frac{1}{M_4}M_4c_4\ddot{r} \\ \frac{2\omega}{c_3r^3}c_3\dot{r} - \frac{2\omega}{c_4r^3}c_4\dot{r} \\ -H_{r_2^2}c_2\dot{r} - H_{r_2,r_3}c_3\dot{r} - H_{r_2,r_4}c_4\dot{r} \\ -H_{r_3,r_2}c_2\dot{r} - H_{r_3^2}c_3\dot{r} - H_{r_3,r_4}c_4\dot{r} \\ 0 \\ -H_{r_4,r_2}c_2\dot{r} - H_{r_4,r_3}c_3\dot{r} - H_{r_4^2}c_4\dot{r} \\ 0 \end{bmatrix} = \begin{bmatrix} c_2\ddot{r} \\ c_3\ddot{r} \\ 0 \\ c_4\ddot{r} \\ 0 \\ -H_{r_2^2}c_2\dot{r} - H_{r_2,r_3}c_3\dot{r} - H_{r_2,r_4}c_4\dot{r} \\ -H_{r_3,r_2}c_2\dot{r} - H_{r_3^2}c_3\dot{r} - H_{r_3,r_4}c_4\dot{r} \\ 0 \\ -H_{r_4,r_2}c_2\dot{r} - H_{r_4,r_3}c_3\dot{r} - H_{r_4^2}c_4\dot{r} \\ 0 \end{bmatrix} \tag{4.123}$$

According to Eqs. (4.119) and (4.122) we should have

$$\begin{aligned} -H_{r_2^2}c_2\dot{r} - H_{r_2,r_3}c_3\dot{r} - H_{r_2,r_4}c_4\dot{r} &= M_2c_2\left(-\frac{3\omega^2}{r^4} + \frac{2}{r^3}\right)\dot{r} \\ -H_{r_3,r_2}c_2\dot{r} - H_{r_3^2}c_3\dot{r} - H_{r_3,r_4}c_4\dot{r} &= M_3c_3\left(-\frac{3\omega^2}{r^4} + \frac{2}{r^3}\right)\dot{r} \\ -H_{r_4,r_2}c_2\dot{r} - H_{r_4,r_3}c_3\dot{r} - H_{r_4^2}c_4\dot{r} &= M_4c_4\left(-\frac{3\omega^2}{r^4} + \frac{2}{r^3}\right)\dot{r} \end{aligned} \tag{4.124}$$

Here we verify that this is indeed the case. Using

$$\begin{aligned} -H_{r_2^2} &= -3M_2\frac{\omega^2}{r^4} + 2\frac{Gmm}{r^3c_2^3} + 4\frac{Gmm_3}{r^3c_2^3}\left(3\cos^5\alpha - \cos^3\alpha\right) + 4\frac{Gmm_4}{r^3c_2^3}\left(3\cos^5\beta - \cos^3\beta\right) \\ -H_{r_2,r_3} &= 3\frac{Gmm_3}{r^3c_3^3}\cos\alpha\sin^4\alpha - 3\frac{Gmm_4}{r^3c_3^3}M_{33}\cos^4\beta\sin\beta\tan^3\alpha \\ -H_{r_2,r_4} &= 3\frac{Gmm_4}{r^3c_4^3}\cos^4\beta\sin\beta\left(M_{33}\tan\alpha + \tan\beta\right)^3 \end{aligned}$$

and Eqs. (4.20) and (4.34), we have

$$\begin{aligned} &-H_{r_2^2}c_2\dot{r} - H_{r_2,r_3}c_3\dot{r} - H_{r_2,r_4}c_4\dot{r} = \\ &= -3M_2\frac{\omega^2}{r^4}c_2\dot{r} + 2\frac{Gmm}{r^3c_2^2}\dot{r} + 4\frac{Gmm_3}{r^3c_2^2}\left(3\cos^5\alpha - \cos^3\alpha\right)\dot{r} + 4\frac{Gmm_4}{r^3c_2^2}\left(3\cos^5\beta - \cos^3\beta\right)\dot{r} \\ &\quad + 3\frac{Gmm_3}{r^3c_3^2}\cos\alpha\sin^4\alpha\dot{r} - 3\frac{Gmm_4}{r^3c_3^2}M_{33}\cos^4\beta\sin\beta\tan^3\alpha\dot{r} + 3\frac{Gmm_4}{r^3c_4^2}\cos^4\beta\sin\beta\left(M_{33}\tan\alpha + \tan\beta\right)^3\dot{r} \\ &= -3M_2\frac{\omega^2}{r^4}c_2\dot{r} + \frac{1}{2}\frac{Gmm}{r^3y^2}\dot{r} + \frac{Gmm_3}{r^3y^2}\left(3\cos^5\alpha - \cos^3\alpha\right)\dot{r} + \frac{Gmm_4}{r^3y^2}\left(3\cos^5\beta - \cos^3\beta\right)\dot{r} \\ &\quad + 3\frac{Gmm_3}{r^3y^2}\cos^3\alpha\sin^2\alpha\dot{r} - 3\frac{Gmm_4}{r^3y^2}M_{33}\cos^4\beta\sin\beta\tan\alpha\dot{r} + 3\frac{Gmm_4}{r^3y^2}\cos^4\beta\sin\beta\left(M_{33}\tan\alpha + \tan\beta\right)\dot{r} \end{aligned}$$

now using

$$\begin{aligned} 3\cos^5\alpha - \cos^3\alpha + 3\cos^3\alpha\sin^2\alpha &= \cos^3\alpha\left(3\cos^2\alpha - 1 + 3\sin^2\alpha\right) = 2\cos^3\alpha \\ 3\cos^5\beta - \cos^3\beta + 3\cos^4\beta\sin\beta\tan\beta &= 3\cos^5\beta - \cos^3\beta + 3\cos^3\beta\sin^2\beta = 2\cos^3\beta \end{aligned}$$

and Eqs. (4.26) and (4.29) we get

$$\begin{aligned}
&-H_{r_2^2}c_2\dot{r}-H_{r_2,r_3}c_3\dot{r}-H_{r_2,r_4}c_4\dot{r}=\\
&=-3M_2\frac{\omega^2}{r^4}c_2\dot{r}+\frac{1}{2}\frac{Gmm}{r^3y^2}\dot{r}+2\frac{Gmm_3}{r^3y^2}\cos^3\alpha\dot{r}+2\frac{Gmm_4}{r^3y^2}\cos^3\beta\dot{r}\\
&=-3M_2\frac{\omega^2}{r^4}c_2\dot{r}+\frac{c_2}{4}\frac{Gmm}{r^3y^3}\dot{r}+c_2\frac{Gmm_3}{r^3y^3}\cos^3\alpha\dot{r}+c_2\frac{Gmm_4}{r^3y^3}\cos^3\beta\dot{r}\\
&=-3M_2\frac{\omega^2}{r^4}c_2\dot{r}+\frac{c_2Gm\dot{r}}{r^3}\frac{\frac{m}{4}+m_3\cos^3\alpha+m_4\cos^3\beta}{G\left(\frac{m}{4}+m_3\cos^3\alpha+m_4\cos^3\beta\right)}=-3M_2\frac{\omega^2}{r^4}c_2\dot{r}+\frac{c_2m\dot{r}}{r^3}\\
&=-3M_2\frac{\omega^2}{r^4}c_2\dot{r}+2\frac{c_2M_2\dot{r}}{r^3}=\\
&=M_2c_2\left(-\frac{3\omega^2}{r^4}+\frac{2}{r^3}\right)\dot{r}
\end{aligned}\tag{4.125}$$

We use the property that a skew-orthogonal complement (defined below) to an invariant subspace of a Hamiltonian matrix is also invariant [27] to come up with the bases for two invariant subspaces, together spanning the whole 10-dimensional vector space. Denote by b_1 and b_2 the bases of two invariant subspaces of a square matrix A and introduce the matrix $P=\begin{bmatrix}b_1 & b_2\end{bmatrix}$. Then, the coordinate change $\boldsymbol{x}=P\boldsymbol{\xi}$ will decouple the system $\dot{\boldsymbol{x}}=A\boldsymbol{x}$ as follows:

$$\begin{aligned}
P\dot{\boldsymbol{\xi}}&=AP\boldsymbol{\xi}\\
\dot{\boldsymbol{\xi}}&=P^{-1}AP\boldsymbol{\xi}\\
\dot{\boldsymbol{\xi}}&=P^{-1}\begin{bmatrix}a_{11} & a_{12}\\ a_{21} & a_{22}\end{bmatrix}\begin{bmatrix}b_1 & b_2\end{bmatrix}\boldsymbol{\xi}\\
\dot{\boldsymbol{\xi}}&=P^{-1}\begin{bmatrix}v_1 & v_2\end{bmatrix}\boldsymbol{\xi}
\end{aligned}$$

where $v_1=Ab_1$ and $v_2=Ab_2$ are matrices containing vectors in the first invariant subspace and the second invariant subspace, respectively, by definition of b_1 and b_2. Note that $\boldsymbol{\xi}=P^{-1}\boldsymbol{x}$ can be thought of as $\boldsymbol{x}$ written in the basis of the columns of P, because mutiplying them by entries of $\boldsymbol{\xi}$ yields $\boldsymbol{x}$. In the same way $P^{-1}v_1$ will give the vectors v_1 written in the basis (b_1,b_2):

$$\dot{\boldsymbol{\xi}}=\begin{bmatrix}c_{11} & 0\\ 0 & c_{22}\end{bmatrix}\boldsymbol{\xi}$$

where we have the block diagonal form, because v_1 written in the basis (b_1,b_2) will only have non-zero entries that scale the columns of b_1 and, likewise v_2 will only have non-zero entries that lie in the second invariant subspace and, hence are formed by a linear combination of basis vectors b_2.

Define the *skew-inner product* of two vectors $\boldsymbol{v},\boldsymbol{w}\in\mathbb{R}^{10}$ as [27]

$$\Omega(\boldsymbol{v},\boldsymbol{w})=\boldsymbol{v}^TJ\boldsymbol{w}\tag{4.126}$$

Two vectors are then called *skew-orthogonal* if their skew-inner product is zero. Given an invariant subspace W of the matrix $JD^2H(\boldsymbol{\gamma}(t))$, Lemma 3.1 in [27] then states that the skew-orthogonal complement of W, defined as $W^\perp=\{\boldsymbol{v}:\Omega(\boldsymbol{v},\boldsymbol{w})=0,\forall\,\boldsymbol{w}\in W\}$, is also an invariant subspace of $JD^2H(t)$.

Using the fact that $\dot{\boldsymbol{\gamma}}(t)$ satisfies the variational equations (Eq. (4.119)) and looking at the expressions for $\dot{\boldsymbol{\gamma}}(t)$ and $\ddot{\boldsymbol{\gamma}}(t)$ Eq. (4.122) we identify the basis vectors of our first invariant subspace:

$$\begin{bmatrix}c_2\\ c_3\\ 0\\ c_4\\ 0\\ 0\\ 0\\ 0\\ 0\\ 0\end{bmatrix}\qquad\begin{bmatrix}0\\ 0\\ 0\\ 0\\ 0\\ M_2c_2\\ 0\\ M_3c_3\\ M_4c_4\\ 0\end{bmatrix}\tag{4.127}$$

Looking at Eqs. (4.122) and (4.123) we see that the first basis vector multiplying $JD^2H(\boldsymbol{\gamma}(t))$ produces the second basis vector scaled by

$$\left(-\frac{3\omega^2}{r^4}+\frac{2}{r^3}\right)$$

and the second basis vector produces the first.

To find the skew-orthogonal complement we take the skew-inner product of a general vector $\boldsymbol{w} = [ac_2 \quad ac_3 \quad 0 \quad ac_4 \quad 0 \quad bM_2c_2 \quad bM_3c_3 \quad 0 \quad bM_4c_4 \quad 0]^T$ from the first invariant subspace with an arbitrary vector $\boldsymbol{v}$ containing 10 unknowns:

$$\begin{aligned}\Omega(\boldsymbol{v},\boldsymbol{w}) = \boldsymbol{v}^T J\boldsymbol{w} = \begin{bmatrix} v_1 & v_2 & v_3 & v_4 & v_5 & v_6 & v_7 & v_8 & v_9 & v_{10}\end{bmatrix}\begin{bmatrix} bM_2c_2 \\ bM_3c_3 \\ 0 \\ bM_4c_4 \\ 0 \\ -ac_2 \\ -ac_3 \\ 0 \\ -ac_4 \\ 0 \end{bmatrix} \\ = b(v_1M_2c_2 + v_2M_3c_3 + v_4M_4c_4) - a(v_6c_2 + v_7c_3 + v_9c_4) + 0(v_3 + v_5 + v_8 + v_{10}) = 0\end{aligned} \tag{4.128}$$

Thus we have to satisfy two equations with 6 unknowns:

$$\begin{aligned} v_1M_2c_2 + v_2M_3c_3 + v_4M_4c_4 = 0 &\implies v_4 = -\frac{v_1M_2c_2 + v_2M_3c_3}{M_4c_4} \\ v_6c_2 + v_7c_3 + v_9c_4 = 0 &\implies v_9 = -\frac{v_6c_2 + v_7c_3}{c_4}\end{aligned} \tag{4.129}$$

We make a choice for v_1, v_2, v_6 and v_7:

$$\begin{aligned} v_1 = v_2 = -M_4c_4 &\implies v_4 = M_2c_2 + M_3c_3 \\ v_6 = v_7 = -c_4 &\implies v_9 = c_2 + c_3\end{aligned} \tag{4.130}$$

We make four independent basis vectors out of the remaining four free variables and set them to $v_3 = v_5 = v_8 = v_{10} = 1$. This gives us six basis vectors for the skew-orthogonal subspace:

$$\begin{bmatrix} -M_4c_4 \\ -M_4c_4 \\ 0 \\ M_2c_2 + M_3c_3 \\ 0 \\ 0 \\ 0 \\ 0 \\ 0 \\ 0 \end{bmatrix} \quad \begin{bmatrix} 0 \\ 0 \\ 0 \\ 0 \\ 0 \\ -c_4 \\ -c_4 \\ 0 \\ c_2 + c_3 \\ 0 \end{bmatrix} \quad \begin{bmatrix} 0 \\ 0 \\ 1 \\ 0 \\ 0 \\ 0 \\ 0 \\ 0 \\ 0 \\ 0 \end{bmatrix} \quad \begin{bmatrix} 0 \\ 0 \\ 0 \\ 0 \\ 1 \\ 0 \\ 0 \\ 0 \\ 0 \\ 0 \end{bmatrix} \quad \begin{bmatrix} 0 \\ 0 \\ 0 \\ 0 \\ 0 \\ 0 \\ 0 \\ 1 \\ 0 \\ 0 \end{bmatrix} \quad \begin{bmatrix} 0 \\ 0 \\ 0 \\ 0 \\ 0 \\ 0 \\ 0 \\ 0 \\ 0 \\ 1 \end{bmatrix} \tag{4.131}$$

We need two more linearly independent vectors to have a basis that spans an eight-dimensional subspace of $JD^2H(\boldsymbol{\gamma}(t))$. Towards that end, we set v_1 equal to v_4 in Eq. (4.129) and v_6 equal to v_9:

$$\begin{aligned} v_1 = v_4 = -M_3c_3 &\implies v_2 = -\frac{v_1M_2c_2 + v_4M_4c_4}{M_3c_3} = M_2c_2 + M_4c_4 \\ v_6 = v_9 = -c_3 &\implies v_7 = -\frac{v_6c_2 + v_9c_4}{c_3} = c_2 + c_4\end{aligned} \tag{4.132}$$

This gives us the two desired extra basis vectors:

$$\begin{bmatrix} -M_3c_3 \\ M_2c_2+M_4c_4 \\ 0 \\ -M_3c_3 \\ 0 \\ 0 \\ 0 \\ 0 \\ 0 \\ 0 \end{bmatrix} \quad \begin{bmatrix} 0 \\ 0 \\ 0 \\ 0 \\ 0 \\ -c_3 \\ c_2+c_4 \\ 0 \\ -c_3 \\ 0 \end{bmatrix} \tag{4.133}$$

It can be checked that all vectors in Eqs. (4.131) and (4.133) are linearly independent and, therefore, span an eight-dimensional subspace of $JD^2H(\boldsymbol{\gamma}(t))$. Furthermore, by construction, any linear combination of these basis vectors $\boldsymbol{v}$ will satisfy the criterion $\Omega(\boldsymbol{v},\boldsymbol{w})=0$ (with $\boldsymbol{w}$ as in Eq. (4.128)) and, therefore, the subspace they span is invariant by Lemma 3.1 in [27].

As explained above, we construct a matrix P out of the basis vectors of the two invariant subspaces (vectors (4.127) being the basis of the first and vectors (4.131) and (4.133) making up the basis of the second subspace) and introduce a coordinate change $\boldsymbol{\xi}=P^{-1}\boldsymbol{x}$.

$$P=\begin{bmatrix} c_2 & 0 & -M_4c_4 & -M_3c_3 & 0 & 0 & 0 & 0 & 0 & 0 \\ c_3 & 0 & -M_4c_4 & M_2c_2+M_4c_4 & 0 & 0 & 0 & 0 & 0 & 0 \\ 0 & 0 & 0 & 0 & 0 & 0 & 1 & 0 & 0 & 0 \\ c_4 & 0 & M_2c_2+M_3c_3 & -M_3c_3 & 0 & 0 & 0 & 0 & 0 & 0 \\ 0 & 0 & 0 & 0 & 0 & 0 & 0 & 1 & 0 & 0 \\ 0 & M_2c_2 & 0 & 0 & -c_4 & -c_3 & 0 & 0 & 0 & 0 \\ 0 & M_3c_3 & 0 & 0 & -c_4 & c_2+c_4 & 0 & 0 & 0 & 0 \\ 0 & 0 & 0 & 0 & 0 & 0 & 0 & 0 & 1 & 0 \\ 0 & M_4c_4 & 0 & 0 & c_2+c_3 & -c_3 & 0 & 0 & 0 & 0 \\ 0 & 0 & 0 & 0 & 0 & 0 & 0 & 0 & 0 & 1 \end{bmatrix} \tag{4.134}$$

Inverting P with Mathematica we find:

$$P^{-1}=$$

$$\frac{\omega}{c}\begin{bmatrix} c_2M_2 & c_3M_3 & 0 & c_4M_4 & 0 & 0 & 0 & 0 & 0 & 0 \\ 0 & 0 & 0 & 0 & 0 & c_2 & c_3 & 0 & c_4 & 0 \\ -\frac{c_2c_4M_2+c_3^2M_3+c_4^2M_4}{k_0} & \frac{(c_2-c_4)c_3M_3}{k_0} & 0 & \frac{c_2^2M_2+c_3^2M_3+c_2c_4M_4}{k_0} & 0 & 0 & 0 & 0 & 0 & 0 \\ -\frac{c_2c_3M_2+c_3^2M_3+c_4^2M_4}{k_0} & \frac{c_2^2M_2+c_2c_3M_3+c_4^2M_4}{k_0} & 0 & \frac{(c_2-c_3)c_4M_4}{k_0} & 0 & 0 & 0 & 0 & 0 & 0 \\ 0 & 0 & 0 & 0 & 0 & -\frac{c_3^2M_3+c_2c_4M_4+c_4^2M_4}{k} & \frac{c_3(c_2M_2-c_4M_4)}{k} & 0 & \frac{c_2^2M_2+c_2c_4M_2+c_3^2M_3}{k} & 0 \\ 0 & 0 & 0 & 0 & 0 & -\frac{c_2c_3M_3+c_3^2M_3+c_4^2M_4}{k} & \frac{c_2^2M_2+c_2c_3M_2+c_4^2M_4}{k} & 0 & \frac{c_4(c_2M_2-c_3M_3)}{k} & 0 \\ 0 & 0 & \frac{c}{\omega} & 0 & 0 & 0 & 0 & 0 & 0 & 0 \\ 0 & 0 & 0 & 0 & \frac{c}{\omega} & 0 & 0 & 0 & 0 & 0 \\ 0 & 0 & 0 & 0 & 0 & 0 & 0 & \frac{c}{\omega} & 0 & 0 \\ 0 & 0 & 0 & 0 & 0 & 0 & 0 & 0 & 0 & \frac{c}{\omega} \end{bmatrix}$$

$$=\frac{\omega}{c}\begin{bmatrix} c_2M_2 & c_3M_3 & 0 & c_4M_4 & 0 & 0 & 0 & 0 & 0 & 0 \\ 0 & 0 & 0 & 0 & 0 & c_2 & c_3 & 0 & c_4 & 0 \\ -\frac{\frac{c}{\omega}-c_2M_2(c_2-c_4)}{k_0} & \frac{c_3M_3(c_2-c_4)}{k_0} & 0 & \frac{\frac{c}{\omega}+c_4M_4(c_2-c_4)}{k_0} & 0 & 0 & 0 & 0 & 0 & 0 \\ -\frac{\frac{c}{\omega}-c_2M_2(c_2-c_3)}{k_0} & \frac{\frac{c}{\omega}+c_3M_3(c_2-c_3)}{k_0} & 0 & \frac{c_4M_4(c_2-c_3)}{k_0} & 0 & 0 & 0 & 0 & 0 & 0 \\ 0 & 0 & 0 & 0 & 0 & -\frac{\frac{c}{\omega}-c_2(c_2M_2-c_4M_4)}{k} & \frac{c_3(c_2M_2-c_4M_4)}{k} & 0 & \frac{\frac{c}{\omega}+c_4(c_2M_2-c_4M_4)}{k} & 0 \\ 0 & 0 & 0 & 0 & 0 & -\frac{\frac{c}{\omega}-c_2(c_2M_2-c_3M_3)}{k} & \frac{\frac{c}{\omega}+c_3(c_2M_2-c_3M_3)}{k} & 0 & \frac{c_4(c_2M_2-c_3M_3)}{k} & 0 \\ 0 & 0 & \frac{c}{\omega} & 0 & 0 & 0 & 0 & 0 & 0 & 0 \\ 0 & 0 & 0 & 0 & \frac{c}{\omega} & 0 & 0 & 0 & 0 & 0 \\ 0 & 0 & 0 & 0 & 0 & 0 & 0 & \frac{c}{\omega} & 0 & 0 \\ 0 & 0 & 0 & 0 & 0 & 0 & 0 & 0 & 0 & \frac{c}{\omega} \end{bmatrix} \tag{4.135}$$

where we used definition (4.23) and introduced

$$k=c_2+c_3+c_4$$
$$k_0=c_2M_2+c_3M_3+c_4M_4$$

Since $\boldsymbol{\xi} = \begin{bmatrix} \xi_1 \\ \xi_2 \\ \xi_3 \\ \xi_4 \\ \xi_5 \\ \xi_6 \\ \xi_7 \\ \xi_8 \\ \xi_9 \\ \xi_{10} \end{bmatrix} = P^{-1} \begin{bmatrix} r_2 \\ r_3 \\ \gamma \\ r_4 \\ \phi \\ R_2 \\ R_3 \\ \Gamma \\ R_4 \\ \Phi \end{bmatrix}$ we have the expressions for the new variables:

$$
\begin{aligned}
\xi_1 &= \frac{\omega}{c}\left(c_2 M_2 r_2 + c_3 M_3 r_3 + c_4 M_4 r_4\right) = \frac{c_2 M_2 r_2 + c_3 M_3 r_3 + c_4 M_4 r_4}{c_2^2 M_2 + c_3^2 M_3 + c_4^2 M_4} \\
\xi_2 &= \frac{\omega}{c}\left(c_2 R_2 + c_3 R_3 + c_4 R_4\right) = \frac{c_2 R_2 + c_3 R_3 + c_4 R_4}{c_2^2 M_2 + c_3^2 M_3 + c_4^2 M_4} = \frac{c_2 M_2 \dot{r}_2 + c_3 M_3 \dot{r}_3 + c_4 M_4 \dot{r}_4}{c_2^2 M_2 + c_3^2 M_3 + c_4^2 M_4} \\
\xi_3 &= \frac{\omega}{c}\left(-\frac{\frac{c}{\omega} - c_2 M_2 \left(c_2 - c_4\right)}{c_2 M_2 + c_3 M_3 + c_4 M_4} r_2 + \frac{c_3 M_3 \left(c_2 - c_4\right)}{c_2 M_2 + c_3 M_3 + c_4 M_4} r_3 + \frac{\frac{c}{\omega} + c_4 M_4 \left(c_2 - c_4\right)}{c_2 M_2 + c_3 M_3 + c_4 M_4} r_4\right) \\
\xi_4 &= \frac{\omega}{c}\left(-\frac{\frac{c}{\omega} - c_2 M_2 \left(c_2 - c_3\right)}{c_2 M_2 + c_3 M_3 + c_4 M_4} r_2 + \frac{\frac{c}{\omega} + c_3 M_3 \left(c_2 - c_3\right)}{c_2 M_2 + c_3 M_3 + c_4 M_4} r_3 + \frac{\left(c_2 - c_3\right) c_4 M_4}{c_2 M_2 + c_3 M_3 + c_4 M_4} r_4\right) \\
\xi_5 &= \frac{\omega}{c}\left(-\frac{\frac{c}{\omega} - c_2 \left(c_2 M_2 - c_4 M_4\right)}{c_2 + c_3 + c_4} R_2 + \frac{c_3 \left(c_2 M_2 - c_4 M_4\right)}{c_2 + c_3 + c_4} R_3 + \frac{\frac{c}{\omega} + c_4 \left(c_2 M_2 - c_4 M_4\right)}{c_2 + c_3 + c_4} R_4\right) \\
\xi_6 &= \frac{\omega}{c}\left(-\frac{\frac{c}{\omega} - c_2 \left(c_2 M_2 - c_3 M_3\right)}{c_2 + c_3 + c_4} R_2 + \frac{\frac{c}{\omega} + c_3 \left(c_2 M_2 - c_3 M_3\right)}{c_2 + c_3 + c_4} R_3 + \frac{c_4 \left(c_2 M_2 - c_3 M_3\right)}{c_2 + c_3 + c_4} R_4\right) \\
\xi_7 &= \gamma \\
\xi_8 &= \phi \\
\xi_9 &= \Gamma \\
\xi_{10} &= \Phi
\end{aligned}
\tag{4.136}
$$

Notice that the first six variables are divided by the moment of inertia of the four-body system $\frac{c}{\omega}$. We see that ξ_1 represents the scaling of the configuration, weighted by the first moments of mass of the kite configuration. ξ_2 is the time derivative of ξ_1, e.g. its momentum. ξ_3, ξ_4 represent geometric deviations from the central configuration in two independent directions, while ξ_5 and ξ_6 represent the respective momenta of these deviations. Finally, ξ_7 and ξ_8 represent the angles γ and ϕ, while ξ_9 and ξ_{10} are equal to the respective momenta Γ and Φ. Expressing the periodic solution in the new variables (plugging in expressions from Eqs. (4.19) and (4.23) into expressions (4.136)) we have:

$$
\begin{aligned}
\xi_1 &= \frac{1}{c_2^2 M_2 + c_3^2 M_3 + c_4^2 M_4}\left(c_2^2 M_2 r + c_3^2 M_3 r + c_4^2 M_4 r\right) = r \\
\xi_2 &= \frac{1}{c_2^2 M_2 + c_3^2 M_3 + c_4^2 M_4}\left(c_2^2 M_2 R + c_3^2 M_3 R + c_4^2 M_4 R\right) = R \\
\xi_3 &= \frac{\omega r}{c\left(c_2 M_2 + c_3 M_3 + c_4 M_4\right)}\left(-c_2^2 c_4 M_2 - c_3^2 c_2 M_3 - c_4^2 c_2 M_4 + \left(c_2 - c_4\right) c_3^2 M_3 + c_2^2 c_4 M_2 + c_3^2 c_4 M_3 + c_2 c_4^2 M_4\right) = 0 \\
\xi_4 &= \frac{\omega r}{c\left(c_2 M_2 + c_3 M_3 + c_4 M_4\right)}\left(-c_2^2 c_3 M_2 - c_3^2 c_2 M_3 - c_4^2 c_2 M_4 + c_2^2 c_3 M_2 + c_3^2 c_2 M_3 + c_4^2 c_3 M_4 + c_4^2 \left(c_2 - c_3\right) M_4\right) = 0 \\
\xi_5 &= \\
&= \omega R \frac{-c_3^2 M_3 c_2 M_2 - c_2^2 M_2 c_4 M_4 - c_4^2 M_4 c_2 M_2 + c_3^2 M_3 c_2 M_2 - c_3^2 M_3 c_4 M_4 + c_2^2 M_2 c_4 M_4 + c_4^2 M_4 c_2 M_2 + c_3^2 M_3 c_4 M_4}{c\left(c_2 + c_3 + c_4\right)} \\
&= 0 \\
\xi_6 &= \\
&= \omega R \frac{-c_2^2 M_2 c_3 M_3 - c_3^2 M_3 c_2 M_2 - c_4^2 M_4 c_2 M_2 + c_2^2 M_2 c_3 M_3 + c_3^2 M_3 c_2 M_2 + c_4^2 M_4 c_3 M_3 + c_4^2 M_4 c_2 M_2 - c_4^2 M_4 c_3 M_3}{c\left(c_2 + c_3 + c_4\right)} \\
&= 0
\end{aligned}
$$

$$\begin{aligned}\xi_7 &= -\frac{\pi}{2} \\ \xi_8 &= \pi \\ \xi_9 &= \omega\left(M_3 c_3^2 + M_4 c_4^2\right) \\ \xi_{10} &= \omega M_4 c_4^2\end{aligned} \tag{4.137}$$

The decoupled system in the new coordinates is

$$\dot{\boldsymbol{\xi}} = P^{-1} J D^2 H(\boldsymbol{\gamma}(t)) P \boldsymbol{\xi} = V(t)\boldsymbol{\xi} \tag{4.138}$$

We will now compute the new coefficient matrix V. Starting with $JD^2H(\boldsymbol{\gamma}(t))P$, we have:

$$\begin{aligned}&JD^2 H(\boldsymbol{\gamma}(t))P = \\ &= \begin{bmatrix}
0 & c_2 & 0 & 0 & -\frac{c_4}{M_2} & -\frac{c_3}{M_2} & 0 & 0 & 0 & 0 \\
0 & c_3 & 0 & 0 & -\frac{c_4}{M_3} & \frac{c_2+c_4}{M_3} & 0 & 0 & 0 & 0 \\
\frac{2\omega}{r^3} - \frac{2\omega}{r^3} & 0 & -2M_4\frac{c_4}{c_2}\frac{\omega}{r^3} + 2M_4\frac{c_4}{c_3}\frac{\omega}{r^3} & -2M_3\frac{c_3}{c_2}\frac{\omega}{r^3} - 2M_2\frac{c_2}{c_3}\frac{\omega}{r^3} - 2M_4\frac{c_4}{c_3}\frac{\omega}{r^3} & 0 & 0 & 0 & 0 & H_{\Gamma^2} & -\frac{1}{M_3 c_3^2 r^2} \\
0 & c_4 & 0 & 0 & \frac{c_2+c_3}{M_4} & -\frac{c_3}{M_4} & 0 & 0 & 0 & 0 \\
\frac{2\omega}{r^3} - \frac{2\omega}{r^3} & 0 & -2M_4\frac{c_4}{c_3}\frac{\omega}{r^3} - 2M_2\frac{c_2}{c_4}\frac{\omega}{r^3} - 2M_3\frac{c_3}{c_4}\frac{\omega}{r^3} & 2M_2\frac{c_2}{c_3}\frac{\omega}{r^3} + 2M_4\frac{c_4}{c_3}\frac{\omega}{r^3} + 2M_3\frac{c_3}{c_4}\frac{\omega}{r^3} & 0 & 0 & 0 & 0 & -\frac{1}{M_3 c_3^2 r^2} & H_{\Phi^2} \\
a_{61} & 0 & a_{63} & a_{64} & 0 & 0 & 0 & 0 & -\frac{2\omega}{c_2 r^3} & 0 \\
a_{71} & 0 & a_{73} & a_{74} & 0 & 0 & 0 & 0 & \frac{2\omega}{c_3 r^3} & -\frac{2\omega}{c_3 r^3} \\
0 & 0 & 0 & 0 & 0 & 0 & -H_{\gamma^2} & -H_{\gamma,\phi} & 0 & 0 \\
a_{91} & 0 & a_{93} & a_{94} & 0 & 0 & 0 & 0 & 0 & \frac{2\omega}{c_4 r^3} \\
0 & 0 & 0 & 0 & 0 & 0 & -H_{\phi,\gamma} & -H_{\phi^2} & 0 & 0
\end{bmatrix} \\
&= \begin{bmatrix}
0 & c_2 & 0 & 0 & -\frac{c_4}{M_2} & -\frac{c_3}{M_2} & 0 & 0 & 0 & 0 \\
0 & c_3 & 0 & 0 & -\frac{c_4}{M_3} & \frac{c_2+c_4}{M_3} & 0 & 0 & 0 & 0 \\
0 & 0 & 2M_4\frac{\omega}{r^3}\left(\frac{c_4}{c_3} - \frac{c_4}{c_2}\right) & 2\frac{\omega}{r^3}\left(-M_3\frac{c_3}{c_2} - M_2\frac{c_2}{c_3} - M_4\frac{c_4}{c_3}\right) & 0 & 0 & 0 & 0 & H_{\Gamma^2} & -\frac{1}{M_3 c_3^2 r^2} \\
0 & c_4 & 0 & 0 & \frac{c_2+c_3}{M_4} & -\frac{c_3}{M_4} & 0 & 0 & 0 & 0 \\
0 & 0 & 2\frac{\omega}{r^3}\left(-M_4\frac{c_4}{c_3} - M_2\frac{c_2}{c_4} - M_3\frac{c_3}{c_4}\right) & 2\frac{\omega}{r^3}\left(M_2\frac{c_2}{c_3} + M_4\frac{c_4}{c_3} + M_3\frac{c_3}{c_4}\right) & 0 & 0 & 0 & 0 & -\frac{1}{M_3 c_3^2 r^2} & H_{\Phi^2} \\
a_{61} & 0 & a_{63} & a_{64} & 0 & 0 & 0 & 0 & -\frac{2\omega}{c_2 r^3} & 0 \\
a_{71} & 0 & a_{73} & a_{74} & 0 & 0 & 0 & 0 & \frac{2\omega}{c_3 r^3} & -\frac{2\omega}{c_3 r^3} \\
0 & 0 & 0 & 0 & 0 & 0 & -H_{\gamma^2} & -H_{\gamma,\phi} & 0 & 0 \\
a_{91} & 0 & a_{93} & a_{94} & 0 & 0 & 0 & 0 & 0 & \frac{2\omega}{c_4 r^3} \\
0 & 0 & 0 & 0 & 0 & 0 & -H_{\phi,\gamma} & -H_{\phi^2} & 0 & 0
\end{bmatrix}\end{aligned} \tag{4.139}$$

where

$$\begin{aligned}a_{61} &= -c_2 H_{r_2^2} - c_3 H_{r_2,r_3} - c_4 H_{r_2,r_4} & a_{63} &= M_4 c_4 H_{r_2^2} + M_4 c_4 H_{r_2,r_3} - (M_2 c_2 + M_3 c_3) H_{r_2,r_4} \\ a_{71} &= -c_2 H_{r_3,r_2} - c_3 H_{r_3^2} - c_4 H_{r_3,r_4} & a_{73} &= M_4 c_4 H_{r_3,r_2} + M_4 c_4 H_{r_3^2} - (M_2 c_2 + M_3 c_3) H_{r_3,r_4} \\ a_{91} &= -c_2 H_{r_4,r_2} - c_3 H_{r_4,r_3} - c_4 H_{r_4^2} & a_{93} &= M_4 c_4 H_{r_4,r_2} + M_4 c_4 H_{r_4,r_3} - (M_2 c_2 + M_3 c_3) H_{r_4^2}\end{aligned}$$

$$\begin{aligned}a_{64} &= M_3 c_3 H_{r_2^2} - (M_2 c_2 + M_4 c_4) H_{r_2,r_3} + M_3 c_3 H_{r_2,r_4} \\ a_{74} &= M_3 c_3 H_{r_3,r_2} - (M_2 c_2 + M_4 c_4) H_{r_3^2} + M_3 c_3 H_{r_3,r_4} \\ a_{94} &= M_3 c_3 H_{r_4,r_2} - (M_2 c_2 + M_4 c_4) H_{r_4,r_3} + M_3 c_3 H_{r_4^2}\end{aligned}$$

The coefficient matrix of the transformed system is then:

$$V = \begin{bmatrix} 0 & v_{12} & 0 & 0 & 0 & 0 & 0 & 0 & 0 & 0 \\ v_{21} & 0 & v_{23} & v_{24} & 0 & 0 & 0 & 0 & 0 & 0 \\ 0 & 0 & 0 & 0 & v_{35} & v_{36} & 0 & 0 & 0 & 0 \\ 0 & 0 & 0 & 0 & v_{45} & v_{46} & 0 & 0 & 0 & 0 \\ v_{51} & 0 & v_{53} & v_{54} & 0 & 0 & 0 & 0 & v_{59} & v_{5,10} \\ v_{61} & 0 & v_{63} & v_{64} & 0 & 0 & 0 & 0 & v_{69} & v_{6,10} \\ 0 & 0 & v_{73} & v_{74} & 0 & 0 & 0 & 0 & H_{\Gamma^2} & -\frac{1}{M_3 c_3^2 r^2} \\ 0 & 0 & v_{83} & v_{84} & 0 & 0 & 0 & 0 & -\frac{1}{M_3 c_3^2 r^2} & H_{\Phi^2} \\ 0 & 0 & 0 & 0 & 0 & 0 & -H_{\gamma^2} & -H_{\gamma,\phi} & 0 & 0 \\ 0 & 0 & 0 & 0 & 0 & 0 & -H_{\phi,\gamma} & -H_{\phi^2} & 0 & 0 \end{bmatrix} \tag{4.140}$$

where

$$\begin{aligned}
v_{21} &= \frac{\omega}{c}\left(c_2 a_{61} + c_3 a_{71} + c_4 a_{91}\right) = \\
&= -\frac{\omega}{c}\left[c_2^2 H_{r_2^2} + 2c_2 c_3 H_{r_2,r_3} + 2c_2 c_4 H_{r2,r4} + c_3^2 H_{r_3^2} + 2c_3 c_4 H_{r_3,r_4} + c_4^2 H_{r_4^2}\right] \\
&= -\frac{\omega}{c}\left[c_2\left(c_2 H_{r_2^2} + c_3 H_{r_2,r_3} + c_4 H_{r_2,r_4}\right) + c_3\left(c_2 H_{r_3,r_2} + c_3 H_{r_3^2} + c_4 H_{r_3,r_4}\right) + c_4\left(c_2 H_{r_4,r_2} + c_3 H_{r_4,r_3} + c_4 H_{r_4^2}\right)\right] \\
&= -\frac{\omega}{c}\left[-c_2^2 M_2\left(-\frac{3\omega^2}{r^4} + \frac{2}{r^3}\right) - c_3^2 M_3\left(-\frac{3\omega^2}{r^4} + \frac{2}{r^3}\right) - c_4^2 M_4\left(-\frac{3\omega^2}{r^4} + \frac{2}{r^3}\right)\right] \\
&= -\frac{1}{c_2^2 + c_3^2 M_3 + c_4^2 M_4} \cdot -\left(c_2^2 M_2 + c_3^2 M_3 + c_4^2 M_4\right)\left(-\frac{3\omega^2}{r^4} + \frac{2}{r^3}\right) \\
&= \boxed{-\frac{3\omega^2}{r^4} + \frac{2}{r^3}}
\end{aligned}$$

$$\begin{aligned}
v_{51} &= -\frac{\omega}{c\left(c_2 + c_3 + c_4\right)}\left[\left(c_3^2 M_3 + c_4\left(c_2 + c_4\right) M_4\right) a_{61} - c_3\left(c_2 M_2 - c_4 M_4\right) a_{71} - \left(c_2\left(c_2 + c_4\right) M_2 + c_3^2 M_3\right) a_{91}\right] \\
&= \boxed{\frac{\omega}{ck}\left[-H_{r_2^2} k_1 - H_{r_2,r_3} k_2 - H_{r_2,r_4} k_3 - H_{r_3^2} k_4 - H_{r_3,r_4} k_5 - H_{r_4^2} k_6\right]}
\end{aligned}$$

$$\begin{aligned}
k &= c_2 + c_3 + c_4 \\
k_1 &= c_2\left(-M_3 c_3^2 - M_4 c_4\left(c_2 + c_4\right)\right) \\
k_2 &= c_3\left(M_2 c_2^2 - M_4 c_4\left(2c_2 + c_4\right) - M_3 c_3^2\right) \\
k_3 &= M_2 c_2^2\left(c_2 + c_4\right) + M_3 c_3^2\left(c_2 - c_4\right) - M_4 c_4^2\left(c_2 + c_4\right) \\
k_4 &= c_3^2\left(M_2 c_2 - M_4 c_4\right) \\
k_5 &= M_3 c_3^3 - M_4 c_3 c_4^2 + M_2 c_2 c_3\left(c_2 + 2c_4\right) \\
k_6 &= c_4\left(M_2 c_2\left(c_2 + c_4\right) + M_3 c_3^2\right)
\end{aligned} \tag{4.141}$$

$$\begin{aligned}
v_{61} &= -\frac{\omega}{ck}\left[\left(c_3\left(c_2 + c_3\right) M_3 + c_4^2 M_4\right) a_{61} - \left(c_2\left(c_2 + c_3\right) M_2 + c_4^2 M_4\right) a_{71} - c_4\left(c_2 M_2 - c_3 M_3\right) a_{91}\right] = \\
&= \boxed{\frac{\omega}{ck}\left[-H_{r_2^2} k_7 - H_{r_2,r_3} k_8 - H_{r_2,r_4} k_9 - H_{r_3^2} k_{10} - H_{r_3,r_4} k_{11} - H_{r_4^2} k_{12}\right]}
\end{aligned}$$

$$\begin{aligned}
k_7 &= c_2\left(-M_3 c_3\left(c_2 + c_3\right) - M_4 c_4^2\right) \\
k_8 &= M_2 c_2^2\left(c_2 + c_3\right) - M_3 c_3^2\left(c_2 + c_3\right) + M_4 c_4^2\left(c_2 - c_3\right) \\
k_9 &= c_4\left(M_2 c_2^2 - M_3 c_3\left(2c_2 + c_3\right) - M_4 c_4^2\right) \\
k_{10} &= c_3\left(M_2 c_2\left(c_2 + c_3\right) + M_4 c_4^2\right) \\
k_{11} &= c_4\left(M_2 c_2\left(c_2 + 2c_3\right) - M_3 c_3^2 + M_4 c_4^2\right) \\
k_{12} &= c_4^2\left(M_2 c_2 - M_3 c_3\right)
\end{aligned} \tag{4.142}$$

$$v_{12} = \frac{\omega}{c}\left(M_2 c_2^2 + M_3 c_3^2 + M_4 c_4^2\right) = \boxed{1} \tag{4.143}$$

$$
\begin{aligned}
v_{23} =& \frac{\omega}{c}\left(c_2 a_{63} + c_3 a_{73} + c_4 a_{93}\right) = \\
=& \boxed{\frac{\omega}{c}\left[H_{r_2^2} k_{13} + H_{r_2,r_3} k_{14} + H_{r_2,r_4} k_{15} + H_{r_3^2} k_{16} + H_{r_3,r_4} k_{17} + H_{r_4^2} k_{18}\right]} \\
& k_{13} = M_4 c_4 c_2 \\
& k_{14} = M_4 c_4 \left(c_2 + c_3\right) \\
& k_{15} = c_2\left(-M_2 c_2 - M_3 c_3\right) + M_4 c_4^2 \\
& k_{16} = M_4 c_4 c_3 \\
& k_{17} = c_3\left(-M_2 c_2 - M_3 c_3\right) + M_4 c_4^2 \\
& k_{18} = c_4\left(-M_2 c_2 - M_3 c_3\right)
\end{aligned} \tag{4.144}
$$

$$
\begin{aligned}
v_{53} =& -\frac{\omega}{ck}\left[\left(c_3^2 M_3 + c_4\left(c_2 + c_4\right) M_4\right) a_{63} - c_3\left(c_2 M_2 - c_4 M_4\right) a_{73} - \left(c_2\left(c_2 + c_4\right) M_2 + c_3^2 M_3\right) a_{93}\right] \\
=& \boxed{\frac{\omega}{ck}\left[-H_{r_2^2} k_{19} - H_{r_2,r_3} k_{20} - H_{r_2,r_4} k_{21} - H_{r_3^2} k_{22} - H_{r_3,r_4} k_{23} - H_{r_4^2} k_{24}\right]} \\
& k_{19} = M_4 c_4\left(M_3 c_3^2 + M_4 c_4\left(c_2 + c_4\right)\right) \\
& k_{20} = M_2 c_2\left(-M_4 c_4 c_3\right) + M_4^2 c_4^2 k + M_3 c_3^2 M_4 c_4 \\
& k_{21} = M_2 c_2\left(-2 M_4 c_4\left(c_2 + c_4\right) - M_3 c_3^2\right) - M_3 c_3 M_4 c_4 k - M_3^2 c_3^3 \\
& k_{22} = M_4 c_4\left(-M_2 c_2 c_3 + M_4 c_4 c_3\right) \\
& k_{23} = M_2^2 c_2^2 c_3 - M_2 c_2 M_4 c_4 k + M_3 c_3^2\left(M_2 c_2 - 2 M_4 c_4\right) \\
& k_{24} = M_2^2 c_2^2\left(c_2 + c_4\right) + M_2 c_2 M_3 c_3 k + M_3^2 c_3^3
\end{aligned} \tag{4.145}
$$

$$
\begin{aligned}
v_{63} =& -\frac{\omega}{ck}\left[\left(c_3\left(c_2 + c_3\right) M_3 + c_4^2 M_4\right) a_{63} - \left(c_2\left(c_2 + c_3\right) M_2 + c_4^2 M_4\right) a_{73} - c_4\left(c_2 M_2 - c_3 M_3\right) a_{93}\right] \\
=& \boxed{\frac{\omega}{ck}\left[-H_{r_2^2} k_{25} - H_{r_2,r_3} k_{26} - H_{r_2,r_4} k_{27} - H_{r_3^2} k_{28} - H_{r_3,r_4} k_{29} - H_{r_4^2} k_{30}\right]} \\
& k_{25} = M_4 c_4\left(M_3 c_3\left(c_2 + c_3\right) + M_4 c_4^2\right) \\
& k_{26} = M_4 c_4\left(-M_2 c_2 + M_3 c_3\right)\left(c_2 + c_3\right) \\
& k_{27} = -M_2 c_2\left(2 M_4 c_4^2 + M_3 c_3\left(c_2 + c_3\right)\right) - M_3^2 c_3^2\left(c_2 + c_3\right) \\
& k_{28} = -M_4 c_4\left(M_2 c_2\left(c_2 + c_3\right) + M_4 c_4^2\right) \\
& k_{29} = M_2 c_2\left(M_2 c_2 + M_3 c_3\right)\left(c_2 + c_3\right) + 2 M_3 c_3 M_4 c_4^2 \\
& k_{30} = c_4\left(M_2^2 c_2^2 - M_3^2 c_3^2\right)
\end{aligned} \tag{4.146}
$$

$$
\begin{aligned}
v_{73} &= \boxed{2 M_4 \frac{\omega}{r^3}\left(\frac{c_4}{c_3} - \frac{c_4}{c_2}\right)} \\
v_{83} &= \boxed{2 \frac{\omega}{r^3}\left(-M_4 \frac{c_4}{c_3} - M_2 \frac{c_2}{c_4} - M_3 \frac{c_3}{c_4}\right)}
\end{aligned} \tag{4.147}
$$

$$
\begin{aligned}
v_{24} =& \frac{\omega}{c}\left[c_2 a_{64} + c_3 a_{74} + c_4 a_{94}\right] = \\
=& \boxed{\frac{\omega}{c}\left[H_{r_2^2} k_{31} + H_{r_2,r_3} k_{32} + H_{r_2,r_4} k_{33} + H_{r_3^2} k_{34} + H_{r_3,r_4} k_{35} + H_{r_4^2} k_{36}\right]} \\
& k_{31} = M_3 c_3 c_2 \\
& k_{32} = -M_2 c_2^2 + M_3 c_3^2 - M_4 c_4 c_2 \\
& k_{33} = M_3 c_3\left(c_2 + c_4\right) \\
& k_{34} = -M_2 c_2 c_3 - M_4 c_4 c_3 \\
& k_{35} = M_3 c_3^2 - M_4 c_4^2 - M_2 c_2 c_4 \\
& k_{36} = M_3 c_3 c_4
\end{aligned} \tag{4.148}
$$

$$
\begin{aligned}
v_{54} &= -\frac{\omega}{ck}\left[\left(c_3^2 M_3 + c_4\left(c_2+c_4\right)M_4\right)a_{64} - c_3\left(M_2 c_2 - M_4 c_4\right)a_{74} - \left(c_2\left(c_2+c_4\right)M_2 + c_3^2 M_3\right)a_{94}\right] = \\
&= \boxed{\frac{\omega}{ck}\left[-H_{r_2^2}k_{37} - H_{r_2,r_3}k_{38} - H_{r_2,r_4}k_{39} - H_{r_3^2}k_{40} - H_{r_3,r_4}k_{41} - H_{r_4^2}k_{42}\right]} \\
k_{37} &= M_3 c_3\left(M_3 c_3^2 + M_4 c_4\left(c_2+c_4\right)\right) \\
k_{38} &= M_3 c_3^2\left(-2M_2 c_2\right) - M_4 c_4\left(M_2 c_2 + M_4 c_4\right)\left(c_2+c_4\right) \\
k_{39} &= M_3 c_3\left(-M_2 c_2 + M_4 c_4\right)\left(c_2+c_4\right) \\
k_{40} &= c_3\left(M_2^2 c_2^2 - M_4^2 c_4^2\right) \\
k_{41} &= M_2 c_2\left(M_2 c_2 + M_4 c_4\right)\left(c_2+c_4\right) + 2M_3 c_3^2\left(M_4 c_4\right) \\
k_{42} &= -M_2 c_2 M_3 c_3\left(c_2+c_4\right) - M_3^2 c_3^3
\end{aligned}
\tag{4.149}
$$

$$
\begin{aligned}
v_{64} &= -\frac{\omega}{ck}\left[\left(c_3\left(c_2+c_3\right)M_3 + c_4^2 M_4\right)a_{64} - \left(c_2\left(c_2+c_3\right)M_2 + c_4^2 M_4\right)a_{74} - c_4\left(M_2 c_2 - M_3 c_3\right)a_{94}\right] = \\
&= \boxed{\frac{\omega}{ck}\left[-H_{r_2^2}k_{43} - H_{r_2,r_3}k_{44} - H_{r_2,r_4}k_{45} - H_{r_3^2}k_{46} - H_{r_3,r_4}k_{47} - H_{r_4^2}k_{48}\right]} \\
k_{43} &= M_3 c_3\left(M_3 c_3\left(c_2+c_3\right) + M_4 c_4^2\right) \\
k_{44} &= \left(c_2+c_3\right)\left(-2M_2 c_2 M_3 c_3 - M_4 c_4 M_3 c_3\right) - M_4 c_4^2\left(M_2 c_2 + M_3 c_3 + M_4 c_4\right) \\
k_{45} &= M_3 c_3\left(-M_2 c_2 c_4 + M_3 c_3 k + M_4 c_4^2\right) \\
k_{46} &= M_2^2 c_2^2\left(c_2+c_3\right) + M_2 c_2 M_4 c_4 k + M_4^2 c_4^3 \\
k_{47} &= M_2^2 c_2^2 c_4 + M_2 c_2\left(M_4 c_4^2 - M_3 c_3 k\right) - M_3 c_3\left(2M_4 c_4^2\right) \\
k_{48} &= -M_2 c_2 M_3 c_3 c_4 + M_3^2 c_3^2 c_4
\end{aligned}
\tag{4.150}
$$

$$
\begin{aligned}
v_{74} &= \boxed{2\frac{\omega}{r^3}\left(-M_3\frac{c_3}{c_2} - M_2\frac{c_2}{c_3} - M_4\frac{c_4}{c_3}\right)} \\
v_{84} &= \boxed{2\frac{\omega}{r^3}\left(M_2\frac{c_2}{c_3} + M_4\frac{c_4}{c_3} + M_3\frac{c_3}{c_4}\right)}
\end{aligned}
\tag{4.151}
$$

$$
\begin{aligned}
v_{35} &= \frac{\omega}{c\left(c_2 M_2 + c_3 M_3 + c_4 M_4\right)}\left(c_2 c_4^2 + c_3 c_4^2 + c_2^2 c_4 + \frac{M_3 c_3^2 c_4 + M_4 c_4^3}{M_2} + \frac{M_2\left(c_2^3 + c_2^2 c_3\right) + M_3\left(c_3^3 + c_2 c_3^2\right)}{M_4}\right) \\
&= \frac{\left(c_2+c_3\right)M_2 + c_4 M_4}{M_2 M_4\left(c_2 M_2 + c_3 M_3 + c_4 M_4\right)} = \boxed{\frac{\left(c_2+c_3\right)M_2 + c_4 M_4}{M_2 M_4 k_0}} \\
v_{45} &= \frac{\omega}{c\left(c_2 M_2 + c_3 M_3 + c_4 M_4\right)}\left(c_2^2 c_4 - c_3^2 c_4 + \frac{M_3 c_3^2 c_4 + M_4 c_4^3}{M_2} - \frac{M_2 c_2^2 c_4 + M_4 c_4^3}{M_3}\right) \\
&= \frac{c_4\left(-M_2 + M_3\right)}{M_2 M_3\left(c_2 M_2 + c_3 M_3 + c_4 M_4\right)} = \boxed{\frac{c_4\left(-M_2 + M_3\right)}{M_2 M_3 k_0}} \\
v_{36} &= \frac{\omega}{c\left(c_2 M_2 + c_3 M_3 + c_4 M_4\right)} c_3\left(c_2^2 - c_4^2 + \frac{M_3 c_3^2 + M_4 c_4^2}{M_2} - \frac{M_2 c_2^2 + M_3 c_3^2}{M_4}\right) \\
&= \frac{c_3\left(-M_2 + M_4\right)}{M_2 M_4\left(c_2 M_2 + c_3 M_3 + c_4 M_4\right)} = \boxed{\frac{c_3\left(-M_2 + M_4\right)}{M_2 M_4 k_0}} \\
v_{46} &= \frac{\omega}{c\left(c_2 M_2 + c_3 M_3 + c_4 M_4\right)}\left(c_2 c_3^2 + c_2^2 c_3 + c_3^2 c_4 + \frac{M_3 c_3^3 + M_4 c_3 c_4^2}{M_2} + \frac{M_2 c_2^2\left(c_2+c_4\right) + M_4 c_4^2\left(c_2+c_4\right)}{M_3}\right) \\
&= \frac{\left(c_2+c_4\right)M_2 + c_3 M_3}{M_2 M_3\left(c_2 M_2 + c_3 M_3 + c_4 M_4\right)} = \boxed{\frac{\left(c_2+c_4\right)M_2 + c_3 M_3}{M_2 M_3 k_0}}
\end{aligned}
\tag{4.152}
\tag{4.153}
$$

$$
\begin{aligned}
v_{59} &= \frac{2\omega^2}{cr^3 k}\left(\frac{c_3^2}{c_2}M_3 + \frac{c_4^2}{c_2}M_4 + c_2 M_2\right) = \boxed{\frac{2\omega}{r^3}\frac{1}{c_2 k}} \\
v_{69} &= \frac{2\omega^2}{cr^3 k}\left(\frac{c_3}{c_2}\left(c_2+c_3\right)M_3 + \frac{c_4^2}{c_2}M_4 + \frac{c_2}{c_3}\left(c_2+c_3\right)M_2 + \frac{c_4^2}{c_3}M_4\right) = \boxed{\frac{2\omega}{r^3}\frac{c_2+c_3}{c_2 c_3 k}}
\end{aligned}
\tag{4.154}
$$

$$\begin{aligned} v_{5,10} &= \frac{2\omega^2}{cr^3k}\left(c_4M_4+\frac{c_2^2}{c_4}M_2+\frac{c_3^2}{c_4}M_3\right)=\boxed{\frac{2\omega}{r^3}\frac{1}{c_4k}} \\ v_{6,10} &= -\frac{2\omega^2}{cr^3k}\left(\frac{c_2^2}{c_3}M_2+\frac{c_4^2}{c_3}M_4+c_3M_3\right)=\boxed{-\frac{2\omega}{r^3}\frac{1}{c_3k}} \end{aligned} \tag{4.155}$$

Using Eq. (4.124) we get

$$\begin{aligned} v_{51} =& -H_{r_2^2}k_1-H_{r_2,r_3}k_2-H_{r_2,r_4}k_3-H_{r_3^2}k_4-H_{r_3,r_4}k_5-H_{r_4^2}k_6 \\ =& -H_{r_2^2}c_2\left(-M_3c_3^2-M_4c_4\left(c_2+c_4\right)\right)-H_{r_2,r_3}c_3\left(M_2c_2^2-M_4c_4\left(2c_2+c_4\right)-M_3c_3^2\right) \\ & -H_{r_2,r_4}\left(M_2c_2^2\left(c_2+c_4\right)+M_3c_3^2\left(c_2-c_4\right)-M_4c_4^2\left(c_2+c_4\right)\right)-H_{r_3^2}c_3^2\left(M_2c_2-M_4c_4\right) \\ & -H_{r_3,r_4}\left(M_3c_3^3-M_4c_3c_4^2+M_2c_2c_3\left(c_2+2c_4\right)\right)-H_{r_4^2}c_4\left(M_2c_2\left(c_2+c_4\right)+M_3c_3^2\right) \\ =& M_2c_2^2\left(-H_{r_4,r_2}c_2-H_{r_4,r_3}c_3-H_{r_4^2}c_4\right) \\ & +M_3c_3^2\left(H_{r_2^2}c_2+H_{r_2,r_3}c_3-H_{r_2,r_4}\left(c_2-c_4\right)-H_{r_3,r_4}c_3-H_{r_4^2}c_4\right)+M_4c_4^2\left(H_{r_2^2}c_2+H_{r_2,r_3}c_3+H_{r_2,r_4}c_4\right) \\ & +M_2c_2c_3\left(-H_{r_3,r_2}c_2-H_{r_3^2}c_3-H_{r_3,r_4}c_4\right)+M_2c_2c_4\left(-H_{r_4,r_2}c_2-H_{r_4,r_3}c_3-H_{r_4^2}c_4\right) \\ & +M_4c_4c_2\left(H_{r_2^2}c_2+H_{r_2,r_3}c_3+H_{r_2,r_4}c_4\right)+M_4c_4c_3\left(H_{r_3,r_2}c_2+H_{r_3^2}c_3+H_{r_3,r_4}c_4\right) \\ =& M_2c_2^2M_4c_4\left(-\frac{3\omega^2}{r^4}+\frac{2}{r^3}\right)-M_3c_3^2M_2c_2\left(-\frac{3\omega^2}{r^4}+\frac{2}{r^3}\right)+M_3c_3^2M_4c_4\left(-\frac{3\omega^2}{r^4}+\frac{2}{r^3}\right)-M_4c_4^2M_2c_2\left(-\frac{3\omega^2}{r^4}+\frac{2}{r^3}\right) \\ & +M_2c_2c_3M_3c_3\left(-\frac{3\omega^2}{r^4}+\frac{2}{r^3}\right)-M_4c_4c_2M_2c_2\left(-\frac{3\omega^2}{r^4}+\frac{2}{r^3}\right) \\ & +M_2c_2c_4M_4c_4\left(-\frac{3\omega^2}{r^4}+\frac{2}{r^3}\right)-M_4c_4c_3M_3c_3\left(-\frac{3\omega^2}{r^4}+\frac{2}{r^3}\right) \\ =& \boxed{0} \end{aligned} \tag{4.156}$$

Similarly,

$$\begin{aligned} v_{61} =& -H_{r_2^2}k_7-H_{r_2,r_3}k_8-H_{r_2,r_4}k_9-H_{r_3^2}k_{10}-H_{r_3,r_4}k_{11}-H_{r_4^2}k_{12} \\ =& -H_{r_2^2}c_2\left(-M_3c_3\left(c_2+c_3\right)-M_4c_4^2\right)-H_{r_2,r_3}\left(M_2c_2^2\left(c_2+c_3\right)-M_3c_3^2\left(c_2+c_3\right)+M_4c_4^2\left(c_2-c_3\right)\right) \\ & -H_{r_2,r_4}c_4\left(M_2c_2^2-M_3c_3\left(2c_2+c_3\right)-M_4c_4^2\right)-H_{r_3^2}c_3\left(M_2c_2\left(c_2+c_3\right)+M_4c_4^2\right) \\ & -H_{r_3,r_4}c_4\left(M_2c_2\left(c_2+2c_3\right)-M_3c_3^2+M_4c_4^2\right)-H_{r_4^2}c_4^2\left(M_2c_2-M_3c_3\right) \\ =& M_2c_2^2\left(-H_{r_3,r_2}c_2-H_{r_3^2}c_3-H_{r_3,r_4}c_4\right)+M_3c_3^2\left(H_{r_2^2}c_2+H_{r_2,r_3}c_3+H_{r_2,r_4}c_4\right) \\ & +M_4c_4^2\left(H_{r_2^2}c_2+H_{r_2,r_3}c_3+H_{r_2,r_4}c_4-H_{r_3,r_2}c_2-H_{r_3^2}c_3-H_{r_3,r_4}c_4\right) \\ & M_2c_2c_3\left(-H_{r_3,r_2}c_2-H_{r_3^2}c_3-H_{r_3,r_4}c_4\right)+M_2c_2c_4\left(-H_{r_4,r_2}c_2-H_{r_4,r_3}c_3-H_{r_4^2}c_4\right) \\ & M_3c_3c_2\left(H_{r_2^2}c_2+H_{r_2,r_3}c_3+H_{r_2,r_4}c_4\right)+M_3c_3c_4\left(H_{r_4,r_2}c_2+H_{r_4,r_3}c_3+H_{r_4^2}c_4\right) \\ =& M_2c_2^2M_3c_3\left(-\frac{3\omega^2}{r^4}+\frac{2}{r^3}\right)+M_3c_3^2\left(-M_2c_2\right)\left(-\frac{3\omega^2}{r^4}+\frac{2}{r^3}\right) \\ & +M_4c_4^2\left(-M_2c_2+M_3c_3\right)\left(-\frac{3\omega^2}{r^4}+\frac{2}{r^3}\right) \\ & +M_2c_2c_3M_3c_3\left(-\frac{3\omega^2}{r^4}+\frac{2}{r^3}\right)+M_2c_2c_4M_4c_4\left(-\frac{3\omega^2}{r^4}+\frac{2}{r^3}\right) \\ & +M_3c_3c_2\left(-M_2c_2\right)\left(-\frac{3\omega^2}{r^4}+\frac{2}{r^3}\right)+M_3c_3c_4\left(-M_4c_4\right)\left(-\frac{3\omega^2}{r^4}+\frac{2}{r^3}\right) \\ =& \boxed{0} \end{aligned} \tag{4.157}$$

and

$$\begin{aligned}
v_{23} &= H_{r_2^2} k_{13} + H_{r_2,r_3} k_{14} + H_{r_2,r_4} k_{15} + H_{r_3^2} k_{16} + H_{r_3,r_4} k_{17} + H_{r_4^2} k_{18} \\
&= H_{r_2^2} M_4 c_4 c_2 + H_{r_2,r_3} M_4 c_4 (c_2 + c_3) + H_{r_2,r_4} \left(c_2 (-M_2 c_2 - M_3 c_3) + M_4 c_4^2 \right) \\
&\quad + H_{r_3^2} M_4 c_4 c_3 + H_{r_3,r_4} \left(c_3 (-M_2 c_2 - M_3 c_3) + M_4 c_4^2 \right) + H_{r_4^2} c_4 (-M_2 c_2 - M_3 c_3) \\
&= M_4 c_4 \left(H_{r_2^2} c_2 + H_{r_2,r_3} c_3 + H_{r_2,r_4} c_4 + H_{r_3,r_2} c_2 + H_{r_3^2} c_3 + H_{r_3,r_4} c_4 \right) - (M_2 c_2 + M_3 c_3) \left(H_{r_4^2} c_2 + H_{r_4,r_3} c_3 + H_{r_4^2} c_4 \right) \\
&= M_4 c_4 \left(-\frac{3\omega^2}{r^4} + \frac{2}{r^3} \right) (-M_2 c_2 - M_3 c_3) - (M_2 c_2 + M_3 c_3) \left(-\frac{3\omega^2}{r^4} + \frac{2}{r^3} \right) (-M_4 c_4) \\
&= \boxed{0}
\end{aligned} \tag{4.158}$$

and

$$\begin{aligned}
v_{24} &= H_{r_2^2} k_{31} + H_{r_2,r_3} k_{32} + H_{r_2,r_4} k_{33} + H_{r_3^2} k_{34} + H_{r_3,r_4} k_{35} + H_{r_4^2} k_{36} \\
&= H_{r_2^2} M_3 c_3 c_2 + H_{r_2,r_3} \left(-M_2 c_2^2 + M_3 c_3^2 - M_4 c_4 c_2 \right) + H_{r_2,r_4} M_3 c_3 (c_2 + c_4) \\
&\quad + H_{r_3^2} (-M_2 c_2 c_3 - M_4 c_4 c_3) + H_{r_3,r_4} \left(-M_2 c_2 c_4 + M_3 c_3^2 - M_4 c_4^2 \right) + H_{r_4^2} M_3 c_3 c_4 \\
&= M_2 c_2 \left(-H_{r_3,r_2} c_2 - H_{r_3^2} c_3 - H_{r_3,r_4} c_4 \right) \\
&\quad + M_3 c_3 \left(H_{r_2^2} c_2 + H_{r_2,r_3} c_3 + H_{r_2,r_4} c_4 + H_{r_4,r_2} c_2 + H_{r_4,r_3} c_3 + H_{r_4^2} c_4 \right) \\
&\quad + M_4 c_4 \left(-H_{r_3,r_2} c_2 - H_{r_3^2} c_3 - H_{r_3,r_4} c_4 \right) \\
&= M_2 c_2 \left(-\frac{3\omega^2}{r^4} + \frac{2}{r^3} \right) M_3 c_3 + M_3 c_3 \left(-\frac{3\omega^2}{r^4} + \frac{2}{r^3} \right) (-M_2 c_2 - M_4 c_4) + M_4 c_4 \left(-\frac{3\omega^2}{r^4} + \frac{2}{r^3} \right) M_3 c_3 \\
&= \boxed{0}
\end{aligned} \tag{4.159}$$

We find that, as expected, the new system is decoupled into 2x2 and 8x8 systems

$$\begin{bmatrix} \dot{\xi}_1 \\ \dot{\xi}_2 \\ \dot{\xi}_3 \\ \dot{\xi}_4 \\ \dot{\xi}_5 \\ \dot{\xi}_6 \\ \dot{\xi}_7 \\ \dot{\xi}_8 \\ \dot{\xi}_9 \\ \dot{\xi}_{10} \end{bmatrix} = \begin{bmatrix} 0 & 1 & 0 & 0 & 0 & 0 & 0 & 0 & 0 & 0 \\ -\frac{3\omega^2}{r^4} + \frac{2}{r^3} & 0 & 0 & 0 & 0 & 0 & 0 & 0 & 0 & 0 \\ 0 & 0 & 0 & 0 & v_{35} & v_{36} & 0 & 0 & 0 & 0 \\ 0 & 0 & 0 & 0 & v_{45} & v_{46} & 0 & 0 & 0 & 0 \\ 0 & 0 & v_{53} & v_{54} & 0 & 0 & 0 & 0 & \frac{2\omega}{r^3} \frac{1}{c_2 k} & \frac{2\omega}{r^3} \frac{1}{c_4 k} \\ 0 & 0 & v_{63} & v_{64} & 0 & 0 & 0 & 0 & \frac{2\omega}{r^3} \frac{c_2 + c_3}{c_2 c_3 k} & -\frac{2\omega}{r^3} \frac{1}{c_3 k} \\ 0 & 0 & v_{73} & v_{74} & 0 & 0 & 0 & 0 & H_{\Gamma^2} & -\frac{1}{M_3 c_3^2 r^2} \\ 0 & 0 & v_{83} & v_{84} & 0 & 0 & 0 & 0 & -\frac{1}{M_3 c_3^2 r^2} & H_{\Phi^2} \\ 0 & 0 & 0 & 0 & 0 & 0 & -H_{\gamma^2} & -H_{\gamma,\phi} & 0 & 0 \\ 0 & 0 & 0 & 0 & 0 & 0 & -H_{\phi,\gamma} & -H_{\phi^2} & 0 & 0 \end{bmatrix} \begin{bmatrix} \xi_1 \\ \xi_2 \\ \xi_3 \\ \xi_4 \\ \xi_5 \\ \xi_6 \\ \xi_7 \\ \xi_8 \\ \xi_9 \\ \xi_{10} \end{bmatrix} \tag{4.160}$$

The 2x2 system is

$$\begin{aligned}
\dot{\xi}_1 &= \xi_2 \\
\dot{\xi}_2 &= \left(-\frac{3\omega^2}{r^4} + \frac{2}{r^3} \right) \xi_1
\end{aligned} \tag{4.161}$$

Making use of Eq. (4.121), we find as a solution

$$\begin{aligned}
\xi_1(t) &= k \dot{r}(t) \\
\xi_2(t) &= k \ddot{r}(t)
\end{aligned} \tag{4.162}$$

If we set the initial conditions to $\xi_1(0) = 0$, $\xi_2(0) = 1$, we obtain

$$k = \frac{\omega^4}{e(1+e)^2} \tag{4.163}$$

Since our solution is periodic we have that $x(T) = x(0) = 0$ and $X(T) = X(0) = 1$. We set the fundamental matrix at initial time $X(0)$ to the identity matrix. Then,

$$X(0) = \begin{bmatrix} 1 & 0 \\ 0 & 1 \end{bmatrix} \qquad X(T) = \begin{bmatrix} \star & 0 \\ \star & 1 \end{bmatrix} \tag{4.164}$$

because we know that (0,1) is the initial condition of the periodic solution. Further, we know that the monodromy matrix $X(T)$ is symplectic and, therefore has 1 as its determinant. That means

$$X(T) = \begin{bmatrix} 1 & 0 \\ \star & 1 \end{bmatrix} \tag{4.165}$$

and we have that the two eigenvalues are both 1. So, we confirmed that the two remaining +1 characteristic multipliers are contained in the 2x2 system and linear stability is determined by the remaining 8x8 system:

$$\begin{bmatrix} \dot{\xi}_3 \\ \dot{\xi}_4 \\ \dot{\xi}_5 \\ \dot{\xi}_6 \\ \dot{\xi}_7 \\ \dot{\xi}_8 \\ \dot{\xi}_9 \\ \dot{\xi}_{10} \end{bmatrix} = \begin{bmatrix} 0 & 0 & v_{35} & v_{36} & 0 & 0 & 0 & 0 \\ 0 & 0 & v_{45} & v_{46} & 0 & 0 & 0 & 0 \\ v_{53} & v_{54} & 0 & 0 & 0 & 0 & \frac{2\omega}{r^3}\frac{1}{c_2 k} & \frac{2\omega}{r^3}\frac{1}{c_4 k} \\ v_{63} & v_{64} & 0 & 0 & 0 & 0 & \frac{2\omega}{r^3}\frac{c_2+c_3}{c_2 c_3 k} & -\frac{2\omega}{r^3}\frac{1}{c_3 k} \\ v_{73} & v_{74} & 0 & 0 & 0 & 0 & H_{\Gamma^2} & -\frac{1}{M_3 c_3^2 r^2} \\ v_{83} & v_{84} & 0 & 0 & 0 & 0 & -\frac{1}{M_3 c_3^2 r^2} & H_{\Phi^2} \\ 0 & 0 & 0 & 0 & -H_{\gamma^2} & -H_{\gamma,\phi} & 0 & 0 \\ 0 & 0 & 0 & 0 & -H_{\phi,\gamma} & -H_{\phi^2} & 0 & 0 \end{bmatrix} \begin{bmatrix} \xi_3 \\ \xi_4 \\ \xi_5 \\ \xi_6 \\ \xi_7 \\ \xi_8 \\ \xi_9 \\ \xi_{10} \end{bmatrix} \tag{4.166}$$

From Eq. (4.115) we see that all radius double derivatives take the form

$$\frac{m}{r^3}\left[K(\alpha,\beta) + \frac{\omega^2}{r} W(\alpha,\beta)\right]$$

while the v coefficients are scaled by

Coefficient	v_{53}		v_{63}		v_{54}		v_{64}	
Term	k_{19-24}	$\frac{\omega}{ck}$	k_{25-30}	$\frac{\omega}{ck}$	k_{37-42}	$\frac{\omega}{ck}$	k_{43-48}	$\frac{\omega}{ck}$
Scaling	m^2y^3	$\frac{1}{my^3}$	m^2y^3	$\frac{1}{my^3}$	m^2y^3	$\frac{1}{my^3}$	m^2y^3	$\frac{1}{my^3}$

Thus the coefficients take the forms

$$\begin{aligned} v_{53} &= \frac{m^2}{r^3}\left[K_{31}(\alpha,\beta) + W_{31}(\alpha,\beta)\frac{\omega^2}{r}\right] & v_{54} &= \frac{m^2}{r^3}\left[K_{32}(\alpha,\beta) + W_{32}(\alpha,\beta)\frac{\omega^2}{r}\right] & v_{35} &= \frac{1}{m^2}K_{13}(\alpha,\beta) \\ v_{63} &= \frac{m^2}{r^3}\left[K_{41}(\alpha,\beta) + W_{41}(\alpha,\beta)\frac{\omega^2}{r}\right] & v_{64} &= \frac{m^2}{r^3}\left[K_{42}(\alpha,\beta) + W_{42}(\alpha,\beta)\frac{\omega^2}{r}\right] & v_{45} &= \frac{1}{m^2}K_{23}(\alpha,\beta) \\ v_{73} &= \frac{m\omega}{r^3}K_{51}(\alpha,\beta) & v_{74} &= \frac{m\omega}{r^3}K_{52}(\alpha,\beta) & v_{36} &= \frac{1}{m^2}K_{14}(\alpha,\beta) \\ v_{83} &= \frac{m\omega}{r^3}K_{61}(\alpha,\beta) & v_{84} &= \frac{m\omega}{r^3}K_{62}(\alpha,\beta) & v_{46} &= \frac{1}{m^2}K_{24}(\alpha,\beta) \end{aligned} \tag{4.167}$$

while

$$\begin{aligned} v_{59} &= \frac{2\omega}{r^3}\frac{1}{c_2 k} = \frac{\omega}{r^3 y^2}K_{37}(\alpha,\beta) & v_{5,10} &= \frac{2\omega}{r^3}\frac{1}{c_4 k} = \frac{\omega}{r^3 y^2}K_{38}(\alpha,\beta) & -\frac{1}{M_3 c_3^2 r^2} &= \frac{1}{my^2 r^2}K_{67}(\alpha,\beta) \\ v_{69} &= \frac{2\omega}{r^3}\frac{c_2+c_3}{c_2 c_3 k} = \frac{\omega}{r^3 y^2}K_{47}(\alpha,\beta) & v_{6,10} &= -\frac{2\omega}{r^3}\frac{1}{c_3 k} = \frac{\omega}{r^3 y^2}K_{48}(\alpha,\beta) & & \end{aligned} \tag{4.168}$$

To summarize, we have obtained an 8x8 linear periodic system of differential equations which describes the stability-determining part of the linearized dynamics of perturbations from the periodic solution. We have conveniently collected all geometric terms involving trigonometric functions of α and β into dimensionless K and W variables, while the dimensional quantities are all pulled out as factors multiplying the K and W coefficients in Eqs. (4.167) and (4.168). This suggests a possibility to cancel out some of the dimensional factors by linear coordinate changes, as done in the next section.

4.5. Simplification

A linear change of variables does not change the characteristic multipliers [27]. In this section an attempt is made to simplify the reduced system (4.166) as much as possible to make visible only the essential factors

that determine the stability. To that end, we change the independent variable from t to θ and scale the eight state variables by appropriate factors.

From Eq. (4.7)

$$\dot{\xi} = \frac{d\xi}{dt} = \frac{d\xi}{d\theta}\frac{d\theta}{dt} = \frac{d\xi}{d\theta}\frac{\omega}{r^2} = \xi'\frac{\omega}{r^2} \tag{4.169}$$

Plugging it into Eq. (4.166) gives

$$\begin{aligned}
\begin{bmatrix} \xi_3' \\ \xi_4' \\ \xi_5' \\ \xi_6' \\ \xi_7' \\ \xi_8' \\ \xi_9' \\ \xi_{10}' \end{bmatrix} &= \frac{r^2}{\omega}\begin{bmatrix} 0 & 0 & v_{35} & v_{36} & 0 & 0 & 0 & 0 \\ 0 & 0 & v_{45} & v_{46} & 0 & 0 & 0 & 0 \\ v_{53} & v_{54} & 0 & 0 & 0 & 0 & \frac{2\omega}{r^3}\frac{1}{c_2k} & \frac{2\omega}{r^3}\frac{1}{c_4k} \\ v_{63} & v_{64} & 0 & 0 & 0 & 0 & \frac{2\omega}{r^3}\frac{c_2+c_3}{c_2c_3k} & -\frac{2\omega}{r^3}\frac{1}{c_3k} \\ v_{73} & v_{74} & 0 & 0 & 0 & 0 & H_{\Gamma^2} & -\frac{1}{M_3c_3^2r^2} \\ v_{83} & v_{84} & 0 & 0 & 0 & 0 & -\frac{1}{M_3c_3^2r^2} & H_{\Phi^2} \\ 0 & 0 & 0 & 0 & -H_{\gamma^2} & -H_{\gamma,\phi} & 0 & 0 \\ 0 & 0 & 0 & 0 & -H_{\phi,\gamma} & -H_{\phi^2} & 0 & 0 \end{bmatrix}\begin{bmatrix} \xi_3 \\ \xi_4 \\ \xi_5 \\ \xi_6 \\ \xi_7 \\ \xi_8 \\ \xi_9 \\ \xi_{10} \end{bmatrix} \\
&= \begin{bmatrix} 0 & 0 & \frac{r^2}{\omega}v_{35} & \frac{r^2}{\omega}v_{36} & 0 & 0 & 0 & 0 \\ 0 & 0 & \frac{r^2}{\omega}v_{45} & \frac{r^2}{\omega}v_{46} & 0 & 0 & 0 & 0 \\ \frac{r^2}{\omega}v_{53} & \frac{r^2}{\omega}v_{54} & 0 & 0 & 0 & 0 & \frac{2}{r}\frac{1}{c_2k} & \frac{2}{r}\frac{1}{c_4k} \\ \frac{r^2}{\omega}v_{63} & \frac{r^2}{\omega}v_{64} & 0 & 0 & 0 & 0 & \frac{2}{r}\frac{c_2+c_3}{c_2c_3k} & -\frac{2}{r}\frac{1}{c_3k} \\ \frac{r^2}{\omega}v_{73} & \frac{r^2}{\omega}v_{74} & 0 & 0 & 0 & 0 & \frac{r^2}{\omega}H_{\Gamma^2} & -\frac{1}{M_3c_3^2\omega} \\ \frac{r^2}{\omega}v_{83} & \frac{r^2}{\omega}v_{84} & 0 & 0 & 0 & 0 & -\frac{1}{M_3c_3^2\omega} & \frac{r^2}{\omega}H_{\Phi^2} \\ 0 & 0 & 0 & 0 & -\frac{r^2}{\omega}H_{\gamma^2} & -\frac{r^2}{\omega}H_{\gamma,\phi} & 0 & 0 \\ 0 & 0 & 0 & 0 & -\frac{r^2}{\omega}H_{\phi,\gamma} & -\frac{r^2}{\omega}H_{\phi^2} & 0 & 0 \end{bmatrix}\begin{bmatrix} \xi_3 \\ \xi_4 \\ \xi_5 \\ \xi_6 \\ \xi_7 \\ \xi_8 \\ \xi_9 \\ \xi_{10} \end{bmatrix}
\end{aligned} \tag{4.170}$$

Using Eqs. (4.115) and (4.167) we obtain the coefficient matrix

$$\begin{bmatrix} 0 & 0 & \frac{r^2}{m^2\omega}K_{13}(\alpha) & \frac{r^2}{m^2\omega}K_{14}(\alpha) & 0 & 0 & 0 & 0 \\ 0 & 0 & \frac{r^2}{m^2\omega}K_{23}(\alpha) & \frac{r^2}{m^2\omega}K_{24}(\alpha) & 0 & 0 & 0 & 0 \\ \frac{m^2}{r\omega}\left[K_{31}(\alpha)+W_{31}(\alpha)\frac{\omega^2}{r}\right] & \frac{m^2}{r\omega}\left[K_{32}(\alpha)+W_{32}(\alpha)\frac{\omega^2}{r}\right] & 0 & 0 & 0 & 0 & \frac{K_{37}}{ry^2} & \frac{K_{38}}{ry^2} \\ \frac{m^2}{r\omega}\left[K_{41}(\alpha)+W_{41}(\alpha)\frac{\omega^2}{r}\right] & \frac{m^2}{r\omega}\left[K_{42}(\alpha)+W_{42}(\alpha)\frac{\omega^2}{r}\right] & 0 & 0 & 0 & 0 & \frac{K_{47}}{ry^2} & \frac{K_{48}}{ry^2} \\ \frac{m}{r}K_{51}(\alpha) & \frac{m}{r}K_{52}(\alpha) & 0 & 0 & 0 & 0 & \frac{K_{\Gamma^2}}{m\omega y^2} & \frac{K_{67}}{m\omega y^2} \\ \frac{m}{r}K_{61}(\alpha) & \frac{m}{r}K_{62}(\alpha) & 0 & 0 & 0 & 0 & \frac{K_{67}}{m\omega y^2} & \frac{K_{\Phi^2}}{m\omega y^2} \\ 0 & 0 & 0 & 0 & \frac{Gm^2r}{y\omega}K_{\gamma^2} & \frac{Gm^2r}{y\omega}K_{\gamma,\phi} & 0 & 0 \\ 0 & 0 & 0 & 0 & \frac{Gm^2r}{y\omega}K_{\gamma,\phi} & \frac{Gm^2r}{y\omega}K_{\phi^2} & 0 & 0 \end{bmatrix} \tag{4.171}$$

Introducing

$$\xi_5 = \frac{m^2}{r}\hat{\xi}_5 \qquad \xi_6 = \frac{m^2}{r}\hat{\xi}_6 \tag{4.172}$$

and applying the chain rule we get

$$\xi_5' = \frac{m^2}{r}\hat{\xi}_5' - \frac{m^2r'}{r^2}\hat{\xi}_5 \qquad \xi_6' = \frac{m^2}{r}\hat{\xi}_6' - \frac{m^2r'}{r^2}\hat{\xi}_6 \tag{4.173}$$

and thus

$$\hat{\xi}_5' = \frac{r}{m^2}\xi_5' + \frac{r'}{r}\hat{\xi}_5 \qquad \hat{\xi}_6' = \frac{r}{m^2}\xi_6' + \frac{r'}{r}\hat{\xi}_6 \tag{4.174}$$

the matrix for $\hat{\xi}$ variables is then

$$\begin{bmatrix} 0 & 0 & \frac{r}{\omega}K_{13}(\alpha) & \frac{r}{\omega}K_{14}(\alpha) & 0 & 0 & 0 & 0 \\ 0 & 0 & \frac{r}{\omega}K_{23}(\alpha) & \frac{r}{\omega}K_{24}(\alpha) & 0 & 0 & 0 & 0 \\ \frac{1}{\omega}\left[K_{31}(\alpha)+W_{31}(\alpha)\frac{\omega^2}{r}\right] & \frac{1}{\omega}\left[K_{32}(\alpha)+W_{32}(\alpha)\frac{\omega^2}{r}\right] & \frac{r'}{r} & 0 & 0 & 0 & \frac{K_{37}}{m^2y^2} & \frac{K_{38}}{m^2y^2} \\ \frac{1}{\omega}\left[K_{41}(\alpha)+W_{41}(\alpha)\frac{\omega^2}{r}\right] & \frac{1}{\omega}\left[K_{42}(\alpha)+W_{42}(\alpha)\frac{\omega^2}{r}\right] & 0 & \frac{r'}{r} & 0 & 0 & \frac{K_{47}}{m^2y^2} & \frac{K_{48}}{m^2y^2} \\ \frac{m}{r}K_{51}(\alpha) & \frac{m}{r}K_{52}(\alpha) & 0 & 0 & 0 & 0 & \frac{K_{\Gamma^2}}{m\omega y^2} & \frac{K_{67}}{m\omega y^2} \\ \frac{m}{r}K_{61}(\alpha) & \frac{m}{r}K_{62}(\alpha) & 0 & 0 & 0 & 0 & \frac{K_{67}}{m\omega y^2} & \frac{K_{\Phi^2}}{m\omega y^2} \\ 0 & 0 & 0 & 0 & \frac{Gm^2r}{y\omega}K_{\gamma^2} & \frac{Gm^2r}{y\omega}K_{\gamma,\phi} & 0 & 0 \\ 0 & 0 & 0 & 0 & \frac{Gm^2r}{y\omega}K_{\gamma,\phi} & \frac{Gm^2r}{y\omega}K_{\phi^2} & 0 & 0 \end{bmatrix} \tag{4.175}$$

Introducing

$$\begin{aligned} \xi_9 &= m^2y^2\hat{\xi}_9 \qquad \xi_{10} = m^2y^2\hat{\xi}_{10} \\ \xi'_9 &= m^2y^2\hat{\xi}'_9 \qquad \xi'_{10} = m^2y^2\hat{\xi}'_{10} \end{aligned} \tag{4.176}$$

gives

$$\begin{bmatrix} 0 & 0 & \frac{r}{\omega}K_{13}(\alpha) & \frac{r}{\omega}K_{14}(\alpha) & 0 & 0 & 0 & 0 \\ 0 & 0 & \frac{r}{\omega}K_{23}(\alpha) & \frac{r}{\omega}K_{24}(\alpha) & 0 & 0 & 0 & 0 \\ \frac{1}{\omega}\left[K_{31}(\alpha)+W_{31}(\alpha)\frac{\omega^2}{r}\right] & \frac{1}{\omega}\left[K_{32}(\alpha)+W_{32}(\alpha)\frac{\omega^2}{r}\right] & \frac{r'}{r} & 0 & 0 & 0 & K_{37} & K_{38} \\ \frac{1}{\omega}\left[K_{41}(\alpha)+W_{41}(\alpha)\frac{\omega^2}{r}\right] & \frac{1}{\omega}\left[K_{42}(\alpha)+W_{42}(\alpha)\frac{\omega^2}{r}\right] & 0 & \frac{r'}{r} & 0 & 0 & K_{47} & K_{48} \\ \frac{m}{r}K_{51}(\alpha) & \frac{m}{r}K_{52}(\alpha) & 0 & 0 & 0 & 0 & \frac{mK_{\Gamma^2}}{\omega} & \frac{mK_{67}}{\omega} \\ \frac{m}{r}K_{61}(\alpha) & \frac{m}{r}K_{62}(\alpha) & 0 & 0 & 0 & 0 & \frac{mK_{67}}{\omega} & \frac{mK_{\Phi^2}}{\omega} \\ 0 & 0 & 0 & 0 & \frac{Gr}{y^3\omega}K_{\gamma^2} & \frac{Gr}{y^3\omega}K_{\gamma,\phi} & 0 & 0 \\ 0 & 0 & 0 & 0 & \frac{Gr}{y^3\omega}K_{\gamma,\phi} & \frac{Gr}{y^3\omega}K_{\phi^2} & 0 & 0 \end{bmatrix} \tag{4.177}$$

and setting

$$\begin{aligned} \xi_3 &= \frac{r}{\omega}\hat{\xi}_3 \qquad \xi_4 = \frac{r}{\omega}\hat{\xi}_4 \\ \xi'_3 &= \frac{r}{\omega}\hat{\xi}'_3 + \frac{r'}{\omega}\hat{\xi}_3 \qquad \xi'_4 = \frac{r}{\omega}\hat{\xi}'_4 + \frac{r'}{\omega}\hat{\xi}_4 \end{aligned} \tag{4.178}$$

gives

$$\begin{bmatrix} -\frac{r'}{r} & 0 & K_{13} & K_{14} & 0 & 0 & 0 & 0 \\ 0 & -\frac{r'}{r} & K_{23} & K_{24} & 0 & 0 & 0 & 0 \\ \frac{r}{\omega^2}K_{31}+W_{31} & \frac{r}{\omega^2}K_{32}+W_{32} & \frac{r'}{r} & 0 & 0 & 0 & K_{37} & K_{38} \\ \frac{r}{\omega^2}K_{41}+W_{41} & \frac{r}{\omega^2}K_{42}+W_{42} & 0 & \frac{r'}{r} & 0 & 0 & K_{47} & K_{48} \\ \frac{m}{\omega}K_{51} & \frac{m}{\omega}K_{52} & 0 & 0 & 0 & 0 & \frac{mK_{\Gamma^2}}{\omega} & \frac{mK_{67}}{\omega} \\ \frac{m}{\omega}K_{61} & \frac{m}{\omega}K_{62} & 0 & 0 & 0 & 0 & \frac{mK_{67}}{\omega} & \frac{mK_{\Phi^2}}{\omega} \\ 0 & 0 & 0 & 0 & \frac{Gr}{y^3\omega}K_{\gamma^2} & \frac{Gr}{y^3\omega}K_{\gamma,\phi} & 0 & 0 \\ 0 & 0 & 0 & 0 & \frac{Gr}{y^3\omega}K_{\gamma,\phi} & \frac{Gr}{y^3\omega}K_{\phi^2} & 0 & 0 \end{bmatrix} \tag{4.179}$$

Finally, setting

$$\begin{aligned} \xi_7 &= \frac{m}{\omega}\hat{\xi}_7 \qquad \xi_8 = \frac{m}{\omega}\hat{\xi}_8 \\ \xi'_7 &= \frac{m}{\omega}\hat{\xi}'_7 \qquad \xi'_8 = \frac{m}{\omega}\hat{\xi}'_8 \end{aligned} \tag{4.180}$$

we obtain

$$\begin{bmatrix} -\frac{r'}{r} & 0 & K_{13} & K_{14} & 0 & 0 & 0 & 0 \\ 0 & -\frac{r'}{r} & K_{23} & K_{24} & 0 & 0 & 0 & 0 \\ \frac{r}{\omega^2}K_{31}+W_{31} & \frac{r}{\omega^2}K_{32}+W_{32} & \frac{r'}{r} & 0 & 0 & 0 & K_{37} & K_{38} \\ \frac{r}{\omega^2}K_{41}+W_{41} & \frac{r}{\omega^2}K_{42}+W_{42} & 0 & \frac{r'}{r} & 0 & 0 & K_{47} & K_{48} \\ K_{51} & K_{52} & 0 & 0 & 0 & 0 & K_{\Gamma^2} & K_{67} \\ K_{61} & K_{62} & 0 & 0 & 0 & 0 & K_{67} & K_{\Phi^2} \\ 0 & 0 & 0 & 0 & \frac{Gm}{y^3}\frac{r}{\omega^2}K_{\gamma^2} & \frac{Gm}{y^3}\frac{r}{\omega^2}K_{\gamma,\phi} & 0 & 0 \\ 0 & 0 & 0 & 0 & \frac{Gm}{y^3}\frac{r}{\omega^2}K_{\gamma,\phi} & \frac{Gm}{y^3}\frac{r}{\omega^2}K_{\phi^2} & 0 & 0 \end{bmatrix} \tag{4.181}$$

where

$$\frac{Gm}{y^3} = \left(\frac{1}{4} + \frac{m_3}{m}\cos^3\alpha + \frac{m_4}{m}\cos^3\beta\right)^{-1}$$

is a function of the angles α, β only and

$$\frac{r}{\omega^2} = (1 + e\cos\theta)^{-1}$$

together with

$$\frac{r'}{r} = \frac{e\sin\theta}{1+e\cos\theta}$$

are functions of e and θ, which means that the matrix (4.181) and, in turn, the linear stability of our system depends only on the eccentricity e and the angles α, β (θ is the independent variable). It is notable that, similarly to the case of the elliptic Lagrangian triangle [27], ω and G are eliminated and do not affect linear stability. Actually, the fact that G is irrelevant to stability can easily be seen, as changing G effectively only changes the units of length and mass and the relationship between size and mass of the configuration Eq. (4.26). The irrelevance of ω can be explained by the fact that for a choice of $r(0)$ (the simplest choice is 1, which sets the initial positions to $r_2(0) = c_2$, $r_3(0) = c_3$ and $r_4(0) = c_4$), and a choice of eccentricity e, ω is uniquely determined by Eq. (4.18) (assuming $\omega > 0$).

4.6. Circular square case

So far, linearized variational equations have been developed for the assessment of stability of general convex kite central configurations. Before turning to that, it is insightful to take a look at a special case: the circular square configuration. Owing to the symmetry of the square configuration, the equations of motion become relatively simple and the linear stability of the circular solution has already been determined analytically, allowing us to validate our equations and methods.

Towards that end, we set the angles to $\alpha = \beta = 45°$, such that the four bodies are positioned at the corners of a square. In that case, from Fig. 4.2 and Eqs. (4.27) to (4.29) we find:

$$\begin{aligned} &c_3 = y = \frac{1}{2}c_2 && m_1 = m_2 = m_3 = m_4 = m && M_{c3} = M_{13} + M_{23} = \frac{2}{3} \\ &c_4 = \frac{4}{3}y = \frac{4}{3}c_3 = \frac{2}{3}c_2 && M_{13} = M_{23} = \frac{1}{3} && M_3 = \frac{2}{3}m \\ & && M_{33} = \frac{1}{3} && M_4 = \frac{3}{4}m \end{aligned} \tag{4.182}$$

Furthermore, Equation 4.26 becomes

$$y^3 = Gm\left(\frac{1}{4} + \cos^3\alpha + \cos^3\beta\right) = Gm\left(\frac{1}{4} + \frac{1}{\sqrt{2}}\right) \tag{4.183}$$

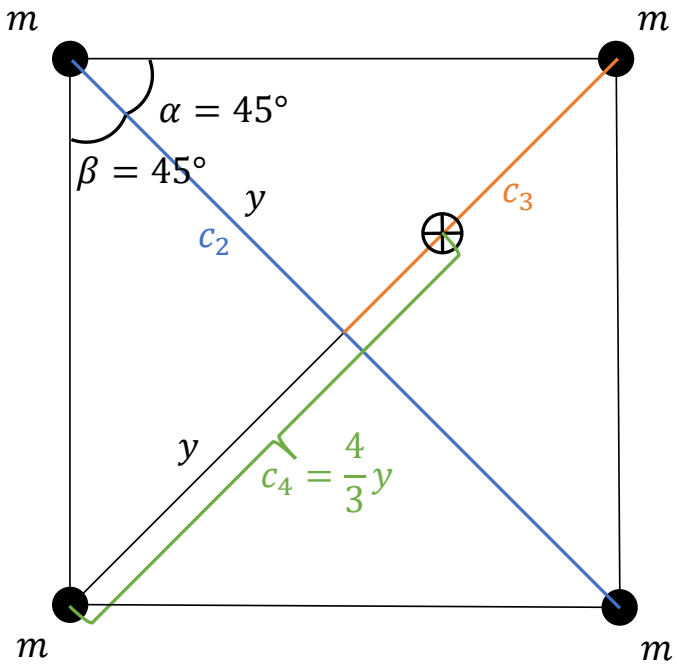

Figure 4.2: The square configuration. Rotated 45° w.r.t. previous plots.

The double derivatives then become, from Eqs. (4.106) to (4.108)

$$
\begin{aligned}
-H_{r_2^2} &= -\frac{3}{2}\frac{m}{r^3}(1+e\cos\theta)+\frac{m}{r^3}\frac{1+6\cdot 2^{-\frac{5}{2}}-2\cdot 2^{-\frac{3}{2}}+6\cdot 2^{-\frac{5}{2}}-2\cdot 2^{-\frac{3}{2}}}{1+4\cdot 2^{-\frac{3}{2}}+4\cdot 2^{-\frac{3}{2}}} = \boxed{-\frac{3}{2}\frac{m}{r^3}(1+e\cos\theta)+\frac{m}{r^3}\frac{1}{14}\left(2+3\sqrt{2}\right)} \\
-H_{r_2,r_3} &= \frac{m}{r^3}\frac{3\cdot 2^{-\frac{4}{2}}\cdot 2^{-\frac{1}{2}}-2^{-\frac{4}{2}}\cdot 2^{-\frac{1}{2}}}{\frac{1}{4}+2^{-\frac{3}{2}}+2^{-\frac{3}{2}}} = \boxed{\frac{m}{r^3}\frac{1}{7}\left(4-\sqrt{2}\right)} \\
-H_{r_2,r_4} &= 3\frac{Gm^2}{r^3y^3}\cos^4\beta\sin\beta = 3\frac{m}{r^3}\frac{\cos^4\beta\sin\beta}{\frac{1}{4}+\cos^3\alpha+\cos 3\beta} = \frac{m}{r^3}\frac{3\cdot 2^{-\frac{4}{2}}\cdot 2^{-\frac{1}{2}}}{2^{-2}+2^{-\frac{3}{2}}+2^{-\frac{3}{2}}} = \boxed{\frac{m}{r^3}\frac{3}{14}\left(4-\sqrt{2}\right)}
\end{aligned}
\tag{4.184}
$$

From Eqs. (4.109) and (4.110)

$$
\begin{aligned}
-H_{r_3^2} &= -3\frac{2}{3}m\frac{\omega^2}{r^4}+2\frac{Gm^2}{r^3y^3}\left(2\cos^3\alpha-3\cos^5\alpha\right)+2\frac{Gm^2}{r^3y^3}\frac{1}{9}\left(2\cos^3\beta-3\cos^5\beta\right)+2\frac{Gm^2}{r^3y^3}\frac{4}{9}\left(\tan\alpha+\tan\beta\right)^{-3} \\
&= -2m\frac{\omega^2}{r^4}+2\frac{m}{r^3}\frac{2\cos^3\alpha-3\cos^5\alpha+\frac{2}{9}\cos^3\beta-\frac{1}{3}\cos^5\beta+\frac{4}{9}\left(\tan\alpha+\tan\beta\right)^{-3}}{\frac{1}{4}+\cos^3\alpha+\cos^3\beta} \\
&= -2\frac{m}{r^3}(1+e\cos\theta)+2\frac{m}{r^3}\frac{2\cdot 2^{-\frac{3}{2}}-3\cdot 2^{-\frac{5}{2}}+\frac{2}{9}\cdot 2^{-\frac{3}{2}}-\frac{1}{3}\cdot 2^{-\frac{5}{2}}+\frac{4}{9}\cdot 2^{-3}}{2^{-2}+2^{-\frac{3}{2}}+2^{-\frac{3}{2}}} \\
&= \boxed{-2\frac{m}{r^3}(1+e\cos\theta)+\frac{m}{r^3}\frac{2}{63}\left(18-\sqrt{2}\right)} \\
-H_{r_3,r_4} &= -2\frac{Gm^2}{r^3y^3}\frac{1}{3}\left(2\cos^3\beta-3\cos^5\beta\right)+2\frac{Gm^2}{r^3y^3}\frac{2}{3}\left(\tan\alpha+\tan\beta\right)^{-3} \\
&= \frac{1}{3}\frac{m}{r^3}\frac{-4\cos^3\beta+6\cos^5\beta+4\left(\tan\alpha+\tan\beta\right)^{-3}}{\frac{1}{4}+\cos^3\alpha+\cos^3\beta} = \frac{1}{3}\frac{m}{r^3}\frac{-4\cdot 2^{-\frac{3}{2}}+6\cdot 2^{-\frac{5}{2}}+4\cdot 2^{-3}}{\frac{1}{4}+2^{-\frac{3}{2}}+2^{-\frac{3}{2}}} = \boxed{\frac{m}{r^3}\frac{1}{21}\left(-6+5\sqrt{2}\right)}
\end{aligned}
\tag{4.185}
$$

From Eqs. (4.111) and (4.112)

$$\begin{aligned} -H_{\gamma^2} &= 6\frac{Gm^2}{ry}\cos^3\alpha\sin^2\alpha + 6\frac{Gm^2}{ry}\cos^3\beta\sin^2\beta = 6\frac{Gm^2}{ry}\left(2^{-\frac{3}{2}}\cdot 2^{-\frac{2}{2}} + 2^{-\frac{3}{2}}\cdot 2^{-\frac{2}{2}}\right) = \boxed{\frac{Gm^2}{ry}\frac{3}{2}\sqrt{2}} \\ -H_{\gamma,\phi} &= 6\frac{Gm^2}{ry}\cos^4\beta\sin\beta\left(\frac{1}{3}\tan\alpha + \tan\beta\right) = \frac{Gm^2}{ry}6\cdot 2^{-\frac{4}{2}}\cdot 2^{-\frac{1}{2}}\cdot\left(\frac{1}{3}+1\right) = \boxed{\frac{Gm^2}{ry}\sqrt{2}} \end{aligned} \tag{4.186}$$

From Eq. (4.113)

$$\begin{aligned} -H_{r_4^2} &= -3\frac{3}{4}m\frac{\omega^2}{r^4} + 2\frac{Gm^2}{r^3y^3}\left(2\cos^3\beta - 3\cos^5\beta\right) + 2\frac{Gm^2}{r^3y^3}\left(\tan\alpha+\tan\beta\right)^{-3} \\ &= -\frac{9}{4}m\frac{\omega^2}{r^4} + \frac{m}{r^3}\frac{4\cos^3\beta - 6\cos^5\beta + 2\left(\tan\alpha+\tan\beta\right)^{-3}}{\frac{1}{4}+\cos^3\alpha+\cos^3\beta} = \boxed{-\frac{9}{4}\frac{m}{r^3}(1+e\cos\theta) + \frac{1}{7}\frac{m}{r^3}\left(3+\sqrt{2}\right)} \end{aligned} \tag{4.187}$$

From Eq. (4.114)

$$\begin{aligned} -H_{\phi^2} &= -2\frac{Gm^2}{ry}\left(\frac{1}{3}\tan\alpha+\tan\beta\right)\cos^3\beta\left(\frac{1}{3}\tan\alpha\left(1-3\cos^2\beta\right) - 3\cos\beta\sin\beta\right) \\ &\quad + \frac{Gm^2}{ry}\left(\tan\alpha+\tan\beta\right)^{-3}\cdot\frac{2}{3}\tan\alpha\left(\frac{1}{3}\tan\alpha+\tan\beta\right) = \boxed{\frac{1}{9}\frac{Gm^2}{ry}\left(1+10\sqrt{2}\right)} \end{aligned} \tag{4.188}$$

From Eqs. (4.104) and (4.105)

$$\begin{aligned} H_{\Gamma^2} &= \frac{1}{r^2y^2}\left(\frac{1}{2m} + \frac{1}{\frac{2}{3}m\tan^2\alpha}\right) = \frac{1}{r^2y^2}\frac{4}{2m} = \boxed{\frac{2}{r^2y^2m}} \\ H_{\Phi^2} &= \frac{1}{r^2y^2}\left(\frac{1}{\frac{2}{3}m\tan^2\alpha} + \frac{1}{\frac{3}{4}m\left(\frac{1}{3}\tan\alpha+\tan\beta\right)^2}\right) = \frac{1}{r^2y^2}\left(\frac{3}{2m}+\frac{3}{4m}\right) = \boxed{\frac{9}{4}\frac{1}{r^2y^2m}} \end{aligned} \tag{4.189}$$

With the values for c_2, c_3, c_4, M_2, M_3 and M_4 the k coefficients from Eqs. (4.145) to (4.147), (4.149) and (4.150) become:

$$\begin{aligned} k &= \frac{13}{3}y & k_{19} &= 4m^2y^3 & k_{25} &= \frac{10}{3}m^2y^3 & k_{37} &= \frac{8}{3}m^2y^3 & k_{43} &= \frac{20}{9}m^2y^3 \\ \frac{c}{\omega} &= 4my^2 & k_{20} &= 4m^2y^3 & k_{26} &= -m^2y^3 & k_{38} &= -8m^2y^3 & k_{44} &= -\frac{86}{9}m^2y^3 \\ & & k_{21} &= -\frac{32}{3}m^2y^3 & k_{27} &= -6m^2y^3 & k_{39} &= 0 & k_{45} &= \frac{52}{27}m^2y^3 \\ & & k_{22} &= 0 & k_{28} &= -\frac{13}{3}m^2y^3 & k_{40} &= 0 & k_{46} &= \frac{26}{3}m^2y^3 \\ & & k_{23} &= -4m^2y^3 & k_{29} &= \frac{61}{9}m^2y^3 & k_{41} &= 8m^2y^3 & k_{47} &= -2m^2y^3 \\ & & k_{24} &= \frac{20}{3}m^2y^3 & k_{30} &= \frac{20}{27}m^2y^3 & k_{42} &= -\frac{8}{3}m^2y^3 & k_{48} &= -\frac{8}{27}m^2y^3 \end{aligned}$$

The relevant v coefficients follow from Eqs. (4.145) to (4.147) and (4.149) to (4.155) using the values of the radius double derivatives in Eqs. (4.184), (4.185) and (4.187) combined with the k coefficients above:

$$\begin{aligned} v_{53} &= \frac{m^2}{r^3}\left[\frac{3}{182}\left(-8+9\sqrt{2}\right) - \frac{63}{52}(1+e\cos\theta)\right] & v_{83} &= -\frac{9}{2}\frac{\omega m}{r^3} & v_{74} &= -\frac{14}{3}\frac{\omega m}{r^3} \\ &= \frac{m^2}{r^3}\left[\frac{3}{364}\left(-163+18\sqrt{2}\right) - \frac{63}{52}e\cos\theta\right] & v_{54} &= \frac{m^2}{r^3}\left[\frac{1}{91}\left(-40+17\sqrt{2}\right) + \frac{3}{26}(1+e\cos\theta)\right] & v_{84} &= 5\frac{\omega m}{r^3} \\ v_{63} &= \frac{m^2}{r^3}\left[\frac{1}{13}\left(-7+3\sqrt{2}\right) + \frac{3}{26}(1+e\cos\theta)\right] & &= \frac{m^2}{r^3}\left[\frac{1}{182}\left(-59+34\sqrt{2}\right) + \frac{3}{26}e\cos\theta\right] & v_{35} &= \frac{5}{2m^2} \\ &= \frac{m^2}{r^3}\left[\frac{1}{26}\left(-11+6\sqrt{2}\right) + \frac{3}{26}e\cos\theta\right] & v_{64} &= \frac{m^2}{r^3}\left[\frac{10}{273}\left(3+\sqrt{2}\right) - \frac{15}{13}(1+e\cos\theta)\right] & v_{45} &= \frac{1}{4m^2} \\ v_{73} &= \frac{\omega m}{r^3} & &= \frac{m^2}{r^3}\left[\frac{5}{273}\left(-57+2\sqrt{2}\right) - \frac{15}{13}e\cos\theta\right] & v_{36} &= \frac{1}{4m^2} \\ & & & & v_{46} &= \frac{21}{8m^2} \end{aligned} \tag{4.190}$$

and

$$\begin{aligned} v_{59} &= \frac{3}{13}\frac{\omega}{r^3y^2} \qquad v_{5,10} = \frac{9}{26}\frac{\omega}{r^3y^2} \qquad -\frac{1}{M_3c_3^2r^2} = -\frac{3}{2my^2r^2} \\ v_{69} &= \frac{9}{13}\frac{\omega}{r^3y^2} \qquad v_{6,10} = -\frac{6}{13}\frac{\omega}{r^3y^2} \end{aligned} \tag{4.191}$$

Comparing Eqs. (4.190) and (4.191) with Eqs. (4.167) and (4.168) and Eqs. (4.186), (4.188) and (4.189) with Eq. (4.115) we find the K and W coefficients:

$$\begin{array}{lllllll} K_{13} = \frac{5}{2} & K_{14} = \frac{1}{4} & K_{23} = \frac{1}{4} & K_{24} = \frac{21}{8} & & & \\ K_{31} = \frac{3}{182}\left(-8+9\sqrt{2}\right) & W_{31} = -\frac{63}{52} & K_{32} = \frac{1}{91}\left(-40+17\sqrt{2}\right) & W_{32} = \frac{3}{26} & K_{37} = \frac{3}{13} & K_{38} = \frac{9}{26} & \\ K_{41} = \frac{1}{13}\left(-7+3\sqrt{2}\right) & W_{41} = \frac{3}{26} & K_{42} = \frac{10}{273}\left(3+\sqrt{2}\right) & W_{42} = -\frac{15}{13} & K_{47} = \frac{9}{13} & K_{48} = -\frac{6}{13} & \\ K_{51} = 1 & K_{52} = -\frac{14}{3} & K_{61} = -\frac{9}{2} & K_{62} = 5 & K_{67} = -\frac{3}{2} & & \\ K_{\gamma^2} = \frac{3}{2}\sqrt{2} & K_{\gamma,\phi} = \sqrt{2} & K_{\phi^2} = \frac{1+10\sqrt{2}}{9} & K_{\Gamma^2} = 2 & K_{\Phi^2} = \frac{9}{4} & & \end{array}$$

Using the K and W coefficients and the angle double derivatives Eqs. (4.186), (4.188) and (4.189), the 8x8 linear system (4.181) becomes:

$$\begin{bmatrix} -\frac{r'}{r} & 0 & \frac{5}{2} & \frac{1}{4} & 0 & 0 & 0 & 0 \\ 0 & -\frac{r'}{r} & \frac{1}{4} & \frac{21}{8} & 0 & 0 & 0 & 0 \\ \frac{r}{\omega^2}\frac{3}{182}\left(-8+9\sqrt{2}\right)-\frac{63}{52} & \frac{r}{\omega^2}\frac{1}{91}\left(-40+17\sqrt{2}\right)+\frac{3}{26} & \frac{r'}{r} & 0 & 0 & 0 & \frac{3}{13} & \frac{9}{26} \\ \frac{r}{\omega^2}\frac{1}{13}\left(-7+3\sqrt{2}\right)+\frac{3}{26} & \frac{r}{\omega^2}\frac{10}{273}\left(3+\sqrt{2}\right)-\frac{15}{13} & 0 & \frac{r'}{r} & 0 & 0 & \frac{9}{13} & -\frac{6}{13} \\ 1 & -\frac{14}{3} & 0 & 0 & 0 & 0 & 2 & -\frac{3}{2} \\ -\frac{9}{2} & 5 & 0 & 0 & 0 & 0 & -\frac{3}{2} & \frac{9}{4} \\ 0 & 0 & 0 & 0 & \frac{Gm}{y^3}\frac{r}{\omega^2}\frac{3}{2}\sqrt{2} & \frac{Gm}{y^3}\frac{r}{\omega^2}\sqrt{2} & 0 & 0 \\ 0 & 0 & 0 & 0 & \frac{Gm}{y^3}\frac{r}{\omega^2}\sqrt{2} & \frac{Gm}{y^3}\frac{r}{\omega^2}\frac{1+10\sqrt{2}}{9} & 0 & 0 \end{bmatrix} \tag{4.192}$$

Taking $e = 0$ and, therefore, $r = \omega^2$, $\frac{r'}{r} = 0$ and plugging in Eq. (4.183) we get

$$\begin{bmatrix} 0 & 0 & \frac{5}{2} & \frac{1}{4} & 0 & 0 & 0 & 0 \\ 0 & 0 & \frac{1}{4} & \frac{21}{8} & 0 & 0 & 0 & 0 \\ \frac{3}{364}\left(-163+18\sqrt{2}\right) & \frac{1}{182}\left(-59+34\sqrt{2}\right) & 0 & 0 & 0 & 0 & \frac{3}{13} & \frac{9}{26} \\ \frac{1}{26}\left(-11+6\sqrt{2}\right) & \frac{5}{273}\left(-57+2\sqrt{2}\right) & 0 & 0 & 0 & 0 & \frac{9}{13} & -\frac{6}{13} \\ 1 & -\frac{14}{3} & 0 & 0 & 0 & 0 & 2 & -\frac{3}{2} \\ -\frac{9}{2} & 5 & 0 & 0 & 0 & 0 & -\frac{3}{2} & \frac{9}{4} \\ 0 & 0 & 0 & 0 & -\frac{6}{7}\left(-4+\sqrt{2}\right) & -\frac{4}{7}\left(-4+\sqrt{2}\right) & 0 & 0 \\ 0 & 0 & 0 & 0 & -\frac{4}{7}\left(-4+\sqrt{2}\right) & -\frac{4}{63}\left(-39+8\sqrt{2}\right) & 0 & 0 \end{bmatrix} \tag{4.193}$$

Eq. (4.193) is a constant, exact Hamiltonian matrix, which means we can obtain the exact eigenvalues of the square circular case. Calculating the characteristic equation with Mathematica gives:

$$\lambda^8 + \frac{\left(11+8\sqrt{2}\right)}{9+4\sqrt{2}}\lambda^6 + \frac{5\left(7+6\sqrt{2}\right)}{9+4\sqrt{2}}\lambda^4 + \frac{5\left(75+4\sqrt{2}\right)}{7\left(9+4\sqrt{2}\right)}\lambda^2 + \frac{-2160+4194\sqrt{2}}{49\left(9+4\sqrt{2}\right)} = 0 \tag{4.194}$$

We see that the characteristic polynomial is even, as expected of a Hamiltonian matrix [17].

We now exploit this evenness and apply the technique of a reduced characteristic polynomial where we substitute a new variable, conventionally $\tau = -\lambda^2$, into the characteristic equation, which reduces the order by half [12]. If the equilibrium is *spectrally stable* all eigenvalues have to lie on the imaginary axis and thus all roots of the reduced characteristic equation have to be positive real numbers. Spectral stability is a weaker form of linear stability, where eigenvalues are allowed to have algebraic multiplicity larger than the geometric multiplicity, meaning that the system can be on the verge of losing stability: as we will see later, stability can only be gained or lost from a point of repeated eigenvalues. So, determining the roots of the reduced

polynomial is enough to determine spectral stability. The reduced characteristic equation of the square configuration is:

$$\tau^4 - \frac{\left(11+8\sqrt{2}\right)}{9+4\sqrt{2}}\tau^3 + \frac{5\left(7+6\sqrt{2}\right)}{9+4\sqrt{2}}\tau^2 - \frac{5\left(75+4\sqrt{2}\right)}{7\left(9+4\sqrt{2}\right)}\tau + \frac{-2160+4194\sqrt{2}}{49\left(9+4\sqrt{2}\right)} = 0 \tag{4.195}$$

This is a fourth-degree polynomial equation whose roots can be found analytically. The roots are:

$$\begin{aligned} &\frac{1}{7}\left(-1+2\sqrt{2}-2i\sqrt{56-14\sqrt{2}}\right) \qquad \frac{1}{14}\left(7-i\sqrt{-625+648\sqrt{2}}\right) \\ &\frac{1}{7}\left(-1+2\sqrt{2}+2i\sqrt{56-14\sqrt{2}}\right) \qquad \frac{1}{14}\left(7+i\sqrt{-625+648\sqrt{2}}\right) \end{aligned} \tag{4.196}$$

The eigenvalues are then found by the relation $\lambda = (-\tau)^{\frac{1}{2}}$ and by virtue of the fact that the eigenvalues of a real Hamiltonian matrix are symmetric across the real and imaginary axes [17]:

$$\begin{aligned} \lambda_{sq,1} &= \sqrt{\frac{1}{7}\left(1-2\sqrt{2}+2i\sqrt{56-14\sqrt{2}}\right)} & \lambda_{sq,5} &= \sqrt{\frac{1}{14}\left(-7+i\sqrt{-625+648\sqrt{2}}\right)} \\ \lambda_{sq,2} &= \sqrt{\frac{1}{7}\left(1-2\sqrt{2}-2i\sqrt{56-14\sqrt{2}}\right)} & \lambda_{sq,6} &= \sqrt{\frac{1}{14}\left(-7-i\sqrt{-625+648\sqrt{2}}\right)} \\ \lambda_{sq,3} &= -\sqrt{\frac{1}{7}\left(1-2\sqrt{2}+2i\sqrt{56-14\sqrt{2}}\right)} & \lambda_{sq,7} &= -\sqrt{\frac{1}{14}\left(-7+i\sqrt{-625+648\sqrt{2}}\right)} \\ \lambda_{sq,4} &= -\sqrt{\frac{1}{7}\left(1-2\sqrt{2}-2i\sqrt{56-14\sqrt{2}}\right)} & \lambda_{sq,8} &= -\sqrt{\frac{1}{14}\left(-7-i\sqrt{-625+648\sqrt{2}}\right)} \end{aligned} \tag{4.197}$$

In decimal approximation the eigenvalues for the square configuration are:

$$\begin{aligned} \lambda_{sq,1} &= -0.859533+i & \lambda_{sq,5} &= -0.639481+0.953381i \\ \lambda_{sq,2} &= +0.859533-i & \lambda_{sq,6} &= +0.639481-0.953381i \\ \lambda_{sq,3} &= -0.859533-i & \lambda_{sq,7} &= -0.639481-0.953381i \\ \lambda_{sq,4} &= +0.859533+i & \lambda_{sq,8} &= +0.639481+0.953381i \end{aligned} \tag{4.198}$$

Thus, as is well known [5, 9, 14, 29, 39], we find that the square configuration is unstable in the circular case. The eigenvalues match with the ones obtained in [18] for the restricted five-body configuration of a square with a small mass in the middle. Figures 4.3 and 4.4, taken from [18], show the eigenvalues of the configuration for a varying mass of the small body. The marked points correspond to 0 central mass, which is just our square central configuration, but with an additional body of no mass and, therefore, no effect on the dynamics of the bodies on the vertices. As a result, eight of the eigenvalues match and there are four others, which correspond to the additional degrees of freedom introduced by the 0-mass. These matching eigenvalues verify that the derived system of equations (4.181) and our procedure to obtain eigenvalues are correct.

4.7. Circular cases

As Eq. (4.181) depends only on the angles α, β, the eccentricity e and true anomaly θ, by setting $e = 0$ we obtain a constant matrix of coefficients of our linear system of differential equations, whose eigenvalues can be calculated to directly determine the linear stability for the full range of α and β.

If ρ is an eigenvalue, then we know that $e^{2\pi\rho}$ is a characteristic multiplier [27]. For a complex eigenvalue $\rho = a + ib$, we have

$$e^{2\pi(a+ib)} = e^{2\pi a}\left(\cos(2\pi b) + i\sin(2\pi b)\right)$$

and, therefore, in order for the characteristic multipliers to lie on the unit circle, we must have $e^{2\pi a} = 1$, which requires that $a = 0$. Hence, all the eigenvalues have to be purely imaginary for linear stability [12]. Strictly speaking, all imaginary eigenvalues only guarantee *spectral stability*, whereas for linear stability it is also required that the matrix be diagonalizable, i.e. that the geometric multiplicity of each eigenvalue is not less than its algebraic multiplicity [12]. In other words still, the eigenvalues must have as many unique eigenvectors

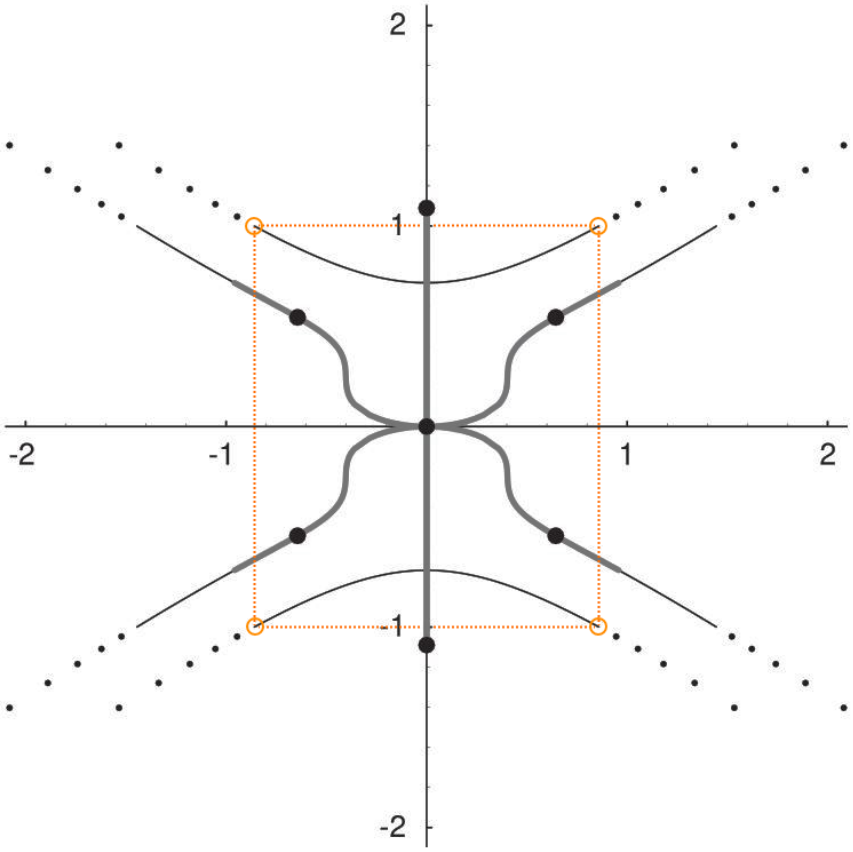

Figure 4.3: Eigenvalues $\pm 0.859533 \pm i$ of the square from [18].

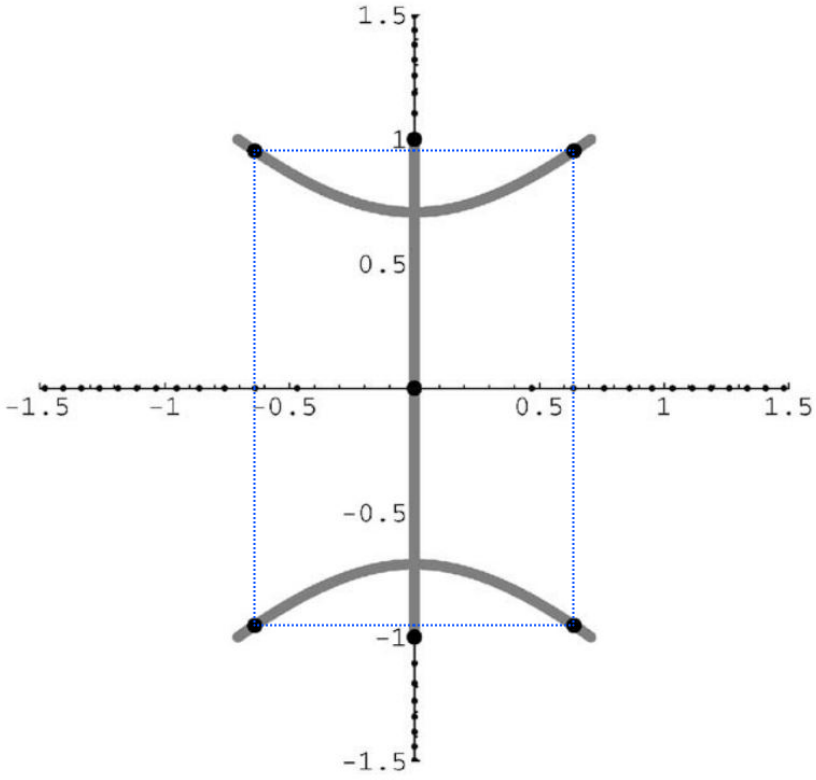

Figure 4.4: Eigenvalues $\pm 0.639481 \pm 0.953381\,i$ of the square from [18].

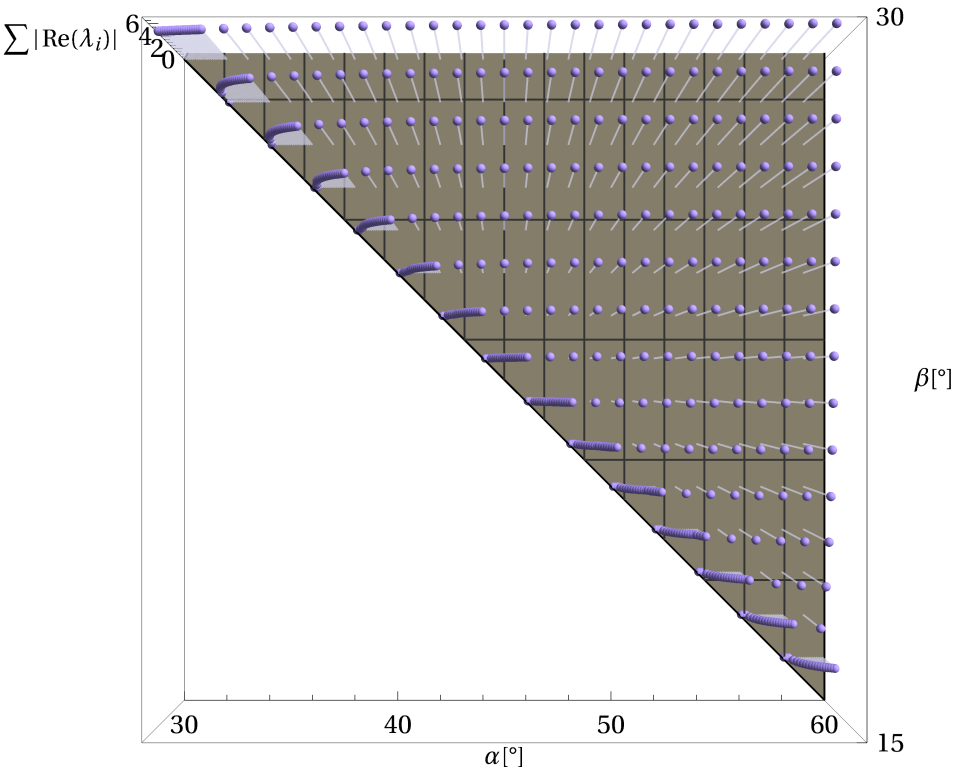

Figure 4.5: Top view of the sums of the magnitudes of the real parts of the eigenvalues sampled from the convex domain. The coloured region denotes the zero-plane.

associated to them as is their algebraic multiplicity, so there must be eight imaginary eigenvalues with eight distinct eigenvectors to have linear stability. If all eigenvalues are unique then their algebraic and geometric multiplicity is necessarily one and spectral stability implies linear stability. In the case of repeated eigenvalues on the imaginary axis, resonance type instabilities with linear growth rates may occur if the solution is only spectrally stable [11]. Because of the symmetry of the characteristic multipliers around the unit circle, stability is only gained or lost at a collision of two multipliers, therefore the boundary of linear and spectral stability coincides.

4.7.1. Mathematica procedure

We calculate the eigenvalues for a sampling of the convex domain with Mathematica. Sums of the real parts of these eigenvalues are plotted in Figs. 4.5 to 4.8. In Figs. 4.6 to 4.8 we see that some eigenvalues near the edge of minimum β lie on the zero-plane. This implies that the real parts are all zero, which implies linear stability. The line of minimum β corresponds to the case where all the mass of the system is in a single body,

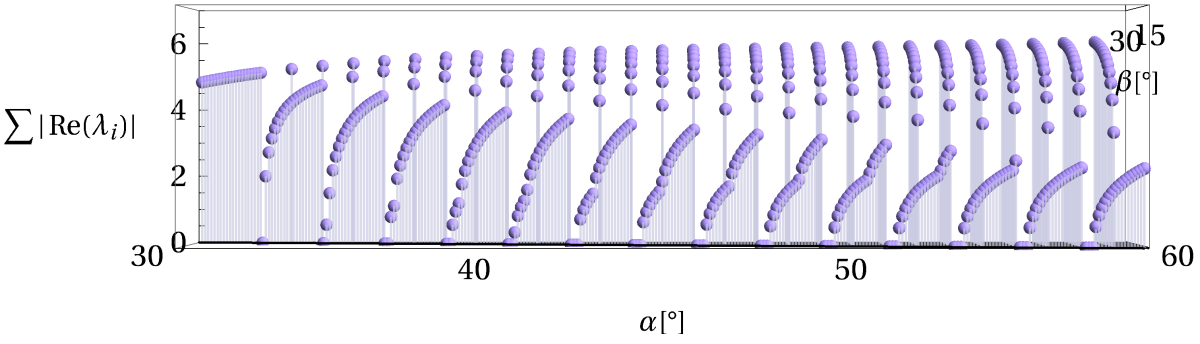

Figure 4.6: Front view of sums of magnitudes of real parts of the eigenvalues of RE's sampled from the convex domain. The coloured region denotes the zero-plane.

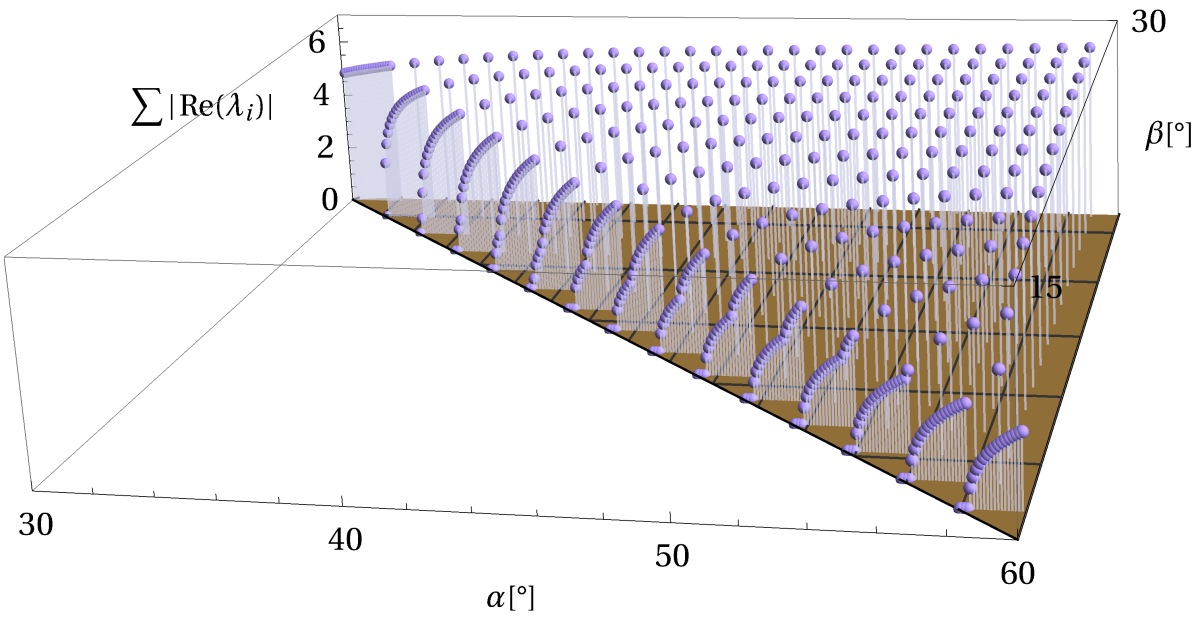

Figure 4.7: Sums of magnitudes of real parts of the eigenvalues of RE's sampled from the convex domain. The coloured region denotes the zero-plane.

while the three other bodies have zero mass. We have divisions by zero if we attempt to find the eigenvalues on this line. Close to it, however, we have cases where most of the mass of the system is in one body, while the other three have relatively small masses. It makes sense that we find stable solutions in this region, since every known example of a linearly stable RE has a dominant mass [19], such as in the cases of Lagrangian triangle central configurations [27, 28] and planetary rings. The stability region near the line of minimum β will be explored and analyzed in higher resolution in Section 4.9.

4.8. Perturbations in eccentricity

In this section we develop a method to determine the effect on linear stability of four-body central configurations when small perturbations to the eccentricity e are applied. The basis of the method is a naive expansion perturbation method, which is used to estimate the coefficients of the characteristic equation of the monodromy matrix.

4.8.1. Method

The monodromy matrix of a Hamiltonian system is a symplectic transformation, because it takes a state of the system to a future state, according to the phase flow of the system, which is volume preserving [3]. The characteristic polynomial of a symplectic matrix is always reciprocal (also called symmetric or reflexive in literature) [3], meaning that coefficients of the polynomial

$$a_0 + a_1 x + a_2 x^2 + \ldots + a_n x^n$$

satisfy

$$a_i = a_{n-i}, \quad \forall i$$

A key property of reciprocal polynomials is that if λ is a root, then so is $\frac{1}{\lambda}$ [3]. Combined with the fact that complex conjugates $\bar{\lambda}$ are also roots we get the following relationship between eigenvalues

$$\frac{1}{\lambda} = \frac{1}{a+ib} = \frac{a-ib}{a^2+b^2} = \frac{1}{R^2}(a-ib) = \frac{1}{R^2}\bar{\lambda} \tag{4.199}$$

where $R = |\lambda|$. For linear stability, we require that the characteristic multipliers ρ lie on the unit circle in the complex plane, $|\rho| = 1$. In that case $R = 1$ and $\bar{\lambda} = \frac{1}{\lambda}$.

In our problem the characteristic equation of the 8×8 monodromy matrix will take the form

$$p(\rho) = \rho^8 + a\rho^7 + b\rho^6 + c\rho^5 + d\rho^4 + c\rho^3 + b\rho^2 + a\rho + 1 = 0 \tag{4.200}$$

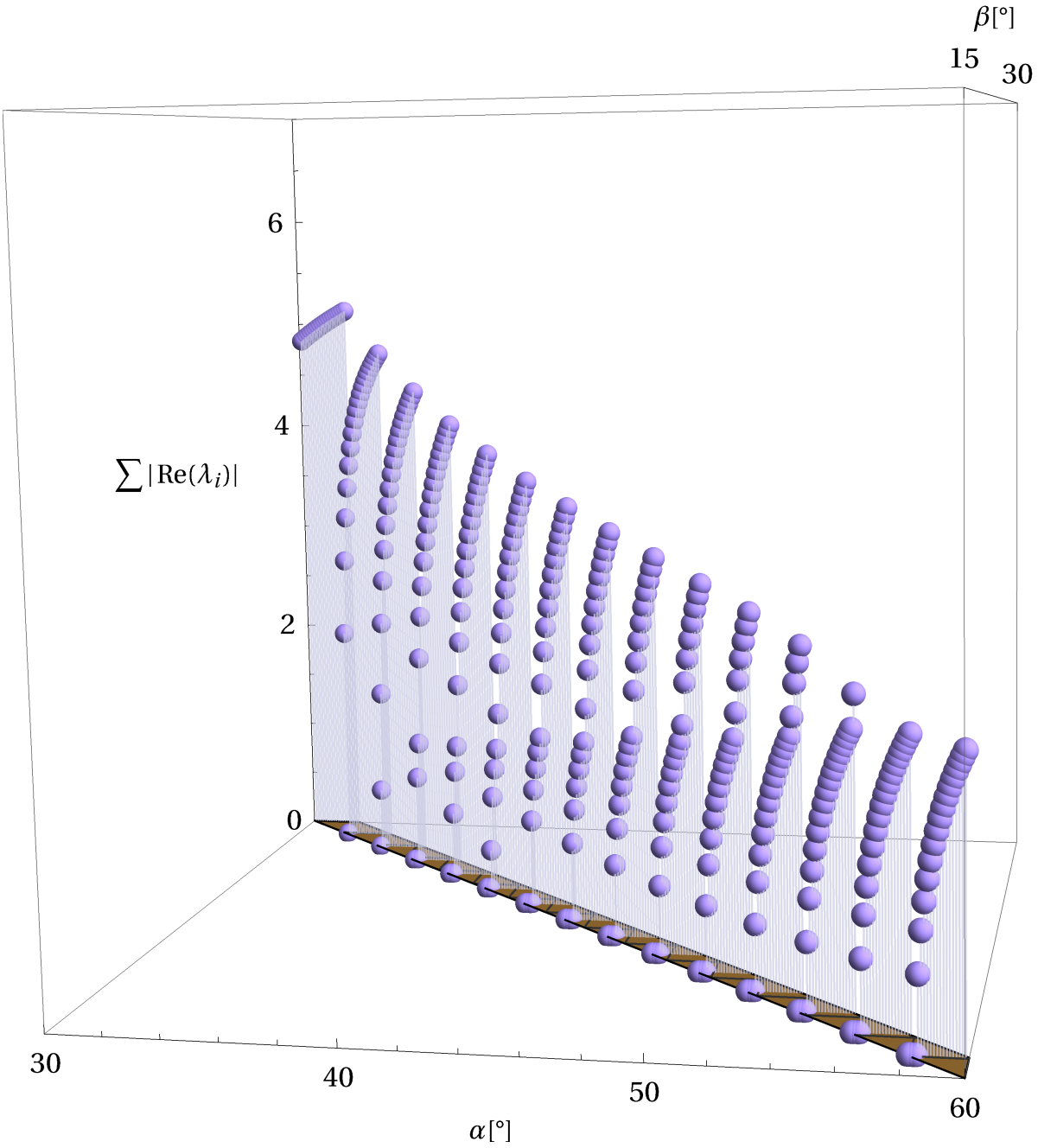

Figure 4.8: Zoom view of sums of magnitudes of real parts of the eigenvalues of RE's sampled from the convex domain. The coloured region denotes the zero-plane.

We would like to derive relations between a, b, c and d for which we have roots on the unit circle, $|\rho| = 1$. However, this polynomial equation is of the 8-th degree, which is impossible to solve analytically. Still, we can use yet another property of reciprocal polynomials, namely that for every reciprocal univariate polynomial f of even degree $2n$:

$$f(t) = \Sigma_{k=0}^{2n} a_k t^k$$

where $a_{2n-k} = a_k$ for all $k \in \{0,\dots,2n\}$, there exists a univariate polynomial (polynomial in one variable) g [1]:

$$g(u) := a_n + \sum_{j=1}^{n} 2a_{n-j}\mathcal{T}_j(u/2) \tag{4.201}$$

such that

$$f(t) = t^n g(t + t^{-1}) \tag{4.202}$$

where $\mathcal{T}_j$ is the j-th Chebychev polynomial. We use this fact to write our 8-th degree characteristic equation in the form $\rho^4 g(\rho + \rho^{-1})$ where g is a 4-th degree polynomial.

The first five Chebychev polynomials are:

$$\begin{aligned}
\mathcal{T}_0(u) &= 1 \\
\mathcal{T}_1(u) &= u \\
\mathcal{T}_2(u) &= 2u^2 - 1 \\
\mathcal{T}_3(u) &= 4u^3 - 3u \\
\mathcal{T}_4(u) &= 8u^4 - 8u^2 + 1
\end{aligned} \tag{4.203}$$

Applying Eq. (4.201) to Eq. (4.200) we get

$$\begin{aligned}
g(u) &= a_4 + \Sigma_{j=1}^{4} 2a_{4-j}\mathcal{T}_j(u/2) \\
&= d + 2c\frac{u}{2} + 2b\left(2\frac{u^2}{4} - 1\right) + 2a\left(4\frac{u^3}{8} - 3\frac{u}{2}\right) + 2\left(8\frac{u^4}{16} - 8\frac{u^2}{4} + 1\right) \\
&= u^4 + au^3 + (b-4)\,u^2 + (c-3a)\,u + d - 2b + 2
\end{aligned} \tag{4.204}$$

It was checked that indeed

$$\rho^4 g(\rho + \rho^{-1}) = p(\rho)$$

We also know that if τ is a root of g, then ρ and ρ^{-1} which satisfy $\tau = \rho + \rho^{-1}$ are roots of p [1]. Therefore, we can analyze the four roots of g to find out about the characteristic multipliers ρ, since we assume that $\rho \neq 0$. For stability we require $|\rho| = 1$ and thus:

$$\rho + \rho^{-1} = \rho + \bar{\rho} = \tau \in \mathbb{R} \tag{4.205}$$

So, the roots of g must be real for linear stability. Writing g as

$$g(u) = u^4 + Bu^3 + Cu^2 + Du + E \tag{4.206}$$

the discriminant of this quartic polynomial is then:

$$\begin{aligned}
\Delta =& 256E^3 - 192BDE^2 - 128C^2E^2 + 144CD^2E - 27D^4 + 144B^2CE^2 \\
&- 6B^2D^2E - 80BC^2DE + 18BCD^3 + 16C^4E - 4C^3D^2 - 27B^4E^2 \\
&+ 18B^3CDE - 4B^3D^3 - 4B^2C^3E + B^2C^2D^2
\end{aligned} \tag{4.207}$$

Now our goal is to find expansions for the coefficients $B(e)$, $C(e)$, $D(e)$, $E(e)$. We start by naive expansion of our linear system:

$$\boldsymbol{\xi}' = \left(A_0 + eA_1(\theta) + e^2A_2(\theta) + \cdots\right)\boldsymbol{\xi} \tag{4.208}$$

and we substitute an expansion of the solution

$$\boldsymbol{\xi}(\theta) = \boldsymbol{\xi_0}(\theta) + e\boldsymbol{\xi_1}(\theta) + e^2\boldsymbol{\xi_2}(\theta) \tag{4.209}$$

into Eq. (4.208) to get:

$$\begin{aligned}\boldsymbol{\xi}_0' &= A_0\boldsymbol{\xi_0}\\ \boldsymbol{\xi}_1' &= A_0\boldsymbol{\xi_1} + A_1(\theta)\boldsymbol{\xi}_0\\ \boldsymbol{\xi}_2' &= A_0\boldsymbol{\xi_2} + A_1(\theta)\boldsymbol{\xi}_1 + A_2(\theta)\boldsymbol{\xi}_0\end{aligned} \tag{4.210}$$

Now writing the fundamental matrix solution as

$$X(\theta) = X_0(\theta) + eX_1(\theta) + e^2X_2(\theta) + \cdots \tag{4.211}$$

with $X_0(0) = I_4$, $X_1(0) = 0$, $X_2(0) = 0$, …. Solving the system differential equations Eq. (4.210) we obtain

$$\begin{aligned}X_0(\theta) &= e^{A_0\theta}\\ X_1(\theta) &= e^{A_0\theta}\int_0^\theta e^{-A_0 s}A_1(s)e^{A_0 s}ds\\ X_2(\theta) &= e^{A_0\theta}\int_0^\theta e^{-A_0 s}\left(A_1(s)X_1(s) + A_2(s)e^{A_0 s}\right)ds\end{aligned} \tag{4.212}$$

The coefficients of the characteristic polynomial of the monodromy matrix M (Eq. (4.200)) are given by the Newton's identities:

$$\begin{aligned}a &= -Tr(M) = -Tr(X(2\pi))\\ b &= \frac{1}{2}\left(Tr(M)^2 - Tr(M^2)\right) = \frac{1}{2}\left(Tr(X(2\pi))^2 - Tr(X(4\pi))\right)\\ c &= -\frac{1}{6}Tr(M)^3 + \frac{1}{2}Tr(M)Tr(M^2) - \frac{1}{3}Tr(M^3)\\ d &= \frac{1}{24}Tr(M)^4 - \frac{1}{4}Tr(M)^2Tr(M^2) + \frac{1}{3}Tr(M)Tr(M^3) + \frac{1}{8}Tr(M^2)^2 - \frac{1}{4}Tr(M^4)\end{aligned} \tag{4.213}$$

Then, we have that:

$$\begin{aligned}B &= a = -Tr(X(2\pi))\\ C &= b - 4 = \frac{1}{2}Tr(X(2\pi))^2 - \frac{1}{2}Tr(X(4\pi)) - 4\\ D &= c - 3a = -\frac{1}{6}Tr(X(2\pi))^3 + Tr(X(2\pi))\left(3 + \frac{1}{2}Tr(X(4\pi))\right) - \frac{1}{3}Tr(X(6\pi))\\ E &= d - 2b + 2\\ &= \frac{1}{24}Tr(X(2\pi))^4 - Tr(X(2\pi))^2\left(1 + \frac{1}{4}Tr(X(4\pi))\right) + \frac{1}{3}Tr(X(2\pi))Tr(X(6\pi))\\ &+ Tr(X(4\pi))\left(1 + \frac{1}{8}Tr(X(4\pi))\right) - \frac{1}{4}Tr(X(8\pi)) + 2\end{aligned} \tag{4.214}$$

To expand the matrix (4.181) in a Taylor series we find partial derivatives of the e-dependent terms:

$$\begin{aligned}\left.\frac{r'}{r}\right|_{e=0} &= \left.\frac{e\sin\theta}{1+e\cos\theta}\right|_{e=0} = 0\\ \left.\frac{\partial}{\partial e}\frac{r'}{r}\right|_{e=0} &= \left.\left(\frac{\sin\theta}{1+e\cos\theta} - \frac{e\sin\theta\cos\theta}{(1+e\cos\theta)^2}\right)\right|_{e=0} = \sin\theta\\ \left.\frac{\partial^2}{\partial e^2}\frac{r'}{r}\right|_{e=0} &= \left.\left(-2\frac{\sin\theta\cos\theta}{(1+e\cos\theta)^2} + 2\frac{e\sin\theta\cos^2\theta}{(1+e\cos\theta)^3}\right)\right|_{e=0} = -2\sin\theta\cos\theta\\ \left.\frac{r}{\omega^2}\right|_{e=0} &= \left.\frac{1}{1+e\cos\theta}\right|_{e=0} = 1\\ \left.\frac{\partial}{\partial e}\frac{r}{\omega^2}\right|_{e=0} &= \left.-\frac{\cos\theta}{(1+e\cos\theta)^2}\right|_{e=0} = -\cos\theta\\ \left.\frac{\partial^2}{\partial e^2}\frac{r}{\omega^2}\right|_{e=0} &= \left.2\frac{\cos^2\theta}{(1+e\cos\theta)^3}\right|_{e=0} = 2\cos^2\theta\end{aligned} \tag{4.215}$$

which gives

$$A_0 = \begin{bmatrix} 0 & 0 & K_{13} & K_{14} & 0 & 0 & 0 & 0 \\ 0 & 0 & K_{23} & K_{24} & 0 & 0 & 0 & 0 \\ K_{31}+W_{31} & K_{32}+W_{32} & 0 & 0 & 0 & 0 & K_{37} & K_{38} \\ K_{41}+W_{41} & K_{42}+W_{42} & 0 & 0 & 0 & 0 & K_{47} & K_{48} \\ K_{51} & K_{52} & 0 & 0 & 0 & 0 & K_{\Gamma^2} & K_{67} \\ K_{61} & K_{62} & 0 & 0 & 0 & 0 & K_{67} & K_{\Phi^2} \\ 0 & 0 & 0 & 0 & \frac{Gm}{y^3}K_{\gamma^2} & \frac{Gm}{y^3}K_{\gamma,\phi} & 0 & 0 \\ 0 & 0 & 0 & 0 & \frac{Gm}{y^3}K_{\gamma,\phi} & \frac{Gm}{y^3}K_{\phi^2} & 0 & 0 \end{bmatrix} \tag{4.216}$$

$$A_1 = \begin{bmatrix} -\sin\theta & 0 & 0 & 0 & 0 & 0 & 0 & 0 \\ 0 & -\sin\theta & 0 & 0 & 0 & 0 & 0 & 0 \\ -\cos\theta K_{31} & -\cos\theta K_{32} & \sin\theta & 0 & 0 & 0 & 0 & 0 \\ -\cos\theta K_{41} & -\cos\theta K_{42} & 0 & \sin\theta & 0 & 0 & 0 & 0 \\ 0 & 0 & 0 & 0 & 0 & 0 & 0 & 0 \\ 0 & 0 & 0 & 0 & 0 & 0 & 0 & 0 \\ 0 & 0 & 0 & 0 & -\cos\theta\frac{Gm}{y^3}K_{\gamma^2} & -\cos\theta\frac{Gm}{y^3}K_{\gamma,\phi} & 0 & 0 \\ 0 & 0 & 0 & 0 & -\cos\theta\frac{Gm}{y^3}K_{\gamma,\phi} & -\cos\theta\frac{Gm}{y^3}K_{\phi^2} & 0 & 0 \end{bmatrix} \tag{4.217}$$

$$\begin{aligned} A_2 &= \begin{bmatrix} \sin\theta\cos\theta & 0 & 0 & 0 & 0 & 0 & 0 & 0 \\ 0 & \sin\theta\cos\theta & 0 & 0 & 0 & 0 & 0 & 0 \\ \cos^2\theta K_{31} & \cos^2\theta K_{32} & -\sin\theta\cos\theta & 0 & 0 & 0 & 0 & 0 \\ \cos^2\theta K_{41} & \cos^2\theta K_{42} & 0 & -\sin\theta\cos\theta & 0 & 0 & 0 & 0 \\ 0 & 0 & 0 & 0 & 0 & 0 & 0 & 0 \\ 0 & 0 & 0 & 0 & 0 & 0 & 0 & 0 \\ 0 & 0 & 0 & 0 & \cos^2\theta\frac{Gm}{y^3}K_{\gamma^2} & \cos^2\theta\frac{Gm}{y^3}K_{\gamma,\phi} & 0 & 0 \\ 0 & 0 & 0 & 0 & \cos^2\theta\frac{Gm}{y^3}K_{\gamma,\phi} & \cos^2\theta\frac{Gm}{y^3}K_{\phi^2} & 0 & 0 \end{bmatrix} \\ &= -\cos\theta \begin{bmatrix} -\sin\theta & 0 & 0 & 0 & 0 & 0 & 0 & 0 \\ 0 & -\sin\theta & 0 & 0 & 0 & 0 & 0 & 0 \\ -\cos\theta K_{31} & -\cos\theta K_{32} & \sin\theta & 0 & 0 & 0 & 0 & 0 \\ -\cos\theta K_{41} & -\cos\theta K_{42} & 0 & \sin\theta & 0 & 0 & 0 & 0 \\ 0 & 0 & 0 & 0 & 0 & 0 & 0 & 0 \\ 0 & 0 & 0 & 0 & 0 & 0 & 0 & 0 \\ 0 & 0 & 0 & 0 & -\cos\theta\frac{Gm}{y^3}K_{\gamma^2} & -\cos\theta\frac{Gm}{y^3}K_{\gamma,\phi} & 0 & 0 \\ 0 & 0 & 0 & 0 & -\cos\theta\frac{Gm}{y^3}K_{\gamma,\phi} & -\cos\theta\frac{Gm}{y^3}K_{\phi^2} & 0 & 0 \end{bmatrix} = -\cos\theta A_1 \end{aligned} \tag{4.218}$$

Now we will obtain expressions for the traces of the fundamental matrix (4.211) appearing in expressions (4.214). Starting with X_1:

$$\begin{aligned} Tr\left(X_1(2\pi)\right) &= Tr\left(e^{A_0 2\pi}\int_0^{2\pi} e^{-A_0 s}A_1(s)e^{A_0 s}\right)ds \\ &= \int_0^{2\pi} Tr\left(e^{A_0(2\pi-s)}A_1(s)e^{A_0 s}\right)ds \\ &= \int_0^{2\pi} Tr\left(A_1(s)e^{A_0 s}e^{A_0(2\pi-s)}\right)ds \\ &= \int_0^{2\pi} Tr\left(e^{A_0 2\pi}A_1(s)\right)ds = Tr\left(e^{A_0 2\pi}\int_0^{2\pi} A_1(s)ds\right) = 0 \\ \implies Tr\left(X_1(4\pi)\right) &= Tr\left(X_1(6\pi)\right) = Tr\left(X_1(8\pi)\right) = 0 \end{aligned} \tag{4.219}$$

since $\int_0^{2\pi} A_1(s)ds = \int_0^{4\pi} A_1(s)ds = \int_0^{6\pi} A_1(s)ds = \int_0^{8\pi} A_1(s)ds = 0$. Moving on to traces of X_2:

$$\begin{aligned}
Tr\left(X_2(2\pi)\right) =& Tr\left[e^{A_0 2\pi}\int_0^{2\pi} e^{-A_0 s}\left(A_1(s)X_1(s) + A_2(s)e^{A_0 s}\right)ds\right] \\
=& Tr\begin{bmatrix} e^{A_0 2\pi}\int_0^{2\pi} e^{-A_0 s}A_1(s)e^{A_0 s}\int_0^{s} e^{-A_0 u}A_1(u)e^{A_0 u}duds \\ -e^{A_0 2\pi}\int_0^{2\pi} e^{-A_0 s}\cos(s)A_1(s)e^{A_0 s}ds \end{bmatrix} \\
=& \int_0^{2\pi} Tr\left[e^{A_0 2\pi}e^{-A_0 s}A_1(s)e^{A_0 s}\int_0^{s} e^{-A_0 u}A_1(u)e^{A_0 u}du\right]ds \\
&-\int_0^{2\pi} Tr\left[e^{A_0 2\pi}e^{-A_0 s}\cos(s)A_1(s)e^{A_0 s}\right]ds \\
=& Tr\left[e^{A_0 2\pi}\int_0^{2\pi} e^{-A_0 s}A_1(s)e^{A_0 s}\int_0^{s} e^{-A_0 u}A_1(u)e^{A_0 u}duds\right] - Tr\left[e^{A_0 2\pi}\int_0^{2\pi}\cos(s)A_1(s)ds\right]
\end{aligned} \tag{4.220}$$

now using $A_1(\theta) = A_1(0)\cos\theta + A_1(\pi/2)\sin\theta$:

$$\begin{aligned}
Tr(X_2(2\pi)) =& \; Tr\left[e^{A_0 2\pi}\int_0^{2\pi} e^{-A_0 s}A_1(s)e^{A_0 s}\int_0^{s} e^{-A_0 u}A_1(u)e^{A_0 u}duds\right] \\
&- Tr\left[e^{A_0 2\pi}A_1(0)\int_0^{2\pi}\cos^2(s)ds\right] - Tr\left[e^{A_0 2\pi}A_1(\pi/2)\int_0^{2\pi}\cos(s)\sin(s)ds\right] \\
=& \; Tr\left[e^{A_0 2\pi}\int_0^{2\pi} e^{-A_0 s}A_1(s)e^{A_0 s}\int_0^{s} e^{-A_0 u}A_1(u)e^{A_0 u}duds\right] - \pi Tr\left[e^{A_0 2\pi}A_1(0)\right] \\
\implies Tr\left[X_2(4\pi)\right] =& \; Tr\left[e^{A_0 4\pi}\int_0^{4\pi} e^{-A_0 s}A_1(s)e^{A_0 s}\int_0^{s} e^{-A_0 u}A_1(u)e^{A_0 u}duds\right] - 2\pi Tr\left[e^{A_0 4\pi}A_1(0)\right] \\
\implies Tr\left[X_2(6\pi)\right] =& \; Tr\left[e^{A_0 6\pi}\int_0^{6\pi} e^{-A_0 s}A_1(s)e^{A_0 s}\int_0^{s} e^{-A_0 u}A_1(u)e^{A_0 u}duds\right] - 3\pi Tr\left[e^{A_0 6\pi}A_1(0)\right] \\
\implies Tr\left[X_2(8\pi)\right] =& \; Tr\left[e^{A_0 8\pi}\int_0^{8\pi} e^{-A_0 s}A_1(s)e^{A_0 s}\int_0^{s} e^{-A_0 u}A_1(u)e^{A_0 u}duds\right] - 4\pi Tr\left[e^{A_0 8\pi}A_1(0)\right]
\end{aligned} \tag{4.221}$$

Finally, combining Eq. (4.211) with Eqs. (4.219) and (4.221), we find the expansions in e for the traces of the fundamental matrix at multiples of 2π:

$$\begin{aligned}
Tr\left[X(2\pi)\right] &= Tr\left[X_0(2\pi)\right] + e^2 Tr\left[X_2(2\pi)\right] + O(e^3) \\
Tr\left[X(4\pi)\right] &= Tr\left[X_0(4\pi)\right] + e^2 Tr\left[X_2(4\pi)\right] + O(e^3) \\
Tr\left[X(6\pi)\right] &= Tr\left[X_0(6\pi)\right] + e^2 Tr\left[X_2(6\pi)\right] + O(e^3) \\
Tr\left[X(8\pi)\right] &= Tr\left[X_0(8\pi)\right] + e^2 Tr\left[X_2(8\pi)\right] + O(e^3)
\end{aligned} \tag{4.222}$$

Notice that, because the X_1 traces vanished in Eq. (4.219), there are no linear terms in e in these expansions, meaning that the coefficients of the reduced characteristic polynomial A, B, C and D (Eq. (4.214)) and, in turn, the discriminant (4.207) also depend on e only quadratically plus higher orders. Perturbing from $e = 0$, this means that the effect of eccentricity on stability is weaker than linear.

Having obtained the expressions for the traces Eqs. (4.219), (4.221) and (4.222) we are now able to estimate the coefficient multiplying e^2 in expanded discriminant, which then determines whether the influence of increasing eccentricity for circular cases is stabilizing or not.

4.8.2. Application

After having derived general expressions, we apply the above method to assess analytically the effect of orbital eccentricity on the stability of a circular periodic solution. To this end, we search for a configuration at the border of a stability region, one whose eigenvalues just collided on the imaginary axis and thus, a multiple eigenvalue is present. This border corresponds to the points where the real parts of the eigenvalues land on the zero plane in Fig. 4.8. In such a case, the discriminant is zero and we are "on the fence" in terms of linear stability, in other words, the solution is spectrally stable. Then, the e^2 term in the expanded discriminant will show whether an increment in eccentricity pushes the solution into the stability region or out of it. We

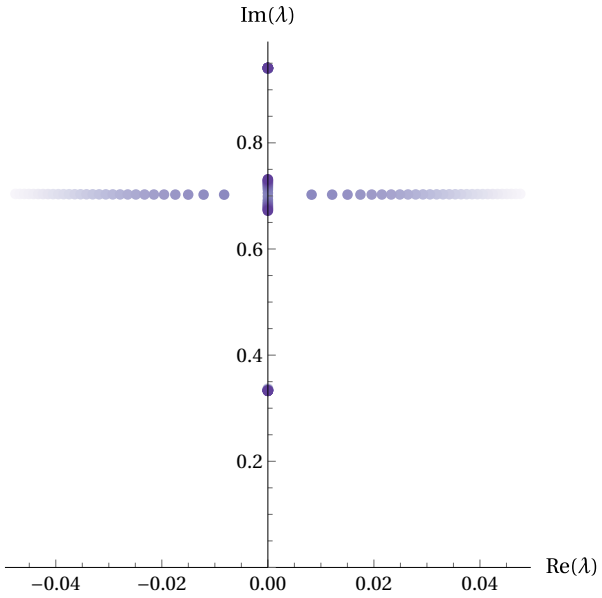

Figure 4.9: Eigenvalue collision on the imaginary axis as $\beta = 24°$ is held fixed and α is decreased from 42.308° to 42.3° in steps of $-0.0002°$. An accurate collision point is given in Table 4.1

α	42.3°
Eigenvalue 1	0.731397831942222453414124645614 i
Eigenvalue 2	0.672029334754486791749030031617 i
α	42.3022276245°
Eigenvalue 1	0.702312251207510903616061876761 i
Eigenvalue 2	0.702299941824885747567900087799 i
α	42.302227624595967248137702253379005337286344800588895316637699446 2°
Eigenvalue 1	0.702306096541656243784464865527342 6 i
Eigenvalue 2	0.702306096541656243784464865283369 4 i
α	42.3022276245959672481377022533790053372863448005888953166376994462°
Eigenvalue 1	0.702306096541656243784464865405356 1 i
Eigenvalue 2	0.702306096541656243784464865405355 9 i

Table 4.1: Bisection results of varying α for $\beta = 24°$ and $e = 0$ to find a configuration with a multiple eigenvalue.

choose to fix $\beta = 24°$ and find the α for which we have all eigenvalues imaginary with two pairs of multiple eigenvalues (two because of symmetry w.r.t. the real axis). This configuration corresponds to the collision point in Fig. 4.9 where the eigenvalues are plotted in the top half of the complex plane for $\beta = 24°$ and a range of α that crosses the stability border. Our task is equivalent to finding a root of the discriminant of the characteristic equation, as the discriminant is zero when multiple eigenvalues are present. However, the characteristic polynomial, even if reduced to a quartic, is messy and complicated with a ton of trigonometric functions of different powers involving α and thus, finding a root of the discriminant analytically is extremely difficult and may be impossible.

Therefore, we have to find an estimate for α numerically. We do this by a simple bisection method using the difference between the eigenvalues as a minimization goal. The results are shown in Table 4.1.

With Mathematica we calculate for $e = 0$, $\beta = 24°$,

$\alpha = 42.302227624595967248137702253379005337286344800588895316637699446 2°$:

$$\begin{aligned}
K_{31} &= 1.881995150123204990973301476482855605863951975791482 62\\
K_{32} &= -1.507612309829512330843055735335966621797567955362627 72\\
K_{41} &= -0.102241967240333138505435018169711918909057761685896786\\
K_{42} &= -0.912610647093293281488821831038534567959645321124341 82\\
K_{75} &= 2.684386506372517090614383756899770388829767503250749261910609332\\
K_{76} &= 0.038884333775630582693508382679357056873402466546710048087827 3335\\
K_{85} &= 0.038884333775630582693508382679357056873402466546710048087827 3335\\
K_{86} &= 0.102487123407347648587370310271673211595886687373693763717854 1492
\end{aligned} \tag{4.223}$$

The traces are then:

$$\begin{aligned}
Tr[X_0(2\pi)] &= -0.32409341519030092276844898787030141019560539842576143276 9649\\
Tr[X_0(4\pi)] &= -2.81928576720868738046085258720152505416965031632990156973 8407\\
Tr[X_0(6\pi)] &= 6.00800985478356358119600309640062891515206627681143960958 1758\\
Tr[X_0(8\pi)] &= 0.59272814681608450337869181409231373860080925317626619312 9046
\end{aligned} \tag{4.224}$$

Surprisingly, all double integrals in expressions (4.221) turn out to be zero and the X_2 traces are determined solely by the trailing terms. They turn out to be:

$$\begin{aligned}
Tr[X_2(2\pi)] &= 17.653002671864455374282529019648468723765434234894850\\
Tr[X_2(4\pi)] &= -136.47917955181061841798517282641199952303872254183446 5\\
Tr[X_2(6\pi)] &= 211.81001980041757744936327855244585691893226095262853 0\\
Tr[X_2(8\pi)] &= 274.12948395782508851235804340139054369890658276858652
\end{aligned} \tag{4.225}$$

We have kept all numbers after the comma, because through a series of multiplications while calculating the discriminant the precision quickly diminishes, as one can see from the amount of certain digits that are left in the expression for Δ below. Plugging in the trace values into Eqs. (4.214) and (4.222) we obtain the reduced polynomial coefficients B, C, D, E and calculate the discriminant with Eq. (4.207):

$$\Delta = 0 - 1800.48887e^2 - 492276.94407e^4 + O(e^6) \tag{4.226}$$

We used automatic precision tracking functionality in Mathematica (discussed more in depth in the next section) to leave in our discriminant expression only the significant digits of which we are certain, such that we eliminate any random errors associated to machine precision. Notice that for $e = 0$ the discrimintant is zero, which verifies the calculations at the multiple root point, because $\Delta = 0$ if and only if at least two roots are equal. Recall that for stability we require all roots of the reduced characteristic polynomial to be real. This tells us with certainty that increasing eccentricity by any positive amount will cause the discriminant to become negative, meaning that we will have two real and two complex conjugate roots of the reduced polynomial, which means four characteristic multipliers lie on the unit circle and four in the complex plane - instability by a Krein bifurcation. Therefore, eccentricity causes a destabilizing effect and whereas in the circular case at this configuration we are at the edge of stability, eccentric cases move into the unstable region, effectively shrinking the stable boundary later seen in Figs. 4.11, 4.15, 4.19, 4.22 and 4.24.

4.9. Eccentric cases

For the eccentric cases the coefficient matrix (4.181) of our linearized system of equations is no longer constant, but periodically varying, so we turn to Floquet theory and numerical simulation to assess the linear stability. The method we use is standard: we integrate the linear system for one period with the identity matrix as the initial state matrix [33]. This yields a fundamental matrix which tells us how each unit vector is mapped from the initial time to one period later. As discussed in Section 4.4, this matrix is the monodromy matrix $X(2\pi)$, which transforms any state vector to a state vector one period later:

$$X(2\pi)\boldsymbol{x}(\theta) = \boldsymbol{x}(\theta + 2\pi)$$

The eigenvalues of the monodromy matrix are called characteristic multipliers and for linear stability we require that each of them has magnitude exactly 1, that is, they lie on the unit circle in the complex plane (the monodromy matrix also has to be diagonalizable, otherwise we have spectral stability).

Method	Time [s]	Precision	Accuracy
Implicit RK10	1.14	14	26
RK9(8)	1.03	12	26
RK5(4)	7.59	12	26
RK8(9)	1.38	13	26
Adams	0.52	14	26
BDF	8.34	16	26

Table 4.2: Integration method comparison. The identity matrix is propagated by one period with each method for the square linearized system (4.193) and the characteristic multipliers are compared with analytically computed ones, resulting in precision and accuracy evaluations. We let the optimal order for Adams and BDF methods be automatically chosen by Mathematica.

4.9.1. Method of integration

We use the built-in Mathematica function **NDSolve** to numerically integrate the linear system of ODEs (4.181). We have a number of built-in integration methods to choose from [26]:

- explicit Runge-Kutta methods with adaptive embedded pairs 2(1) through 9(8),
- predictor-corrector Adams method, orders 1 through 12
- implicit backward differentiation formulas (BDF), orders 1 through 5
- families of arbitrary-order implicit Runge-Kutta methods
- symplectic partitioned Runge-Kutta methods for separable Hamiltonian systems

Even though the linearized system is Hamiltonian, the Hamiltonian function is not separable anymore into kinetic energy, which depends only on momenta, and potential energy that depends only on position variables. Therefore, we cannot use the symplectic partitioned Runge-Kutta methods in this case [37]. The other four methods are tested by integrating the linearized system for the square configuration with zero eccentricity. We set the initial states to the identity matrix, such that integration for one period produces the monodromy matrix. Then, the numerically obtained characteristic multipliers are compared with the analytically computed ones to obtain the precision and accuracy of the numerical method. Adapting the conventions used within Mathematica, by precision we mean the number of correct significant digits and by accuracy we mean the number of correct digits after the comma. These results along with the speed of each method are shown in Table 4.2. We see that the most precise method seems to be BDF, however it is also the slowest. We can sacrifice a couple of digits of accuracy for speed, as we will need to generate monodromy matrices for hundreds of cases. The second-most accurate methods seem to be the Implicit Runge-Kutta (IRK) and Adams methods, which we choose as our candidates to investigate further.

Next, we compare some settings of the integrators. Among the parameters we can choose is *WorkingPrecision*, *AccuracyGoal* and *PrecisionGoal*. These choices will impact the precision of the end result. As *arbitrary precision numbers* are being used (this is the name within Mathematica for numbers that carry precision information with them), Mathematica keeps track of the error internally and estimates the precision of these numbers after calculations automatically. The significant digits of arbitrary precision numbers within the integrator are set by *WorkingPrecision* parameter. In contrast, were we to use machine precision, the digits that are affected by rounding error are kept and can often be completely random, because all machine precision numbers are padded to 16 digits if some of the digits are unknown. With arbitrary precision numbers in Mathematica only the known digits are kept and if no digits are known with certainty anymore, a 0 is displayed with a warning that no digits are known. We cross-verified the computed precision and accuracy results from Table 4.2 with the ones estimated by Mathematica and found perfect agreement. The *PrecisionGoal* setting tells the integrator how many correct significant digits to aim for (relative precision), while *AccuracyGoal* tells how many digits after the floating point should be correct (absolute precision). Both of these settings are half the *WorkingPrecision* by default. The results for various settings combinations for the IRK and Adams integrators are shown in Tables 4.3 and 4.4 respectively.

We see that in all cases, the Adams integrator produces results of the same or better accuracy than IRK and, therefore, we choose it as our integrator with the settings as in the last row of Table 4.4 (a smaller *StartingStepSize* is required for higher precision integration for convergence).

WorkingPrecision	AccuracyGoal	PrecisionGoal	Time [s]	Precision	Accuracy
15	10	10	0.58	5	11
20	10	10	0.58	10	16
20	15	15	1.09	4	16
30	15	15	1.14	14	26
30	20	20	1.67	9	26

Table 4.3: Implicit RK integration precision comparison.

StartingStepSize	WorkingPrecision	AccuracyGoal	PrecisionGoal	Time [s]	Precision	Accuracy
1/10	15	10	10	0.28125	5	11
1/10	20	10	10	0.265625	10	16
1/10	20	15	15	0.53125	5	16
1/10	30	15	15	0.484375	14	26
1/20	30	20	20	0.875	10	26
1/20	40	20	20	0.875	20	36

Table 4.4: Adams integration precision comparison.

4.9.2. Results

The monodromy matrices are symplectic maps, since a state transition matrix of a Hamiltonian system is always symplectic [3]. A known property of symplectic matrices is that their determinant is exactly 1. This provides a way to check the accuracy of our integrations. The determinants of the monodromy matrices are shown in Tables 4.5 and 4.6. We consider the number of significant digits to which the determinants round to exactly 1 as the precision of the matrices. By finding the maximum and minimum determinants of a given set of monodromy matrices we obtain the highest errors in the set and conclude that the monodromy matrices in this set must be at least as precise as the least precise determinant.

The characteristic multipliers of the coarse sampling of the convex configurations domain are shown in Fig. 4.10 for a range of eccentricities. We see that generally, the configurations become more unstable with increasing eccentricity. As we saw before, the stable cases are only plausible near the line of minimum β.

We zoom in to the region near the limit line and calculate the characteristic multipliers for a dense sampling of this region. The multipliers are rounded to 16 digits, as that is the minimum precision of all the monodromy matrices. Then, we simply label each configuration as stable or unstable based on whether the magnitudes of the multipliers are 1 or any other value. This yields the binary plots Figs. 4.11, 4.15, 4.19, 4.22 and 4.24 showing the stability regions for our sampling.

To verify the results shown in Figs. 4.11, 4.15, 4.19, 4.22 and 4.24 we plot the characteristic multipliers along each of the horizontal lines containing stable configurations in Figs. 4.12 to 4.14, 4.16 to 4.18, 4.20, 4.21 and 4.23. We see that in each case stability is lost either through a Krein bifurcation (two multipliers collide

Eccentricity	Precision	Max determinant	Min determinant
0	17	1.00000000000000002009	0.99999999999999990040
0.1	17	1.00000000000000000805	0.99999999999999974418
0.2	17	1.00000000000000001528	0.99999999999999983374
0.3	17	1.00000000000000000792	0.99999999999999974800
0.4	17	1.00000000000000002048	0.99999999999999977990
0.5	17	1.00000000000000002894	0.99999999999999982603
0.6	17	1.00000000000000003231	0.99999999999999978438
0.7	17	1.00000000000000002396	0.99999999999999982907
0.8	16	1.00000000000000004703	0.99999999999999946127
0.9	16	1.00000000000000011508	0.99999999999999768746

Table 4.5: Precision of the monodromy matrices of the coarse sampling of the convex cases, corresponding to Fig. 4.10.

Eccentricity	Precision	Max determinant	Min determinant
0	18	1.000000000000000002652	0.999999999999999995163
0.1	17	1.00000000000000001199	0.99999999999999962165
0.2	17	1.00000000000000004228	0.99999999999999961145
0.3	17	1.00000000000000003863	0.99999999999999969099
0.4	17	1.00000000000000002929	0.99999999999999962863
0.5	17	1.00000000000000004979	0.99999999999999961157
0.6	17	1.00000000000000003779	0.99999999999999966292
0.7	17	1.00000000000000004709	0.99999999999999973380
0.8	16	1.0000000000000013746	0.9999999999999892503
0.9	16	1.0000000000000060294	0.9999999999999562027

Table 4.6: Precision of the monodromy matrices of the fine sampling of the convex cases near the line of minimum β, corresponding to Figs. 4.11, 4.15, 4.19, 4.22 and 4.24.

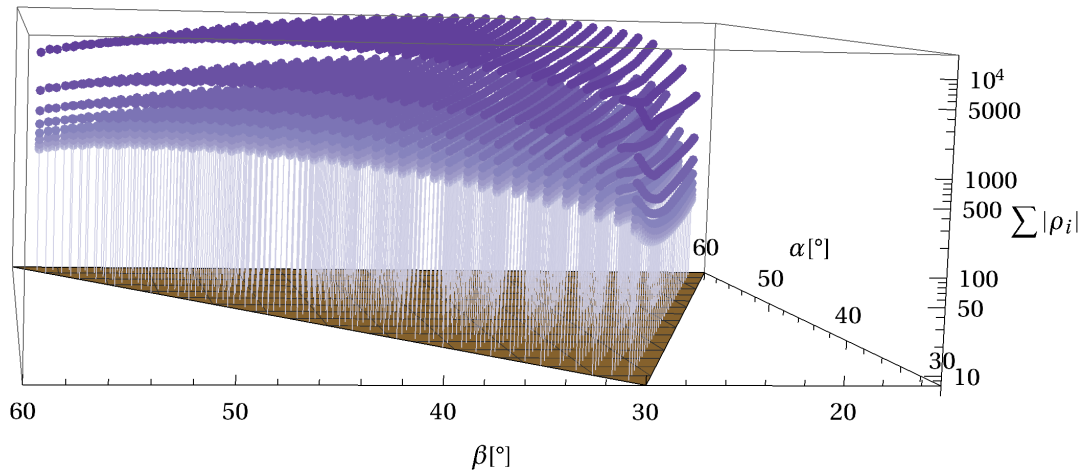

Figure 4.10: Sums of absolute values of characteristic multipliers for a sampling of the possible convex cases for eccentricities from 0 to 0.9. The coloured plane has height 8, which would be the sum of 8 multipliers on the unit circle.

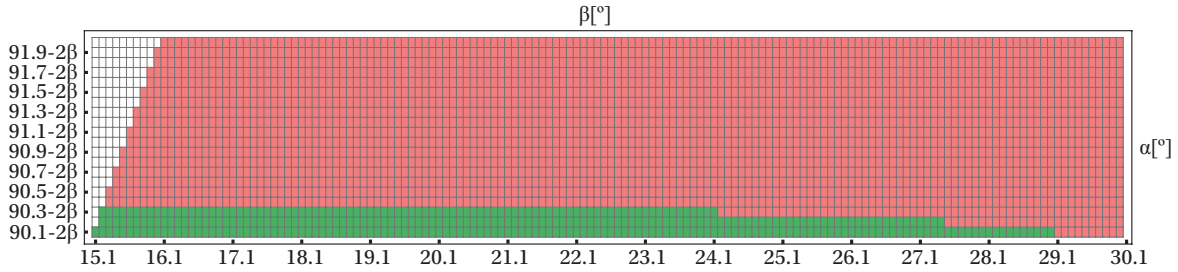

Figure 4.11: Stability diagram for the convex cases near the limit line for $e = 0$. Red means instability and green indicates linear stability.

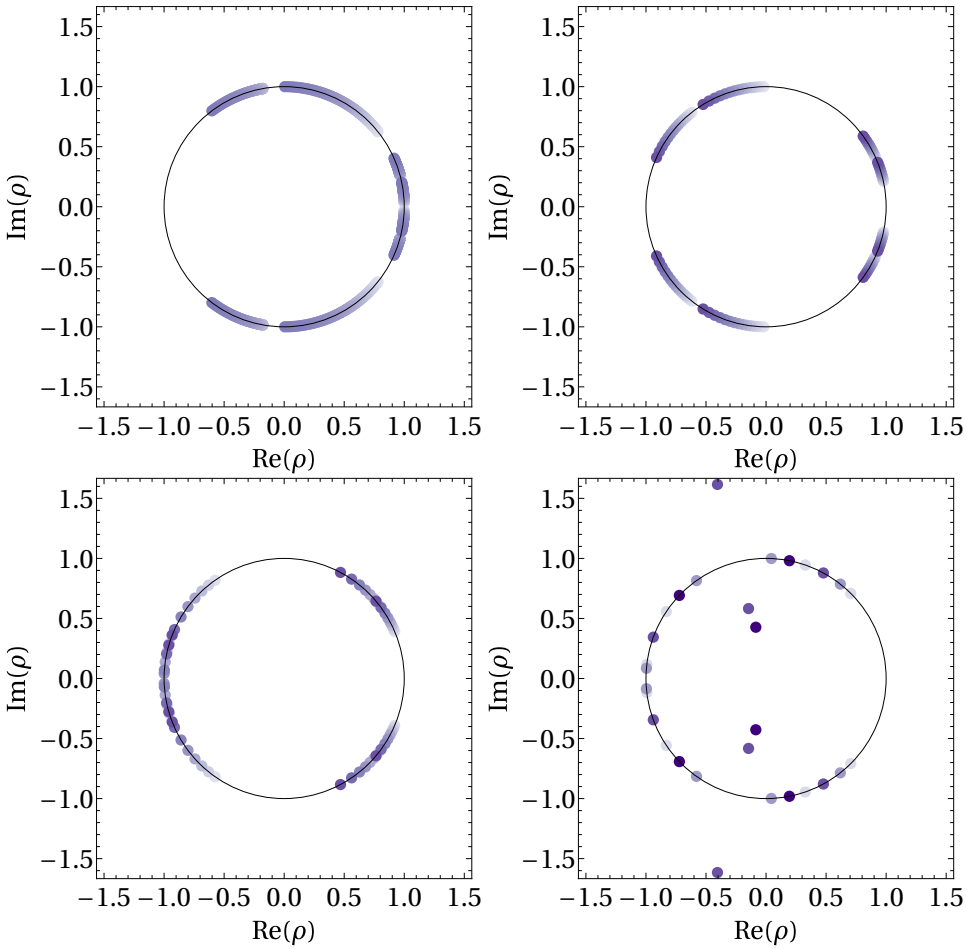

Figure 4.12: Characteristic multipliers along the bottom-most stable line for $e = 0$, $15.1° \leq \beta \leq 29.2°$, $59.9° \geq \alpha \geq 31.7°$. Stability is lost at $\beta = 29.1°$, $\alpha = 31.9°$.

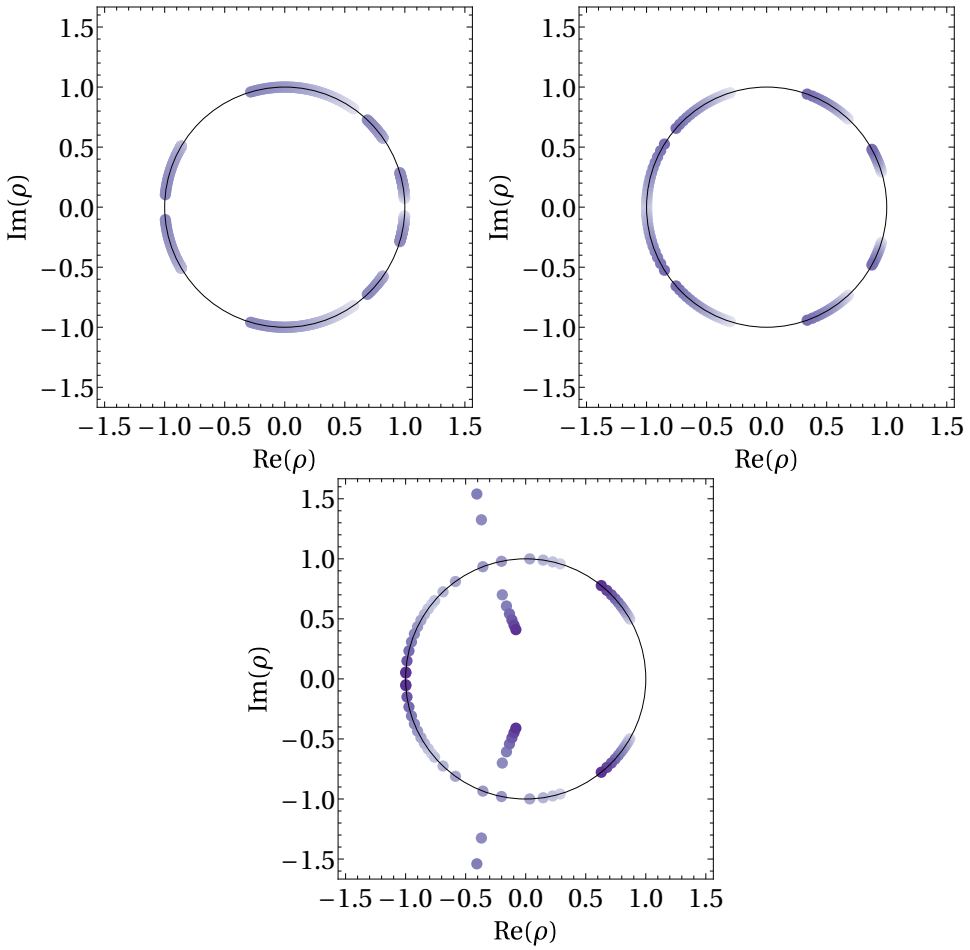

Figure 4.13: Characteristic multipliers along the second bottom-most line for $e = 0$, $15.2° \leq \beta \leq 28°$, $59.8° \geq \alpha \geq 34.2°$. Stability is lost at $\beta = 27.5°$, $\alpha = 35.2°$.

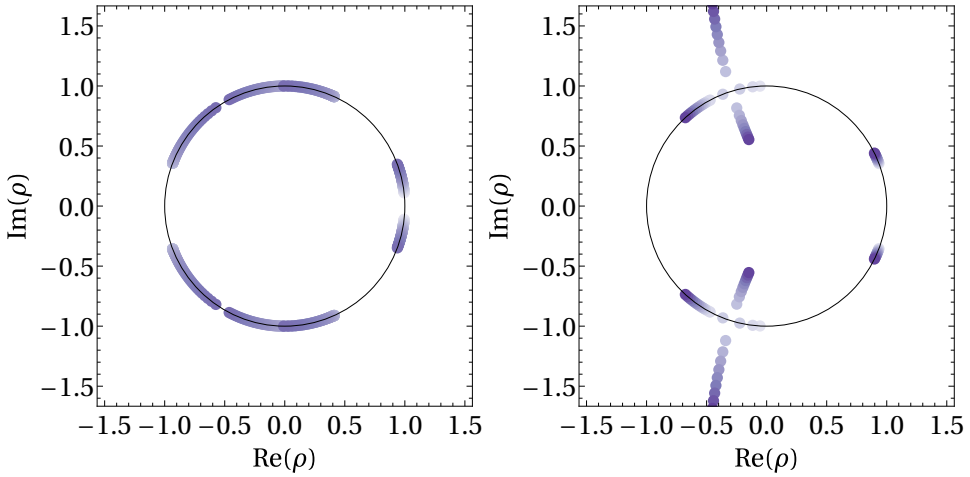

Figure 4.14: Characteristic multipliers along the third bottom-most line for $e = 0$, $15.2° \leq \beta \leq 25°$, $59.9° \geq \alpha \geq 40.3°$. Stability is lost at $\beta = 24.2°$, $\alpha = 41.9°$.

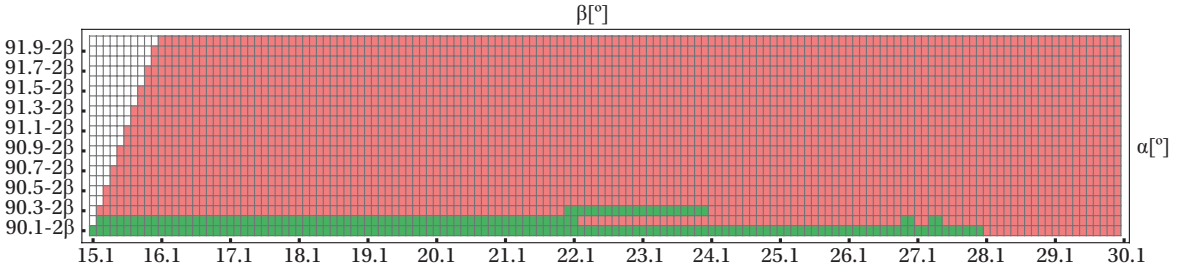

Figure 4.15: Stability diagram for the convex cases near the limit line for $e = 0.1$. Red means instability and green indicates linear stability.

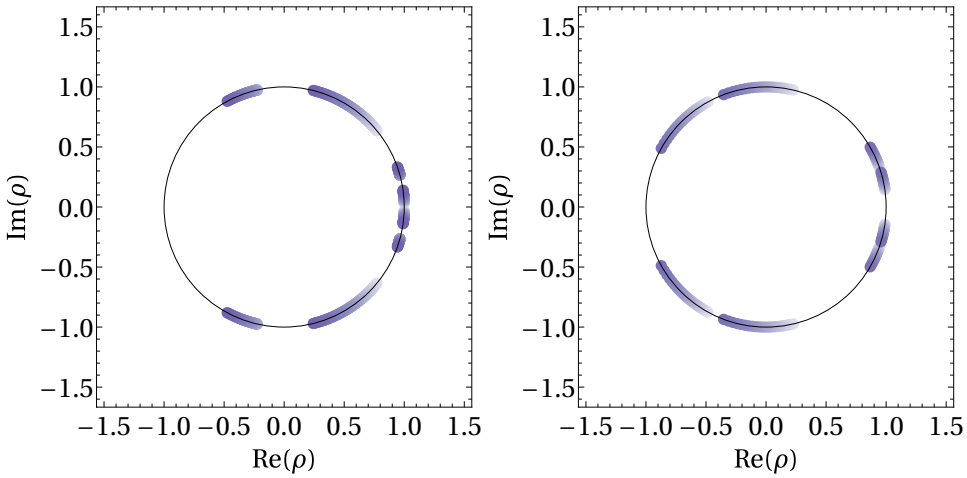

Figure 4.16: Characteristic multipliers along the bottom-most line of Fig. 4.15.

on the unit circle and split off to the complex plane) or a period-doubling bifurcation (two multipliers collide at -1 and split off onto the real axis) [27]. In theory, there is another possibility, which is when two multipliers collide at +1 and split off onto the real axis, but this bifurcation does not seem to appear in any of our cases.

These plots verify that inside the green regions we have 8 multipliers travelling along the unit circle, a qualitative result that was expected and could not possibly be produced by numerical error, i.e. we could not see the multipliers moving in such a fashion were they not actually on the unit circle, which serves as a convincing verification. Moreover, we now see that throughout the absolute majority of the regions we have eight distinct multipliers and the only places where we have multiple eigenvalues is at the collisions, that is, at the boundaries of the stability regions. This means that all the green cases in the stability plots are linearly stable, since none of them are exactly at a collision. Were we to consider a case that was exactly on the boundary, we would have to investigate the dimension of its eigenspace to conclude linear stability, as such cases may only be spectrally stable.

In conclusion, we find that up until at least $e = 0.3$ there is a thin region of stability near the limit case where a single body has all the mass. Increasing the eccentricity generally has the effect of destabilizing the configurations, as is clearly seen from Fig. 4.10 and from the shrinking green region in Figs. 4.11, 4.15, 4.19, 4.22 and 4.24. Even still, we find an anomaly for eccentricity $e = 0.2$, where one isolated sample is stable, as seen in Figs. 4.19 and 4.21, while the same configuration is unstable for lower eccentricities. That region seems to be very sensitive to changes in the parameters, as characterized by the rapidly changing eigenvalues in Fig. 4.21, and so seems to be an almost accidental stable island, for which we can't provide a clear reason.

It is proven in [27] that for the elliptic Lagrangian triangle configurations, there is also a region of mass ratios, which are linearly stable in eccentric cases, but not in the circular ones. Therefore, it is a phenomenon known to occur in central configurations. In our case, however, the stable configuration is isolated from the main region of stability, which makes this result even stranger, but true nevertheless, as seen from Fig. 4.21, where we find eight distinct eigenvalues on the unit circle, with significant digression from the boundary of stability.

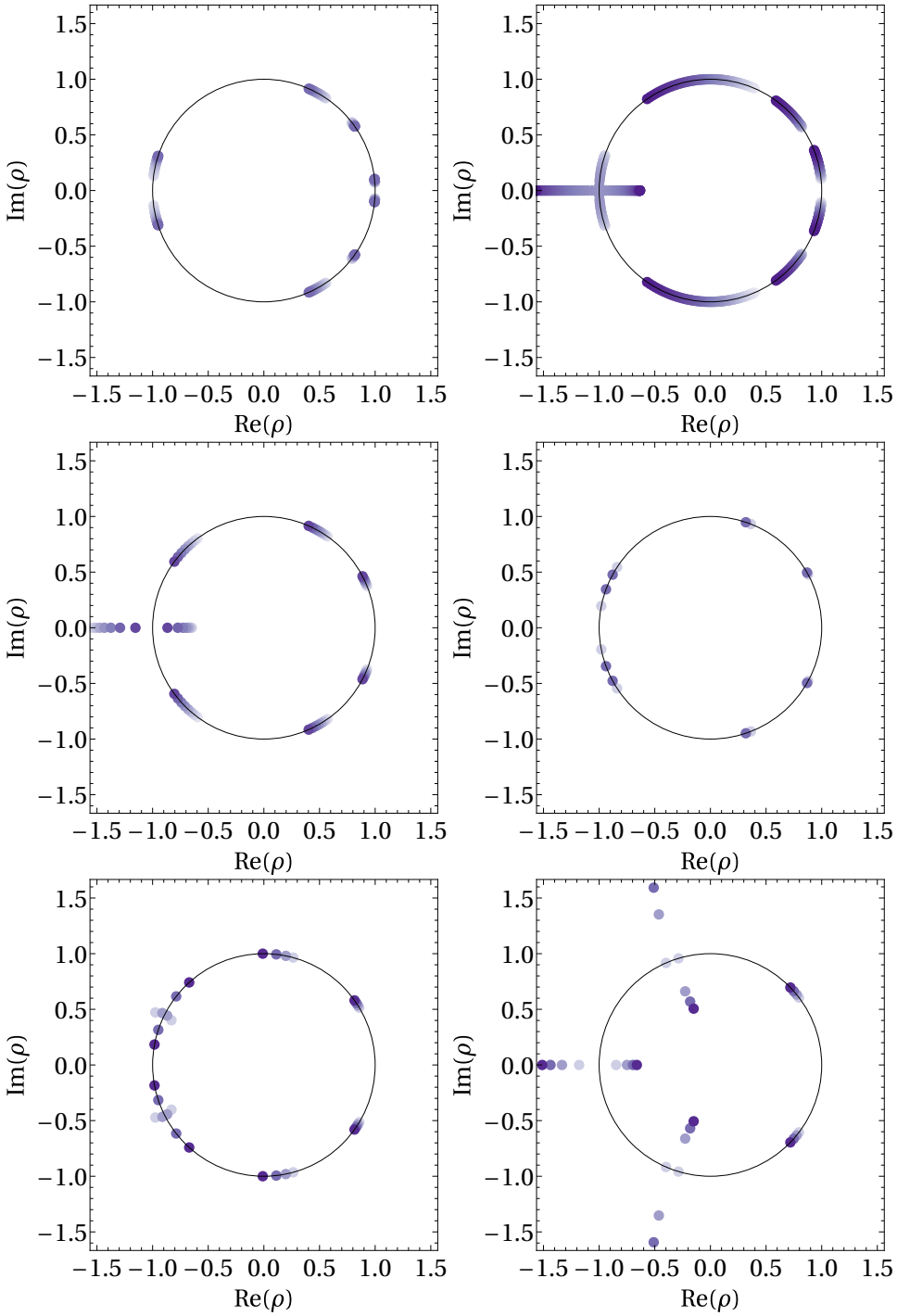

Figure 4.17: Characteristic multipliers along the second bottom-most line of Fig. 4.15, $e = 0.1$, $15.2° \leq \beta \leq 27.8°$, $59.8° \geq \alpha \geq 34.6°$. Stability is lost at $\beta = 22.2°$, $\alpha = 45.8°$ (top right image), then regained at $\beta = 26.9°$, $\alpha = 36.4°$ (middle right image), lost again at $\beta = 27.1°$, $\alpha = 36°$ (bottom left image), regained again at $\beta = 27.3°$, $\alpha = 35.6°$ (bottom left image) and finally lost at $\beta = 27.5°$, $\alpha = 35.2°$ (bottom right image).

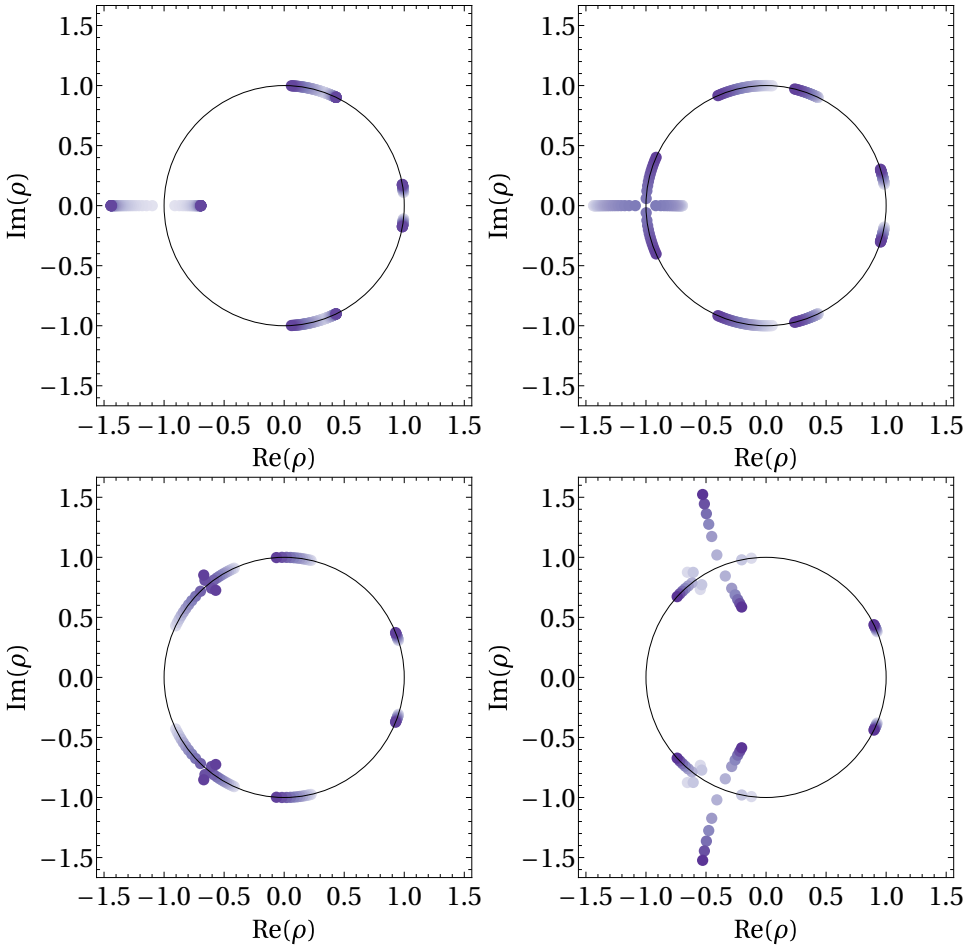

Figure 4.18: Characteristic multipliers along the third bottom-most line of Fig. 4.15, $e = 0.1$, $15.2° \leq \beta \leq 25°$, $59.9° \geq \alpha \geq 40.3°$. Stability is gained at $\beta = 22°$, $\alpha = 46.3°$ (top right image), then lost again at $\beta = 24.1°$, $\alpha = 42.1°$ (bottom left image).

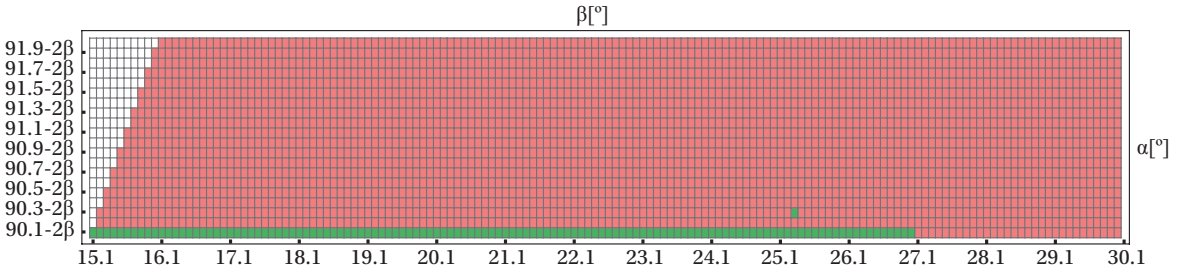

Figure 4.19: Stability diagram for the convex cases near the limit line for $e = 0.2$. Red means instability and green indicates linear stability.

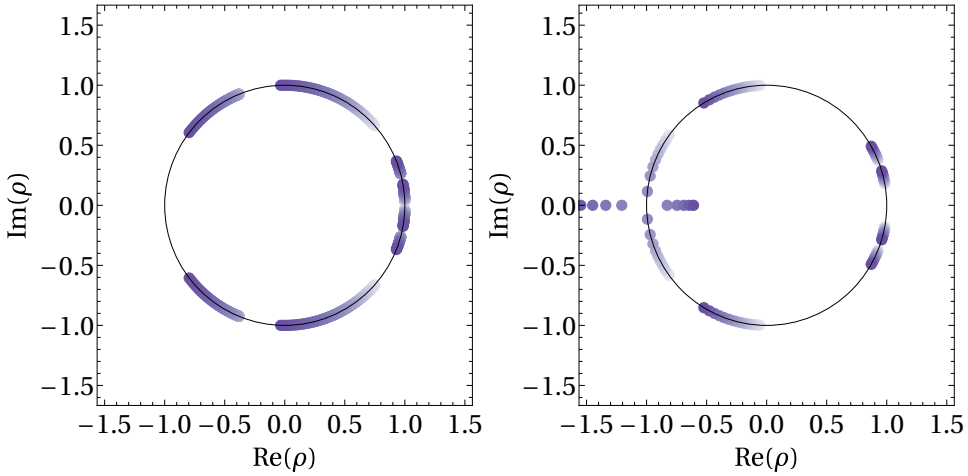

Figure 4.20: Characteristic multipliers along the bottom-most line of Fig. 4.19, $e = 0.2$, $15.1° \leq \beta \leq 27.5°$, $59.9° \geq \alpha \geq 35.1°$. Stability is lost at $\beta = 27.1°$, $\alpha = 35.9°$ (right image).

4.10. Closing remarks

To summarize, we have found that a region of linearly stable solutions exists in the convex case for eccentricities from 0 up to at least 0.3. Each of these solutions describes four bodies moving on Keplerian ellipses in a plane about the common center of mass. Note that we only considered the stability of the planar motion, however, it is an established fact that when considering the out-of-plane perturbations of planar relative equilibria, the variational equations decouple into the part governing the planar motion and another part governing the out-of-plane motion, the latter of which is always linearly stable [29]. This is also intuitive from observations, as many body systems, for example, planetary systems, such as our own Solar System, or rings around planets generally tend to planar motion, therefore out-of-plane motion gets diminished over time. Thus, our linear stability result extends to kite central configurations in three-dimensional space.

A very important observation is that all linearly stable configurations that we found are located within $0.4°$ from the $\alpha + 2\beta = 90°$ line, which, recall from Chapter 2, corresponds to the convex coorbital case with all mass in body 3 with other bodies situated on a 'lumpy ring" around it. The fact that we only find linearly stable solutions near this configuration agrees with the general pattern for stability of relative equilibria, which is that all known examples have a dominant mass and are ring-like, that is the small masses are situated near a circle around the big mass [19]. In fact, it is proven in [29] that RE of four-body problem are only stable in the planetary case, i.e. when there is a dominant mass. Hence, these facts verify that indeed our linear stability assessment produced sensible results and our results, in turn, add to the existing evidence for R. Moeckel's conjecture that all stable relative equilibria are ring-like [19].

Lastly, we remark that our results extend beyond the theory of RE, because we also assessed the linear stability of eccentric cases, which are not equilibria in a rotating frame. The linearly stable eccentric cases that we found are also situated near the co-orbital line, in fact even more so than the circular cases, since the stability region shrank for increasing eccentricity (see Figs. 4.11, 4.15, 4.19, 4.22 and 4.24). This, along with the largely matching trend of multipliers for different eccentricities in Fig. 4.10 suggests that the dominant mass and ring-like structure may also be required for stability of eccentric cases.

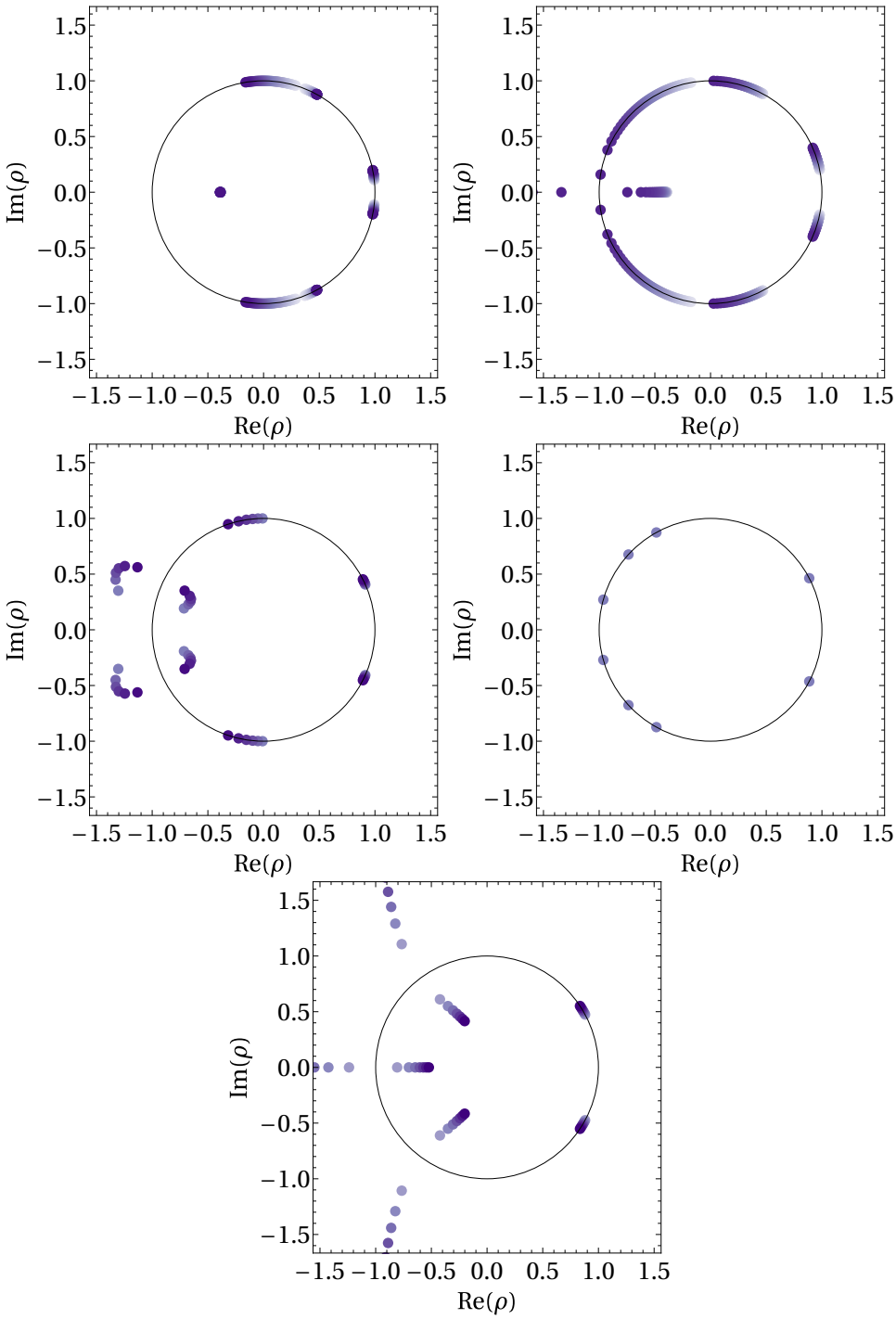

Figure 4.21: Characteristic multipliers along the third bottom-most line of Fig. 4.19, $e = 0.2$, $15.2° \leq \beta \leq 26°$, $59.9° \geq \alpha \geq 38.3°$. We have instability until a linearly stable sample at $\beta = 25.3°$, $\alpha = 39.7°$ (middle right image) is encountered, after which the configurations are again unstable.

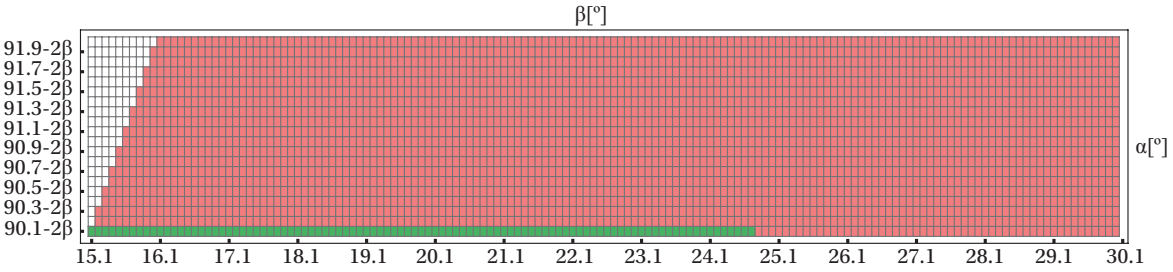

Figure 4.22: Stability diagram for the convex cases near the limit line for $e = 0.3$. Red means instability and green indicates linear stability.

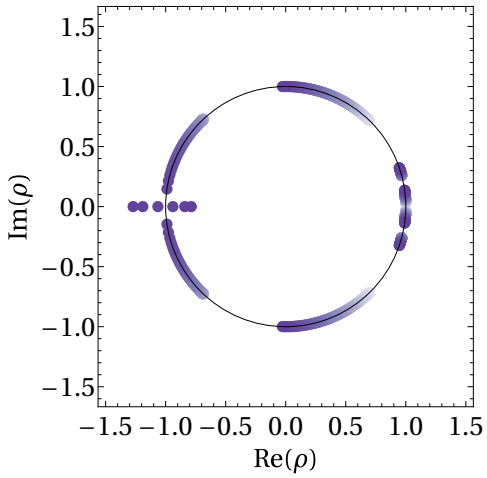

Figure 4.23: Characteristic multipliers along the bottom-most line of Fig. 4.22, $e = 0.3$, $15.1° \leq \beta \leq 25°$, $59.9° \geq \alpha \geq 40.1°$. Stability is lost at $\beta = 24.8°$, $\alpha = 40.5°$.

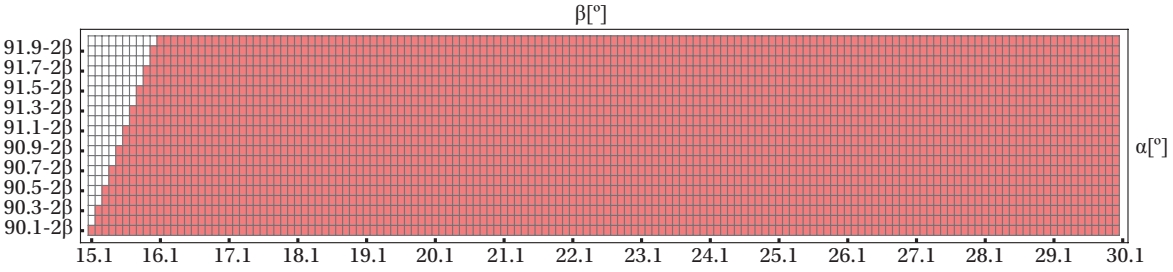

Figure 4.24: Stability diagram for the convex cases near the limit line for $e = 0.4$, $e = 0.5$, $e = 0.6$, $e = 0.7$, $e = 0.8$, $e = 0.9$. Red means instability and green means indicates stability.

5

First concave cases

So far, we have developed the procedure to compute the eigenvalues analytically (be it with the help of a computer algebra system) for the circular periodic solutions and characteristic multipliers for the elliptical solutions with the help of numerical integration. Having applied this to the convex cases, we now move on to the second of the three types of kite central configurations, as described in Chapter 2 - the first concave type. In these configurations, body m_3 lies inside the triangle defined by the other three bodies, while the center of mass lies inside the kite geometry described by all four bodies (see Fig. 2.4). The procedure to determine linear stability is the same, with only some sign changes in the computations, as we will see shortly.

5.1. Linearization

The mass ratios in the first concave case are given by [34]

$$\begin{aligned}\frac{m_3}{m_1} = \frac{m_3}{m_2} = \frac{m_3}{m} &= \frac{\tan\beta\left(\tan\alpha-\tan\beta\right)^2\left(1-8\cos^3\beta\right)}{4\left[\left(\sin\alpha-\cos\alpha\tan\beta\right)^3-1\right]}\\ \frac{m_4}{m_1} = \frac{m_4}{m_2} = \frac{m_4}{m} &= \frac{\tan\alpha\left(\tan\alpha-\tan\beta\right)^2\left(1-8\cos^3\alpha\right)}{4\left[\left(\sin\beta-\cos\beta\tan\alpha\right)^3+1\right]}\end{aligned} \tag{5.1}$$

where α and β must satisfy Eq. (2.2) The initial distances between the bodies are expressed in terms of y, α and β as

$$\begin{aligned} d_1 &= y\sec\alpha = \frac{y}{\cos\alpha}\\ d_2 &= y\sec\beta = \frac{y}{\cos\beta}\\ d_{34} &= y\left(\tan\alpha-\tan\beta\right)\end{aligned} \tag{5.2}$$

where the expression for the distance between the third and fourth bodies differs from that for the convex case by a minus sign, because now both bodies are on the same side of the vertical datum line (Fig. 2.4) and we have to subtract the distance to the inner body from the distance to the outer body. The time-dependent distances between the bodies are again obtained by multiplying with the scaling factor $r(t)$:

$$\begin{aligned}\kappa_1 = \kappa_3 = r_{23} = r_{13} = r d_1 &= \frac{r\,y}{\cos\alpha}\\ \kappa_2 = \kappa_4 = r_{24} = r_{14} = r d_2 &= \frac{r\,y}{\cos\beta}\\ \kappa_5 = r d_{34} &= r\,y\left(\tan\alpha-\tan\beta\right)\end{aligned} \tag{5.3}$$

The canonical coordinates of the linearized system are then

$$\begin{aligned} r_2 = c_2 r = 2yr \quad & R_2 = M_2 c_2 R \\ r_3 = c_3 r = y\tan\alpha\, r \quad & R_3 = M_3 c_3 R \\ r_4 = c_4 r = y\left(M_{33}\tan\alpha - \tan\beta\right) \quad & R_4 = M_4 c_4 R \\ \gamma = -\frac{\pi}{2} \quad & \Gamma = M_3 c_3^2 \omega + M_4 c_4^2 \omega \\ \phi = \pi \quad & \Phi = M_4 c_4^2 \omega \end{aligned} \tag{5.4}$$

where r_4, the length between the center of mass of the first three bodies and the fourth body, now has a minus sign, because, similarly to d_{34}, the two points are now both on the same side of the datum line (see Fig. 2.4), hence we have to subtract the distances.

The expressions for the mass parameters in terms of the masses remain the same:

$$\begin{aligned} M_{12} = M_{22} &= \frac{m_1}{m_1+m_2} = \frac{m_2}{m_1+m_2} = \frac{1}{2} \\ M_{13} = M_{23} &= \frac{m_1}{m_1+m_2+m_3} = \left(\frac{m_1}{m_1}+\frac{m_2}{m_1}+\frac{m_3}{m_1}\right)^{-1} = \left(2+\frac{m_3}{m}\right)^{-1} \\ M_{33} &= \frac{m_3}{m_1+m_2+m_3} = \left(\frac{m_1}{m_3}+\frac{m_2}{m_3}+\frac{m_3}{m_3}\right)^{-1} = \left(2\frac{m}{m_3}+1\right)^{-1} \end{aligned} \tag{5.5}$$

however, the values of M_{13}, M_{23} and M_{33} depend differently on α and β compared to the convex case, because of the different mass-geometry relationships Eq. (5.1).

The double derivatives for the first concave case are given below. Since the periodic solution of the first concave case differs from the convex case only by the sign change in variables κ_5 and c_4, only the derivatives which involve these variables will be different. They are marked orange to make tracking the changes easier. Meanwhile the derivatives not involving these variables are the same as in the convex case and are simply repeated here.

$$\left.\frac{\partial^2 H}{\partial r_2^2}\right|_{\phi(t)} = \boxed{3M_2\frac{\omega^2}{r^4} - \frac{1}{4}\frac{Gm^2}{r^3y^3} - \frac{1}{2}\frac{Gmm_3}{r^3y^3}\left(3\cos^5\alpha - \cos^3\alpha\right) - \frac{1}{2}\frac{Gmm_4}{r^3y^3}\left(3\cos^5\beta - \cos^3\beta\right)} \tag{5.6}$$

$$\begin{aligned} \left.\frac{\partial^2 H}{\partial r_2 \partial r_3}\right|_{\phi(t)} &= -\frac{3}{2}\frac{Gmm_3}{r^3y^5}\cos^5\alpha\, c_3 c_2 - \frac{3}{2}\frac{Gmm_4}{r^3y^5}\cos^5\beta\left(M_{33}^2 c_3 - M_{33}\,c_4\right)c_2 \\ &= -\frac{3}{2}\frac{Gmm_3}{r^3y^3}\cos^5\alpha 2\tan\alpha - \frac{3}{2}\frac{Gmm_4}{r^3y^3}\cos^5\beta\left(M_{33}^2\tan\alpha - M_{33}\left(M_{33}\tan\alpha - \tan\beta\right)\right)2 \\ &= \boxed{-3\frac{Gmm_3}{r^3y^3}\cos^4\alpha\sin\alpha - 3\frac{Gmm_4}{r^3y^3}M_{33}\cos^4\beta\sin\beta} \end{aligned} \tag{5.7}$$

$$\begin{aligned} \left.\frac{\partial^2 H}{\partial r_2 \partial r_4}\right|_{\phi(t)} &= -\frac{3}{2}\frac{Gmm_4}{r^3y^5}\cos^5\beta\left(c_4 - M_{33}c_3\right)c_2 = -\frac{3}{2}\frac{Gmm_4}{r^3y^3}\cos^5\beta\left(M_{33}\tan\alpha - \tan\beta - M_{33}\tan\alpha\right)2 \\ &= +3\frac{Gmm_4}{r^3y^3}\cos^5\beta\tan\beta = \boxed{+3\frac{Gmm_4}{r^3y^3}\cos^4\beta\sin\beta} \end{aligned} \tag{5.8}$$

$$\begin{aligned} \left.\frac{\partial^2 H}{\partial r_2\partial\gamma}\right|_{\phi(t)} &= \boxed{0} \quad \left.\frac{\partial^2 H}{\partial r_2\partial R_2}\right|_{\phi(t)} = \boxed{0} \quad \left.\frac{\partial^2 H}{\partial r_2\partial R_4}\right|_{\phi(t)} = \boxed{0} \\ \left.\frac{\partial^2 H}{\partial r_2\partial\phi}\right|_{\phi(t)} &= \boxed{0} \quad \left.\frac{\partial^2 H}{\partial r_2\partial R_3}\right|_{\phi(t)} = \boxed{0} \quad \left.\frac{\partial^2 H}{\partial r_2\partial\Phi}\right|_{\phi(t)} = \boxed{0} \end{aligned} \tag{5.9}$$

$$\left.\frac{\partial^2 H}{\partial r_2\partial\Gamma}\right|_{\phi(t)} = \boxed{\frac{\omega}{r^3 y}} \tag{5.10}$$

$$
\begin{aligned}
\left.\frac{\partial^2 H}{\partial r_3^2}\right|_{\phi(t)} =& 3\frac{M_3^2 c_3^4 \omega^2}{M_3}\frac{1}{c_3^4 r^4} \\
&-3\frac{Gmm_3}{r^5 y^5}\cos^5\alpha\, c_3^2 r^2 + \frac{Gmm_3}{r^3 y^3}\cos^3\alpha - 3\frac{Gmm_4}{r^5 y^5}\cos^5\beta\left(M_{33}^2 c_3 r - M_{33} c_4 r\right)^2 + \frac{Gmm_4}{r^3 y^3}\cos^3\beta M_{33}^2 \\
&-3\frac{Gmm_3}{r^5 y^5}\cos^5\alpha\,(c_3 r)^2 + \frac{Gmm_3}{r^3 y^3}\cos^3\alpha - 3\frac{Gmm_4}{r^5 y^5}\cos^5\beta\left(M_{33}^2 c_3 r - M_{33} c_4 r\right)^2 + \frac{Gmm_4}{r^3 y^3}\cos^3\beta M_{33}^2 \\
&-3\frac{Gm_3 m_4}{r^5 y^5}\left(\tan\alpha-\tan\beta\right)^{-5}\left(M_{c3}^2 c_3 r + M_{c3} c_4 r\right)^2 + \frac{Gm_3 m_4}{r^3 y^3}\left(\tan\alpha-\tan\beta\right)^{-3} M_{c3}^2 \\
=& 3M_3\frac{\omega^2}{r^4} - 6\frac{Gmm_3}{r^5 y^5}\cos^5\alpha\, c_3^2 r^2 + 2\frac{Gmm_3}{r^3 y^3}\cos^3\alpha \\
&-6\frac{Gmm_4}{r^3 y^3}\cos^5\beta\left(M_{33}^2\tan\alpha - M_{33}\left(M_{33}\tan\alpha-\tan\beta\right)\right)^2 + 2\frac{Gmm_4}{r^3 y^3}M_{33}^2\cos^3\beta \\
&-3\frac{Gm_3 m_4}{r^3 y^3}\left(\tan\alpha-\tan\beta\right)^{-5}\left(M_{c3}^2\tan\alpha + M_{c3}\left(M_{33}\tan\alpha-\tan\beta\right)\right)^2 + \frac{Gm_3 m_4}{r^3 y^3}\left(\tan\alpha-\tan\beta\right)^{-3} M_{c3}^2 \\
=& 3M_3\frac{\omega^2}{r^4} - 2\frac{Gmm_3}{r^3 y^3}\left(3\cos^5\alpha\tan^2\alpha - \cos^3\alpha\right) - 2\frac{Gmm_4}{r^3 y^3}M_{33}^2\left(3\cos^5\beta\tan^2\beta - \cos^3\beta\right) \\
&-\frac{Gm_3 m_4}{r^3 y^3}\left(\tan\alpha-\tan\beta\right)^{-5}\left(3\left(M_{c3}\tan\alpha\left(M_{c3}+M_{33}\right) - M_{c3}\tan\beta\right)^2 - M_{c3}^2\left(\tan\alpha-\tan\beta\right)^2\right) \\
=& \boxed{\begin{aligned}&3M_3\frac{\omega^2}{r^4} - 2\frac{Gmm_3}{r^3 y^3}\left(2\cos^3\alpha - 3\cos^5\alpha\right) - 2\frac{Gmm_4}{r^3 y^3}M_{33}^2\left(2\cos^3\beta - 3\cos^5\beta\right) \\ &\quad -2\frac{Gm_3 m_4}{r^3 y^3}M_{c3}^2\left(\tan\alpha-\tan\beta\right)^{-3}\end{aligned}}
\end{aligned}
\tag{5.11}
$$

$$
\begin{aligned}
\left.\frac{\partial^2 H}{\partial r_3 \partial r_4}\right|_{\phi(t)} =& -\frac{3}{2}\frac{Gmm_4}{r^5 y^5}\cos^5\beta\left(2c_4 r - 2M_{33} c_3 r\right)\left(M_{33}^2 c_3 r - M_{33} c_4 r\right) - \frac{Gmm_4}{r^3 y^3}M_{33}\cos^3\beta \\
&-\frac{3}{2}\frac{Gmm_4}{r^5 y^5}\cos^5\beta\left(2c_4 r - 2M_{33} c_3 r\right)\left(M_{33}^2 c_3 r - M_{33} c_4 r\right) - \frac{Gmm_4}{r^3 y^3}M_{33}\cos^3\beta \\
&-\frac{3}{2}\frac{Gm_3 m_4}{r^5 y^5}\left(\tan\alpha-\tan\beta\right)^{-5}\left(2c_4 r + 2M_{c3} c_3 r\right)\left(M_{c3}^2 c_3 r + M_{c3} c_4 r\right) + \frac{Gm_3 m_4}{r^3 y^3}\left(\tan\alpha-\tan\beta\right)^{-3} M_{c3} \\
=& -3\frac{Gmm_4}{r^3 y^5}\cos^5\beta\left(2c_4 - 2M_{33} c_3\right)\left(M_{33}^2 c_3 - M_{33} c_4\right) - 2\frac{Gmm_4}{r^3 y^3}M_{33}\cos^3\beta \\
&-\frac{3}{2}\frac{Gm_3 m_4}{r^3 y^5}\left(\tan\alpha-\tan\beta\right)^{-5}\left(2c_4 + 2M_{c3} c_3\right)\left(M_{c3}^2 c_3 + M_{c3} c_4\right) + \frac{Gm_3 m_4}{r^3 y^3}M_{c3}\left(\tan\alpha-\tan\beta\right)^{-3} \\
=& 6\frac{Gmm_4}{r^3 y^5}\cos^5\beta M_{33}\left(M_{33} c_3 - c_4\right)^2 - 2\frac{Gmm_4}{r^3 y^3}M_{33}\cos^3\beta \\
&-3\frac{Gm_3 m_4}{r^3 y^5}\left(\tan\alpha-\tan\beta\right)^{-5} M_{c3}\left(M_{c3} c_3 + c_4\right)^2 + \frac{Gm_3 m_4}{r^3 y^3}M_{c3}\left(\tan\alpha-\tan\beta\right)^{-3} \\
=& 6\frac{Gmm_4}{r^3 y^3}\cos^5\beta M_{33}\left(M_{33}\tan\alpha - M_{33}\tan\alpha + \tan\beta\right)^2 - 2\frac{Gmm_4}{r^3 y^3}M_{33}\cos^3\beta \\
&-3\frac{Gm_3 m_4}{r^3 y^3}\left(\tan\alpha-\tan\beta\right)^{-5} M_{c3}\left(M_{c3}\tan\alpha + M_{33}\tan\alpha-\tan\beta\right)^2 + \frac{Gm_3 m_4}{r^3 y^3}M_{c3}\left(\tan\alpha-\tan\beta\right)^{-3} \\
=& 2\frac{Gmm_4}{r^3 y^3}M_{33}\cos^3\beta\left(3\sin^2\beta - 1\right) - 2\frac{Gm_3 m_4}{r^3 y^3}M_{c3}\left(\tan\alpha-\tan\beta\right)^{-3} \\
=& \boxed{2\frac{Gmm_4}{r^3 y^3}M_{33}\left(2\cos^3\beta - 3\cos^5\beta\right) - 2\frac{Gm_3 m_4}{r^3 y^3}M_{c3}\left(\tan\alpha-\tan\beta\right)^{-3}}
\end{aligned}
\tag{5.12}
$$

$$\left.\frac{\partial^2 H}{\partial r_3 \partial \gamma}\right|_{\phi(t)} = \boxed{0} \qquad \left.\frac{\partial^2 H}{\partial r_3 \partial R_2}\right|_{\phi(t)} = \boxed{0}$$
$$\left.\frac{\partial^2 H}{\partial r_3 \partial \phi}\right|_{\phi(t)} = \boxed{0} \qquad \left.\frac{\partial^2 H}{\partial r_3 \partial R_3}\right|_{\phi(t)} = \boxed{0} \tag{5.13}$$
$$\left.\frac{\partial^2 H}{\partial r_3 \partial R_4}\right|_{\phi(t)} = \boxed{0}$$

$$\left.\frac{\partial^2 H}{\partial r_3 \partial \Gamma}\right|_{\phi(t)} = \boxed{-2\frac{\omega}{r^3 y}\tan^{-1}\alpha} \qquad \left.\frac{\partial^2 H}{\partial r_3 \partial \Phi}\right|_{\phi(t)} = \boxed{2\frac{\omega}{r^3 y}\tan^{-1}\alpha} \tag{5.14}$$

$$\begin{aligned}\left.\frac{\partial^2 H}{\partial \gamma^2}\right|_{\phi(t)} &= -6\frac{Gmm_3}{r^5 y^5}\cos^5\alpha\left(-\frac{1}{2}c_2 c_3 r^2\right)^2 - 6\frac{Gmm_4}{r^5 y^5}\cos^5\beta\left(\frac{1}{2}c_2 c_4 r^2 - \frac{1}{2}M_{33}c_2 c_3 r^2\right)^2 \\ &= -\frac{3}{2}\frac{Gmm_3}{ry}\cos^5\alpha\,(2\tan\alpha)^2 - \frac{3}{2}\frac{Gmm_4}{ry}\cos^5\beta\left(2\left(M_{33}\tan\alpha - \tan\beta\right) - M_{33}2\tan\alpha\right)^2 \\ &= \boxed{-6\frac{Gmm_3}{ry}\cos^3\alpha\sin^2\alpha - 6\frac{Gmm_4}{ry}\cos^3\beta\sin^2\beta}\end{aligned} \tag{5.15}$$

$$\left.\frac{\partial^2 H}{\partial \gamma \partial r_4}\right|_{\phi(t)} = \boxed{0} \tag{5.16}$$

$$\begin{aligned}\left.\frac{\partial^2 H}{\partial \gamma \partial \phi}\right|_{\phi(t)} &= -\frac{3}{2}\frac{Gmm_4}{ry^5}\cos^5\beta c_2 c_4\,(c_2 c_4 - M_{33}c_2 c_3) \\ &= -\frac{3}{2}\frac{Gmm_4}{ry^5}\cos^5\beta c_2^2 c_4\,(c_4 - M_{33}c_3) \\ &= -6\frac{Gmm_4}{ry}\cos^5\beta\left(M_{33}\tan\alpha - \tan\beta\right)\left(\left(M_{33}\tan\alpha - \tan\beta\right) - M_{33}\tan\alpha\right) \\ &= \boxed{+6\frac{Gmm_4}{ry}\cos^4\beta\sin\beta\left(M_{33}\tan\alpha - \tan\beta\right)}\end{aligned} \tag{5.17}$$

$$\left.\frac{\partial^2 H}{\partial \gamma \partial R_2}\right|_{\phi(t)} = \left.\frac{\partial^2 H}{\partial \gamma \partial R_3}\right|_{\phi(t)} = \left.\frac{\partial^2 H}{\partial \gamma \partial \Gamma}\right|_{\phi(t)} = \left.\frac{\partial^2 H}{\partial \gamma \partial R_4}\right|_{\phi(t)} = \left.\frac{\partial^2 H}{\partial \gamma \partial \Phi}\right|_{\phi(t)} = \boxed{0} \tag{5.18}$$

$$\begin{aligned}\left.\frac{\partial^2 H}{\partial r_4^2}\right|_{\phi(t)} =& 3\frac{M_4\omega^2}{r^4} - 3\frac{Gmm_4}{r^5 y^5}\cos^5\beta\,(c_4 r - M_{33}c_3 r)^2 + \frac{Gmm_4}{r^3 y^3}\cos^3\beta \\ & - 3\frac{Gmm_4}{r^5 y^5}\cos^5\beta\,(c_4 r - M_{33}c_3 r)^2 + \frac{Gmm_4}{r^3 y^3}\cos^3\beta \\ & - 3\frac{Gm_3 m_4}{r^5 y^5}\left(\tan\alpha - \tan\beta\right)^{-5}(c_4 r + M_{c3}c_3 r)^2 + \frac{Gm_3 m_4}{r^3 y^3}\left(\tan\alpha - \tan\beta\right)^{-3} \\ =& 3\frac{M_4\omega^2}{r^4} - 6\frac{Gmm_4}{r^5 y^5}\cos^5\beta\,(c_4 r - M_{33}c_3 r)^2 + 2\frac{Gmm_4}{r^3 y^3}\cos^3\beta \\ & - 3\frac{Gm_3 m_4}{r^5 y^5}\left(\tan\alpha - \tan\beta\right)^{-5}(c_4 r + M_{c3}c_3 r)^2 + \frac{Gm_3 m_4}{r^3 y^3}\left(\tan\alpha - \tan\beta\right)^{-3} \\ =& 3M_4\frac{\omega^2}{r_4} - 6\frac{Gmm_4}{r^3 y^3}\cos^5\beta\left(M_{33}\tan\alpha - \tan\beta - M_{33}\tan\alpha\right)^2 + 2\frac{Gmm_4}{r^3 y^3}\cos^3\beta \\ & - 3\frac{Gm_3 m_4}{r^3 y^3}\left(\tan\alpha - \tan\beta\right)^{-5}\left(M_{33}\tan\alpha - \tan\beta + M_{c3}\tan\alpha\right)^2 + \frac{Gm_3 m_4}{r^3 y^3}\left(\tan\alpha - \tan\beta\right)^{-3} \\ =& 3M_4\frac{\omega^2}{r^4} - 6\frac{Gmm_4}{r^3 y^3}\cos^3\beta\sin^2\beta + 2\frac{Gmm_4}{r^3 y^3}\cos^3\beta - 2\frac{Gm_3 m_4}{r^3 y^3}\left(\tan\alpha - \tan\beta\right)^{-3} \\ =& \boxed{3M_4\frac{\omega^2}{r^4} - 2\frac{Gmm_4}{r^3 y^3}\left(2\cos^3\beta - 3\cos^5\beta\right) - 2\frac{Gm_3 m_4}{r^3 y^3}\left(\tan\alpha - \tan\beta\right)^{-3}}\end{aligned} \tag{5.19}$$

$$\left.\frac{\partial^2 H}{\partial r_4 \partial \phi}\right|_{\phi(t)} = \left.\frac{\partial^2 H}{\partial r_4 \partial R_2}\right|_{\phi(t)} = \left.\frac{\partial^2 H}{\partial r_4 \partial R_3}\right|_{\phi(t)} = \left.\frac{\partial^2 H}{\partial r_4 \partial \Gamma}\right|_{\phi(t)} = \left.\frac{\partial^2 H}{\partial r_4 \partial R_4}\right|_{\phi(t)} = \boxed{0} \tag{5.20}$$

$$\left.\frac{\partial^2 H}{\partial r_4 \partial \Phi}\right|_{\phi(t)} = -2\frac{\omega}{c_4 r^3} = \boxed{-2\frac{\omega}{r^3 y}\left(M_{33}\tan\alpha - \tan\beta\right)^{-1}} \tag{5.21}$$

$$\begin{aligned}
\left.\frac{\partial^2 H}{\partial \phi^2}\right|_{\phi(t)} &= -3\frac{Gmm_4}{r^5 y^5}\cos^5\beta\left(\frac{1}{2}c_2 r c_4 r\right)^2 - \frac{Gmm_4}{r^3 y^3}\cos^3\beta\cdot -M_{33}c_3 r c_4 r \\
&\quad -3\frac{Gmm_4}{r^5 y^5}\cos^5\beta\left(-\frac{1}{2}c_2 r c_4 r\right)^2 - \frac{Gmm_4}{r^3 y^3}\cos^3\beta\cdot -M_{33}c_3 r c_4 r \\
&\quad -\frac{Gm_3 m_4}{r^3 y^3}\left(\tan\alpha-\tan\beta\right)^{-3} M_{c3}c_3 r c_4 r \\
&= -6\frac{Gmm_4}{r y^5}\cos^5\beta\frac{1}{4}c_2^2 {c_4}^2 + 2\frac{Gmm_4}{r y^3}\cos^3\beta M_{33}c_3 c_4 - \frac{Gm_3 m_4}{r y^3}\left(\tan\alpha-\tan\beta\right)^{-3} M_{c3}c_3 c_4 \\
&= -6\frac{Gmm_4}{r y}\cos^5\beta\left(M_{33}\tan\alpha-\tan\beta\right)^2 + 2\frac{Gmm_4}{r y}\cos^3\beta M_{33}\tan\alpha\left(M_{33}\tan\alpha-\tan\beta\right) \\
&\quad -\frac{Gm_3 m_4}{r y}\left(\tan\alpha-\tan\beta\right)^{-3} M_{c3}\tan\alpha\left(M_{33}\tan\alpha-\tan\beta\right) \\
&= -2\frac{Gmm_4}{r y}\cos^3\beta\left(M_{33}\tan\alpha-\tan\beta\right)\left(3\cos^2\beta\left(M_{33}\tan\alpha-\tan\beta\right) - M_{33}\tan\alpha\right) \\
&\quad -\frac{Gm_3 m_4}{r y}M_{c3}\tan\alpha\left(\tan\alpha-\tan\beta\right)^{-3}\left(M_{33}\tan\alpha-\tan\beta\right) \\
&= \boxed{\begin{aligned}&-2\frac{Gmm_4}{r y}\cos^3\beta\left(M_{33}\tan\alpha-\tan\beta\right)\left(M_{33}\tan\alpha\left(3\cos^2\beta-1\right)-3\cos\beta\sin\beta\right) \\ &-\frac{Gm_3 m_4}{r y}M_{c3}\tan\alpha\frac{M_{33}\tan\alpha-\tan\beta}{\left(\tan\alpha-\tan\beta\right)^3}\end{aligned}}
\end{aligned} \tag{5.22}$$

$$\frac{\partial^2 H}{\partial\phi\partial R_2} = \frac{\partial^2 H}{\partial\phi\partial R_3} = \frac{\partial^2 H}{\partial\phi\partial\Gamma} = \frac{\partial^2 H}{\partial\phi\partial R_4} = \frac{\partial^2 H}{\partial\phi\partial\Phi} = \boxed{0} \tag{5.23}$$

$$\begin{aligned}
\frac{\partial^2 H}{\partial R_2^2} &= \boxed{\frac{1}{M_2}} \\
\frac{\partial^2 H}{\partial R_2\partial R_3} = \frac{\partial^2 H}{\partial R_2\partial\Gamma} = \frac{\partial^2 H}{\partial R_2\partial R_4} = \frac{\partial^2 H}{\partial R_2\partial\Phi} &= \boxed{0}
\end{aligned} \tag{5.24}$$

$$\begin{aligned}
\frac{\partial^2 H}{\partial R_3^2} &= \boxed{\frac{1}{M_3}} \\
\frac{\partial^2 H}{\partial R_3\partial\Gamma} = \frac{\partial^2 H}{\partial R_3\partial R_4} = \frac{\partial^2 H}{\partial R_3\partial\Phi} &= \boxed{0}
\end{aligned} \tag{5.25}$$

$$\left.\frac{\partial^2 H}{\partial\Gamma^2}\right|_{\phi(t)} = \boxed{\frac{1}{4M_2 r^2 y^2} + \frac{1}{M_3 r^2 y^2}\tan^{-2}\alpha} \tag{5.26}$$

$$\frac{\partial^2 H}{\partial\Gamma\partial R_4} = \boxed{0} \qquad \frac{\partial^2 H}{\partial\Gamma\partial\Phi} = \boxed{-\frac{1}{M_3 r^2 y^2}\tan^{-2}\alpha} \tag{5.27}$$

$$\frac{\partial^2 H}{\partial R_4^2} = \boxed{\frac{1}{M_4}} \qquad \frac{\partial^2 H}{\partial R_4\partial\Phi} = \boxed{0} \tag{5.28}$$

$$\left.\frac{\partial^2 H}{\partial\Phi^2}\right|_{\phi(t)} = \frac{1}{r^2}\left(\frac{1}{M_3 c_3^2} + \frac{1}{M_4 {c_4}^2}\right) = \boxed{\frac{1}{r^2 y^2}\left(\frac{1}{M_3}\tan^{-2}\alpha + \frac{1}{M_4}\left(M_{33}\tan\alpha-\tan\beta\right)^{-2}\right)} \tag{5.29}$$

Finally, the coefficient matrix for the linearized system is given by:

$$JD^2H(\gamma(t)) =$$

$$\begin{bmatrix}
0 & 0 & 0 & 0 & 0 & \frac{1}{M_2} & 0 & 0 & 0 & 0 \\
0 & 0 & 0 & 0 & 0 & 0 & \frac{1}{M_3} & 0 & 0 & 0 \\
a_0 & -a_1 & 0 & 0 & 0 & 0 & 0 & H_{\Gamma^2} & 0 & -a_3 \\
0 & 0 & 0 & 0 & 0 & 0 & 0 & 0 & \frac{1}{M_4} & 0 \\
0 & a_1 & 0 & -a_2 & 0 & 0 & 0 & -a_3 & 0 & H_{\Phi^2} \\
-H_{r_2^2} & -H_{r_2,r_3} & 0 & -H_{r_2,r_4} & 0 & 0 & 0 & -a_0 & 0 & 0 \\
-H_{r_3,r_2} & -H_{r_3^2} & 0 & -H_{r_3,r_4} & 0 & 0 & 0 & a_1 & 0 & -a_1 \\
0 & 0 & -H_{\gamma^2} & 0 & -H_{\gamma,\phi} & 0 & 0 & 0 & 0 & 0 \\
-H_{r_4,r_2} & -H_{r_4,r_3} & 0 & -H_{r_4^2} & 0 & 0 & 0 & 0 & 0 & a_2 \\
0 & 0 & -H_{\phi,\gamma} & 0 & -H_{\phi^2} & 0 & 0 & 0 & 0 & 0
\end{bmatrix} \tag{5.30}$$

Having obtained these coefficients, the rest of the procedure to arrive at Eq. (4.181) is exactly the same as in the convex case. The v coefficients are expressed in terms of the double derivatives and the k coefficients in terms of the mass and length variables M_i, c_i. Therefore, all we have to do is substitute the new coefficient values into expressions for the terms of the transformed matrix (4.140) in Mathematica and the reduced 8x8 matrix for the first concave case is obtained. Then, performing the linear coordinate changes from Section 4.5 we arrive at the final matrix in the form of Eq. (4.181), but with new coefficients.

5.2. Circular cases

Linear stability of the circular cases may once again be analyzed using only algebraic computations of the eigenvalues of the coefficient matrix Eq. (4.181) made constant by setting $e = 0$. The domain of the first concave cases is sampled as shown in Fig. 5.1. Throughout most of the region the eigenvalues have real parts whose magnitudes total up to 8. Similarly to the convex case, the real parts are diminished as we approach the line $2\alpha - \beta = 90°$. This line corresponds to the limit case where all the mass is concentrated in body 4 (the interior body). Therefore, we increase the sampling resolution in the β direction near this line, as can be seen in Fig. 5.1. Although the real parts of the eigenvalues approach the zero plane (coloured plane in Figs. 5.1, 5.3 and 5.4) as we move towards the limit line, contrary to the convex case, they do not reach it. At 0.1° in β away from the line the real parts still have magnitudes of order 0.1 (see Figs. 5.2 and 5.4). Hence, we conclude that all circular cases in the first concave domain are linearly unstable.

5.3. Eccentric cases

The monodromy matrices are again found by numerical integration of the identity matrix for one period. The settings given to the **NDSolve** function in Mathematica are the "Adams" method with starting step size of 1/200, working precision 40, precision and accuracy goals 20. We estimate the monodromy matrices for a sampling of the first concave region with 1° resolution for eccentricities 0, 0.1, 0.2, 0.3, 0.4, 0.5, 0.6, 0.7, 0.8 and 0.9. The sums of the magnitudes of the characteristic multipliers for a range of eccentricities are shown in Fig. 5.5.

The precision of the generated monodromy matrices is checked in the same way as for the convex cases. For each eccentricity, the determinants of the 196 monodromy matrices are calculated and checked for the biggest deviation from 1. In this way we obtain a precision estimate for the monodromy matrices for each eccentricity, because they must be at least as precise as their determinants. The results are shown in Table 5.1.

The characteristic multipliers for the coarse sampling of the first concave region are shown in Fig. 5.5 for all eccentricities. We see that, again, eccentricity destabilizes the configurations, because the multipliers grow in magnitude.

Zooming in near the line $2\alpha - \beta = 90°$ and checking the magnitudes of the characteristic multipliers in the same way as in the convex case, we are unable to identify any stable configurations for any eccentricities (Fig. 5.6).

5.4. Closing remarks

One can clearly see from Figs. 5.3 and 5.4 that the real parts of the eigenvalues for the circular solutions of the first concave type are diminishing as the configurations approach the $2\alpha - \beta = 90°$ line. On the line, we have

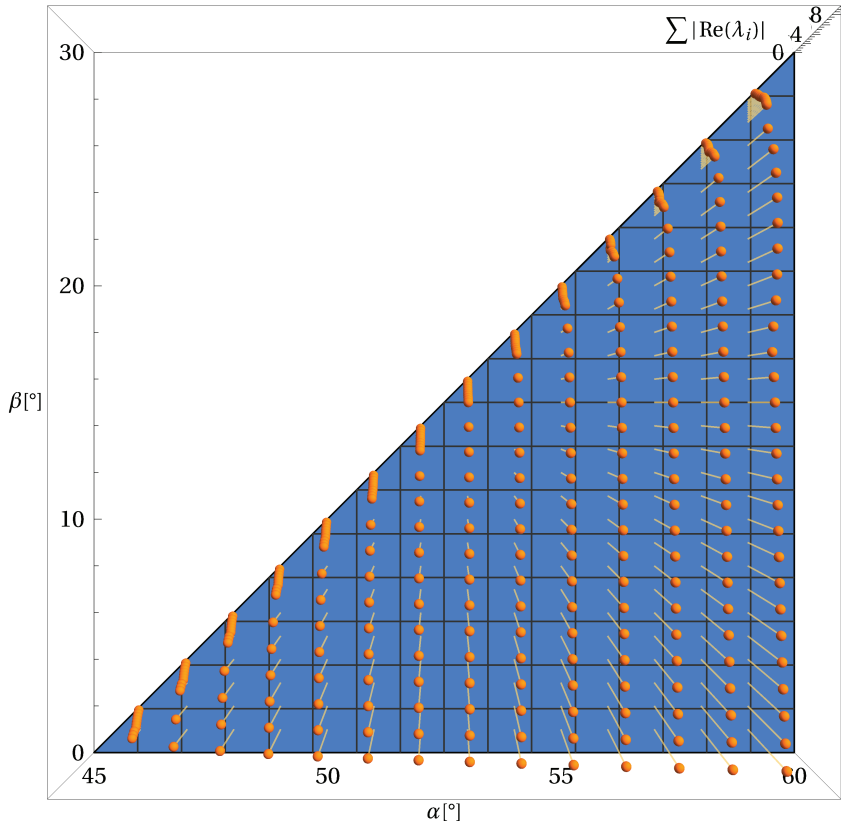

Figure 5.1: Top view of the total magnitudes of the real parts of the eigenvalues for the first concave domain.

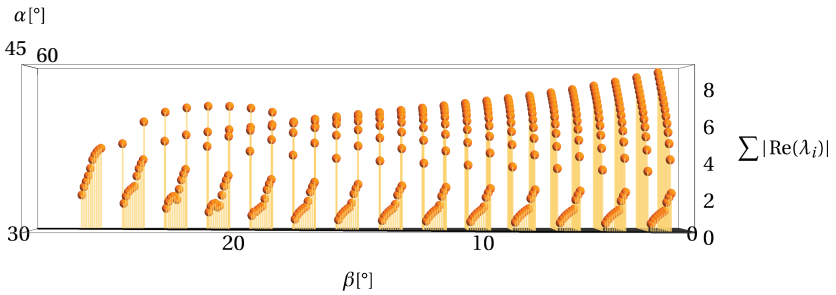

Figure 5.2: Front view of the total magnitudes of the real parts of the eigenvalues for the first concave domain.

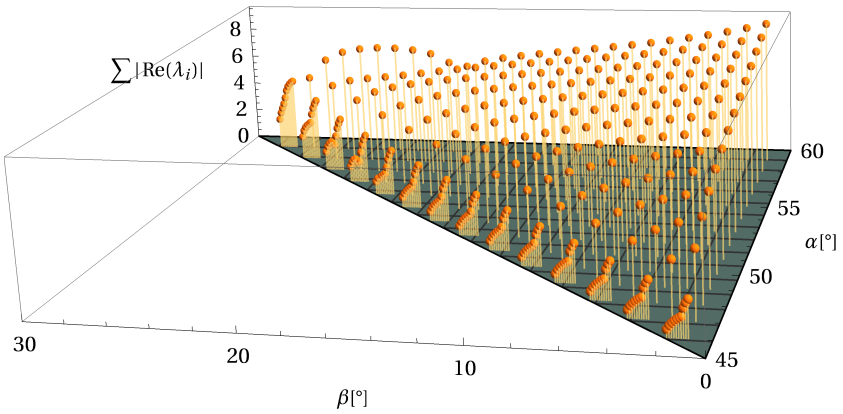

Figure 5.3: Total magnitudes of the real parts of the eigenvalues for the first concave domain.

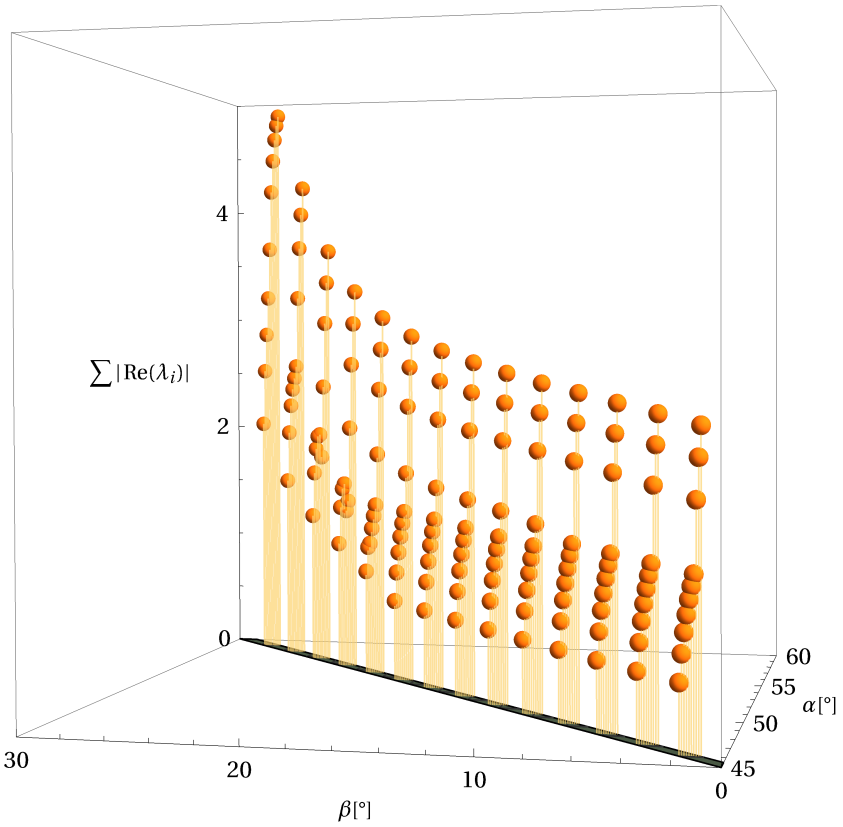

Figure 5.4: Zoom view of the total magnitudes of the real parts of the eigenvalues near the limit line of the first concave domain.

Eccentricity	Precision	Max determinant	Min determinant
0	18	1.000000000000000004381	1.000000000000000000000
0.1	17	1.00000000000000003714	0.999999999999999956707
0.2	17	1.00000000000000003429	0.999999999999999966389
0.3	17	1.00000000000000007273	0.999999999999999960632
0.4	16	1.00000000000000010725	0.999999999999999775570
0.5	16	1.00000000000000049886	0.999999999999999770063
0.6	16	1.00000000000000226624	0.999999999999999788055
0.7	14	1.00000000000000950938	0.999999999999991438185
0.8	14	1.00000000000004880508	0.999999999999968522191
0.9	13	1.00000000000026174559	0.999999999999882456815

Table 5.1: Precision of the monodromy matrices of the coarse sampling of the first concave cases, corresponding to Fig. 5.5.

Eccentricity	Precision	Max determinant	Min determinant
0	17	1.00000000000000009914	0.999999999999999994023
0.1	17	1.00000000000000003849	0.999999999999999970506
0.2	16	1.00000000000000004927	0.999999999999999944167
0.3	16	1.00000000000000008575	0.999999999999999942616
0.4	16	1.00000000000000007012	0.999999999999999888213
0.5	16	1.00000000000000009889	0.999999999999999842099
0.6	16	1.00000000000000019174	0.999999999999999740597
0.7	16	1.00000000000000023999	0.999999999999999839609
0.8	15	1.00000000000000113540	0.999999999999999357822
0.9	15	1.00000000000000924879	0.999999999999998295364

Table 5.2: Precision of the monodromy matrices of the fine sampling of the first concave cases near the line of maximum β, corresponding to Fig. 5.6.

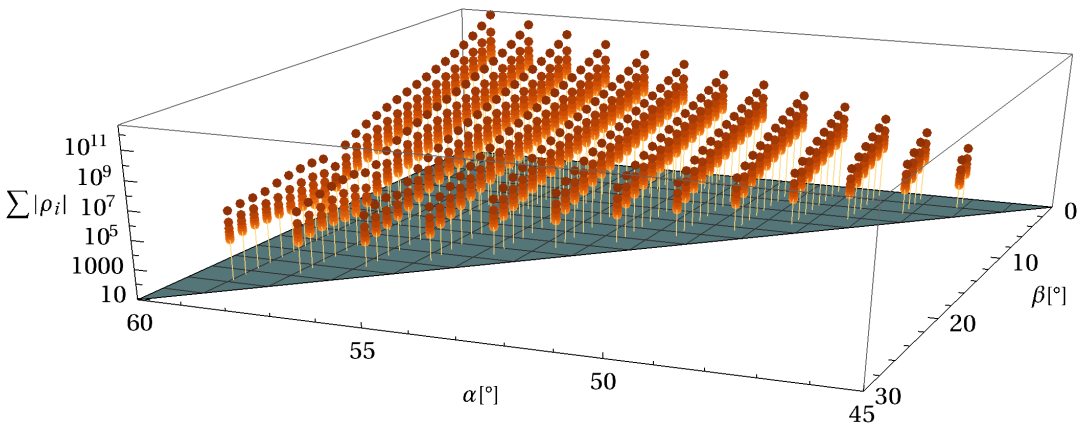

Figure 5.5: Sums of absolute values of characteristic multipliers for a sampling of the possible concave cases of the first kind for eccentricities from 0 to 0.9. The coloured plane has height 8, which would be the sum of 8 multipliers on the unit circle.

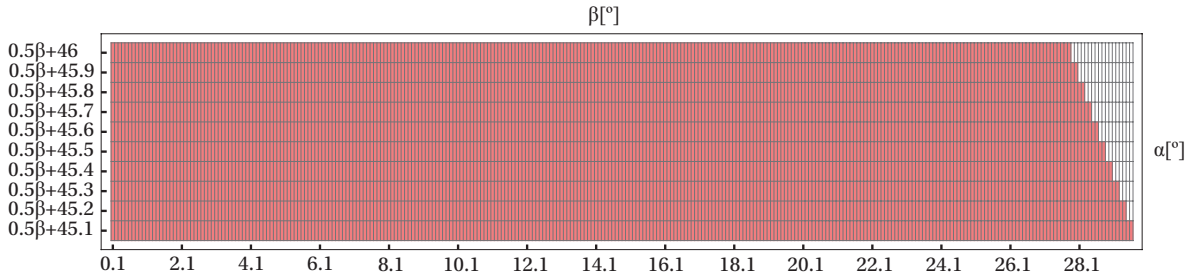

Figure 5.6: Stability diagram for the concave cases of the first kind near the limit line for $e = 0$, $e = 0.1$, $e = 0.2$, $e = 0.3$, $e = 0.4$, $e = 0.5$, $e = 0.6$, $e = 0.7$, $e = 0.8$, $e = 0.9$.

the concave coorbital situation, as discussed in Chapter 2, where three massless bodies orbit the inner body m_4 on a common circle. Similarly to the convex case, linear stability increases when approaching a configuration with a dominant mass and ring-like positioning. However, interestingly, this time linear stability is not reached, not even 0.1° away, as seen in Fig. 5.6. In Fig. 5.4 we see that the real parts of the eigenvalues increase for increasing α and decrease for increasing β. Looking at Fig. 2.6, we see that increasing α (going top to bottom in Fig. 2.6) diminishes the mass of the central body, thus destabilizing the configuration, while increasing β (going left to right in Fig. 2.6) increases the central mass and moves it towards the middle, thus providing a stabilizing effect. However, as we can see the balance works out to instability's side for all sampled concave cases of the first kind and even if for linear stability was found for some very fine sampling of the 0.1° gap near the limit line, for all practical purposes one would already be looking at the degenerate case of three infinitesimal masses orbiting one big mass.

6

Second concave cases

Finally, we are left with the last type of kite central configurations, that is the second concave type. Recall that in these configurations we have body 4 positioned inside the triangle defined by the other bodies, however, differently from the first concave case, the center of mass this time lies outside of the kite described by all four bodies, as shown in Fig. 2.7. We once again apply the procedure of linearization and eigenvalue calculation for the circular cases, complemented with the numerical estimation of characteristic multipliers for the elliptic cases. Also similarly to the last chapter, we encounter a sign change when comparing the expressions developed below with the ones in the previous two chapters.

6.1. Linearization

This time we have the variables ϕ and c_4 that are different from both the convex case and the first concave case. The endpoints of c_4 are now switched, because the center of mass of the first three bodies now switched places with the fourth body. This leads to a c_4 which is negative of the expression for the first concave case and ϕ becomes zero, because r_4 now points in the same direction as r_3.

$$\begin{aligned} c_4 &= y\left(\tan\beta - M_{33}\tan\alpha\right) \\ \phi &= 0 \end{aligned} \tag{6.1}$$

All other variables and mass coefficients are the same as in the first concave case, including the mass ratios Eq. (5.1).

Once again, the double derivatives are given below with the changed variables marked in green, for convenience of tracking the changes.

$$\begin{aligned} \frac{\partial^2 H}{\partial r_2^2} =& 3\frac{(c-\Gamma)^2}{M_2}\frac{1}{r_2^4} - 2\frac{Gm_1m_2}{r_2^3} - 3\frac{Gm_1m_3}{\kappa_1^5}\left(M_{22}^2 r_2 + M_{22}r_3\cos\gamma\right)^2 + \frac{Gm_1m_3}{\kappa_1^3}M_{22}^2 \\ & - 3\frac{Gm_1m_4}{\kappa_2^5}\left(M_{c1}^2 r_2 + M_{c1}r_4\cos(\gamma+\phi) + M_{33}M_{c1}r_3\cos\gamma\right)^2 + \frac{Gm_1m_4}{\kappa_2^3}M_{c1}^2 \\ & - 3\frac{Gm_2m_3}{\kappa_3^5}\left(M_{12}^2 r_2 - M_{12}r_3\cos\gamma\right)^2 + \frac{Gm_2m_3}{\kappa_3^3}M_{12}^2 \\ & - 3\frac{Gm_2m_4}{\kappa_4^5}\left(M_{c2}^2 r_2 + M_{c2}r_4\cos(\gamma+\phi) + M_{33}M_{c2}r_3\cos\gamma\right)^2 + \frac{Gm_2m_4}{\kappa_4^3}M_{c2}^2 \end{aligned} \tag{6.2}$$

$$\begin{aligned}\frac{\partial^2 H}{\partial r_2 \partial r_3} =& -\frac{3}{2}\frac{Gm_1m_3}{\kappa_1^5}\left(2r_3+2M_{22}r_2\cos\gamma\right)\left(M_{22}^2r_2+M_{22}r_3\cos\gamma\right)+\frac{Gm_1m_3}{\kappa_1^3}M_{22}\cos\gamma\\ &-\frac{3}{2}\frac{Gm_1m_4}{\kappa_2^5}\left(2M_{33}^2r_3+2M_{33}r_4\cos\phi+2M_{33}M_{c1}r_2\cos\gamma\right)\left(M_{c1}^2r_2+M_{c1}r_4\cos(\gamma+\phi)+M_{33}M_{c1}r_3\cos\gamma\right)\\ &+\frac{Gm_1m_4}{\kappa_2^3}M_{33}M_{c1}\cos\gamma\\ &-\frac{3}{2}\frac{Gm_2m_3}{\kappa_3^5}\left(2r_3-2M_{12}r_2\cos\gamma\right)\left(M_{12}^2r_2-M_{12}r_3\cos\gamma\right)-\frac{Gm_2m_3}{\kappa_3^3}M_{12}\cos\gamma\\ &-\frac{3}{2}\frac{Gm_2m_4}{\kappa_4^5}\left(2M_{33}^2r_3+2M_{33}r_4\cos\phi+2M_{33}M_{c2}r_2\cos\gamma\right)\left(M_{c2}^2r_2+M_{c2}r_4\cos(\gamma+\phi)+M_{33}M_{c2}r_3\cos\gamma\right)\\ &+\frac{Gm_2m_4}{\kappa_4^3}M_{33}M_{c2}\cos\gamma\end{aligned} \tag{6.3}$$

$$\left.\frac{\partial^2 H}{\partial r_2 \partial r_3}\right|_{\phi(t)} = -\frac{3}{2}\frac{Gmm_3}{r^3y^5}\cos^5\alpha c_3c_2-\frac{3}{2}\frac{Gmm_4}{r^3y^5}\cos^5\beta\left(M_{33}^2c_3+M_{33}c_4\right)c_2 \tag{6.4}$$

$$\begin{aligned}\frac{\partial^2 H}{\partial r_2 \partial \gamma} =& -\frac{3}{2}\frac{Gm_1m_3}{\kappa_1^5}\cdot -2M_{22}r_2r_3\sin\gamma\cdot\left(M_{22}^2r_2+M_{22}r_3\cos\gamma\right)+\frac{Gm_1m_3}{\kappa_1^3}\cdot -M_{22}r_3\sin\gamma\\ &-\frac{3}{2}\frac{Gm_1m_4}{\kappa_2^5}\cdot\left(-2M_{c1}r_2r_4\sin(\gamma+\phi)-2M_{33}M_{c1}r_2r_3\sin\gamma\right)\cdot\left(M_{c1}^2r_2+M_{c1}r_4\cos(\gamma+\phi)+M_{33}M_{c1}r_3\cos\gamma\right)\\ &+\frac{Gm_1m_4}{\kappa_2^3}\cdot\left(-M_{c1}r_4\sin(\gamma+\phi)-M_{33}M_{c1}r_3\sin\gamma\right)\\ &-\frac{3}{2}\frac{Gm_2m_3}{\kappa_3^5}\cdot 2M_{12}r_2r_3\sin\gamma\cdot\left(M_{12}^2r_2-M_{12}r_3\cos\gamma\right)+\frac{Gm_2m_3}{\kappa_3^3}\cdot M_{12}r_3\sin\gamma\\ &-\frac{3}{2}\frac{Gm_2m_4}{\kappa_4^5}\cdot\left(-2M_{c2}r_2r_4\sin(\gamma+\phi)-2M_{33}M_{c2}r_2r_3\sin\gamma\right)\cdot\left(M_{c2}^2r_2+M_{c2}r_4\cos(\gamma+\phi)+M_{33}M_{c2}r_3\cos\gamma\right)\\ &+\frac{Gm_2m_4}{\kappa_4^3}\cdot\left(-M_{c2}r_4\sin(\gamma+\phi)-M_{33}M_{c2}r_3\sin\gamma\right)\end{aligned} \tag{6.5}$$

$$\begin{aligned}\frac{\partial^2 H}{\partial r_2 \partial r_4} =& -\frac{3}{2}\frac{Gm_1m_4}{\kappa_2^5}\cdot\left(2r_4+2M_{c1}r_2\cos(\gamma+\phi)+2M_{33}r_3\cos\phi\right)\cdot\left(M_{c1}^2r_2+M_{c1}r_4\cos(\gamma+\phi)+M_{33}M_{c1}r_3\cos\gamma\right)\\ &+\frac{Gm_1m_4}{\kappa_2^3}\cdot M_{c1}\cos(\gamma+\phi)\\ &-\frac{3}{2}\frac{Gm_2m_4}{\kappa_4^5}\cdot\left(2r_4+2M_{c2}r_2\cos(\gamma+\phi)+2M_{33}r_3\cos\phi\right)\cdot\left(M_{c2}^2r_2+M_{c2}r_4\cos(\gamma+\phi)+M_{33}M_{c2}r_3\cos\gamma\right)\\ &+\frac{Gm_2m_4}{\kappa_4^3}\cdot M_{c2}\cos(\gamma+\phi)\end{aligned} \tag{6.6}$$

at the periodic solution:

$$\begin{aligned}\left.\frac{\partial H}{\partial r_2 \partial r_4}\right|_{\phi_2(t)} =& -3\frac{Gmm_4}{r^5y^5}\cos^5\beta\cdot\left(c_4r+M_{33}c_3r\right)\cdot\left(\frac{1}{4}c_2r\right)+0\\ &-3\frac{Gmm_4}{r^5y^5}\cos^5\beta\cdot\left(c_4r+M_{33}c_3r\right)\cdot\left(\frac{1}{4}c_2r\right)+0\\ =& -\frac{3}{2}\frac{Gmm_4}{r^3y^5}\cos^5\beta\cdot\left(c_4+M_{33}c_3\right)\cdot c_2=-\frac{3}{2}\frac{Gmm_4}{r^3y^5}\cos^5\beta\cdot\left(+y\tan\beta-M_{33}y\tan\alpha+M_{33}y\tan\alpha\right)\cdot 2y\\ =& \boxed{-3\frac{Gmm_4}{r^3y^3}\cos^4\beta\sin\beta}\end{aligned} \tag{6.7}$$

$$\begin{aligned}\frac{\partial^2 H}{\partial r_2 \partial \phi} =& -\frac{3}{2}\frac{Gm_1m_4}{\kappa_2^5}\cdot\left(-2M_{c1}r_2r_4\sin(\gamma+\phi)-2M_{33}r_3r_4\sin\phi\right)\cdot\left(M_{c1}^2r_2+M_{c1}r_4\cos(\gamma+\phi)+M_{33}M_{c1}r_3\cos\gamma\right)\\ &-\frac{Gm_1m_4}{\kappa_2^3}M_{c1}r_4\sin(\gamma+\phi)\\ &-\frac{3}{2}\frac{Gm_2m_4}{\kappa_4^5}\cdot\left(-2M_{c2}r_2r_4\sin(\gamma+\phi)-2M_{33}r_3r_4\sin\phi\right)\cdot\left(M_{c2}^2r_2+M_{c2}r_4\cos(\gamma+\phi)+M_{33}M_{c2}r_3\cos\gamma\right)\\ &-\frac{Gm_2m_4}{\kappa_4^3}M_{c2}r_4\sin(\gamma+\phi)\end{aligned} \tag{6.8}$$

$$\begin{aligned}\frac{\partial^2 H}{\partial r_3^2} =& 3\frac{(\Gamma-\Phi)^2}{M_3}\frac{1}{r_3^4}-3\frac{Gm_1m_3}{\kappa_1^5}\cdot\left(r_3+M_{22}r_2\cos\gamma\right)^2+\frac{Gm_1m_3}{\kappa_1^3}\\ &-3\frac{Gm_1m_4}{\kappa_2^5}\cdot\left(M_{33}^2r_3+M_{33}r_4\cos\phi+M_{33}M_{c1}r_2\cos\gamma\right)^2+\frac{Gm_1m_4}{\kappa_2^3}\cdot M_{33}^2\\ &-3\frac{Gm_2m_3}{\kappa_3^5}\cdot\left(r_3-M_{12}r_2\cos\gamma\right)^2+\frac{Gm_2m_3}{\kappa_3^3}\\ &-3\frac{Gm_2m_4}{\kappa_4^5}\cdot\left(M_{33}^2r_3+M_{33}r_4\cos\phi+M_{33}M_{c2}r_2\cos\gamma\right)^2+\frac{Gm_2m_4}{\kappa_4^3}\cdot M_{33}^2\\ &-3\frac{Gm_3m_4}{\kappa_5^5}\cdot\left(M_{c3}^2r_3-M_{c3}r_4\cos\phi\right)^2+\frac{Gm_3m_4}{\kappa_5^3}\cdot M_{c3}^2\end{aligned} \tag{6.9}$$

$$\begin{aligned}\frac{\partial^2 H}{\partial r_3 \partial \gamma} =& -\frac{3}{2}\frac{Gm_1m_3}{\kappa_1^5}\cdot\left(-2M_{22}r_2r_3\sin\gamma\right)\cdot\left(r_3+M_{22}r_2\cos\gamma\right)+\frac{Gm_1m_3}{\kappa_1^3}\cdot\left(-M_{22}r_2\sin\gamma\right)\\ &-\frac{3}{2}\frac{Gm_1m_4}{\kappa_2^5}\cdot\left(-2M_{c1}r_2r_4\sin(\gamma+\phi)-2M_{33}M_{c1}r_2r_3\sin\gamma\right)\cdot\left(M_{33}^2r_3+M_{33}r_4\cos\phi+M_{33}M_{c1}r_2\cos\gamma\right)\\ &+\frac{Gm_1m_4}{\kappa_2^3}\cdot\left(-M_{33}M_{c1}r_2\sin\gamma\right)\\ &-\frac{3}{2}\frac{Gm_2m_3}{\kappa_3^5}\cdot\left(2M_{12}r_2r_3\sin\gamma\right)\cdot\left(r_3-M_{12}r_2\cos\gamma\right)+\frac{Gm_2m_3}{\kappa_3^3}\cdot\left(M_{12}r_2\sin\gamma\right)\\ &-\frac{3}{2}\frac{Gm_2m_4}{\kappa_4^5}\cdot\left(-2M_{c2}r_2r_4\sin(\gamma+\phi)-2M_{33}M_{c2}r_2r_3\sin\gamma\right)\cdot\left(M_{33}^2r_3+M_{33}r_4\cos\phi+M_{33}M_{c2}r_2\cos\gamma\right)\\ &+\frac{Gm_2m_4}{\kappa_4^3}\cdot\left(-M_{33}M_{c2}r_2\sin\gamma\right)\end{aligned} \tag{6.10}$$

$$\begin{aligned}\frac{\partial^2 H}{\partial r_3 \partial r_4} =& -\frac{3}{2}\frac{Gm_1m_4}{\kappa_2^5}\cdot\left(2r_4+2M_{c1}r_2\cos(\gamma+\phi)+2M_{33}r_3\cos\phi\right)\cdot\left(M_{33}^2r_3+M_{33}r_4\cos\phi+M_{33}M_{c1}r_2\cos\gamma\right)\\ &+\frac{Gm_1m_4}{\kappa_2^3}\cdot\left(M_{33}\cos\phi\right)\\ &-\frac{3}{2}\frac{Gm_2m_4}{\kappa_4^5}\cdot\left(2r_4+2M_{c2}r_2\cos(\gamma+\phi)+2M_{33}r_3\cos\phi\right)\cdot\left(M_{33}^2r_3+M_{33}r_4\cos\phi+M_{33}M_{c2}r_2\cos\gamma\right)\\ &+\frac{Gm_2m_4}{\kappa_4^3}\cdot\left(M_{33}\cos\phi\right)\\ &-\frac{3}{2}\frac{Gm_3m_4}{\kappa_5^5}\cdot\left(2r_4-2M_{c3}r_3\cos\phi\right)\cdot\left(M_{c3}^2r_3-M_{c3}r_4\cos\phi\right)+\frac{Gm_3m_4}{\kappa_5^3}\cdot\left(-M_{c3}\cos\phi\right)\end{aligned} \tag{6.11}$$

at the periodic solution:

$$
\begin{aligned}
\left.\frac{\partial^2 H}{\partial r_3 \partial r_4}\right|_{\phi_2(t)} =& -3\frac{Gmm_4}{r^5y^5}\cos^5\beta\cdot(c_4r+M_{33}c_3r)\cdot\left(M_{33}^2c_3r+M_{33}c_4r\right)+\frac{Gmm_4}{r^3y^3}\cos^3\beta\cdot M_{33}\\
&-3\frac{Gmm_4}{r^5y^5}\cos^5\beta\cdot(c_4r+M_{33}c_3r)\cdot\left(M_{33}^2c_3r+M_{33}c_4r\right)+\frac{Gmm_4}{r^3y^3}\cos^3\beta\cdot M_{33}\\
&-3\frac{Gm_3m_4}{r^5y^5\left(\tan\alpha-\tan\beta\right)^5}\cdot(c_4r-M_{c3}c_3r)\cdot\left(M_{c3}^2c_3r-M_{c3}c_4r\right)-\frac{Gm_3m_4}{r^3y^3\left(\tan\alpha-\tan\beta\right)^3}\cdot M_{c3}\\
=&-6\frac{Gmm_4}{r^3y^5}\cos^5\beta\cdot M_{33}\left(c_4+M_{33}c_3\right)^2+2\frac{Gmm_4}{r^3y^3}\cos^3\beta\cdot M_{33}\\
&+3\frac{Gm_3m_4}{r^3y^5\left(\tan\alpha-\tan\beta\right)^5}\cdot M_{c3}\left(c_4-M_{c3}c_3\right)^2-\frac{Gm_3m_4}{r^3y^3\left(\tan\alpha-\tan\beta\right)^3}\cdot M_{c3}\\
=&-6\frac{Gmm_4}{r^3y^5}\cos^5\beta\cdot M_{33}\left(+y\tan\beta-M_{33}y\tan\alpha+M_{33}y\tan\alpha\right)^2+2\frac{Gmm_4}{r^3y^3}\cos^3\beta\cdot M_{33}\\
&+3\frac{Gm_3m_4}{r^3y^5\left(\tan\alpha-\tan\beta\right)^5}\cdot M_{c3}\left(+y\tan\beta-M_{33}y\tan\alpha-M_{c3}y\tan\alpha\right)^2-\frac{Gm_3m_4}{r^3y^3\left(\tan\alpha-\tan\beta\right)^3}\cdot M_{c3}\\
=&-6\frac{Gmm_4}{r^3y^3}\cos^5\beta\cdot M_{33}\tan^2\beta+2\frac{Gmm_4}{r^3y^3}\cos^3\beta\cdot M_{33}\\
&+3\frac{Gm_3m_4}{r^3y^3\left(\tan\alpha-\tan\beta\right)^3}\cdot M_{c3}-\frac{Gm_3m_4}{r^3y^3\left(\tan\alpha-\tan\beta\right)^3}\cdot M_{c3}\\
=&2\frac{Gmm_4}{r^3y^3}M_{33}\left(-3\cos^5\beta\tan^2\beta+\cos^3\beta\right)+2\frac{Gm_3m_4}{r^3y^3}\frac{M_{c3}}{\left(\tan\alpha-\tan\beta\right)^3}\\
=&\boxed{-2\frac{Gmm_4}{r^3y^3}M_{33}\left(2\cos^3\beta-3\cos^5\beta\right)+2\frac{Gm_3m_4}{r^3y^3}M_{c3}\left(\tan\alpha-\tan\beta\right)^{-3}}
\end{aligned}
\tag{6.12}
$$

$$
\begin{aligned}
\frac{\partial^2 H}{\partial\gamma^2} =& \frac{3}{2}\frac{Gm_1m_3}{\kappa_1^5}\cdot\left(-2M_{22}r_2r_3\sin\gamma\right)\cdot\left(M_{22}r_2r_3\sin\gamma\right)-\frac{Gm_1m_3}{\kappa_1^3}M_{22}r_2r_3\cos\gamma\\
&+\frac{3}{2}\frac{Gm_1m_4}{\kappa_2^5}\cdot\left(-2M_{c1}r_2r_4\sin(\gamma+\phi)-2M_{33}M_{c1}r_2r_3\sin\gamma\right)\cdot\left(M_{c1}r_2r_4\sin(\gamma+\phi)+M_{33}M_{c1}r_2r_3\sin\gamma\right)\\
&-\frac{Gm_1m_4}{\kappa_2^3}\left(M_{c1}r_2r_4\cos(\gamma+\phi)+M_{33}M_{c1}r_2r_3\cos\gamma\right)\\
&-\frac{3}{2}\frac{Gm_2m_3}{\kappa_3^5}\cdot\left(2M_{12}r_2r_3\sin\gamma\right)\cdot\left(M_{12}r_2r_3\sin\gamma\right)+\frac{Gm_2m_3}{\kappa_3^3}M_{12}r_2r_3\cos\gamma\\
&+\frac{3}{2}\frac{Gm_2m_4}{\kappa_4^5}\cdot\left(-2M_{c2}r_2r_4\sin(\gamma+\phi)-2M_{33}M_{c2}r_2r_3\sin\gamma\right)\cdot\left(M_{c2}r_2r_4\sin(\gamma+\phi)+M_{33}M_{c2}r_2r_3\sin\gamma\right)\\
&-\frac{Gm_2m_4}{\kappa_4^3}\cdot\left(M_{c2}r_2r_4\cos(\gamma+\phi)+M_{33}M_{c2}r_2r_3\cos\gamma\right)
\end{aligned}
\tag{6.13}
$$

$$
\begin{aligned}
\frac{\partial^2 H}{\partial\gamma\partial r_4} =& \frac{3}{2}\frac{Gm_1m_4}{\kappa_2^5}\cdot\left(2r_4+2M_{c1}r_2\cos(\gamma+\phi)+2M_{33}r_3\cos\phi\right)\cdot\left(M_{c1}r_2r_4\sin(\gamma+\phi)+M_{33}M_{c1}r_2r_3\sin\gamma\right)\\
&-\frac{Gm_1m_4}{\kappa_2^3}\cdot M_{c1}r_2\sin(\gamma+\phi)\\
&+\frac{3}{2}\frac{Gm_2m_4}{\kappa_4^5}\cdot\left(2r_4+2M_{c2}r_2\cos(\gamma+\phi)+2M_{33}r_3\cos\phi\right)\cdot\left(M_{c2}r_2r_4\sin(\gamma+\phi)+M_{33}M_{c2}r_2r_3\sin\gamma\right)\\
&-\frac{Gm_2m_4}{\kappa_4^3}\cdot M_{c2}r_2\sin(\gamma+\phi)
\end{aligned}
\tag{6.14}
$$

$$\begin{aligned}\left.\frac{\partial^2 H}{\partial\gamma\partial r_4}\right|_{\phi_2(t)} =& 3\frac{Gmm_4}{r^5y^5}\cos^5\beta\cdot(c_4r+M_{33}c_3r)\cdot\left(-\frac{1}{2}c_2c_4r^2-M_{33}\frac{1}{2}c_2c_3r^2\right)+\frac{Gmm_4}{r^3y^3}\cos^3\beta\cdot\frac{1}{2}c_2r\\ &+3\frac{Gmm_4}{r^5y^5}\cos^5\beta\cdot(c_4r+M_{33}c_3r)\cdot\left(+\frac{1}{2}c_2c_4r^2+M_{33}\frac{1}{2}c_2c_3r^2\right)-\frac{Gmm_4}{r^3y^3}\cos^3\beta\cdot\frac{1}{2}c_2r\\ =&\boxed{0}\end{aligned} \tag{6.15}$$

$$\begin{aligned}\frac{\partial^2 H}{\partial\gamma\partial\phi} =& \frac{3}{2}\frac{Gm_1m_4}{\kappa_2^5}\cdot\left(-2M_{c1}r_2r_4\sin(\gamma+\phi)-2M_{33}r_3r_4\sin\phi\right)\cdot\left(M_{c1}r_2r_4\sin(\gamma+\phi)+M_{33}M_{c1}r_2r_3\sin\gamma\right)\\ &-\frac{Gm_1m_4}{\kappa_2^3}\cdot M_{c1}r_2r_4\cos(\gamma+\phi)\\ &+\frac{3}{2}\frac{Gm_2m_4}{\kappa_4^5}\cdot\left(-2M_{c2}r_2r_4\sin(\gamma+\phi)-2M_{33}r_3r_4\sin\phi\right)\cdot\left(M_{c2}r_2r_4\sin(\gamma+\phi)+M_{33}M_{c2}r_2r_3\sin\gamma\right)\\ &-\frac{Gm_2m_4}{\kappa_4^3}\cdot M_{c2}r_2r_4\cos(\gamma+\phi)\end{aligned} \tag{6.16}$$

$$\begin{aligned}\frac{\partial^2 H}{\partial r_4^2} =& \quad 3\frac{\Phi^2}{M_4}\frac{1}{{r_4}^4}-3\frac{Gm_1m_4}{\kappa_2^5}\left(r_4+M_{c1}r_2\cos(\gamma+\phi)+M_{33}r_3\cos\phi\right)^2+\frac{Gm_1m_4}{\kappa_2^3}\\ &-3\frac{Gm_2m_4}{\kappa_4^5}\left(r_4+M_{c2}r_2\cos(\gamma+\phi)+M_{33}r_3\cos\phi\right)^2+\frac{Gm_2m_4}{\kappa_4^3}-3\frac{Gm_3m_4}{\kappa_5^5}\left(r_4-M_{c3}r_3\cos\phi\right)^2+\frac{Gm_3m_4}{\kappa_5^3}\end{aligned} \tag{6.17}$$

$$\begin{aligned}\left.\frac{\partial^2 H}{\partial r_4^2}\right|_{\phi_2(t)} =& 3\frac{M_4^2{c_4}^4\omega^2}{M_4}\frac{1}{{c_4}^4r^4}-3\frac{Gmm_4}{r^5y^5}\cos^5\beta\,(c_4r+M_{33}c_3r)^2+\frac{Gmm_4}{r^3y^3}\cos^3\beta\\ &-3\frac{Gmm_4}{r^5y^5}\cos^5\beta\,(c_4r+M_{33}c_3r)^2+\frac{Gmm_4}{r^3y^3}\cos^3\beta\\ &-3\frac{Gm_3m_4}{r^5y^5\left(\tan\alpha-\tan\beta\right)^5}(c_4r-M_{c3}c_3r)^2+\frac{Gm_3m_4}{r^3y^3\left(\tan\alpha-\tan\beta\right)^3}\end{aligned} \tag{6.18}$$

$$\begin{aligned}\frac{\partial^2 H}{\partial r_4\partial\phi} =& -\frac{3}{2}\frac{Gm_1m_4}{\kappa_2^5}\cdot\left(-2M_{c1}r_2r_4\sin(\gamma+\phi)-2M_{33}r_3r_4\sin\phi\right)\cdot\left(r_4+M_{c1}r_2\cos(\gamma+\phi)+M_{33}r_3\cos\phi\right)\\ &+\frac{Gm_1m_4}{\kappa_2^3}\cdot\left(-M_{c1}r_2\sin(\gamma+\phi)-M_{33}r_3\sin\phi\right)\\ &-\frac{3}{2}\frac{Gm_2m_4}{\kappa_4^5}\cdot\left(-2M_{c2}r_2r_4\sin(\gamma+\phi)-2M_{33}r_3r_4\sin\phi\right)\cdot\left(r_4+M_{c2}r_2\cos(\gamma+\phi)+M_{33}r_3\cos\phi\right)\\ &+\frac{Gm_2m_4}{\kappa_4^2}\cdot\left(-M_{c2}r_2\sin(\gamma+\phi)-M_{33}r_3\sin\phi\right)\\ &-\frac{3}{2}\frac{Gm_3m_4}{\kappa_5^5}\cdot\left(2M_{c3}r_3r_4\sin\phi\right)\cdot\left(r_4-M_{c3}r_3\cos\phi\right)+\frac{Gm_3m_4}{\kappa_5^3}\cdot M_{c3}r_3\sin\phi\end{aligned} \tag{6.19}$$

The first four terms change sign, while the last two terms are zero, as before, which gives

$$\left.\frac{\partial^2 H}{\partial r_4\partial\phi}\right|_{\phi_2(t)} =\boxed{0} \tag{6.20}$$

$$\frac{\partial^2 H}{\partial r_4\partial\Phi} =-2\frac{\Phi}{M_4}\frac{1}{{r_4}^3} \tag{6.21}$$

$$\left.\frac{\partial^2 H}{\partial r_4\partial\Phi}\right|_{\gamma(t)} =-2\frac{M_4{c_4}^2\omega}{M_4}\cdot\frac{1}{{c_4}^3r^3}=-2\frac{\omega}{c_4r^3}=\boxed{+2\frac{\omega}{r^3y}\left(M_{33}\tan\alpha-\tan\beta\right)^{-1}} \tag{6.22}$$

$$\begin{aligned}\frac{\partial^2 H}{\partial \phi^2} = &-3\frac{Gm_1m_4}{\kappa_2^5}\cdot\left(M_{c1}r_2r_4\sin(\gamma+\phi)+M_{33}r_3r_4\sin\phi\right)^2-\frac{Gm_1m_4}{\kappa_2^3}\cdot\left(M_{c1}r_2r_4\cos(\gamma+\phi)+M_{33}r_3r_4\cos\phi\right)\\ &-3\frac{Gm_2m_4}{\kappa_4^5}\cdot\left(M_{c2}r_2r_4\sin(\gamma+\phi)+M_{33}r_3r_4\sin\phi\right)^2-\frac{Gm_2m_4}{\kappa_4^3}\cdot\left(M_{c2}r_2r_4\cos(\gamma+\phi)+M_{33}r_3r_4\cos\phi\right)\\ &-3\frac{Gm_3m_4}{\kappa_5^5}\cdot\left(M_{c3}r_3r_4\sin\phi\right)^2+\frac{Gm_3m_4}{\kappa_5^3}\cdot M_{c3}r_3r_4\cos\phi\end{aligned} \tag{6.23}$$

$$\frac{\partial^2 H}{\partial \Phi^2} = \frac{1}{M_3r_3^2}+\frac{1}{M_4{r_4}^2} = \frac{1}{M_3c_3^2r^2}+\frac{1}{M_4{c_4}^2r^2} \tag{6.24}$$

Again, the linearized system becomes:

$$JD^2H(\gamma(t)) = \begin{bmatrix} 0 & 0 & 0 & 0 & 0 & \frac{1}{M_2} & 0 & 0 & 0 & 0\\ 0 & 0 & 0 & 0 & 0 & 0 & \frac{1}{M_3} & 0 & 0 & 0\\ a_0 & -a_1 & 0 & 0 & 0 & 0 & 0 & H_{\Gamma^2} & 0 & -a_3\\ 0 & 0 & 0 & 0 & 0 & 0 & 0 & 0 & \frac{1}{M_4} & 0\\ 0 & a_1 & 0 & -a_2 & 0 & 0 & 0 & -a_3 & 0 & H_{\Phi^2}\\ -H_{r_2^2} & -H_{r_2,r_3} & 0 & -H_{r_2,r_4} & 0 & 0 & 0 & -a_0 & 0 & 0\\ -H_{r_3,r_2} & -H_{r_3^2} & 0 & -H_{r_3,r_4} & 0 & 0 & 0 & a_1 & 0 & -a_1\\ 0 & 0 & -H_{\gamma^2} & 0 & -H_{\gamma,\phi} & 0 & 0 & 0 & 0 & 0\\ -H_{r_4,r_2} & -H_{r_4,r_3} & 0 & -H_{r_4^2} & 0 & 0 & 0 & 0 & 0 & a_2\\ 0 & 0 & -H_{\phi,\gamma} & 0 & -H_{\phi^2} & 0 & 0 & 0 & 0 & 0 \end{bmatrix} \tag{6.25}$$

where

$$a_0 = 2\frac{\omega}{r^3}\frac{1}{c_2} = \frac{\omega}{r^3y} \tag{6.26}$$

$$a_1 = 2\frac{\omega}{r^3}\frac{1}{c_3} = 2\frac{\omega}{r^3y}\tan^{-1}\alpha \tag{6.27}$$

$$a_2 = 2\frac{\omega}{r^3}\frac{1}{c_4} = -\frac{2\omega}{r^3y\left(M_{33}\tan\alpha-\tan\beta\right)} \tag{6.28}$$

$$a_3 = \frac{1}{M_3r^2c_3^2} = \frac{1}{M_3r^2y^2\tan^2\alpha} \tag{6.29}$$

Having obtained these coefficients, the procedure to reach Eq. (4.181) is again exactly the same as before and is executed using the same Mathematica code with the new coefficients substituted.

6.2. Circular cases

The eigenvalues of the circular cases are obtained with the same procedure as before. The totals of the magnitudes of the eigenvalues for a sampling of the second concave region are shown in Figs. 6.1 to 6.4. We find once again that the real parts are diminished as we approach the line $2\alpha-\beta = 90°$, however, just like in the first concave case the real parts do not vanish, not even 0.1° away from this line, as shown in Fig. 6.4 and below in Fig. 6.6.

6.3. Eccentric cases

The monodromy matrices for the eccentric cases are generated with the same integration technique as introduced in Section 4.9. The precision of the generated monodromy matrices is checked using the same method as for the convex and first concave cases. For each eccentricity, the determinants of the 196 monodromy matrices are calculated and checked for the biggest deviation from 1. In this way we obtain a precision estimate for the monodromy matrices for each eccentricity, because they must be at least as precise as their determinants. The results are shown in Tables 6.1 and 6.2.

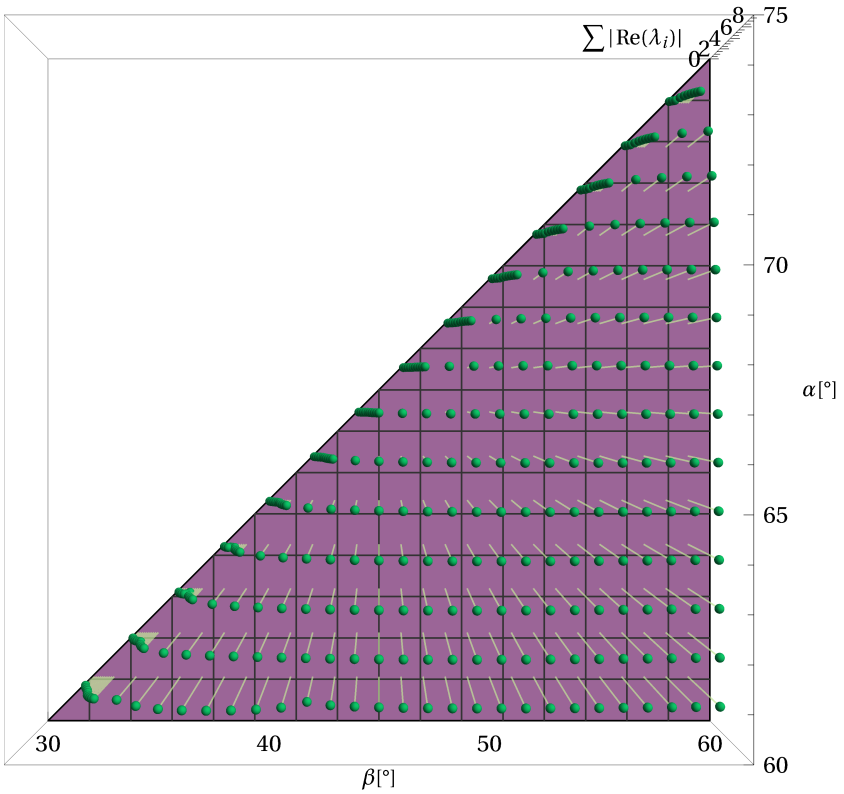

Figure 6.1: Top view of the total magnitudes of the real parts of the eigenvalues for the second concave domain.

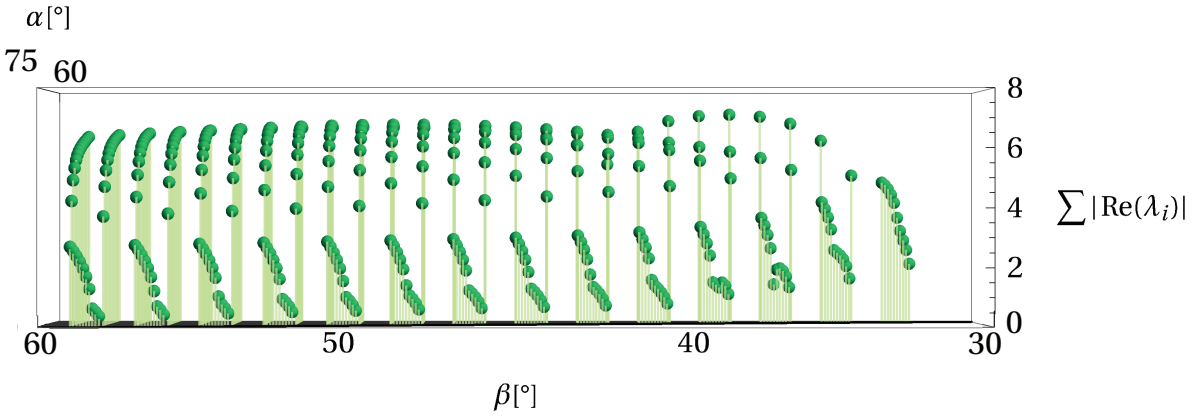

Figure 6.2: Front view of the total magnitudes of the real parts of the eigenvalues for the second concave domain.

Eccentricity	Precision	Max determinant	Min determinant
0	17	1.000000000000000006126	0.999999999999999999997
0.1	17	1.000000000000000002338	0.999999999999999985516
0.2	17	1.000000000000000002559	0.999999999999999982572
0.3	17	1.000000000000000002598	0.999999999999999973959
0.4	16	1.000000000000000004759	0.999999999999999904998
0.5	16	1.000000000000000015420	0.999999999999999740633
0.6	16	1.000000000000000030069	0.999999999999999559660
0.7	15	1.000000000000000288767	0.999999999999999208465
0.8	15	1.000000000000001595564	0.999999999999996372316
0.9	14	1.000000000000009919441	0.999999999999972347007

Table 6.1: Precision of the monodromy matrices of the coarse sampling of the second concave cases, corresponding to Fig. 6.5.

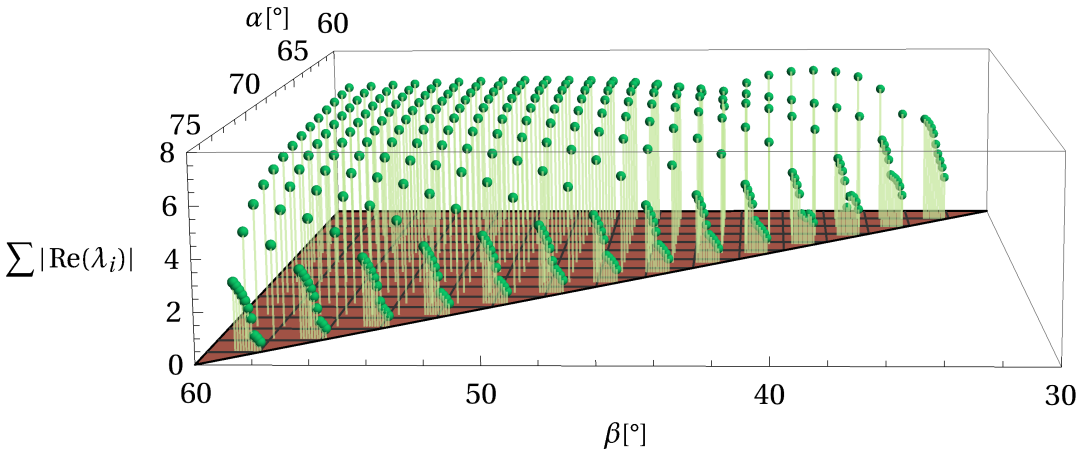

Figure 6.3: Total magnitudes of the real parts of the eigenvalues for the second concave domain.

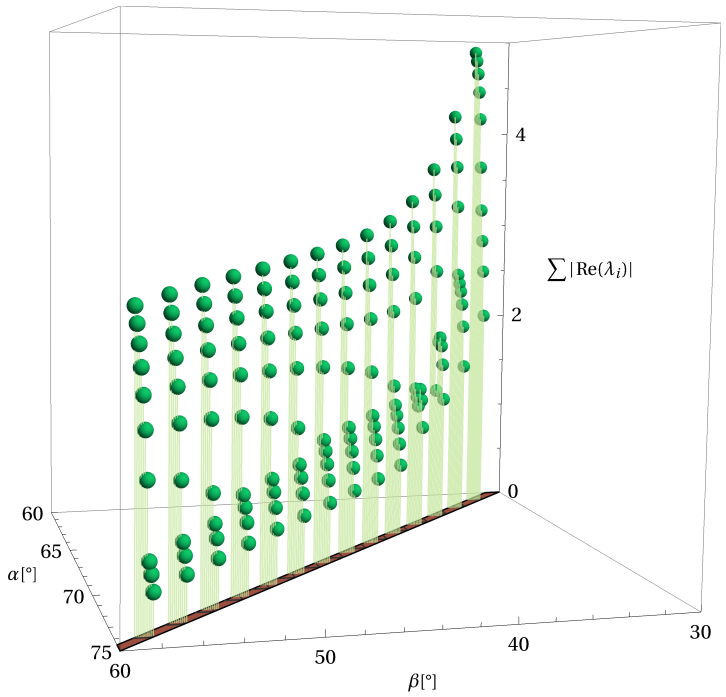

Figure 6.4: Zoom view of the total magnitudes of the real parts of the eigenvalues near the limit line of the second concave domain.

Eccentricity	Precision	Max determinant	Min determinant
0	17	1.000000000000000006782	0.999999999999999999977
0.1	17	1.000000000000000002112	0.999999999999999975577
0.2	17	1.000000000000000003825	0.999999999999999964100
0.3	17	1.000000000000000003528	0.999999999999999963131
0.4	17	1.000000000000000003991	0.999999999999999965337
0.5	16	1.000000000000000004011	0.999999999999999948461
0.6	16	1.000000000000000004375	0.999999999999999944293
0.7	16	1.000000000000000012308	0.999999999999999890511
0.8	16	1.000000000000000023135	0.999999999999999750982
0.9	15	1.000000000000000207090	0.999999999999998990869

Table 6.2: Precision of the monodromy matrices of the fine sampling of the second concave cases near the line of minimum β, corresponding to Fig. 6.6.

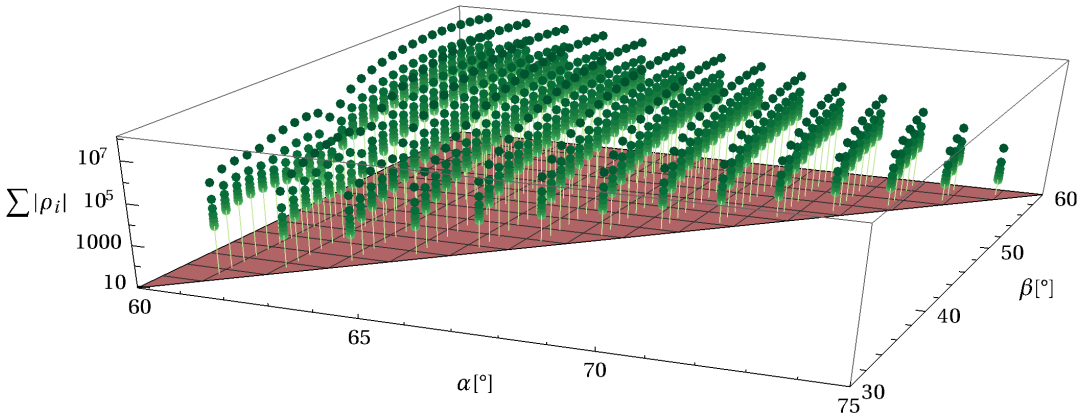

Figure 6.5: Sums of absolute values of characteristic multipliers for a sampling of the possible concave cases of the second kind for eccentricities from 0 to 0.9. The coloured plane has height 8, which would be the sum of 8 multipliers on the unit circle.

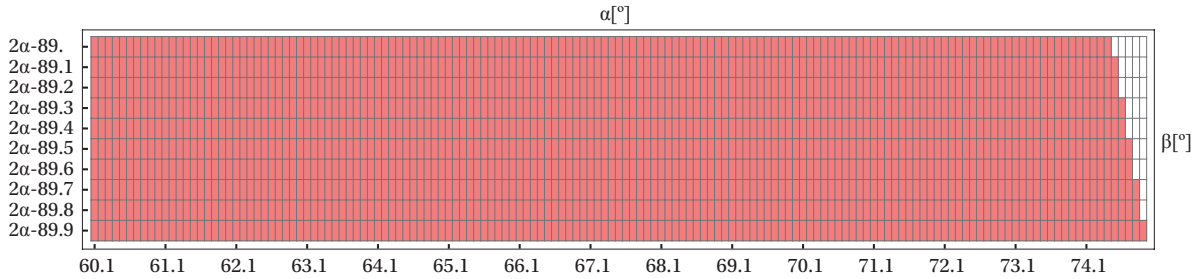

Figure 6.6: Stability diagram for the concave cases of the second kind near the limit line for $e = 0$, $e = 0.1$, $e = 0.2$, $e = 0.3$, $e = 0.4$, $e = 0.5$, $e = 0.6$, $e = 0.7$, $e = 0.8$, $e = 0.9$.

The absolute values of the characteristic multipliers are plotted in Fig. 6.5. Clearly, none of the configurations from the coarse sampling are linearly stable. The linear stability results of a fine sampling near the line of minimum β are represented in Fig. 6.6 for ten values of eccentricity. Given that none of the samples are linearly stable in the circular case and noticing the destabilizing effect of eccentricity in Fig. 6.5, it is not surprising that we do not find any linearly stable configurations for any value of eccentricity.

6.4. Closing remarks

We see that in the second concave case, similarly to the first, linear stability increases as the configurations appoach the coorbital line $2\alpha - \beta = 90°$. This time however, increasing α is stabilizing, since it increases the mass of the central body (Fig. 2.8), while increasing β moves the central body away and reduces its mass, therefore is destabilizing. It is interesting to note that, not unlike for the first concave cases, the eigenvalues in Fig. 6.4 almost become imaginary, but do not quite reach linear stability. Even the bottom-right most configuration in Fig. 6.6, $\alpha = 74.9°$, $\beta = 59.9°$, is unstable, which may be surprising looking at the dominant center mass and surrounding body positions in Fig. 2.8.

The instability of the bottom-left corner ties in with the previously known result that the configuration with three equal masses at the vertices of an equilateral triangle with a body of arbitrary mass in the middle is unstable for all mass ratios [39]. Since the middle body is right in the center of mass, this central configuration is right on the border of the first and second concave cases of the present work (the singular configuration marked 'S' in Fig. 2.5), both of which are found to always be unstable.

The results also tie in with the analysis of the restricted four-body problem in [5], where the author finds that the libration points, obtained by setting either of the masses on the symmetry line in the concave configurations equal to zero, are unstable for any finite masses of the remaining three bodies. Our results show that this property is extended to the non-restricted cases as well.

7

Verification and validation

7.1. Verification of linear stability

While moving through the computations laid down in Part I various verification steps were performed to ascertain the correctness of intermediate and final results and expressions. This section lists the main checks that were performed.

7.1.1. Coefficients of the Hessian

In assessing the linear stability, the linearization procedure is fundamental and, admittedly, a step where mistakes are easy to make due to the big number of similar double derivatives that have to be taken. The correctness of the expressions for the linearization coefficients obtained by evaluating the partial derivatives at the periodic solutions in Sections 4.3, 5.1 and 6.1 was verified with the aid of Mathematica. Using a `FullSimplify` routine the equivalence of each of our expressions with the partial derivatives independently evaluated by Mathematica was checked.

Furthermore, having obtained the linearized matrix $JD^2H(\boldsymbol{\gamma}(t))$ for the convex cases, the fact that $\dot{\boldsymbol{\gamma}}$ satisfies the linearized system was exploited to check in Eqs. (4.123) to (4.125) that indeed $\ddot{\boldsymbol{\gamma}} = JD^2H(\boldsymbol{\gamma}(t)\dot{\boldsymbol{\gamma}}$. This identity only holds if the linearization has been performed correctly.

7.1.2. Decoupling

Next, the v coefficients constituting the transformed matrix (4.140) produce exactly the decoupling which was anticipated, with the two by two matrix $\begin{bmatrix} 0 & v_{12} \\ v_{21} & 0 \end{bmatrix}$ containing exactly the two +1 multipliers that were needed, as shown in Eqs. (4.161) to (4.165). This is evidence that the matrix $V(t) = P^{-1}JD^2H(\boldsymbol{\gamma}(t))P$ was computed correctly, otherwise the terms would be very unlikely to cancel and produce just the decoupling that we were after.

7.1.3. Final matrix

The simplified final form of our linearized equations, given by the coefficient matrix Eq. (4.181) is validated in Section 4.6. It produces the correct eigenvalues for the square circular solution, as demonstrated in Figs. 4.3 and 4.4 through comparison with independently computed eigenvalues in [18].

7.1.4. Perturbation method

The correctness of expressions in Section 4.8 is verified through the fact that the expressions for the coefficients of the reduced polynomial in terms of traces of the fundamental matrix plugged into the disriminant expression (4.207) results in 0 for the zero-degree term in Eq. (4.226) when evaluated at a multiple eigenvalue. At first this was not the case and a mistake was detected using this check, since the discriminant is zero if and only if at least two roots are equal.

7.1.5. Numerical integrators
As mentioned in Section 4.9.1, the precision and accuracy estimates are verified by numerically computing the monodromy matrix for the circular square case and comparing the multipliers with analytically obtained ones.

7.1.6. Monodromy matrices
We exploit the fact that the monodromy matrix of a Hamiltonian system is symplectic and, therefore, has determinant 1 to check the precision of the numerically generated monodromy matrices. The maximum and minimum determinants for all cases are listed in Tables 4.5, 4.6, 5.1, 5.2, 6.1 and 6.2. The biggest detected deviation from 1 in a determinant is 2.6×10^{-14} in the first concave case.

7.1.7. Characteristic multipliers
Plotting the characteristic multipliers for the linearly stable configurations in Figs. 4.12 to 4.14, 4.16 to 4.18, 4.20, 4.21 and 4.23 verifies that eight unique multipliers lie and travel along the unit circle in exactly the symmetric fashion which is expected of eigenvalues of a symplectic matrix. Furthermore, at the places where stability is lost we see multipliers colliding and splitting off into the complex plane (a Krein bifurcation), which again confirms that these numerically computed values are behaving according to their mathematical properties. Finally, seeing that throughout most of the identified linearly stable regions we have eight distinct multipliers on the unit circle offers assurance that our solutions are truly linearly stable: because stability can only be lost through a collision and our coefficient matrix is continuous in terms of α and β, we have that a sudden instability cannot occur until the multipliers traveled on the circle and collided. This is in contrast to if we were to have spectral stability.

7.1.8. Linear stability
As discussed in Sections 4.10, 5.4 and 6.4, the linear stability results are validated by the fact that they show exactly the kind of behaviour as is described in literature (for instance [19, 29]), that is, increased stability around configurations with a dominant mass and ring-like positioning.

Furthermore, the results in Part II serve as validation of the linear stability results. There we numerically integrate the 10-dimensional, non-linear equations with a symplectic integrator for up to 200 periods and compare the observed stability properties with those of Part I. Perfect agreement is found between the results obtained with these two independent approaches, even for the unusual result of the sole linearly stable solution in Fig. 4.19.

II

Non-linear stability

8

Long-term numerical integration

In the previous chapter, the linear stability of a range of central four-body configurations was assessed. In that sense, the conclusions were quite clear. However, some results suggest to have an alternative look at the stability behaviour, if only to verify that results are as they were found. To this aim, we perform direct, long-term numerical integrations of the reduced non-linear system of differential equations (Eqs. (3.62) to (3.68)) for several cases found to be stable or unstable by the linear analysis. This independent approach serves to verify the stability conclusions drawn in the previous part and gain confidence that indeed our periodic solutions behave as expected.

8.1. The system

As explained in Chapter 3, our non-linear system is a conservative Hamiltonian system with the Hamiltonian function Eq. (3.61) constant for all time. The center of mass, linear momentum, rotational symmetry and angular momentum have been eliminated, therefore the system of differential equations Eqs. (3.62) to (3.68) has 10 dimensions, represented by the state variables r_2, R_2, r_3, R_3, γ, Γ, r_4, R_4, ϕ and Φ. As explained in Chapter 3 all relevant dynamics of the entire four-body system are described by the reduced system, therefore we can get our stability results by integrating just the 10 state variables above. Furthermore, for simplicity we choose units such that $G = 1$ and omit them from the rest of this chapter, since the focus here is on the qualitative behaviour of the solutions, on which units have no effect.

8.2. Numerical integration technique

Since we have a Hamiltonian system, a symplectic integrator would be well suited, as, by design, the integration steps yield symplectic maps, which adhere to the rules of Hamiltonian dynamics, namely, the symplectic 2-form (3.6) is preserved between states. When applied to Hamiltonian systems, these integrators keep a nearby Hamiltonian approximately conserved for exponentially long times [37]. This property results in more accurate long-term qualitative behaviour of the solutions, as is especially clear by looking at the phase portraits of Hamiltonian systems obtained with conventional and symplectic integrators [37].

Unfortunately, the built-in *SymplecticPartitionedRungeKutta* methods do not work with our system, because the canonical coordinate changes we used to arrive at the 10-dimensional system made the new momentum variables depend on the position variables, which destroyed the separability of the system (at first the kinetic energy only depended on the momentum variables and the potential energy only on the position). However, there is still a built-in symplectic integrator option, which does not require separability of the kinetic and potential energies. This is the Gauss implicit Runge-Kutta method [37].

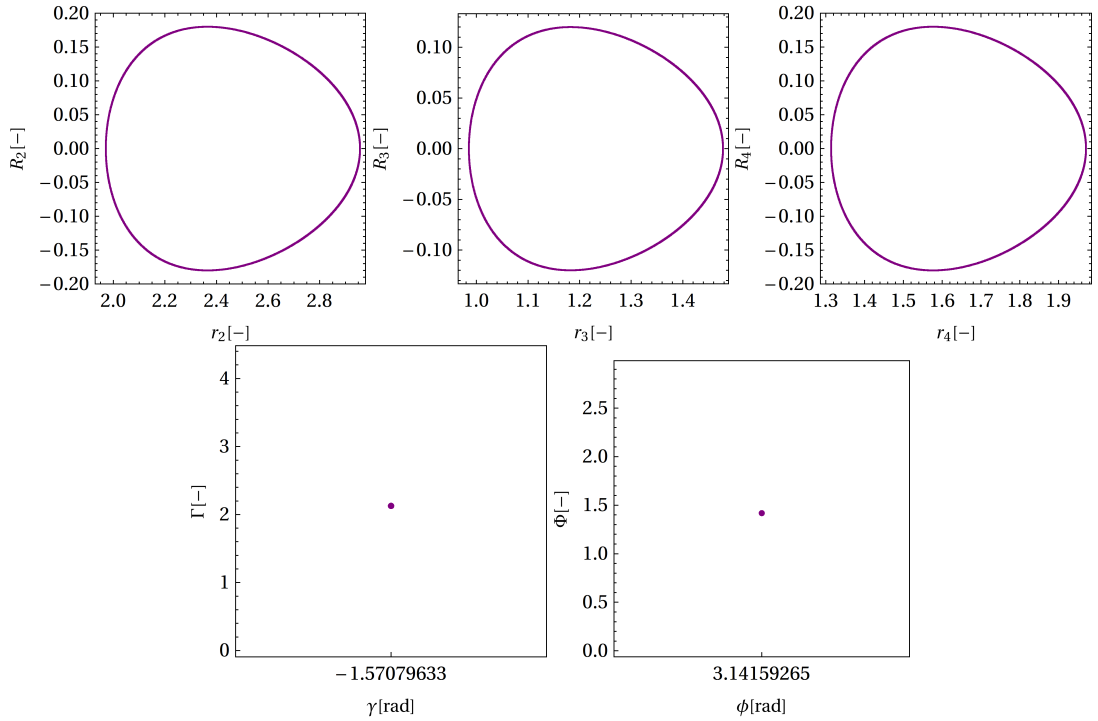

Figure 8.2: Phase portraits of the $e = 0.2$ square case integration with 4th-order Gauss implicit Runge-Kutta method for $4T$.

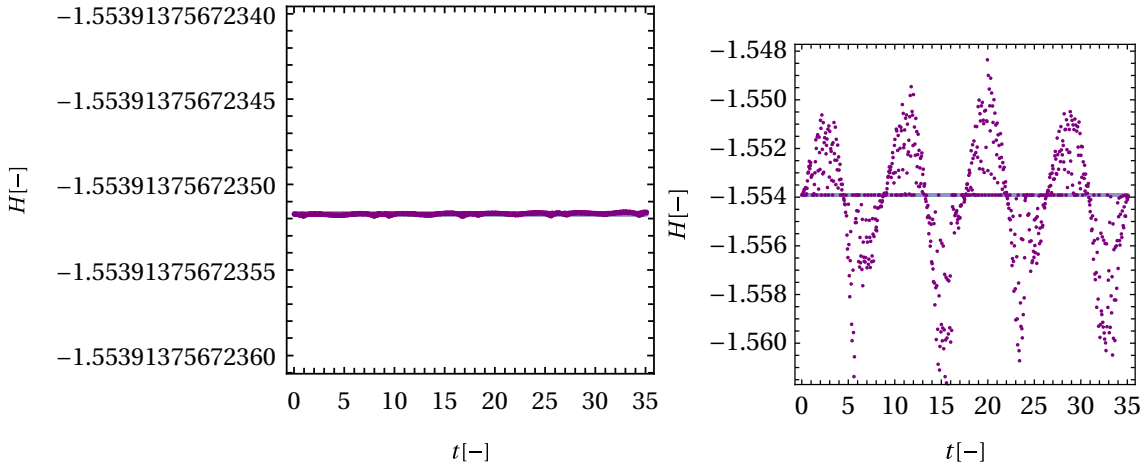

Figure 8.1: Values of the Hamiltonian function at each time step of the Gauss implicit 4th-order Runge-Kutta integration on the left and 12th-order Adams integration on the right.

For comparison we perform a short integration of the square configuration with $e = 0.2$ with the 12th-order Adams method and 4th-order implicit Gauss Runge-Kutta technique. The Hamiltonians for both cases are plotted in Fig. 8.1, while the phase portraits (a dot is placed in phase space at every time step of the integration) are shown in Figs. 8.2 and 8.3. We see clearly how the value of the Hamiltonian fluctuates around the true value with errors as large as 0.004 for the Adams integration, whereas with implicit RK we have only deviations smaller than 10^{-14}. This is reflected in the quality of the phase portraits, which for the symplectic integration show nicely periodic behaviour: the position variables trace out a repeating circular shape and the angle variables stay a constant dot. With the non-symplectic integrator the circular figures are distorted and the angle variables fail to stay constant. Therefore, all the subsequent integrations in this chapter are performed with the Gauss implicit Runge-Kutta method of 4th order. The exact settings are the following:

```
NDSolve[
  Method -> {"ImplicitRungeKutta", "DifferenceOrder" -> 4},
```

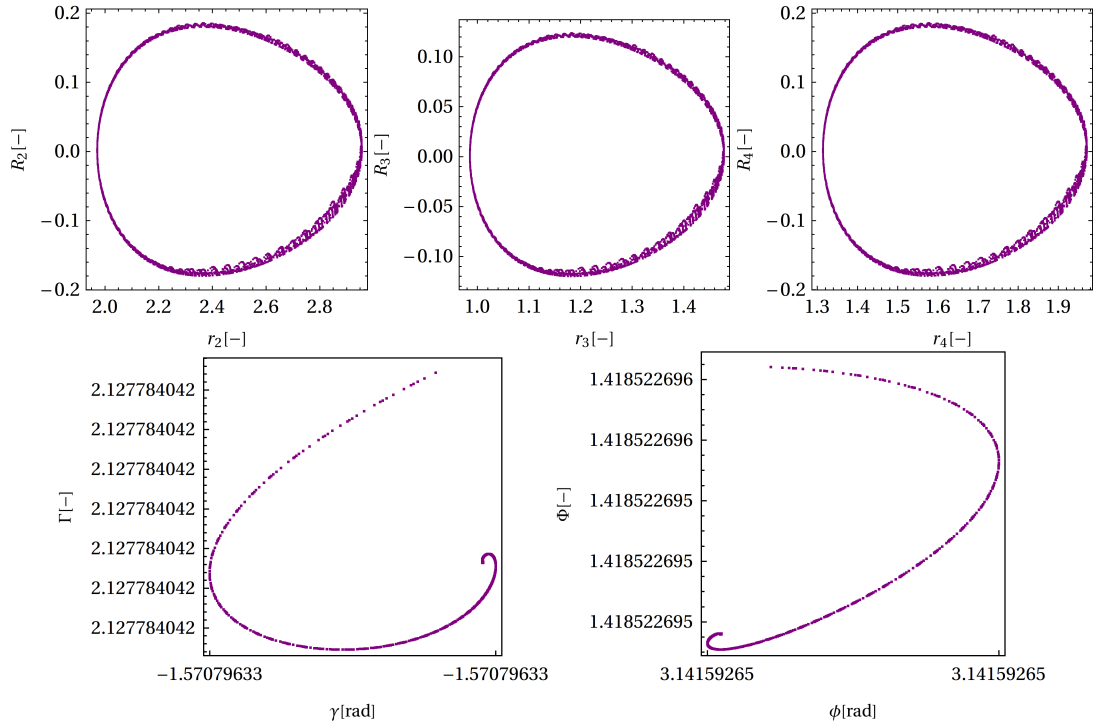

Figure 8.3: Phase portraits of the $e = 0.2$ square case integration with 12th-order Adams method for $4T$.

```
StartingStepSize -> 1/100, MaxSteps -> Infinity,
WorkingPrecision -> 20, PrecisionGoal -> 10, AccuracyGoal -> 10]
```

In principle, to prove non-linear stability with this straight-forward method we would have to run the simulation for an infinite number of periods. However, as mentioned in the introduction to this chapter, we would like to make use of an independent approach to gather evidence that our linear stability analysis has been executed correctly. For this, it will suffice to run the simulations for 200 periods, after which, if the periodic solution has remained bounded we will consider it as stable. Propagating a seemingly stable kite solution for 200 periods on the author's machine takes around 1.5-2 hours.

8.3. Convex configurations

In this section we perform long-time integrations of selected cases from the convex domain and compare the resulting behaviour with the linear stability results of Section 4.9. Since all of our cases are periodic, the symplectic integrator produces nice periodic behaviour like seen in Fig. 8.2 for more than 650 periods, possibly indefinitely. Therefore, to test the stability of the configurations we introduce perturbations in the initial conditions and see whether the bounded periodic behaviour is maintained or broken.

For convenience, we set the nominal initial conditions to be at the periapsis of the periodic solution (Eqs. (4.7) and (4.19)), $\theta(0) = 0$, which, in turn, means that $R(0) = 0$ and

$$r(0) = \frac{\omega^2}{1+e}$$

Without losing generality, we also choose the initial scaling to be $r(0) = 1$. This gives the relation $\omega^2 = 1 + e$ along with the following unperturbed initial state variables:

$$\begin{aligned} r_{2_{k0}} &= c_2 & R_{2_{k0}} &= 0 \\ r_{3_{k0}} &= c_3 & R_{3_{k0}} &= 0 \\ r_{4_{k0}} &= c_4 & R_{4_{k0}} &= 0 \\ \gamma_{k0} &= -\frac{\pi}{2} & \Gamma_{k0} &= \left(M_3 c_3^2 + M_4 c_4^2\right)\omega \\ \phi_{k0} &= \pi & \Phi_{k0} &= M_4 c_4^2 \omega \end{aligned} \tag{8.1}$$

In the following, we will use Eq. (8.1) as nominal initial conditions, to which we will introduce perturbations as a test of non-linear stability.

8.3.1. Square configuration

We choose to start our numerical analysis with the square configuration, shown in Fig. 8.4. Since the square solution is well known to be unstable (see Section 4.6) we use it as a ground case to verify that the numerical simulation produces the expected behabiour.

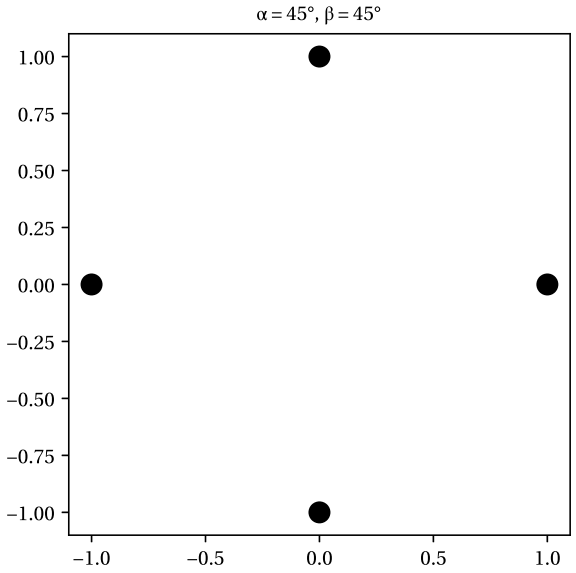

Figure 8.4: The special case of the square central configuration with all masses equal. Periodic solutions in this configurations are well-known to be linearly unstable. Unit radius is chosen for optimal viewing in each case and is not to scale. Unit distance is chosen to be the distance from the axis of symmetry to one of the equal masses.

$e = 0.44$, perturbation in r_2 The period in this case is

$$T = 2\pi\omega^3\left(1-e^2\right)^{-3/2} = 2\pi\sqrt{1+0.44}^3\left(1-0.44^2\right)^{-3/2} = 14.9933 \tag{8.2}$$

We apply a slight perturbation in the r_2 initial value, $r_2(0) = r_{2_{k0}}\left(1+10^{-9}\right)$, and just after 100 time units or 6.6 revolutions we see the solutions becoming unbounded, as seen in the phase portraits in Fig. 8.5. This agrees with the fact that the square configuration was found to be unstable.

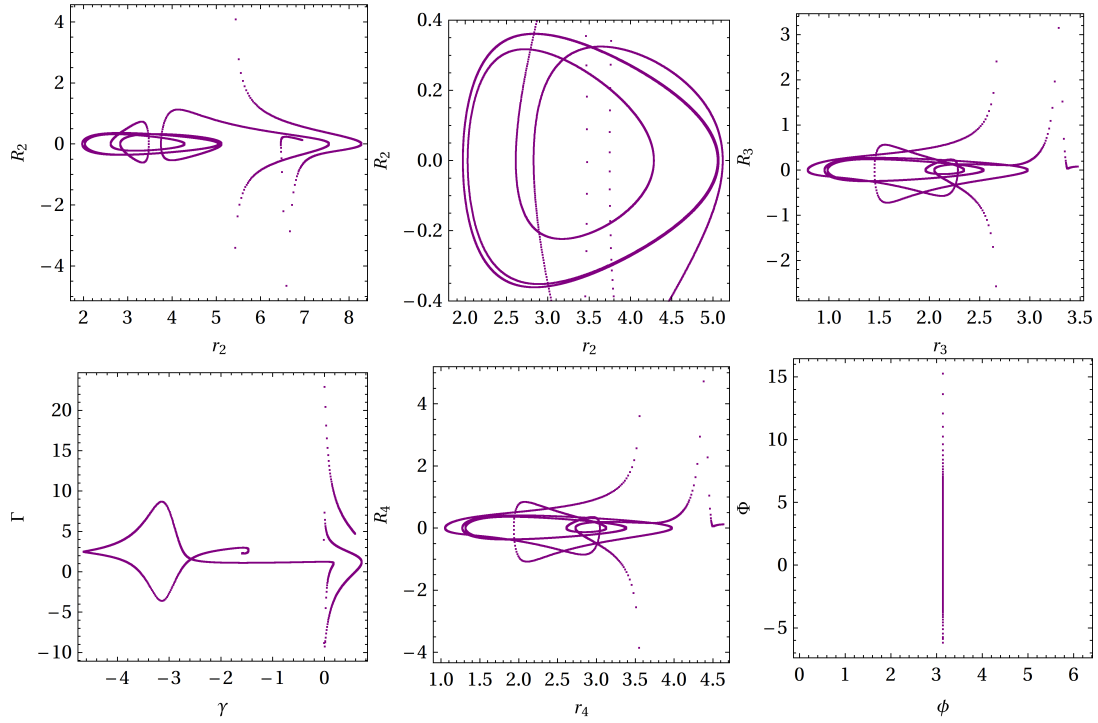

Figure 8.5: Phase portraits of the $e = 0.44$ square case integration with perturbation $r_2(0) = r_{2_{k0}}(1+10^{-9})$ over an interval of $t = 100$.

***e* = 0.2, compensating perturbations in $\gamma(0)$ and $\Gamma(0)$** As a second case we attempt to "compensate" the perturbation to the angle variable by dividing the conjugate momentum variable by the same factor. To this end we apply $\gamma(0) = \gamma_{k0}\left(1+10^{-9}\right)$, $\Gamma(0) = \Gamma_{k0}/\left(1+10^{-9}\right)$. The hypothesis here was that perhaps a perturbation which mimics a symplectic transformation might retain stability. However we see in Fig. 8.6 that stability is lost after four periods.

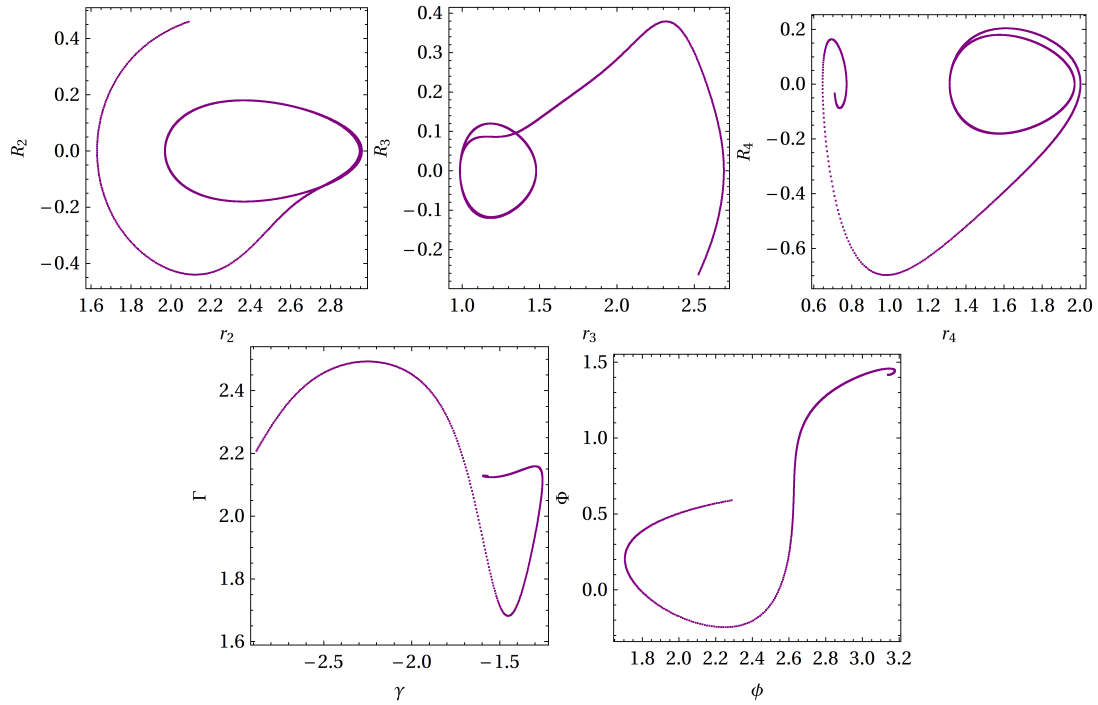

Figure 8.6: Phase portraits of the $e = 0.2$ square case integration with perturbations $\gamma(0) = \gamma_{k0}(1+10^{-9})$, $\Gamma(0) = \Gamma_{k0}/(1+10^{-9})$ over an interval of $t = 4T$.

$e = 0.2$, Hamiltonian preserving perturbations in r_2 and R_2 As a third experiment, we apply a perturbation such that the Hamiltonian function is left unchanged. We use the expression for R_2 in terms of h, given in Eq. (3.73) to calculate the R_2 initial value which compensates the perturbation $r_2(0) = r_{2_{k0}}\left(1+10^{-9}\right)$ and keeps the original Hamiltonian value. The hypothesis that this might preserve stability does not hold up and we again see divergence of the solution just after four periods (Fig. 8.7).

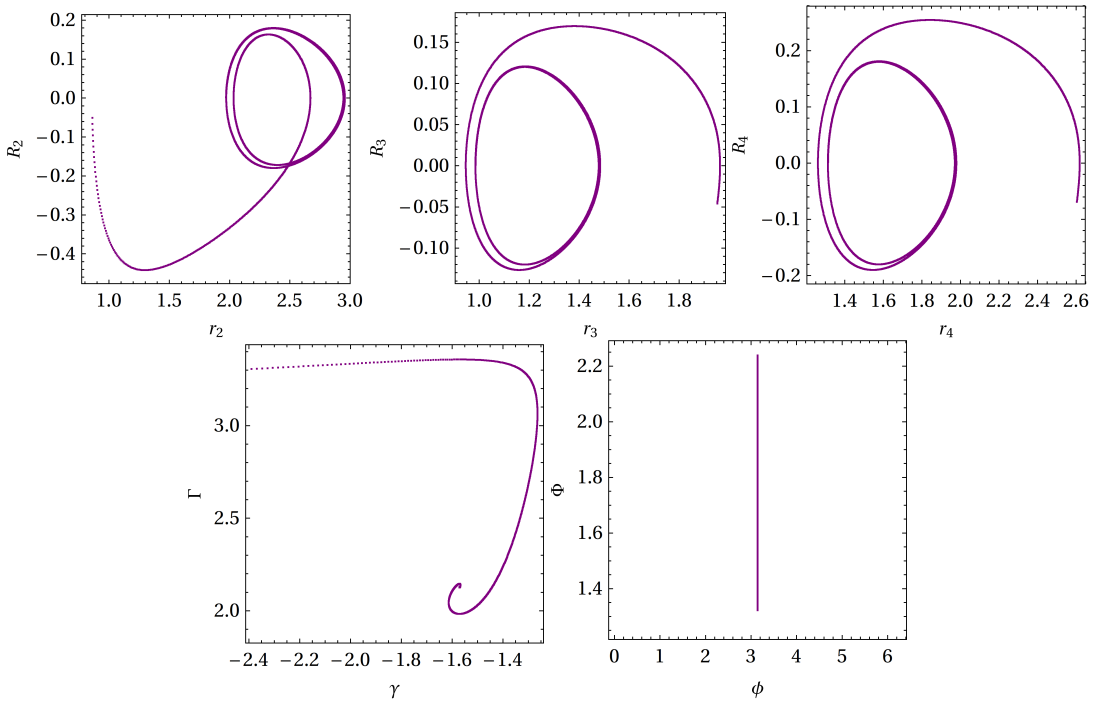

Figure 8.7: Phase portraits of the $e = 0.2$ square case integration with perturbation $r_2(0) = r_{2_{k0}} \cdot (1+10^{-9})$, $R2(0) = \sqrt{\cdots}$ over an interval of $t = 4T$.

Hence, we see that all three perturbations result in divergence of the solution just after a few periods, agreeing with the strong linear instability of the square solutions.

8.3.2. Case $\alpha = 59.9°$, $\beta = 15.1°$, $e = 0.3$

The first linearly stable case we consider is the bottom left case in Fig. 4.22, illustrated in Fig. 8.8. As the solutions generally seem to be more strongly stable in the bottom left direction in the stability plots Figs. 4.15, 4.19 and 4.22 we expect that this solution should pass our test and keep its periodicity.

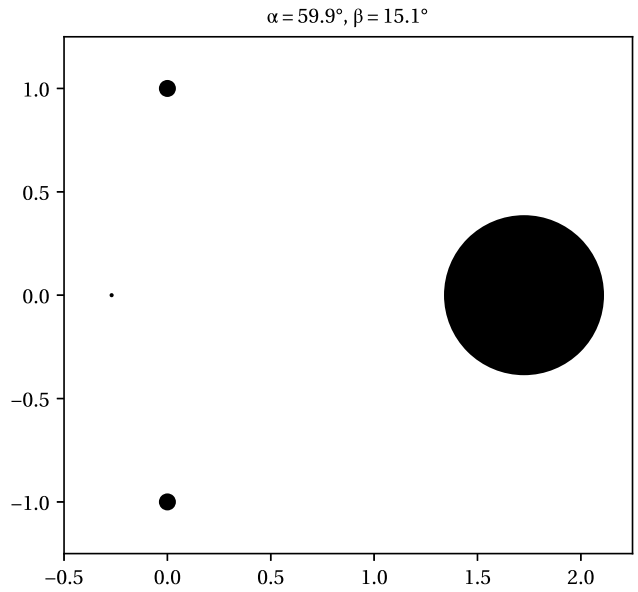

Figure 8.8: The case $\alpha = 59.9°$, $\beta = 15.1°$. The radii of the bodies are proportional to cube roots of the masses, such that the volumes would be directly proportional to the masses. Unit radius is chosen for optimal viewing in each case and is not to scale. Unit distance is chosen to be the distance from the axis of symmetry to one of the equal masses.

The period in this case is

$$T = 2\pi\omega^3\left(1-e^2\right)^{-3/2} = 2\pi\sqrt{1+0.3}^3\left(1-0.3^2\right)^{-3/2} = 10.7283 \tag{8.3}$$

Perturbation in $r_2(0)$ We start by perturbing the initial value $r_2(0) = r_{2_{k0}}\left(1+10^{-9}\right)$. Running the simulation for 200 periods confirms the hypothesis and we see nicely periodic motion in the position variables and semi-periodic motion in the angle variables in Figs. 8.9 and 8.10. The perturbation causes the angle variables to not stay constant anymore, but wiggle around the initial values, however around 199 periods at $t = 2130$ the motion has remained bounded with the angles oscillating in a neighborhood of about 0.00000001 rad.

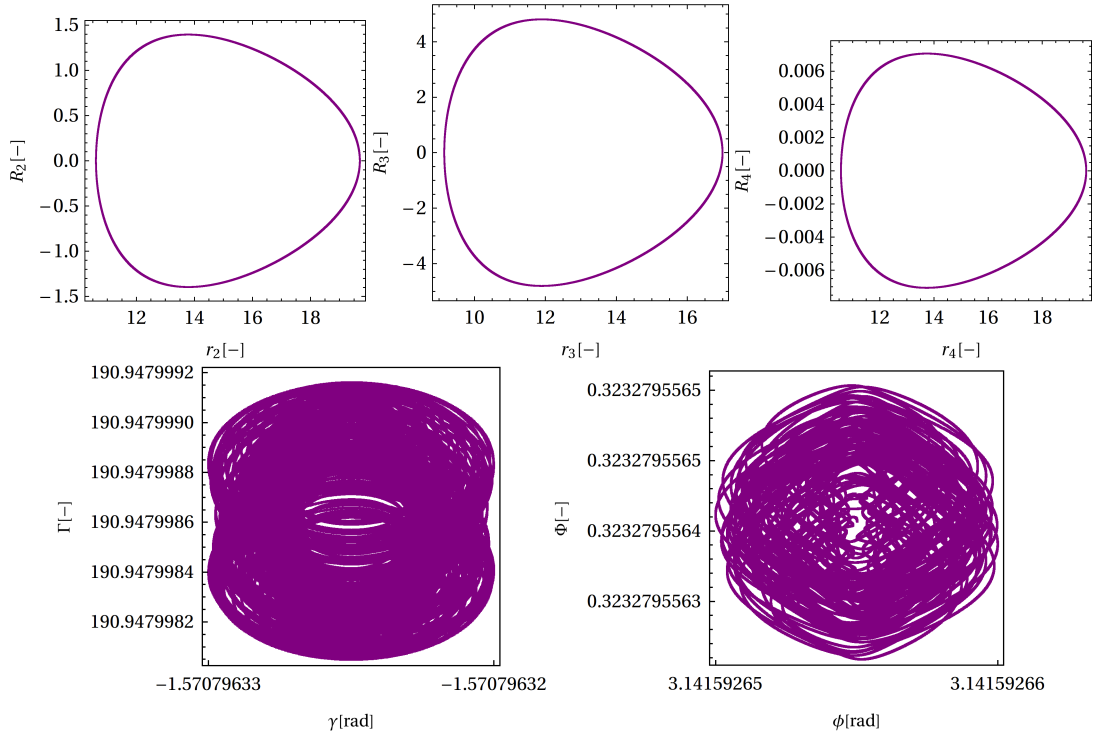

Figure 8.9: Phase portraits of the $e = 0.3$, $\alpha = 59.9°$, $\beta = 15.1°$ case integration with perturbation $r_2(0) = r_{2_{k0}}(1 + 10^{-9})$ over an interval of $t = 2130$.

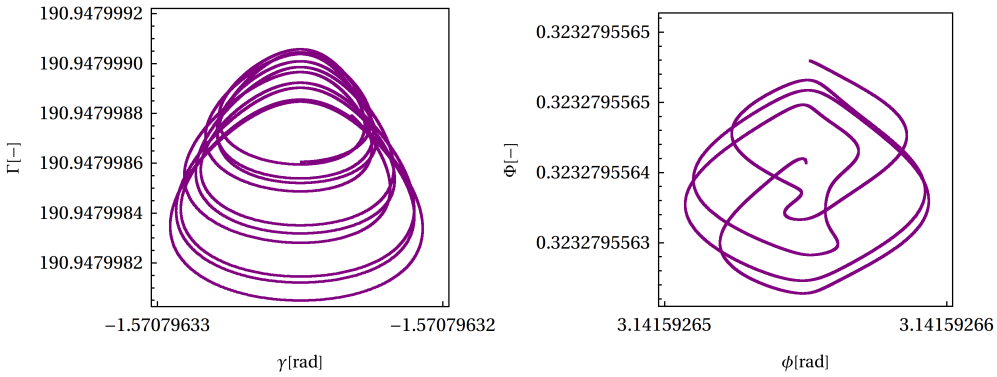

Figure 8.10: Phase portraits of the $e = 0.3$, $\alpha = 59.9°$, $\beta = 15.1°$ case integration with perturbation $r_2(0) = r_{2_{k0}}(1 + 10^{-9})$ over an interval of $t = 10T$.

Perturbation in $r_3(0)$ Applying the perturbation $r_3(0) = r_{3_{k0}}\left(1 + 10^{-9}\right)$ we find the same behaviour as when $r_2(0)$ is perturbed, see Figs. A.1 and A.2.

Perturbation in $\gamma(0)$ Applying $\gamma(0) = \gamma_{k0}\left(1 + 10^{-9}\right)$ we find the same behaviour as when $r_2(0)$ is perturbed, however now the ϕ angle seems to follow even more irregular oscillations, see Figs. A.3 and A.4.

Perturbation in $r_4(0)$ Applying $r_4(0) = r_{4_{k0}}\left(1 + 10^{-9}\right)$ we find again the same behaviour, except now ϕ oscillates with a bigger amplitude, in a neighborhood of about 0.0000003 rad, see Figs. A.5 and A.6.

Perturbation in $\phi(0)$ Perturbation $\phi(0) = \phi_{k0}\left(1 + 10^{-9}\right)$ results in the usual behavior, with angle oscillations in a region of about 0.00000001 rad around the initial values, see Figs. A.7 and A.8.

Perturbation in $R_2(0)$ Now perturbing the momentum variable, we have to add 10^{-9} to it, because the initial value is 0 and cannot be scaled, $R_2(0) = 10^{-9}$. The resulting behaviour is again similar, this time almost identical to the $r_3(0)$ perturbation, see Figs. A.9 and A.10.

Perturbation in $R_3(0)$ Perturbation $R_3(0) = 10^{-9}$ produces almost identical results as the perturbation to $R_2(0)$, see Figs. A.11 and A.12.

Perturbation in $\Gamma(0)$ Applying $\Gamma(0) = \Gamma_{k0}\left(1+10^{-9}\right)$ results in almost identical behaviour as the perturbation in $\gamma(0)$, see Figs. A.13 and A.14.

Perturbation in $R_4(0)$ Perturbation $R_4(0) = 10^{-9}$ results in almost identical behaviour as the perturbation in $r_4(0)$, see Figs. A.15 and A.16.

Perturbation in $\Phi(0)$ Applying $\Phi(0) = \Phi_{k0}\left(1+10^{-9}\right)$ results in almost identical behaviour as perturbation in $\phi(0)$, see Figs. A.17 and A.18

We see that perturbations in all 10 initial conditions resulted in retention of the periodic orbit even after 199 periods, with only small bounded oscillations persisting from the perturbations. This is in accordance with our result of linear stability for this configuration.

8.3.3. Case $\alpha = 39.7°$, $\beta = 25.3°$, $e = 0.2$

Now we turn to the peculiar case of the isolated stable island in Fig. 4.19, illustrated in Fig. 8.11.

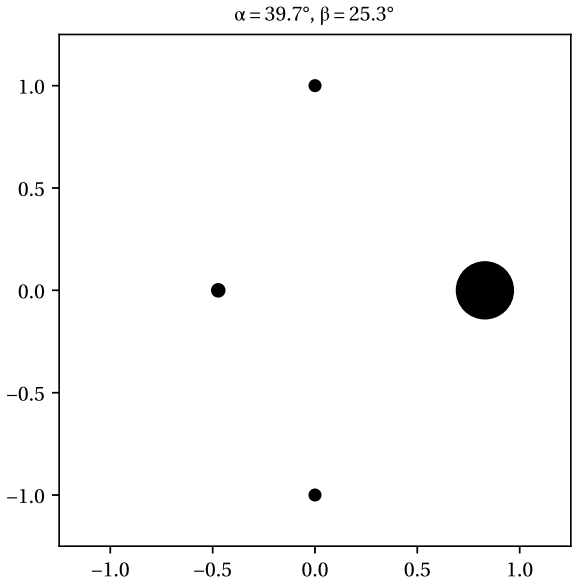

Figure 8.11: The $\alpha = 39.7°$, $\beta = 25.3°$ configuration. The radii of the bodies are proportional to cube roots of the masses, such that the volumes would be directly proportional to the masses. Unit radius is chosen for optimal viewing in each case and is not to scale. Unit distance is chosen to be the distance from the axis of symmetry to one of the equal masses.

The period in this case is

$$T = 2\pi\sqrt{1+0.2}^{3}\left(1-0.2^2\right)^{-3/2} = 8.78102$$

Once again, we perturb each initial condition by 10^{-9} and integrate the system for 200T.

Perturbation in $r_2(0)$ Applying $r_2(0) = r_{2_{k0}}\left(1+10^{-9}\right)$ we find again the nice periodic motions of the radius variables, this time on different scales though, as the geometry is different. The angle variables also follow familiar oscillations, this time γ oscillates in an interval of around 0.00000003 rad, while ϕ moves about in an interval of about 0.00000015 rad around the initial value, see Figs. 8.12 and 8.13.

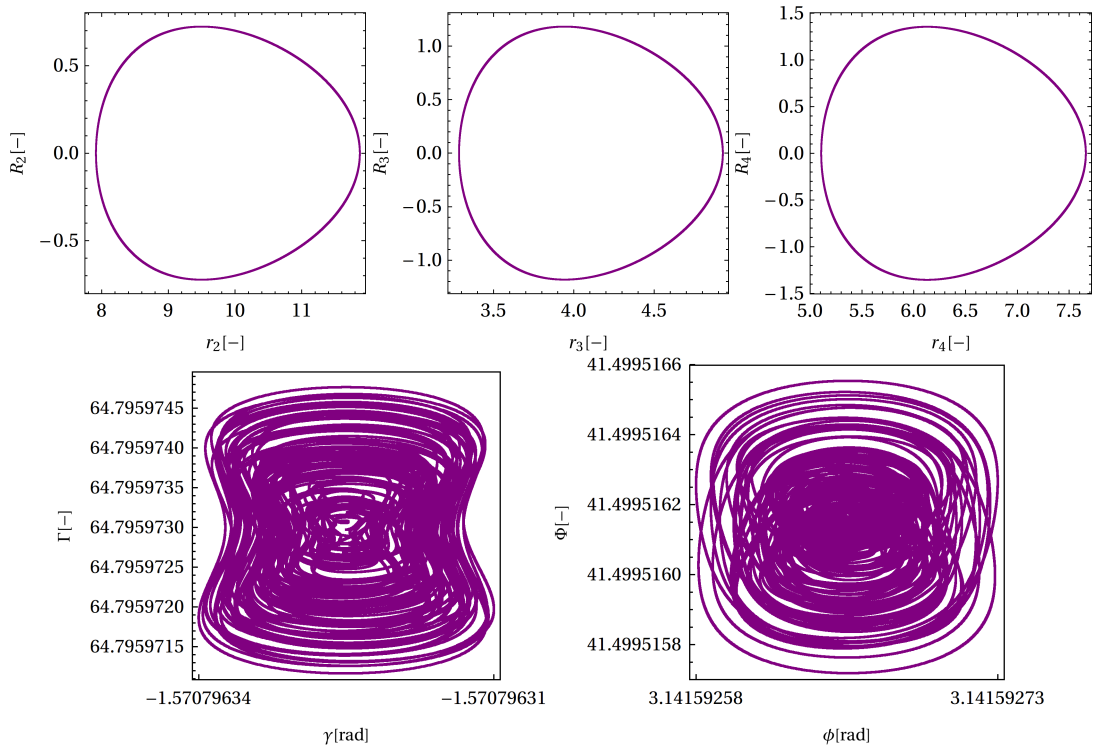

Figure 8.12: Phase portraits of the $e = 0.2$, $\alpha = 39.7°$, $\beta = 25.3°$ case integration with perturbation $r_2(0) = r_{2_{k0}}(1 + 10^{-9})$ over an interval of $t = 1756$.

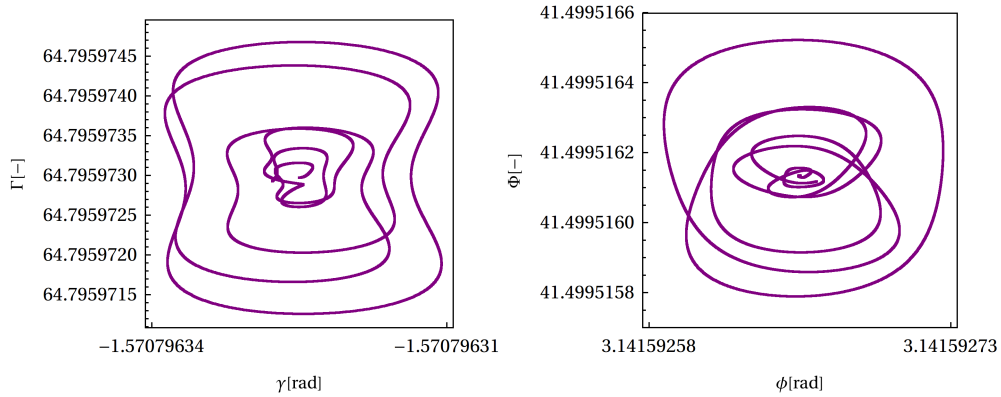

Figure 8.13: Phase portraits of the $e = 0.2$, $\alpha = 39.7°$, $\beta = 25.3°$ case integration with perturbation $e = 0.2$, $r_2(0) = r_{2_{k0}}(1 + 10^{-9})$ over an interval of $t = 10T$.

Perturbation in $r_3(0)$ Perturbation in $r_3(0) = r_{3_{k0}}\left(1 + 10^{-9}\right)$ produces very similar patterns, this time γ varies in a region of around 0.00000001 rad, while ϕ moves about in a neighborhood or around 0.00000003 rad, see Figs. A.19 and A.20.

Perturbation in $\gamma(0)$ Perturbation $\gamma(0) = \gamma_{k0}\left(1 + 10^{-9}\right)$ produces similar results to the $r_2(0)$ perturbation, with the angle variations of the same magnitude, see Figs. A.21 and A.22.

Perturbation in $r_4(0)$ Applying $r_4(0) = r_{4_{k0}}\left(1 + 10^{-9}\right)$ we find very similar results to the r_3 case, with ϕ moving in a neighborhood of around 0.00000007 rad, see Figs. A.23 and A.24.

Perturbation in $\phi(0)$ Perturbing $\phi(0) = \phi_{\phi 0}\left(1 + 10^{-9}\right)$ produces the familiar patterns, but this time the range of motion of the angle variables is larger. Not surprising, as we directly perturbed one of the angle

variables. γ now moves in a region of around 0.0000009 rad, while ϕ moves about in a neighborhood of around 0.000001 rad, see Figs. A.25 and A.26.

Perturbation in $R_2(0)$ Applying $R_2(0) = 10^{-9}$ produces almost identical results to the perturbation in $r_2(0)$, see Figs. A.27 and A.28.

Perturbation in $R_3(0)$ Perturbation $R_3(0) = 10^{-9}$ produces almost identical results to the perturbation in $r_3(0)$, see Figs. A.29 and A.30.

Perturbation in $\Gamma(0)$ Perturbation $\Gamma(0) = \Gamma_{k0}\left(1 + 10^{-9}\right)$ produces almost identical results to the perturbation in $\gamma(0)$, see Figs. A.31 and A.32.

Perturbation in $R_4(0)$ Setting $R_4(0) = 10^{-9}$ produces almost identical results to the perturbation in $r_4(0)$, see Figs. A.33 and A.34.

Perturbation in $\Phi(0)$ Perturbation $\Phi(0) = \Phi_{k0}\left(1 + 10^{-9}\right)$ produces almost identical results to the perturbation in $\phi(0)$, see Figs. A.35 and A.36.

Once again, the long-term integrations confirm the linear stability results for the convex cases, as assessed in Section 4.9, and the perturbed solution in each case remains in the neighborhood of the original solution for $200T$.

8.4. Concave configurations of the first kind

The concave cases of the first kind were all found to be linearly unstable, therefore we expect all solutions to diverge from the periodic solution as perturbations are applied. In this section we choose an arbitrary sample and perform the numerical integration.

8.4.1. Case $\alpha = 50°$, $\beta = 5°$, $e = 0.1$

We choose to test the geometry shown in Fig. 8.14 for eccentricity 0.1.

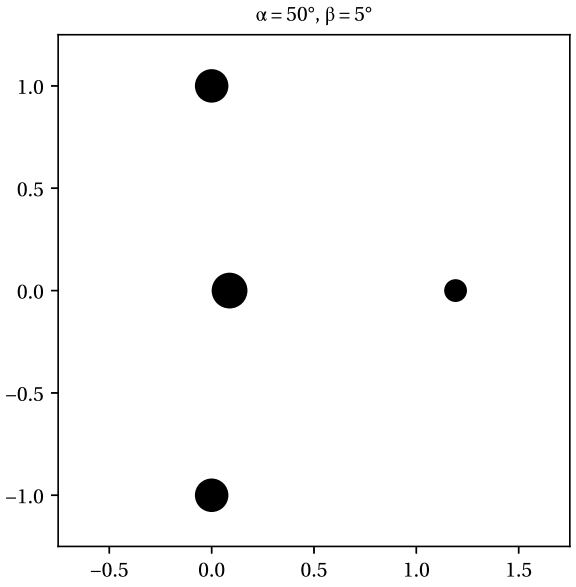

Figure 8.14: The unstable $\alpha = 50°$, $\beta = 5°$ configuration of the first concave type. The radii of the bodies are proportional to cube roots of the masses, such that the volumes would be directly proportional to the masses. Unit radius is chosen for optimal viewing in each case and is not to scale. Unit distance is chosen to be the distance from the axis of symmetry to one of the equal masses.

The period in this case is

$$T = 2\pi\sqrt{1+0.1}^{3}\left(1-0.1^2\right)^{-3/2} = 7.35895 \tag{8.4}$$

Unperturbed $t = 11T$ No perturbation needed in this case, as only after 11 periods we see divergence from the periodic solution, see Fig. 8.15.

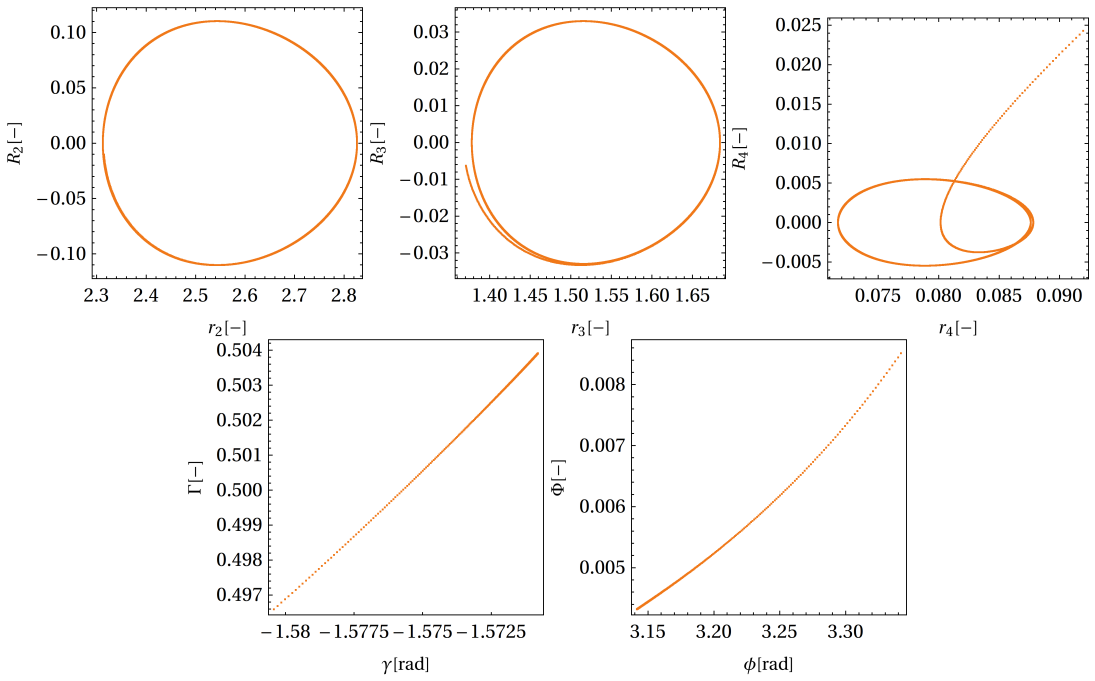

Figure 8.15: Phase portraits of the $e = 0.1$, $\alpha = 50°$, $\beta = 5°$ case integration over an interval of $t = 11T$.

Unperturbed $t = 200$ Integrating for a slightly longer time shows the solutions becoming chaotic and unbounded, see Fig. 8.16.

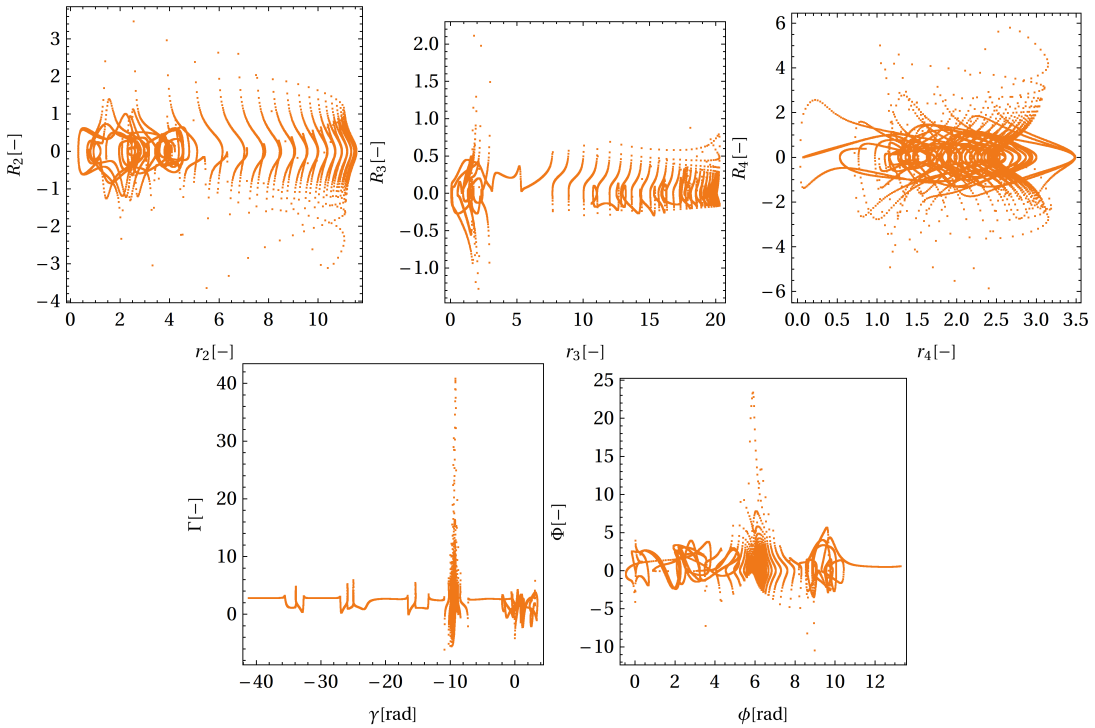

Figure 8.16: Phase portraits of the $e = 0.1$, $\alpha = 50°$, $\beta = 5°$ case integration over an interval of $t = 200$.

8.5. Concave configurations of the second kind

For the second concave cases we again found instability for all periodic solutions. In this section we pick a couple cases and test them against non-linear integration.

8.5.1. Case $\alpha = 74°$, $\beta = 59°$, $e = 0.1$

The first geometry we try is shown in Fig. 8.17, for which we set $e = 0.1$.

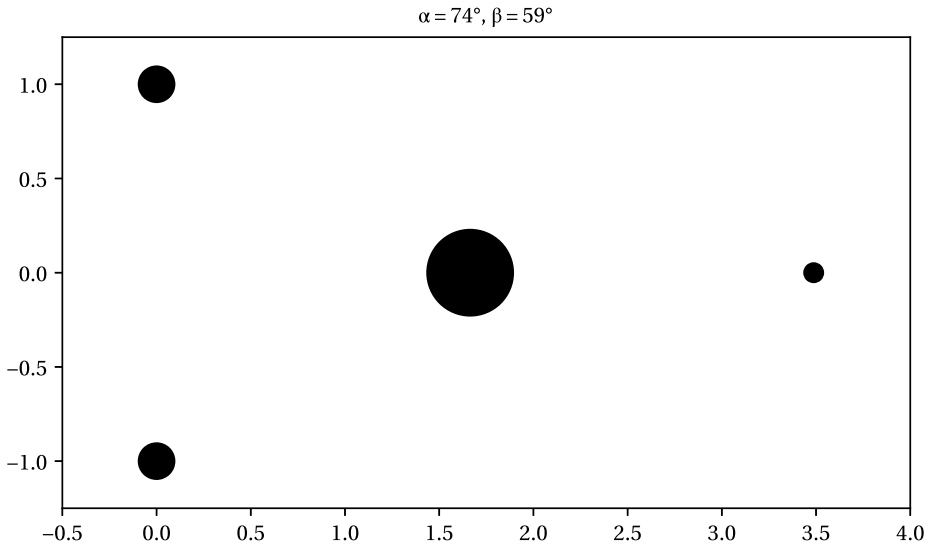

Figure 8.17: The unstable $\alpha = 74°$, $\beta = 59°$ central configuration of the second concave type. The radii of the bodies are proportional to cube roots of the masses, such that the volumes would be directly proportional to the masses. Unit radius is chosen for optimal viewing in each case and is not to scale. Unit distance is chosen to be the distance from the axis of symmetry to one of the equal masses.

The period for $e = 0.1$ is again

$$T = 7.35895$$

.

Unperturbed $t = 300T$ Without perturbations this case remains periodic at least for 300 periods, as seen in Fig. 8.18.

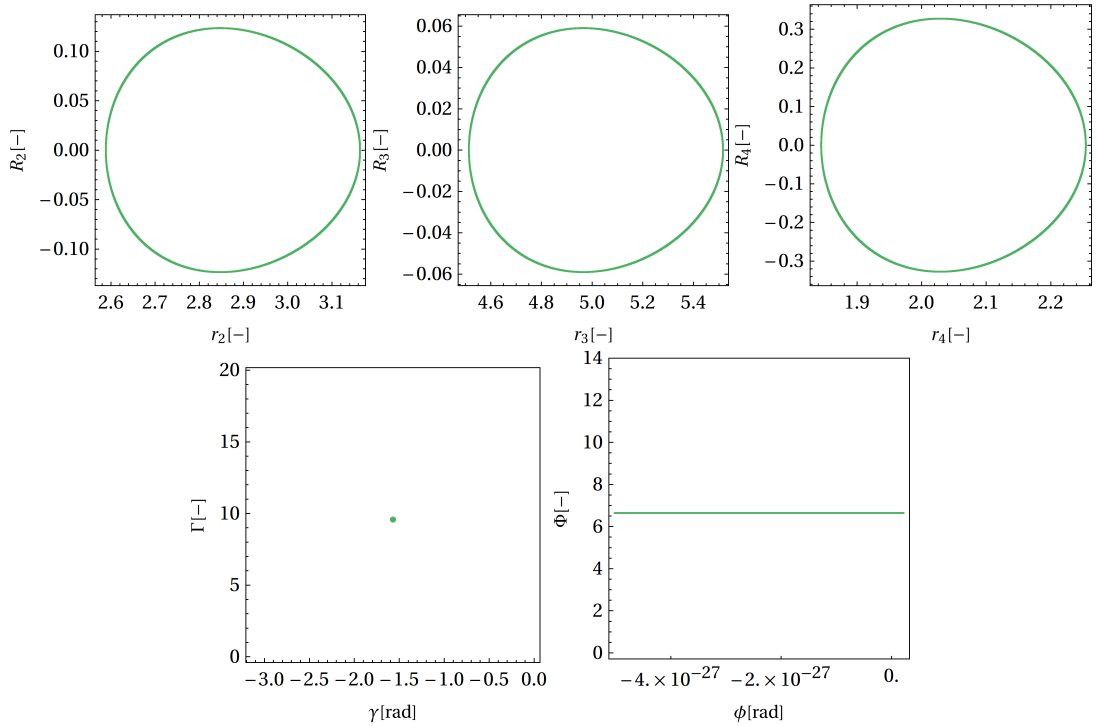

Figure 8.18: Phase portraits of the $e = 0.1$, $\alpha = 74°$, $\beta = 59°$ case integration over an interval of $t = 300T$.

Perturbation in $r_2(0)$ Applying the perturbation $r_2(0) = r_{2_{k0}}\left(1+10^{-9}\right)$ we quickly see the instability arise, with the solutions diverging just after seven periods, see Fig. 8.19.

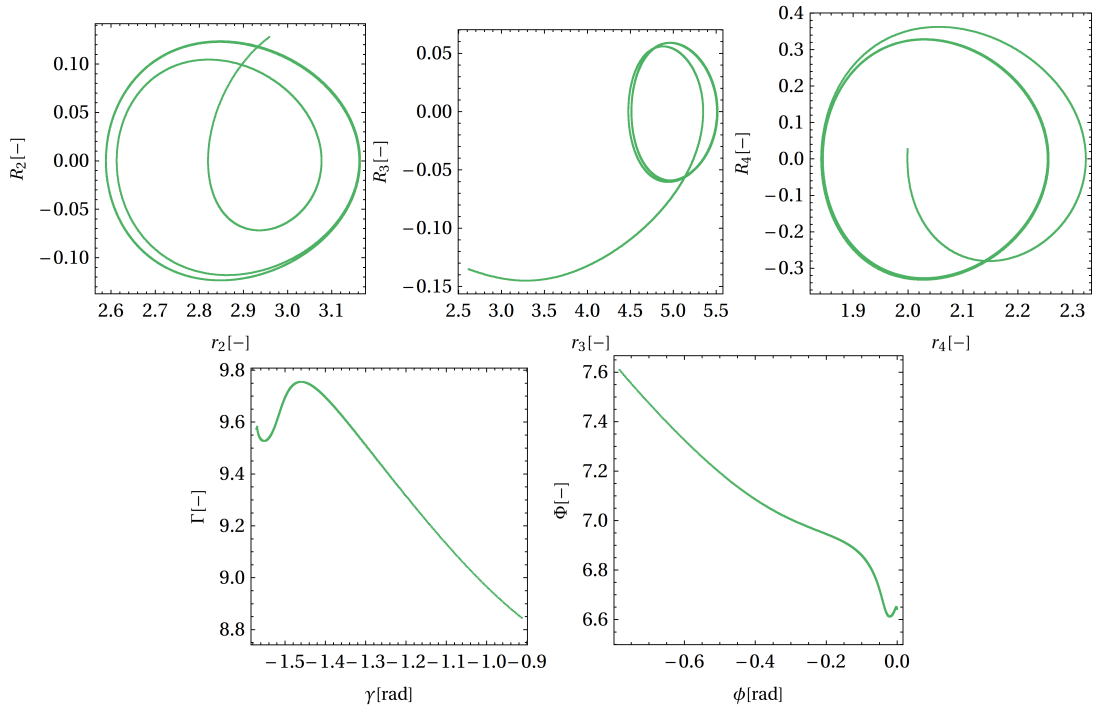

Figure 8.19: Phase portraits of the $e = 0.1$, $\alpha = 74°$, $\beta = 59°$ case integration with perturbation $r2(0) = r_{2_{k0}}(1+1e-9)$ over an interval of $t = 7T$.

Compensating perturbation in $\gamma(0)$ and $\Gamma(0)$ We once again attempt here to "compensate" the perturbation to the angle variable by dividing the conjugate momentum variable by the same factor. To this end we

apply $\gamma(0) = \gamma_{k0}\left(1+10^{-9}\right)$, $\Gamma(0) = \Gamma_{k0}/\left(1+10^{-9}\right)$. We see that after around 30 periods the solutions are fully chaotic, as shown in Fig. 8.20.

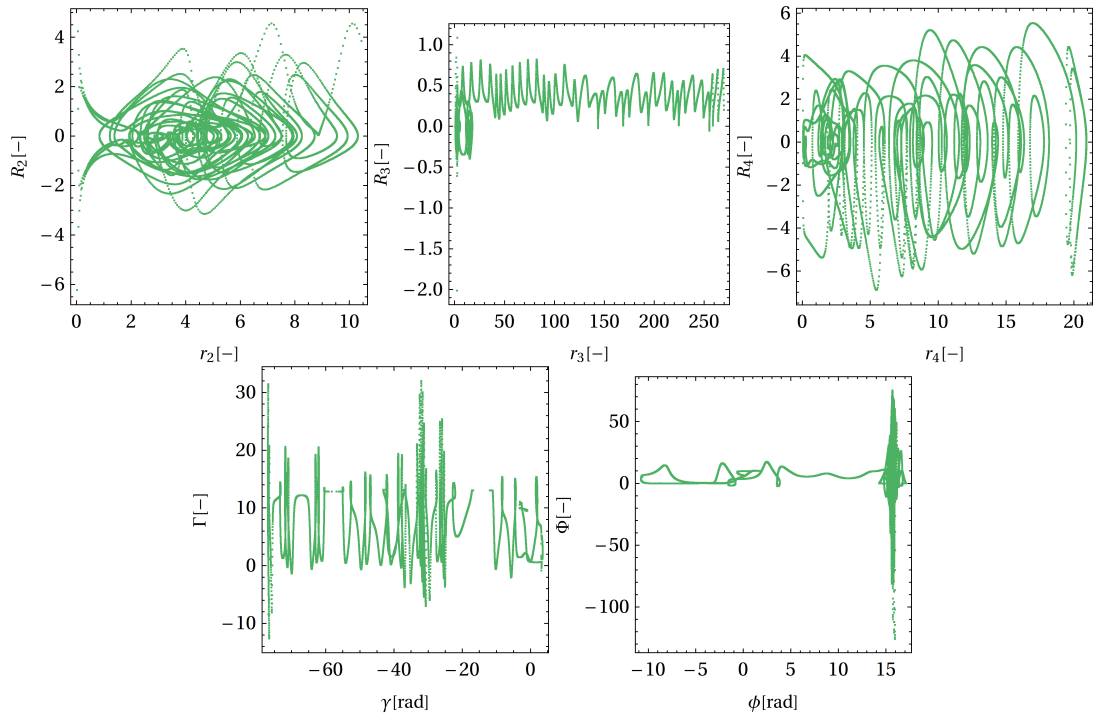

Figure 8.20: Phase portraits of the $e = 0.1$, $\alpha = 74°$, $\beta = 59°$ case integration with perturbations $\gamma(0) = \gamma_{k0}\left(1+10^{-9}\right)$, $\Gamma(0) = \Gamma_{k0}/\left(1+10^{-9}\right)$ over an interval of $t = 218$.

8.5.2. Case $\alpha = 65°$, $\beta = 55°$, $e = 0$

We try another concave case of the second kind, this time for zero eccentricity, with geometry as shown in Fig. 8.21.

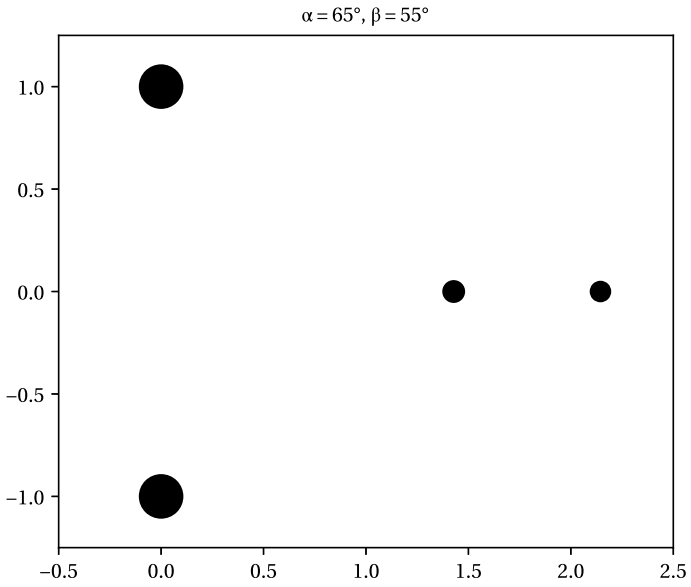

Figure 8.21: The unstable $\alpha = 65°$, $\beta = 55°$ central configuration of the second concave type. The radii of the bodies are proportional to cube roots of the masses, such that the volumes would be directly proportional to the masses. Unit radius is chosen for optimal viewing in each case and is not to scale. Unit distance is chosen to be the distance from the axis of symmetry to one of the equal masses.

The period is

$$T = 2\pi$$

.

Perturbation in $r_2(0)$ Applying $r_2(0) = r_{2_{k0}}\left(1+10^{-9}\right)$ perturbation results in chaos just after four periods, see Fig. 8.22.

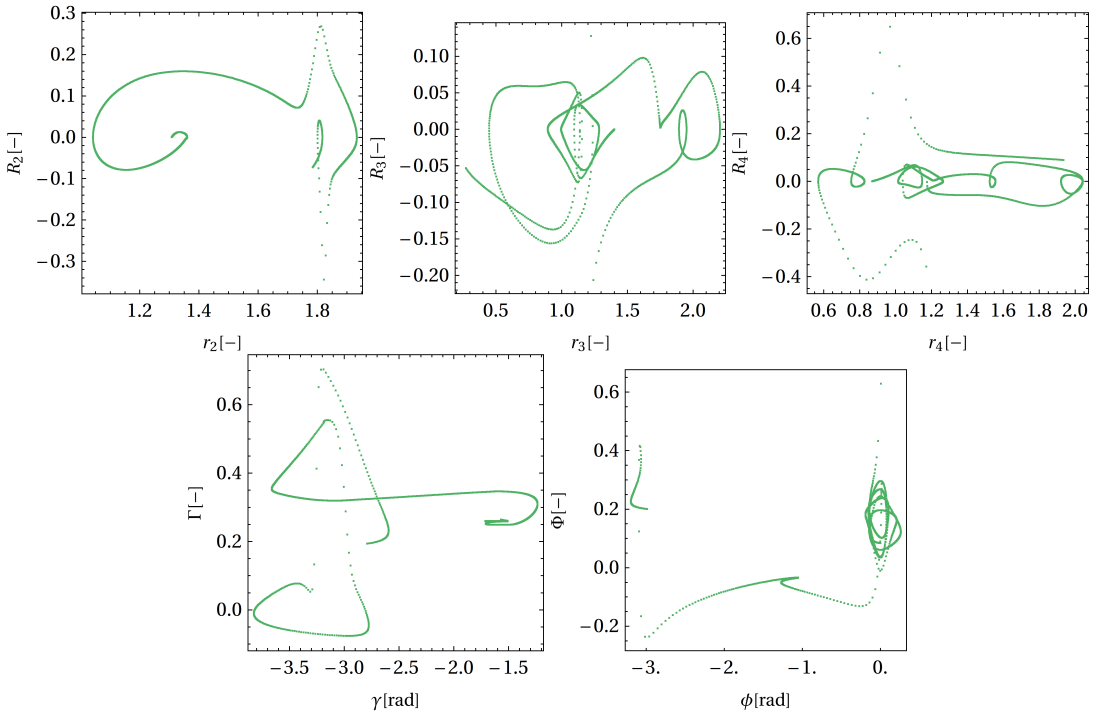

Figure 8.22: Phase portraits of the $e = 0$, $\alpha = 65°$, $\beta = 55°$ case integration with perturbation $r_2(0) = r_{2_{k0}}\left(1+10^{-9}\right)$ over an interval of $t = 4T$.

Perturbation in $\gamma(0)$ We get the same outcome for the $\gamma(0) = \gamma_{k0}\left(1+10^{-9}\right)$ perturbation as well, see Fig. 8.23.

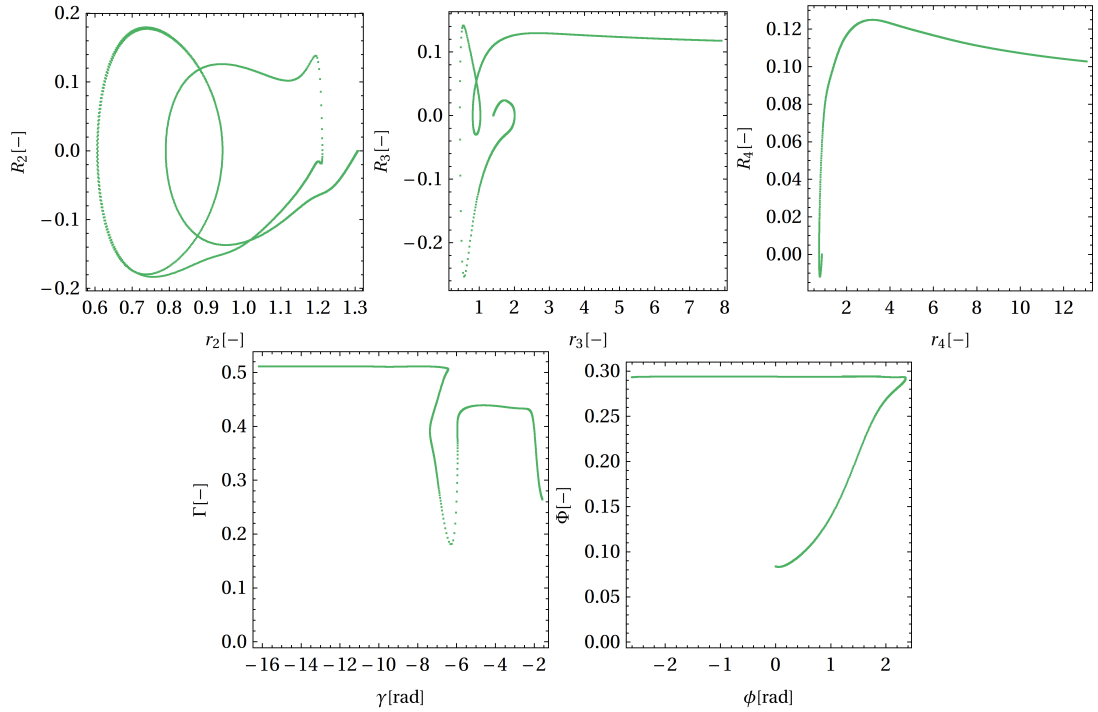

Figure 8.23: Phase portraits of the $e = 0$, $\alpha = 65°$, $\beta = 55°$ case integration with perturbation $\gamma(0) = \gamma_{k0}\left(1 + 10^{-9}\right)$ over an interval of $t = 4T$.

8.6. Conclusions

To review, every case we put to test using non-linear long-time numerical integration behaved as predicted by the linear stability analysis. While the linearly stable cases remained bounded for at least 200 periods for all perturbations, every unstable case subjected to the same perturbations started diverging from the periodic solution just after a few revolutions. The single concave case of the first type that was tested was especially unstable, diverging by itself without any perturbation to the initial conditions (Fig. 8.15). All other solutions needed a perturbation to distinguish the stable or unstable characteristics. Looking at Fig. 8.14, we see that this solution has all four masses of a similar magnitude and is not ring-like in structure. This connects to our remarks in Sections 4.10, 5.4 and 6.4, where we suggested these two properties are the recipe for stability of circular and eccentric orbits alike. Perfect agreement of the linear stability results with the independent approach of this chapter provides validation that the linear stability analysis has been performed correctly. Furthermore, the combined results suggest that the linearly stable convex cases might possibly exist in the universe, as they seem to be robust against various perturbations, whereas the concave cases could not possibly remain in a periodic orbit for long.

III

Conclusions and recommendations

9 Conclusions

9.1. Research questions

To summarize, we have provided answers to the main research question, "What are the stability properties of kite central configurations of four bodies?" using two independent approaches. One of them focused on linear stability, which we determined for samplings of the domains of all three types of kite central configurations. We did this for both the circular and elliptic periodic solutions. The circular ones were treated using an analytical approach (only some algebra was done with the help of Mathematica), whereas numerical integration was employed to compute the Floquet multipliers to determine linear stability of the eccentric orbits. These results answer research sub-question 1 in Section 1.3, "Are the homographic solutions provided by the kite central configurations linearly stable?". Our answer is for the most part not, except a region near co-orbital configurations in the convex case.

The second approach to assess the stability properties was a long-time numerical simulation of the non-linear 10-dimensional system, defined after using first integrals to constrain the phase space. This approach let us to put under test some of the solutions that were found to be linearly stable. Perfect aggreement was found between the two approaches, where two of the convex solutions from the discovered stability region that we tested under perturbations in initial conditions succesfully stayed near the homographic solution until the simulation was stopped after 200 periods. In contrast, the tested unstable configurations usually lost stability after less than 10 revolutions. These results are progress towards definitively answering research sub-question 2, "Do the homographic solutions provided by kite central configurations possess non-linear stability?". The results we obtained do not prove a positive answer to this question, but they do hint that the linearly stable convex periodic solutions, pinpointed in Section 4.9.2, are resilient to perturbations even under the true non-linear dynamics.

Finally, we have decent evidence to attempt to answer the third research sub-question from Section 1.3, "Can kite central configurations occur in real astronomical systems?". Looking at the results from our two stability investigations, it certainly seems possible that, provided four bodies of correct masses were started on one of the stable convex kite homographic solutions, they would stay moving on or in a neighbourhood of this periodic solution. The evidence we have to suggest that is the robustness against perturbations of the two stable test cases, as well as the region of linear stability in the configuration space shown in Figs. 4.11, 4.15, 4.19 and 4.22. Having found not one linearly stable case, but a region, we can more strongly suggest that real life occurence of convex kite periodic solutions is possible. First, because the probability of occurence is simply higher when there is a continuous array of possible configurations, second, because stable neighbouring configurations increase the structural stability of a solution (a perturbation in α is intuitively easier to handle when the neighbouring orbits are also stable). Our analysis for the eccentric cases revealed that the stable region has continuity also in the e direction, further reinforcing the integrity of these solutions.

That being said, celestial bodies have to first find their way into the somewhat thin strip of stability near the co-orbital solutions. The fact that these solutions include a dominating mass, such as the two solutions pictured in Figs. 8.8 and 8.11 help our case, because, as we know from observations, it is very common for a massive body to catch smaller objects from its surroundings, be it asteroids, moons or ring material.

Another promising option for a real manifestation of a kite four-body solution was discussed in Chapter 1, namely a binary star system in a kite central configuration with two other bodies, as proposed in [34]. How-

ever, upon comparing the obtained stability results, it turns out that such a system cannot be stable in a kite configuration. The reason for this is that the only feasible convex kite configurations for such a system were identified in [34] to be close to a rhombus configuration, which we identified as an unstable region. That is, unless two of the masses are so small as to effectively be in the singular configuration, marked 'S' in Fig. 2.2. We have not investigated the stability of such limit cases in the present work.

In any case, we can reasonably expect three satellites to be orbiting a star in a 1:1 resonance close to the co-orbital configuration, or three moons orbiting a huge planet. For instance, in the Solar system, Janus and Epimetheus - moons of Saturn - constitute the largest co-orbital objects [34]. Another co-orbital example is the minor planet orbiting white dwarf WD 1145+017 [34], which has been torn apart by the star and co-orbiting with its scattered fragments. Thus, there are certainly possibilities. Thinking even more broadly, any number of the stable cases may also apply to massive objects on a very large scale, such as star clusters, black holes, galaxies or galaxy clusters, as long as the interaction between them may be approximated as Newtonian gravitational attraction between 4 point masses (and one of them is dominating).

9.2. Research objective

The main objective we set out to achieve in the present work is to contribute to the body of knowledge of celestial mechanics through a stability assessment of the four-body kite central conguration family. We have succeeded in this goal inasmuch as we have the following results:

- Regions of linear stability have been found for the convex kite central configurations for circular as well as eccentric cases.
- No stable cases were found for our sampling of the domains of the first and second concave cases for any eccentricity.
- The linearly stable cases agree with the dominant mass and ring-like linear stability hypotheses.
- Exact eigenvalues were provided for the square central configuration.
- Binary star systems in kite central configurations with two planets were determined to be unplausible.
- A perturbation method utilising properties of reflexive polynomials to allow an analytical assessment of an impact of a parameter on the stability of an eight-dimensional Hamiltonian system.

The perturbation method was developed closely following the method in [27], but nonetheless, it contains new elements which allow an analytical application to an eight-dimensional planar four-body problem by use of special properties of symplectic matrices and reflexive polynomials. This method allows an analytical assessment of the impact of the move to an eccentric orbit from a circular one on the stability of four-body solutions. The author has not seen this or an equivalent method applied to solutions of the four-body problem in literature.

Finally, the correctness of these results has been ensured by validating with existing results and various verification checks, listed in Chapter 7. It must be noted that the stable convex cases found all have one dominant mass, which falls in line with the common axiom that configurations tend to be stable only when a dominant mass is present.

9.3. Recommendations

There are several promising directions from this point, where worthwhile research could be done. First, as mentioned in the previous section, we have not provided absolute proof for non-linear stability of any of the kite configurations. Pursuing such a proof would pose a truly challenging, but exciting endeavour. As mentioned in the present work, Lyapunov methods are known to fail in assessing stability of central configurations [19]. Attempts to apply KAM theory around central configuration periodic solutions could chart new territory.

A second improvement upon this research could be to analyze the limit and singular cases at the borders and vertices of the domains of kite central configurations Figs. 2.2 and 2.5, as in the present work only stability of four-body configurations with all finite masses was considered. The limit cases, however, may offer different possibilities for orbits of small masses or man-made satellites and should be investigated.

Even yet, the results of the present research could be placed in the context of, for example, investigations of the restricted five-body problem, or limit cases of five-body central configurations, similarly to how Lagrangian triangles play a role at limit cases of the kite CCs.

Finally, those well-versed in astronomy can certainly improve on answering our third sub-question, namely whether kite central configurations can be observed in the universe.

Bibliography

[1] P. Alexandersson, L. A. González-Serrano, E. Maximenko, and M. A. Moctezuma-Salazar. Symmetric polynomials in the symplectic alphabet and the change of variables $z_j = x_j + x_j^{-1}$. *The Electronic Journal of Combinatorics*, 28(1), Mar 2021. ISSN 1077-8926. doi: 10.37236/9354.

[2] M. Alvarez-Ramírez and M. Medina. The rhomboidal 4-body problem revisited. *Qualitative Theory of Dynamical Systems*, 14(2):189–207, 2015. ISSN 1662-3592. doi: 10.1007/s12346-015-0151-2.

[3] V. Arnold. *Mathematical Methods of Classical Mechanics*. Springer-Verlag, 1978.

[4] J. Bernoulli. Extrait de la réponse de M. Bernoulli à M. Herman, datée de Basle le 7 Octobre 1710. *Mémoires de l'Académie Royale des Sciences 1710*, pages 521–533, 1712.

[5] V. A. Brumberg. Permanent configurations in the problem of four bodies and their stability. *Soviet Astronomy*, 1:57, February 1957. URL `https://articles.adsabs.harvard.edu/pdf/1957SvA.....1...57B`.

[6] F. Diacu. The solution of the n-body problem. *The Mathematical Intelligencer*, 18(3):66–70, 1996. ISSN 0343-6993. doi: 10.1007/BF03024313.

[7] L. Euler. De motu rectilineo trium corporum se mutuo attrahentium. *Novi Commentarii Academiae Scientiarum Imperialis Petropolitanae*, 11:144–151, 1767.

[8] J. R. Forshaw and A. G. Smith. *Dynamics and Relativity*. Wiley, 2009. ISBN 978-0-470-01459-2.

[9] J. Gomatam, B. A. Steves, and A. E. Roy. Some equal mass four-body equilibrium configurations: linear stability analysis. In *The Dynamics of Small Bodies in the Solar System*, volume 522 of *Nato Science Series C*, pages 373–378. Springer Netherlands, 1999. doi: 10.1007/978-94-015-9221-5.

[10] D. P. Hamilton. Fresh solutions to the four-body problem. *Nature*, 533(7602):187–188, 2016. ISSN 1476-4687. doi: 10.1038/nature17896. URL `https://doi.org/10.1038/nature17896`.

[11] D. D. Holm, J. E. Marsden, T. Ratiu, and A. Weinstein. Nonlinear stability of fluid and plasma equilibria. *Physics Reports*, 123(1):1–116, 1985. ISSN 0370-1573. doi: 10.1016/0370-1573(85)90028-6.

[12] J. Howard. Stability of Hamiltonian equilibria. *Scholarpedia*, 8(10):3627, 2013. doi: 10.4249/scholarpedia.3627. revision #143451.

[13] J.-L. Lagrange. Essai sur le problème des trois corps. *Oeuvres*, 6, 1772.

[14] E. S. G. Leandro. Structure and stability of the rhombus family of relative equilibria under general homogeneous forces. *Journal of Dynamics and Differential Equations*, 31(2):933–958, July 2018. doi: 10.1007/s10884-018-9687-6.

[15] Y. Long and S. Sun. Four-body central configurations with some equal masses. *Archive for Rational Mechanics and Analysis*, 162(1):25–44, March 2002. ISSN 1432-0673. doi: 10.1007/s002050100183.

[16] W. D. MacMillan and W. Bartky. Permanent configurations in the problem of four bodies. *Transactions of the American Mathematical Society*, 34(4):838–875, 1932. ISSN 0002-9947. doi: 10.2307/1989432.

[17] K. R. Meyer and D. C. Offin. *Introduction to Hamiltonian Dynamical Systems and the N-Body Problem*. Springer International Publishing AG, third edition, 2017.

[18] K. R. Meyer and D. S. Schmidt. Elliptic relative equilibria in the n-body problem. *Journal of Differential Equations*, 214(2):256–298, July 2005. doi: 10.1016/j.jde.2004.09.006.

[19] R. Moeckel. Celestial mechanics - especially central configurations, 1994. URL https://www-users.cse.umn.edu/~rmoeckel/notes/CMNotes.pdf.

[20] R. Moeckel. Central configurations. *Scholarpedia*, 9(4):10667, 2014. doi: 10.4249/scholarpedia.10667. revision #142886.

[21] F. R. Moulton. The straight line solutions of the problem of *n* bodies. *Annals of Mathematics*, 12(1):1–17, 1910. ISSN 0003486X. doi: 10.2307/2007159.

[22] I. Newton. *Philosophiæ naturalis principia mathematica*. Royal Society, London, 1687.

[23] B. Oldeman. Analysis of resonances in the three body problem using planar reduction. Master's thesis, University of Groningen, 1998. URL https://fse.studenttheses.ub.rug.nl/id/eprint/8656.

[24] J. E. Pineda, S. S. R. Offner, R. J. Parker, H. G. Arce, A. A. Goodman, P. Caselli, G. A. Fuller, T. L. Bourke, and S. A. Corder. The formation of a quadruple star system with wide separation. *Nature*, 518(7538): 213–215, 2015. ISSN 1476-4687. doi: 10.1038/nature14166.

[25] W. Qiu-Dong. The global solution of the n-body problem. *Celestial Mechanics and Dynamical Astronomy*, 50(1):73–88, 1990. ISSN 1572-9478. doi: 10.1007/BF00048987.

[26] W. Research. NDSolve. https://reference.wolfram.com/language/ref/NDSolve.html, 2019. [Accessed: 5 January 2022].

[27] G. E. Roberts. Linear stability of the elliptic Lagrangian triangle solutions in the three-body problem. *Journal of Differential Equations*, 182:131–218, 2002. doi: 10.1006/jdeq.2001.4089.

[28] E. J. Routh. On Laplace's three particles, with a supplement on the stability of steady motion. *Proceedings of the London Mathematical Society*, s1-6(1):86–97, 11 1874. ISSN 0024-6115. doi: 10.1112/plms/s1-6.1.86.

[29] C. Simó. Relative equilibrium solutions in the four body problem. *Celestial Mechanics*, 18(2):165–184, August 1978. doi: 10.1007/bf01228714.

[30] S. Smale. Mathematical problems for the next century. *The Mathematical Intelligencer*, 20(2):7–15, 1998. ISSN 0343-6993. doi: 10.1007/BF03025291. URL https://doi.org/10.1007/BF03025291.

[31] D. Speiser. The Kepler problem from Newton to Johann Bernoulli. *Archive for History of Exact Sciences*, 50(2):103–116, 1996. ISSN 1432-0657. doi: 10.1007/BF02327155.

[32] M. Spivak. *Calculus on Manifolds: A Modern Approach to Classical Theorems of Advanced Calculus*. CRC Press, 2018. ISBN 978-0-8053-9021-6.

[33] W. van Horssen. Non-linear differential equations. WI4019 lecture, TU Delft, April 2020.

[34] D. Veras. Relating binary-star planetary systems to central configurations. *Monthly Notices of the Royal Astronomical Society*, 462:3368–3375, 2016. doi: 10.1093/mnras/stw1873.

[35] F. Verhulst. *Nonlinear Differential Equations and Dynamical Systems*. Springer-Verlag, second edition, 2000. ISBN 978-3-540-60934-6.

[36] K. Wakker. *Fundamentals of astrodynamics*. TU Delft Library, 2015. ISBN 9789461864192. URL http://resolver.tudelft.nl/uuid:3fc91471-8e47-4215-af43-718740e6694e.

[37] Wolfram Research, Inc. *Wolfram Mathematica Tutorial Collection: Advanced Numerical Differential Equation Solving in Mathematica*. 2008. URL https://library.wolfram.com/infocenter/Books/8503.

[38] Z. Xie. Isosceles trapezoid central configurations of the Newtonian four-body problem. *Proceedings of the Royal Society of Edinburgh: Section A Mathematics*, 142(3):665672, 2012. doi: 10.1017/S0308210511000576.

[39] T. Zhou and Z. Xia. Symmetry in n-body problem via group representations. June 2021. doi: 10.48550/arXiv.2106.06346.

[40] B. Érdi and Z. Czirják. Central configurations of four bodies with an axis of symmetry. *Celestial Mechanics and Dynamical Astronomy*, 125:33–70, 05 2016. doi: 10.1007/s10569-016-9672-5.

Appendices

A

Non-linear numerical integration plots

In this appendix we put the figures with numerical integration results for the two stable convex test cases investigated in Section 8.3 that were too redundant to include in the main body of text. In particular, the following shows the results of long-time integration for perturbations of initial conditions in all other state variables apart from r_2. All of them reinforce the verdict of stability.

A.1. Case $\alpha = 59.9°$, $\beta = 15.1°$, $e = 0.3$

A.1.1. Perturbation in $r_3(0)$

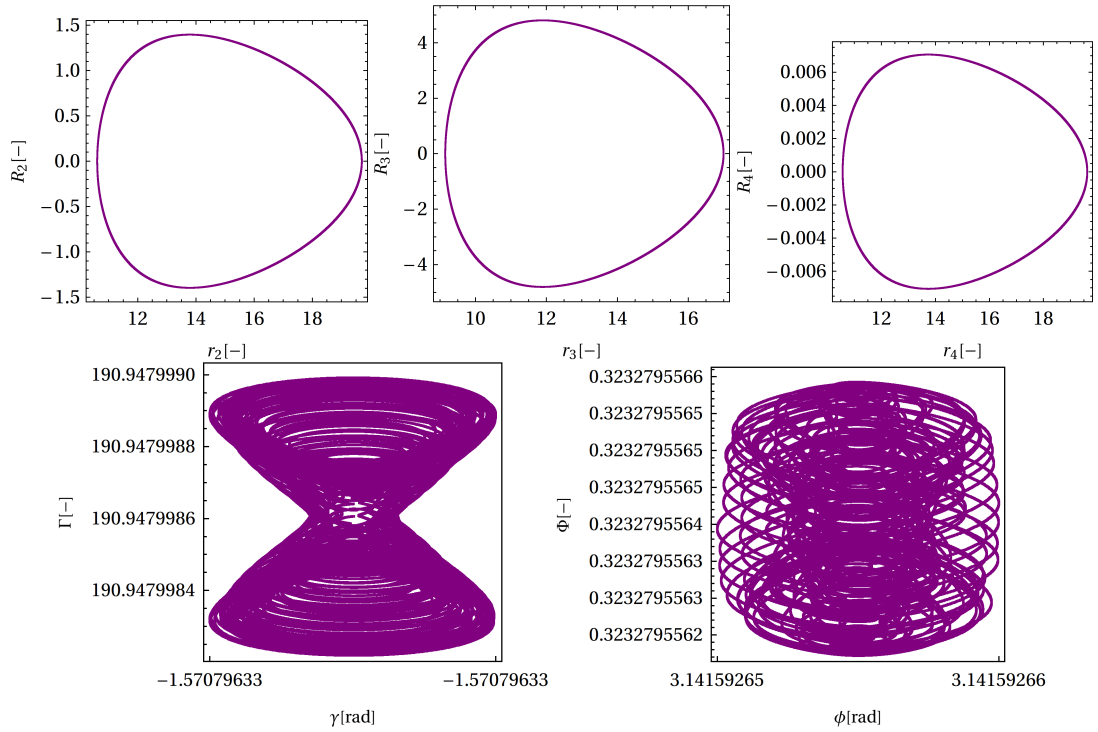

Figure A.1: Phase portraits of the $e = 0.3$, $\alpha = 59.9°$, $\beta = 15.1°$ case integration with perturbation $r_3(0) = r_{3_{k0}} \cdot (1 + 10^{-9})$ over an interval of $t = 2130$.

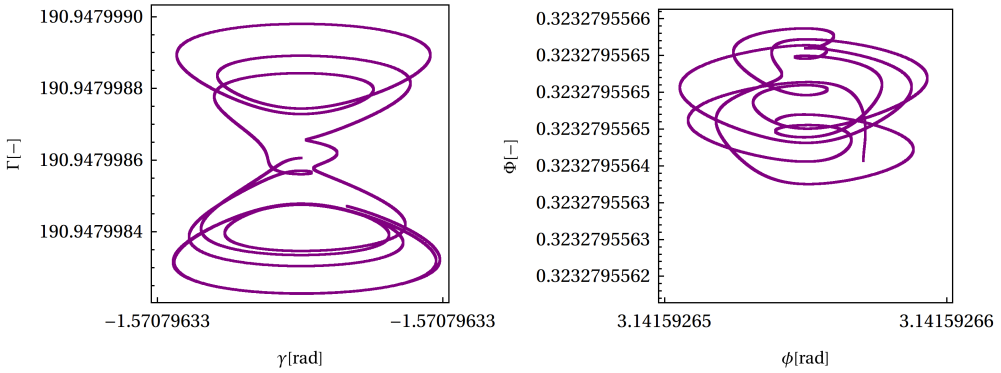

Figure A.2: Phase portraits of the $e = 0.3$, $\alpha = 59.9°$, $\beta = 15.1°$ case integration with perturbation $r_3(0) = r_{3_{k0}} \cdot (1 + 10^{-9})$ over an interval of $t = 10T$.

A.1.2. Perturbation in $\gamma(0)$

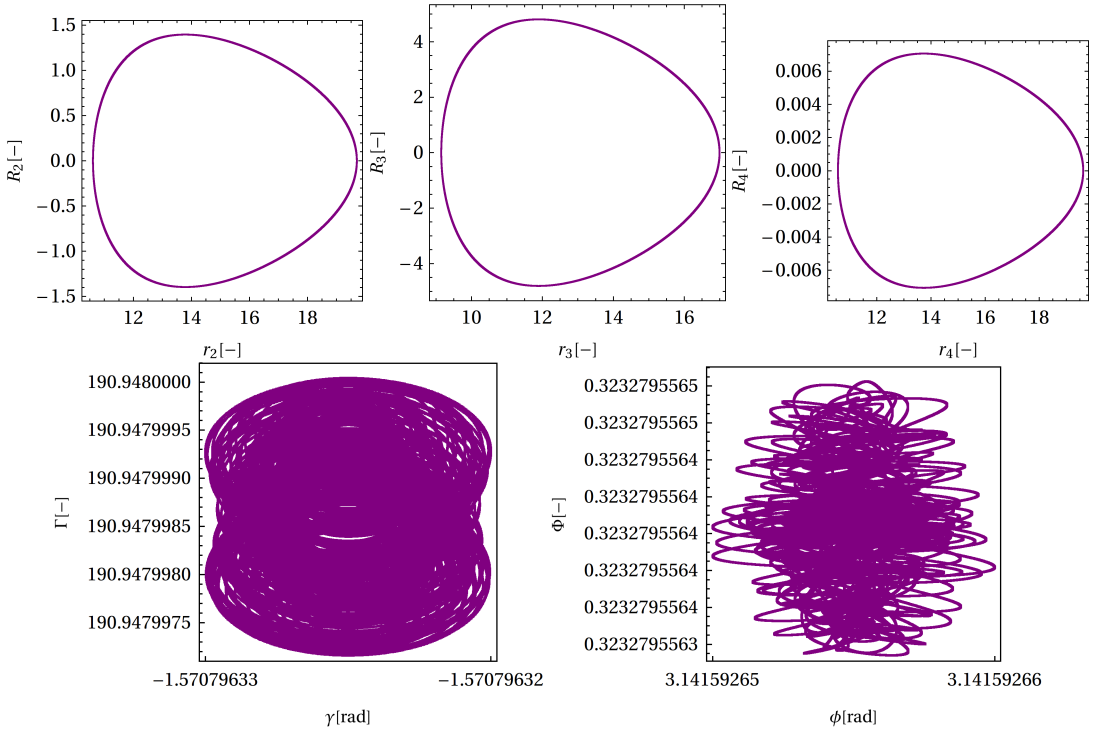

Figure A.3: Phase portraits of the $e = 0.3$, $\alpha = 59.9°$, $\beta = 15.1°$ case integration with perturbation $\gamma(0) = \gamma_{k0} \cdot (1 + 10^{-9})$ over an interval of $t = 2130$.

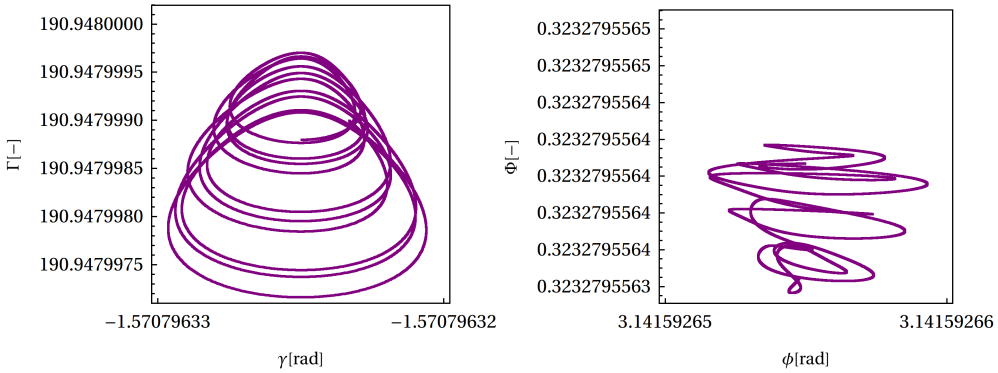

Figure A.4: Phase portraits of the $e = 0.3$, $\alpha = 59.9°$, $\beta = 15.1°$ case integration with perturbation $\gamma(0) = \gamma_{k0} \cdot (1 + 10^{-9})$ over an interval of $t = 10T$.

A.1.3. Perturbation in $r_4(0)$

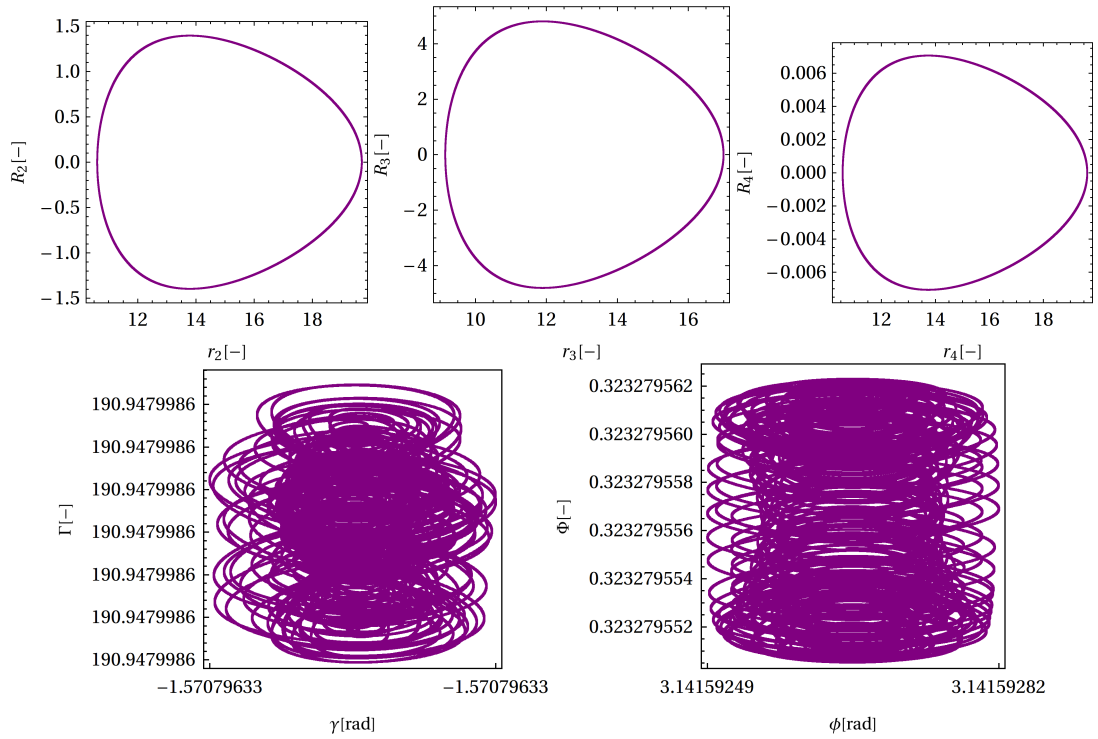

Figure A.5: Phase portraits of the $e = 0.3$, $\alpha = 59.9°$, $\beta = 15.1°$ case integration with perturbation $r_4(0) = r_{4_{k0}} \cdot (1 + 10^{-9})$ over an interval of $t = 2130$.

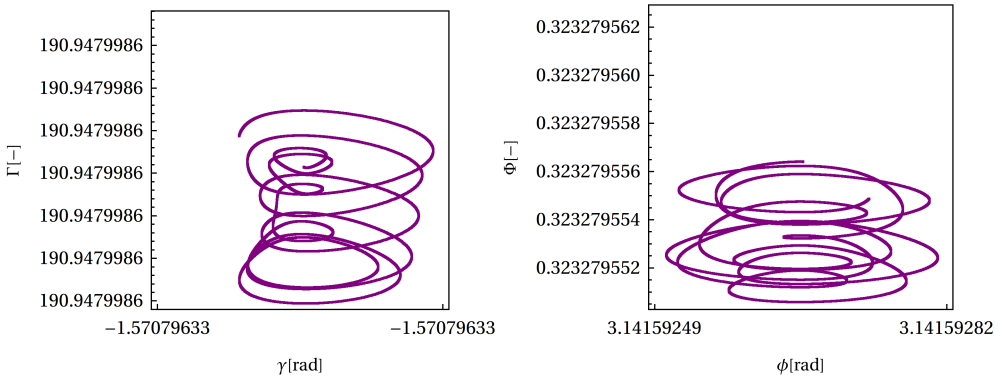

Figure A.6: Phase portraits of the $e = 0.3$, $\alpha = 59.9°$, $\beta = 15.1°$ case integration with perturbation $r_4(0) = r_{4_{k0}} \cdot (1 + 10^{-9})$ over an interval of $t = 10T$.

A.1.4. Perturbation in $\phi(0)$

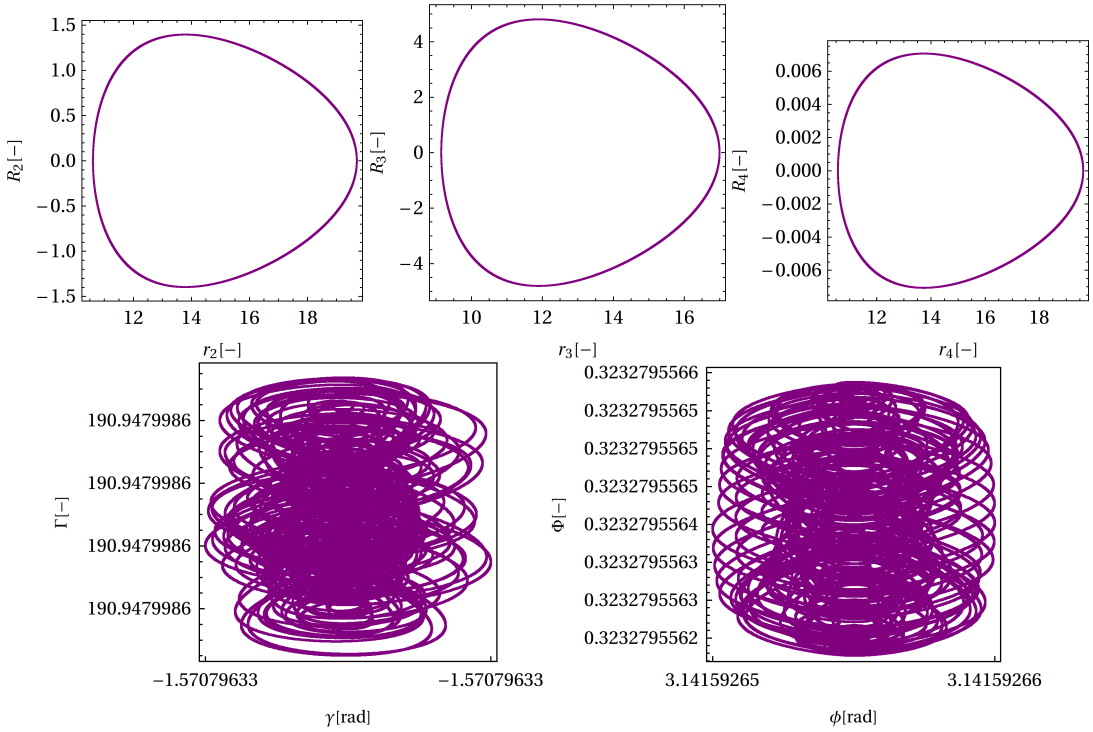

Figure A.7: Phase portraits of the $e = 0.3$, $\alpha = 59.9°$, $\beta = 15.1°$ case integration with perturbation $\phi(0) = \phi_{k0} \cdot (1 + 10^{-9})$ over an interval of $t = 2130$.

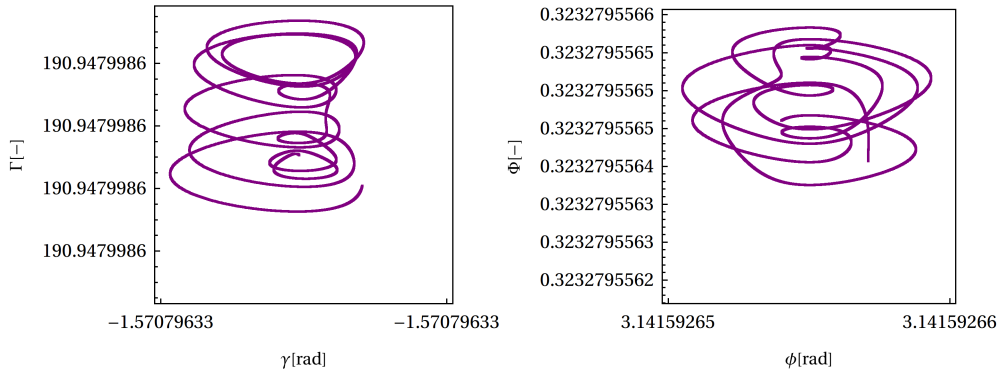

Figure A.8: Phase portraits of the $e = 0.3$, $\alpha = 59.9°$, $\beta = 15.1°$ case integration with perturbation $\phi(0) = \phi_{k0} \cdot (1 + 10^{-9})$ over an interval of $t = 10T$.

A.1.5. Perturbation in $R_2(0)$

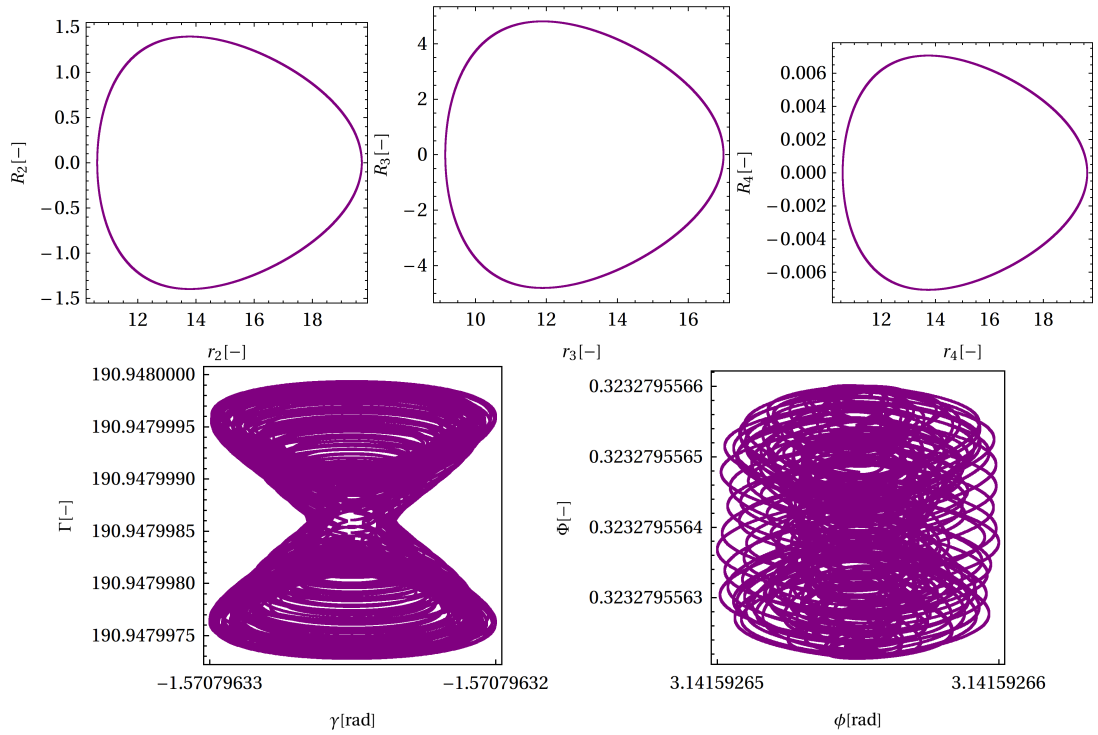

Figure A.9: Phase portraits of the $e = 0.3$, $\alpha = 59.9°$, $\beta = 15.1°$ case integration with perturbation $R_2(0) = 10^{-9}$ over an interval of $t = 2130$.

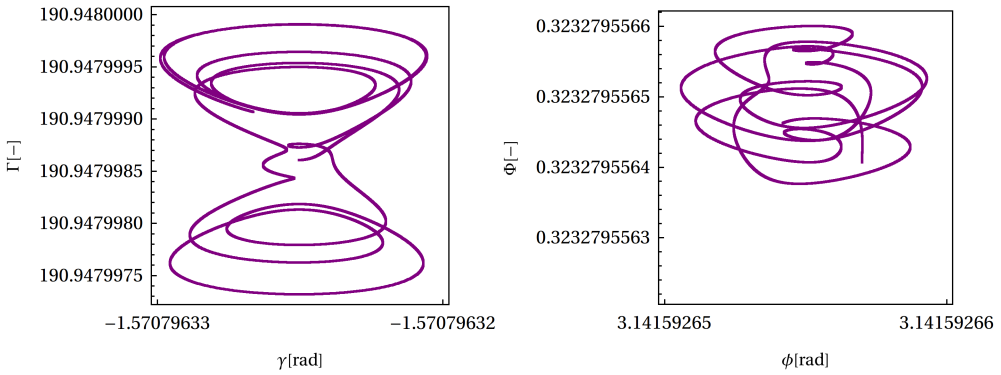

Figure A.10: Phase portraits of the $e = 0.3$, $\alpha = 59.9°$, $\beta = 15.1°$ case integration with perturbation $R_2(0) = 10^{-9}$ over an interval of $t = 10T$.

A.1.6. Perturbation in $R_3(0)$

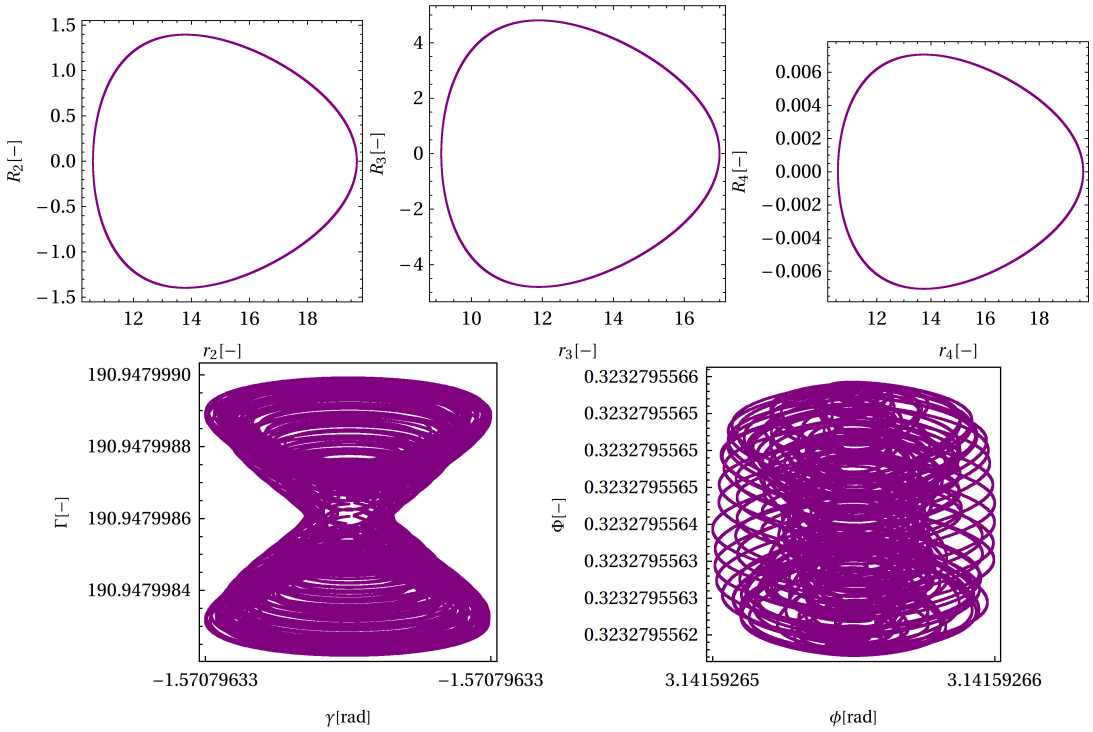

Figure A.11: Phase portraits of the $e = 0.3$, $\alpha = 59.9°$, $\beta = 15.1°$ case integration with perturbation $R_3(0) = 10^{-9}$ over an interval of $t = 2130$.

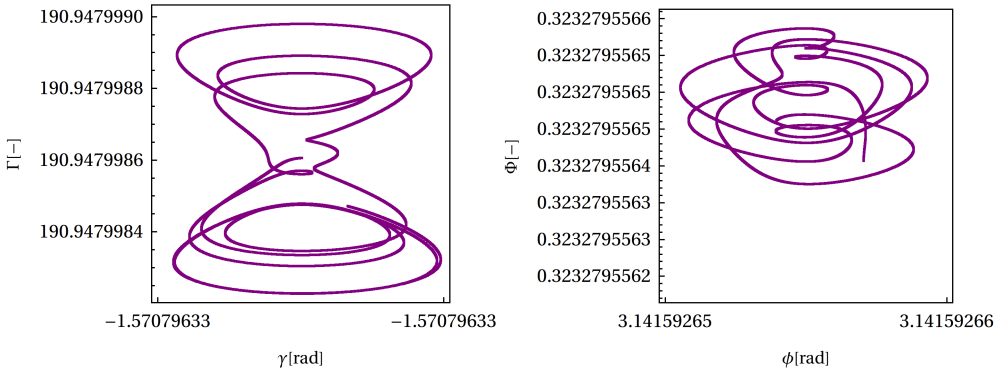

Figure A.12: Phase portraits of the $e = 0.3$, $\alpha = 59.9°$, $\beta = 15.1°$ case integration with perturbation $R_3(0) = 10^{-9}$ over an interval of $t = 10T$.

A.1.7. Perturbation in $\Gamma(0)$

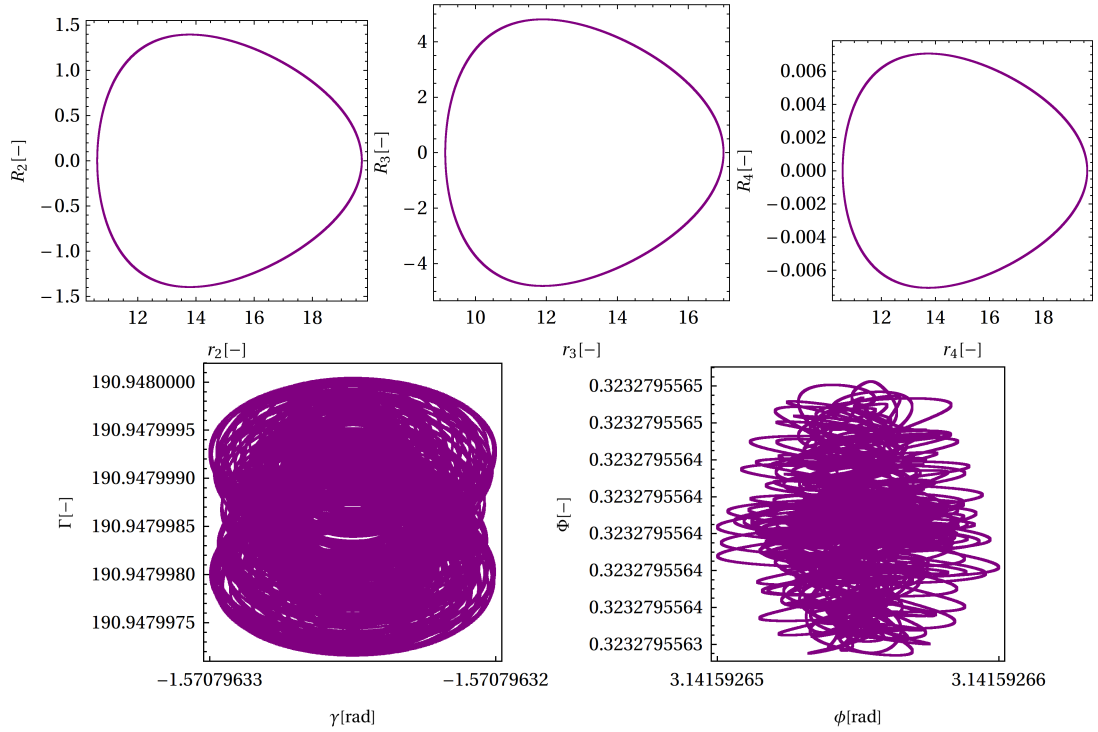

Figure A.13: Phase portraits of the $e = 0.3$, $\alpha = 59.9°$, $\beta = 15.1°$ case integration with perturbation $\Gamma(0) = \Gamma_{k0} \cdot (1 + 10^{-9})$ over an interval of $t = 2130$.

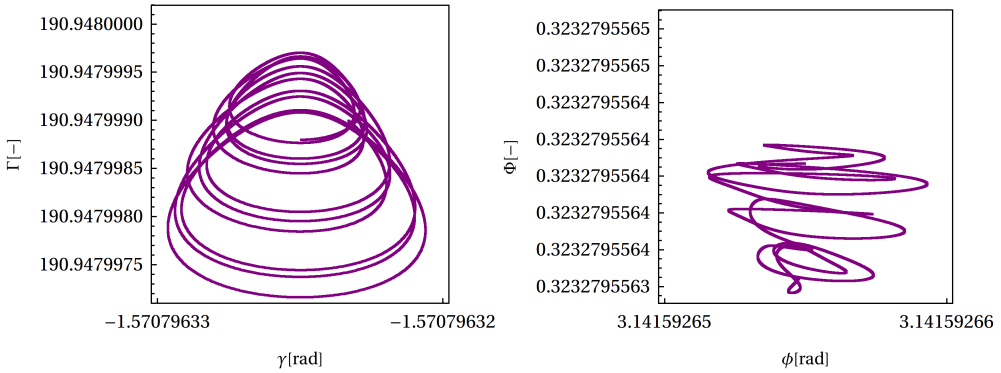

Figure A.14: Phase portraits of the $e = 0.3$, $\alpha = 59.9°$, $\beta = 15.1°$ case integration with perturbation $\Gamma(0) = \Gamma_{k0} \cdot (1 + 10^{-9})$ over an interval of $t = 10T$.

A.1.8. Perturbation in $R_4(0)$

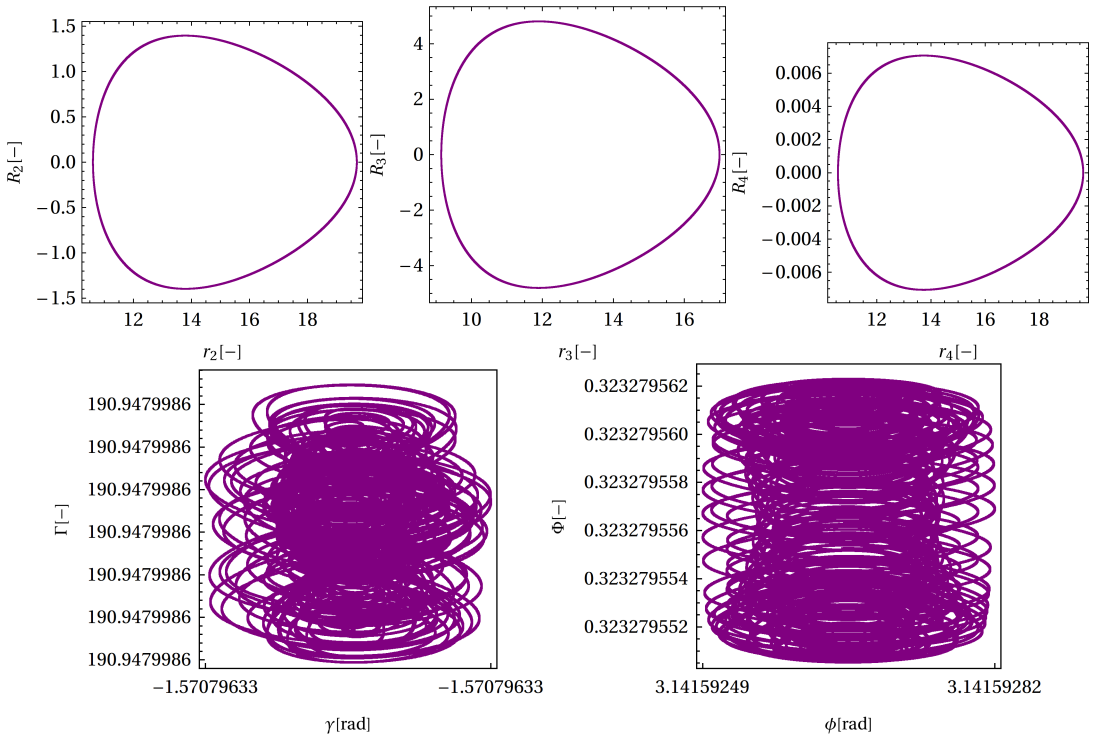

Figure A.15: Phase portraits of the $e = 0.3$, $\alpha = 59.9°$, $\beta = 15.1°$ case integration with perturbation $R_4(0) = 10^{-9}$ over an interval of $t = 2130$.

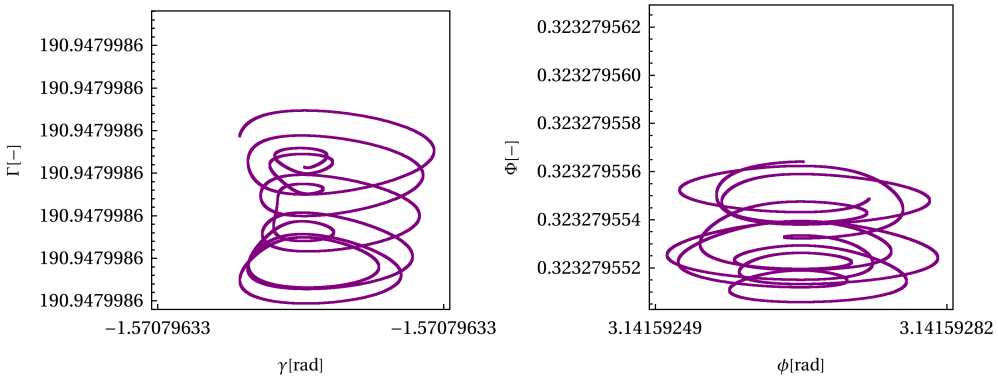

Figure A.16: Phase portraits of the $e = 0.3$, $\alpha = 59.9°$, $\beta = 15.1°$ case integration with perturbation $R_4(0) = 10^{-9}$ over an interval of $t = 10T$.

A.1.9. Perturbation in $\Phi(0)$

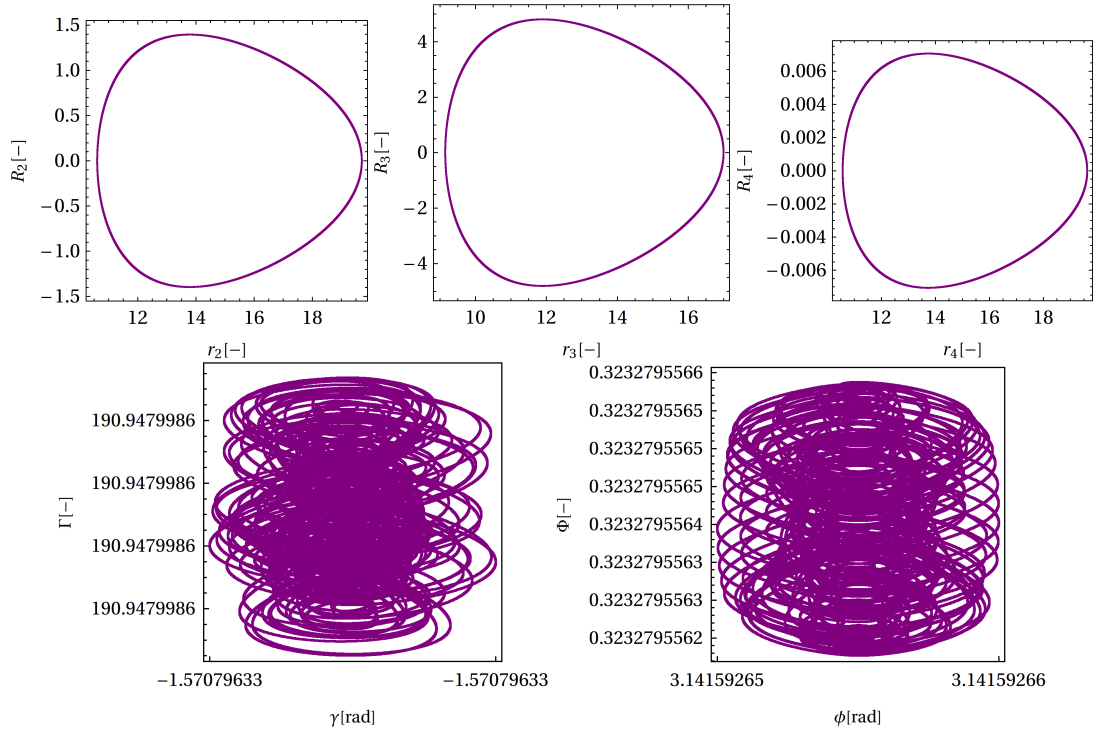

Figure A.17: Phase portraits of the $e = 0.3$, $\alpha = 59.9°$, $\beta = 15.1°$ case integration with perturbation $\Phi(0) = \Phi_{k0} \cdot (1 + 10^{-9})$ over an interval of $t = 2130$.

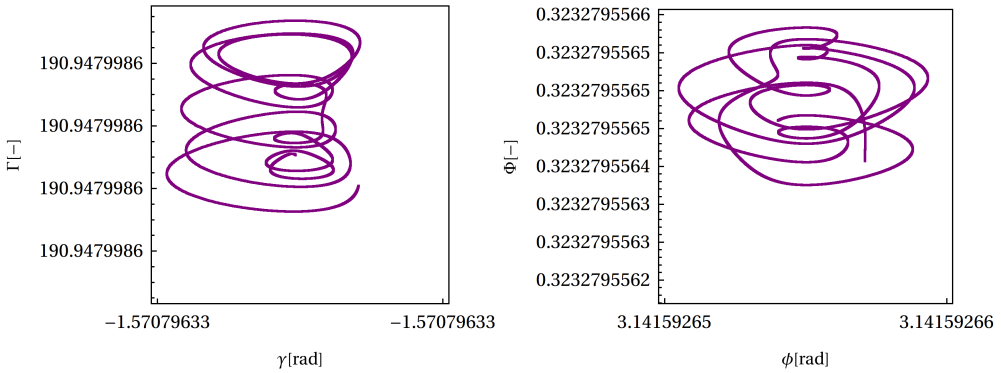

Figure A.18: Phase portraits of the $e = 0.3$, $\alpha = 59.9°$, $\beta = 15.1°$ case integration with perturbation $\Phi(0) = \Phi_{k0} \cdot (1 + 10^{-9})$ over an interval of $t = 10T$.

A.2. Case $\alpha = 39.7°$, $\beta = 25.3°$, $e = 0.2$

A.2.1. Perturbation in $r_3(0)$

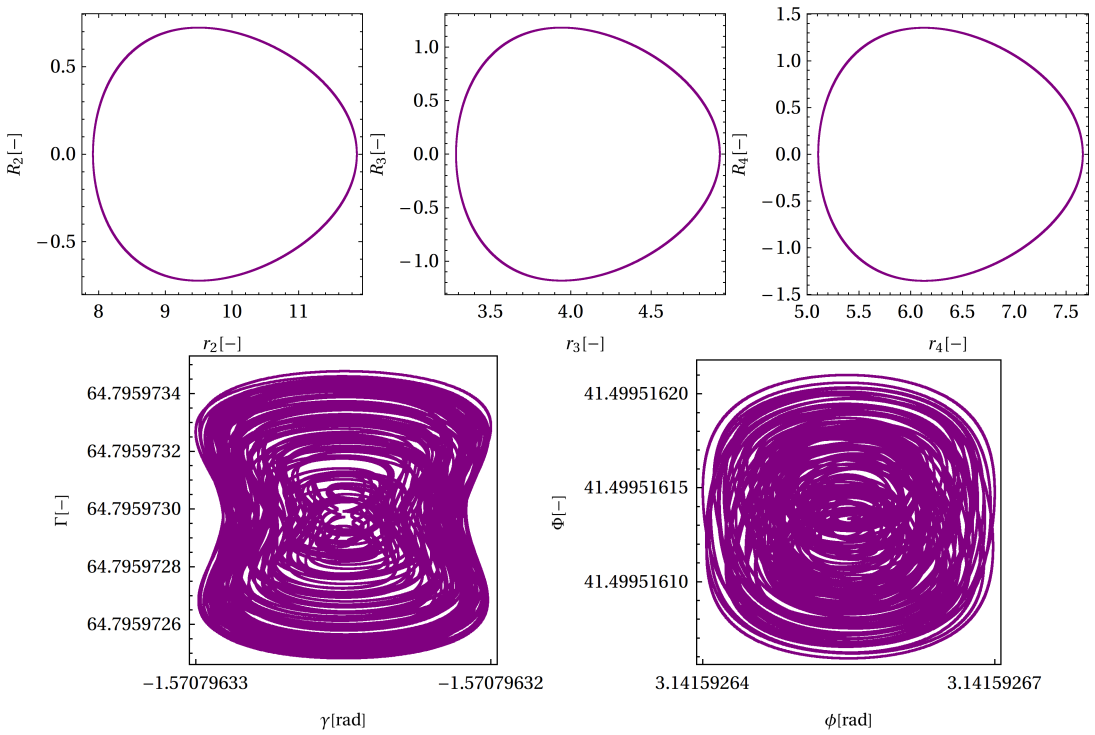

Figure A.19: Phase portraits of the $e = 0.2$, $\alpha = 39.7°$, $\beta = 25.3°$ case integration with perturbation $r_3(0) = r_{3_{k0}} \cdot (1 + 10^{-9})$ over an interval of $t = 1756$.

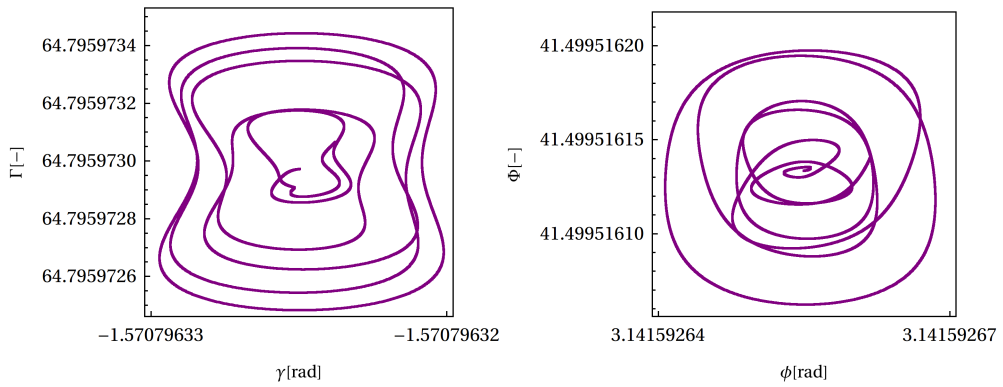

Figure A.20: Phase portraits of the $e = 0.2$, $\alpha = 39.7°$, $\beta = 25.3°$ case integration with perturbation $r_3(0) = r_{3_{k0}} \cdot (1 + 10^{-9})$ over an interval of $t = 10T$.

A.2.2. Perturbation in $\gamma(0)$

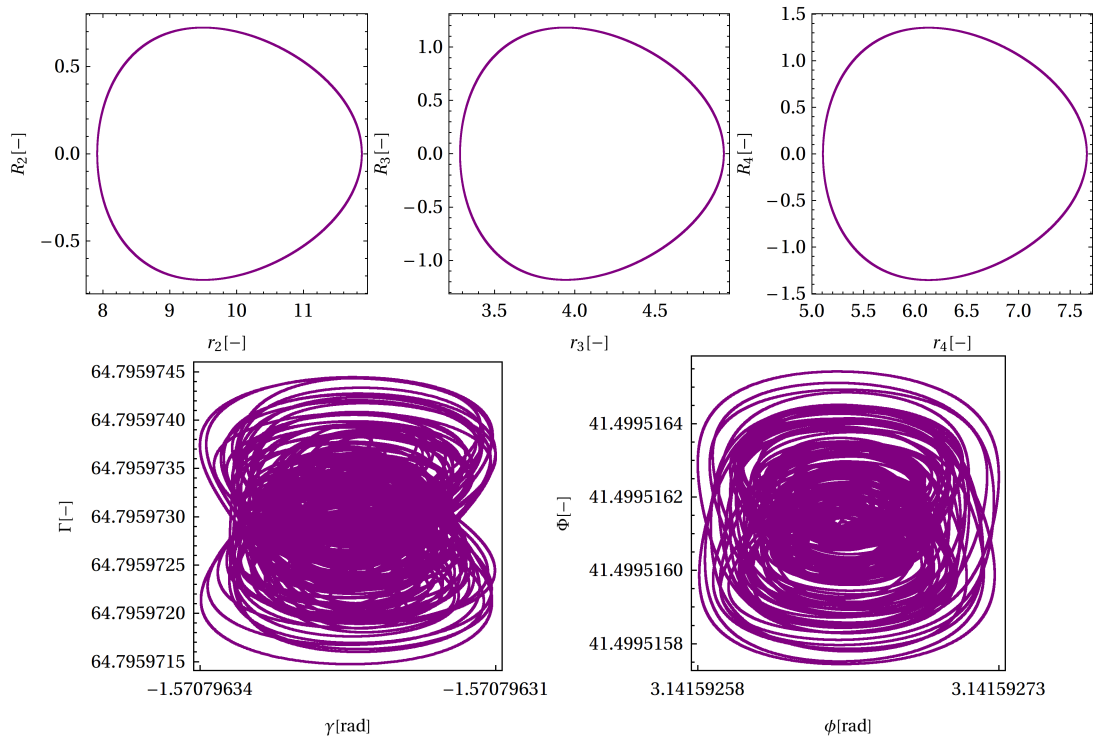

Figure A.21: Phase portraits of the $e = 0.2$, $\alpha = 39.7°$, $\beta = 25.3°$ case integration with perturbation $\gamma(0) = \gamma_{k0} \cdot (1 + 10^{-9})$ over an interval of $t = 1756$.

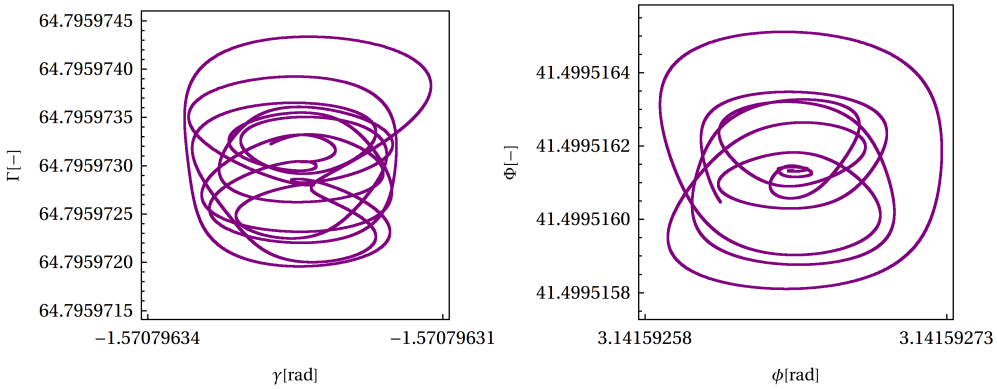

Figure A.22: Phase portraits of the $e = 0.2$, $\alpha = 39.7°$, $\beta = 25.3°$ case integration with perturbation $\gamma(0) = \gamma_{k0} \cdot (1 + 10^{-9})$ over an interval of $t = 10T$.

A.2.3. Perturbation in $r_4(0)$

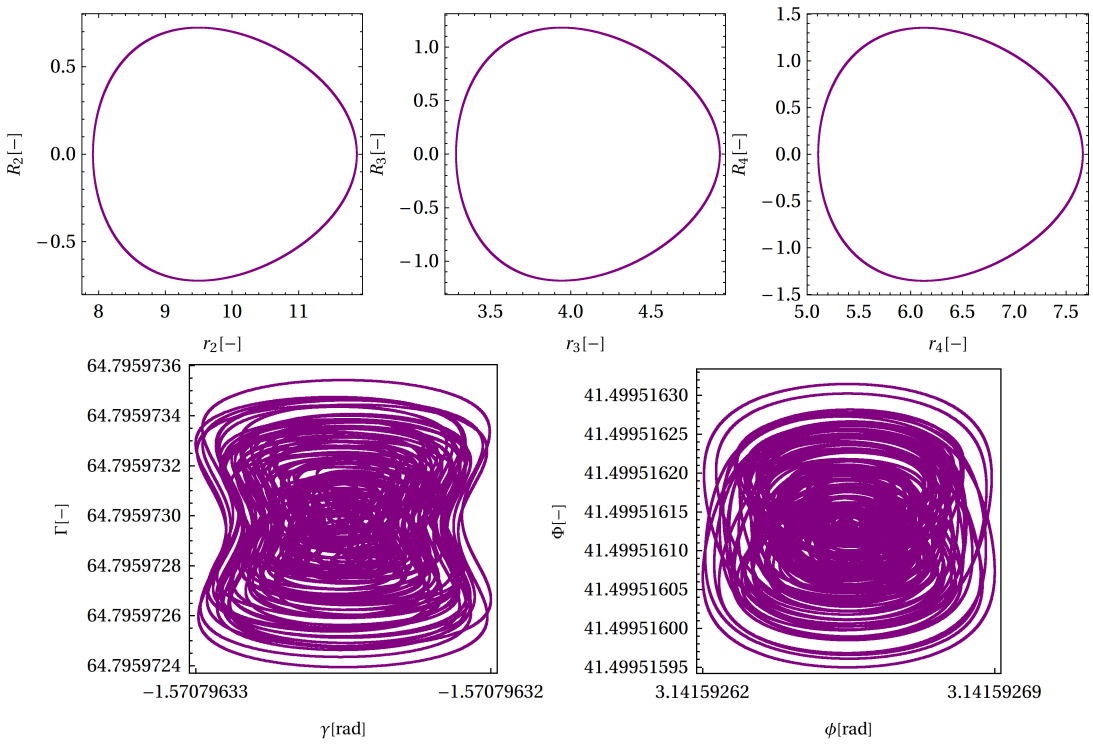

Figure A.23: Phase portraits of the $e = 0.2$, $\alpha = 39.7°$, $\beta = 25.3°$ case integration with perturbation $r_4(0) = r_{4_{k0}} \cdot (1 + 10^{-9})$ over an interval of $t = 1756$.

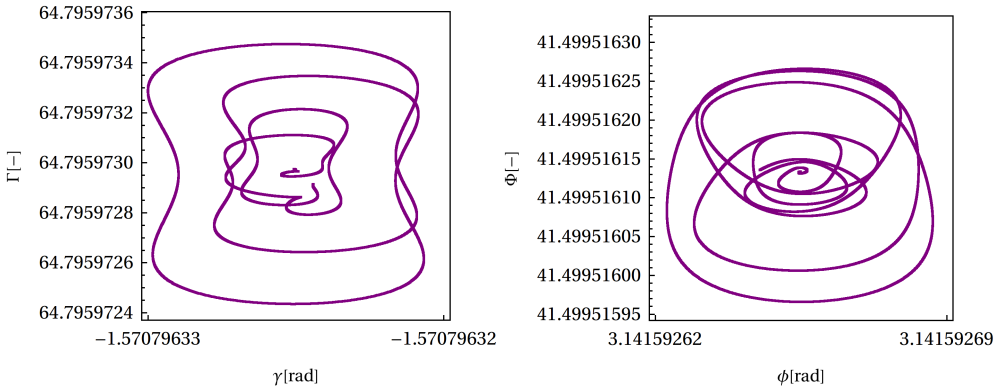

Figure A.24: Phase portraits of the $e = 0.2$, $\alpha = 39.7°$, $\beta = 25.3°$ case integration with perturbation $r_4(0) = r_{4_{k0}} \cdot (1 + 10^{-9})$ over an interval of $t = 10T$.

A.2.4. Perturbation in $\phi(0)$

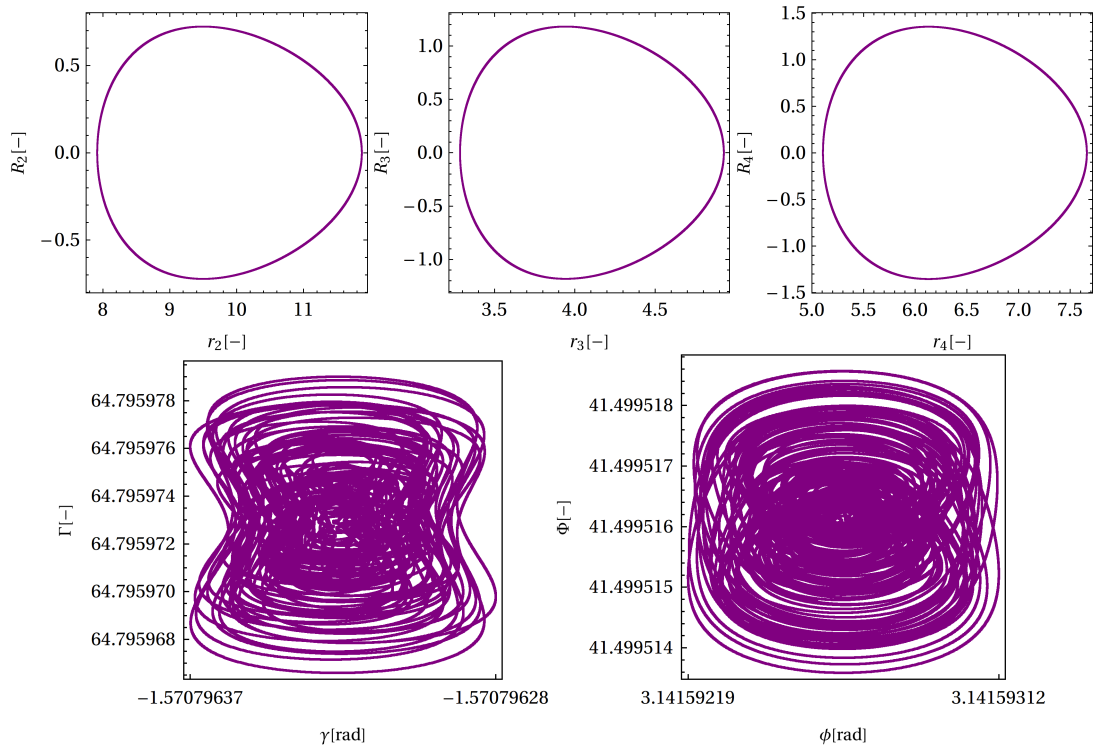

Figure A.25: Phase portraits of the $e = 0.2$, $\alpha = 39.7°$, $\beta = 25.3°$ case integration with perturbation $\phi(0) = \phi_{k0} \cdot (1 + 10^{-9})$ over an interval of $t = 1756$.

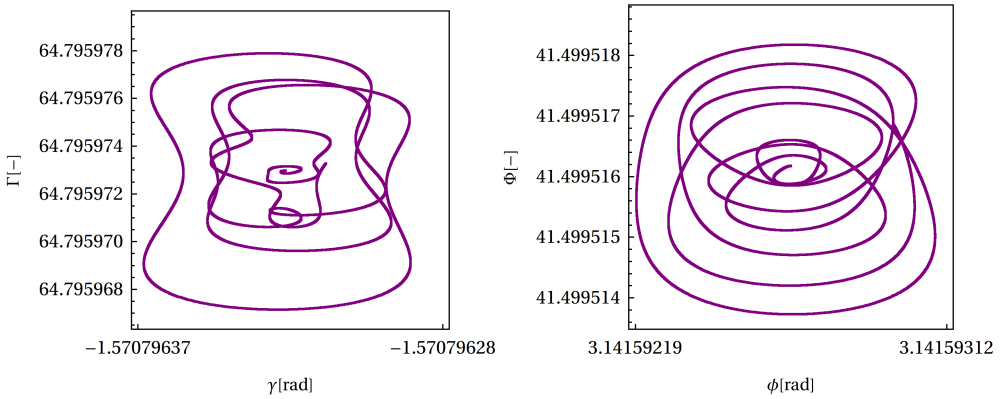

Figure A.26: Phase portraits of the $e = 0.2$, $\alpha = 39.7°$, $\beta = 25.3°$ case integration with perturbation $\phi(0) = \phi_{k0} \cdot (1 + 10^{-9})$ over an interval of $t = 10T$.

A.2.5. Perturbation in $R_2(0)$

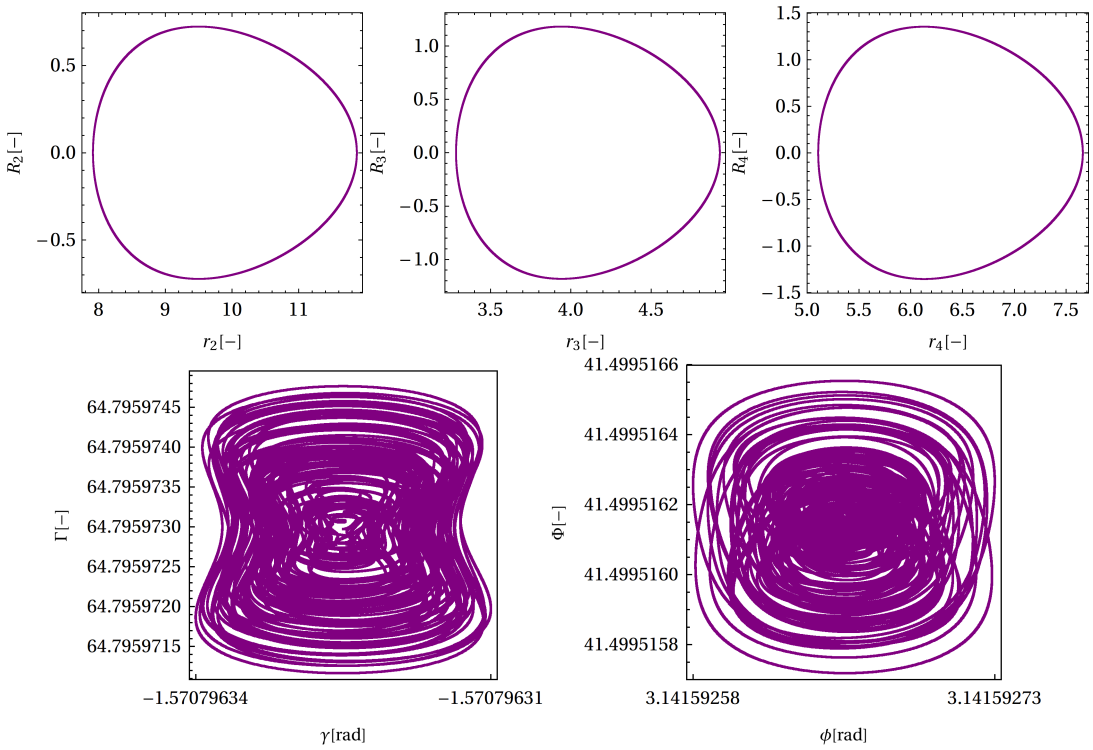

Figure A.27: Phase portraits of the $e = 0.2$, $\alpha = 39.7°$, $\beta = 25.3°$ case integration with perturbation $R_2(0) = 10^{-9}$ over an interval of $t = 1756$.

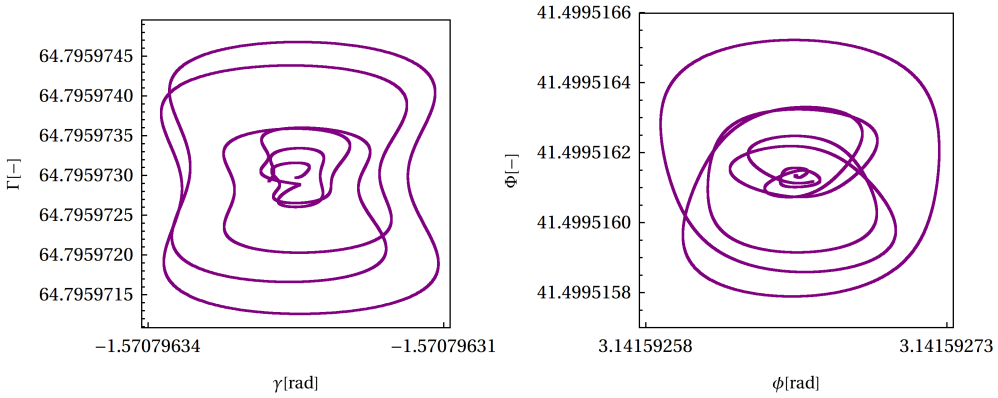

Figure A.28: Phase portraits of the $e = 0.2$, $\alpha = 39.7°$, $\beta = 25.3°$ case integration with perturbation $R_2(0) = 10^{-9}$ over an interval of $t = 10T$.

A.2.6. Perturbation in $R_3(0)$

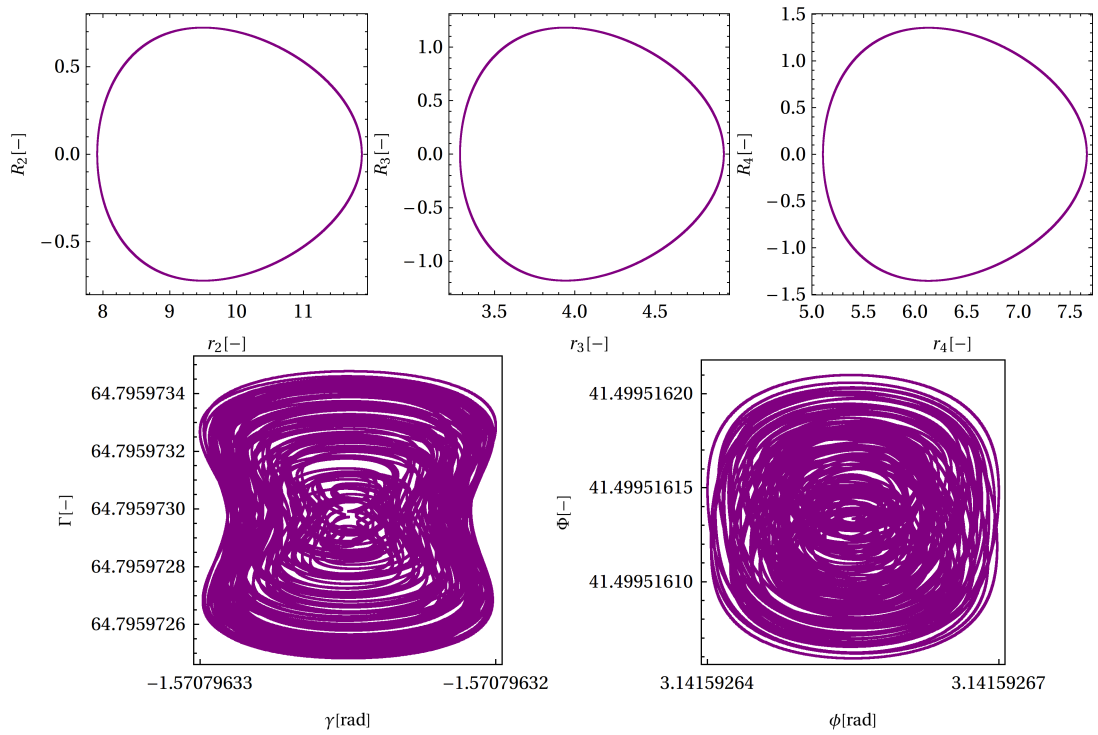

Figure A.29: Phase portraits of the $e = 0.2$, $\alpha = 39.7°$, $\beta = 25.3°$ case integration with perturbation $R_3(0) = 10^{-9}$ over an interval of $t = 1756$.

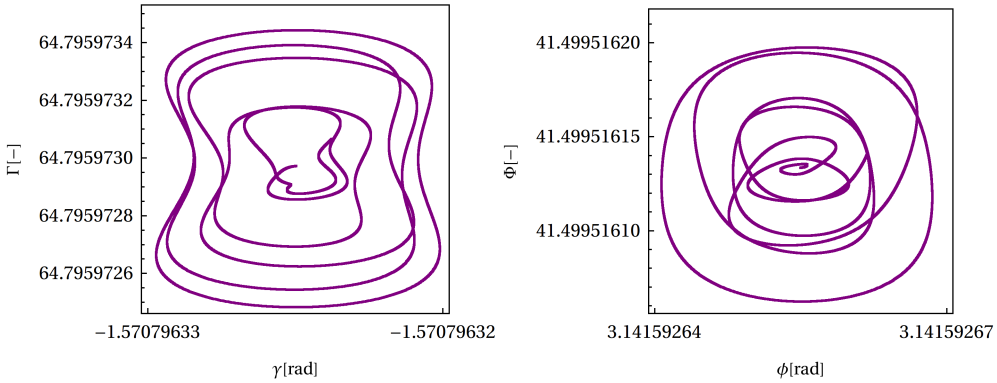

Figure A.30: Phase portraits of the $e = 0.2$, $\alpha = 39.7°$, $\beta = 25.3°$ case integration with perturbation $R_3(0) = 10^{-9}$ over an interval of $t = 10T$.

A.2.7. Perturbation in $\Gamma(0)$

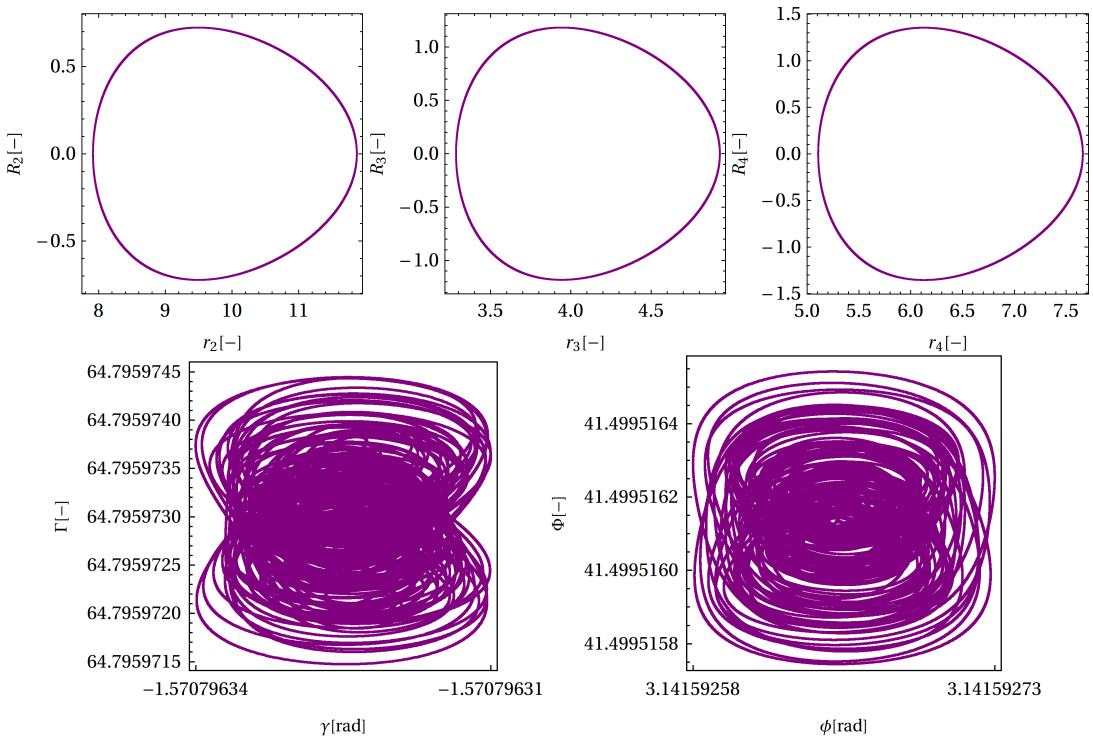

Figure A.31: Phase portraits of the $e = 0.2$, $\alpha = 39.7°$, $\beta = 25.3°$ case integration with perturbation $\Gamma(0) = \Gamma_{k0} \cdot (1 + 10^{-9})$ over an interval of $t = 1756$.

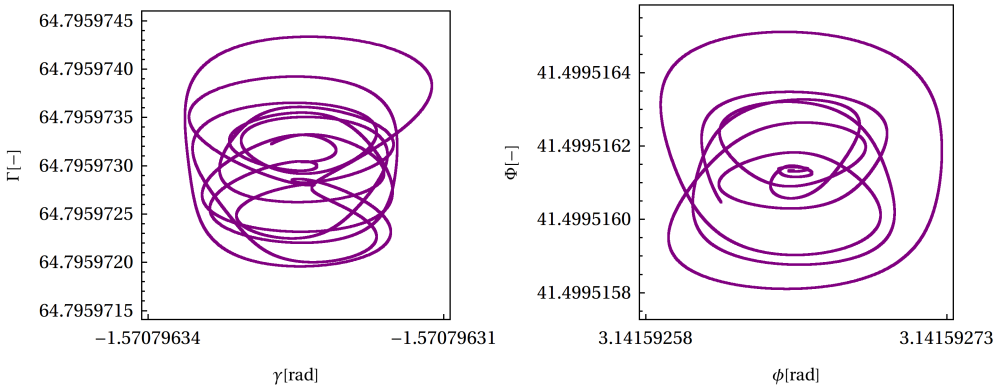

Figure A.32: Phase portraits of the $e = 0.2$, $\alpha = 39.7°$, $\beta = 25.3°$ case integration with perturbation $\Gamma(0) = \Gamma_{k0} \cdot (1 + 10^{-9})$ over an interval of $t = 10T$.

A.2.8. Perturbation in $R_4(0)$

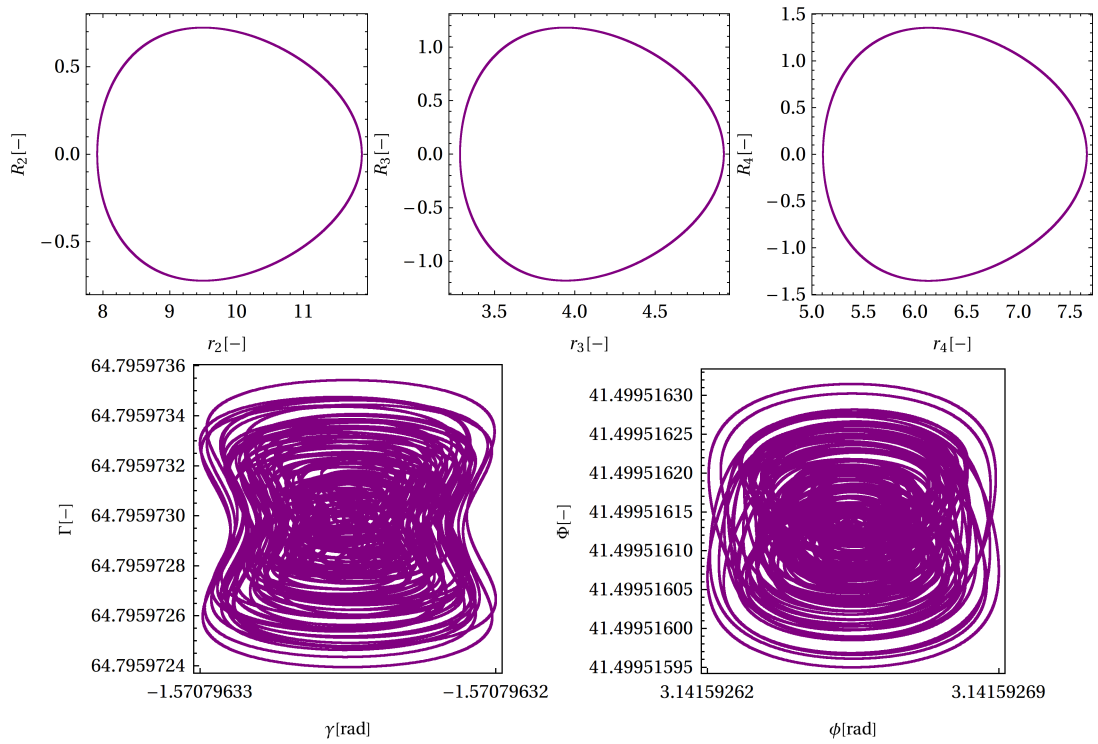

Figure A.33: Phase portraits of the $e = 0.2$, $\alpha = 39.7°$, $\beta = 25.3°$ case integration with perturbation $R_4(0) = 10^{-9}$ over an interval of $t = 1756$.

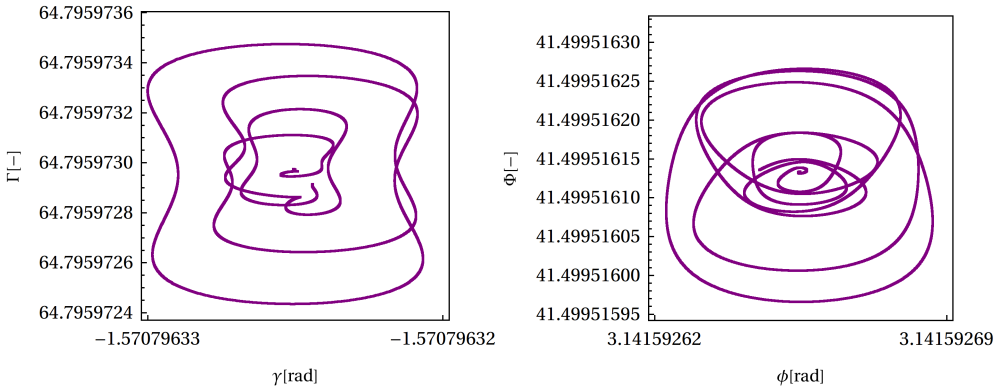

Figure A.34: Phase portraits of the $e = 0.2$, $\alpha = 39.7°$, $\beta = 25.3°$ case integration with perturbation $R_4(0) = 10^{-9}$ over an interval of $t = 10T$.

A.2.9. Perturbation in $\Phi(0)$

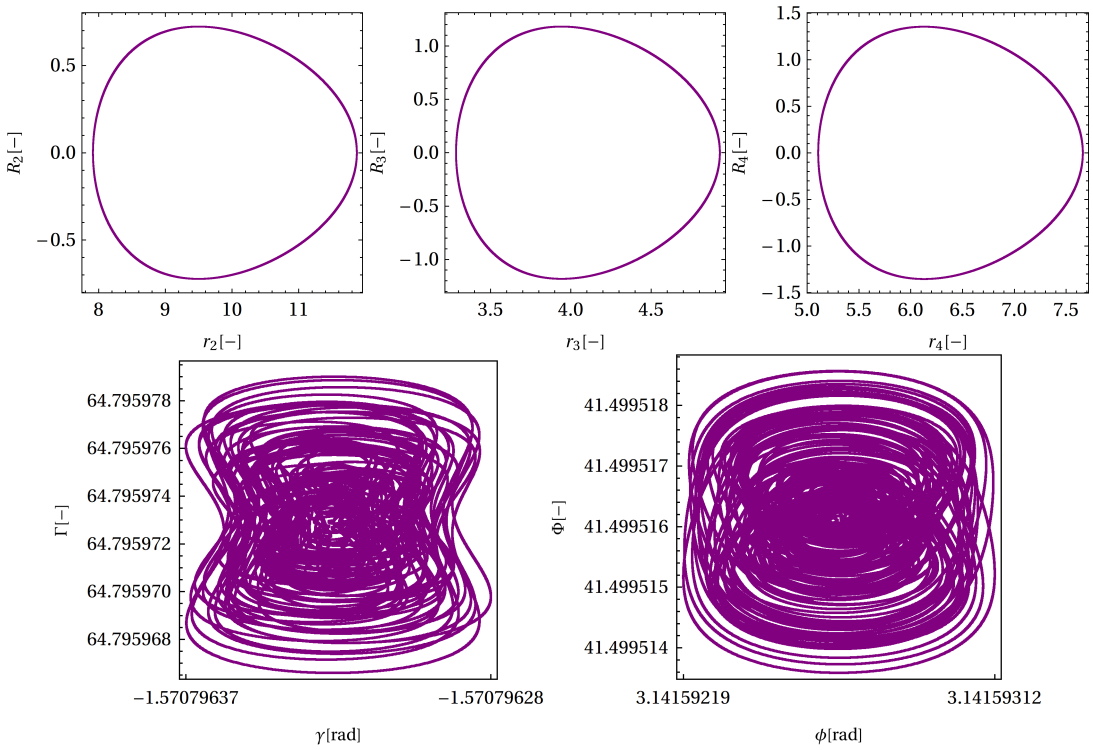

Figure A.35: Phase portraits of the $e = 0.2$, $\alpha = 39.7°$, $\beta = 25.3°$ case integration with perturbation $\Phi(0) = \Phi_{k0} \cdot (1 + 10^{-9})$ over an interval of $t = 1756$.

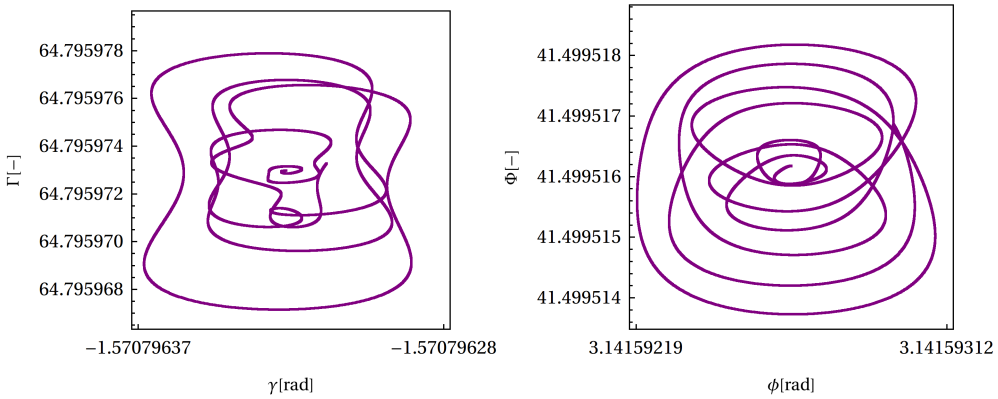

Figure A.36: Phase portraits of the $e = 0.2$, $\alpha = 39.7°$, $\beta = 25.3°$ case integration with perturbation $\Phi(0) = \Phi_{k0} \cdot (1 + 10^{-9})$ over an interval of $t = 10T$.